

Faculty of Resource Science and Technology

Eco-friendly Cellulose Hydrogel as Controlled Release Fertilizer for Sustainable Production of Upland Rice in Sarawak

Dayang Fazirah binti Abg Ahmad

Doctor of Philosophy
2024

Eco-friendly Cellulose Hydrogel as Controlled Release Fertilizer for Sustainable Production of Upland Rice in Sarawak

Dayang Fazirah binti Abg Ahmad

A thesis submitted

In fulfillment of the requirements for the degree of Doctor of Philosophy

(Physical Chemistry)

Faculty of Resources Science and Technology
UNIVERSITI MALAYSIA SARAWAK
2024

DECLARATION

I declare that the work in this thesis was carried out in accordance with the regulations of Universiti Malaysia Sarawak. Except where due acknowledgements have been made, the work is that of the author alone. The thesis has not been accepted for any degree and is not concurrently submitted in candidature of any other degree.



……

Signature

Name: Dayang Fazirah binti Abg Ahmad

Matric No.: 20010084

Faculty of Resource Science and Technology

Universiti Malaysia Sarawak

Date : 24th October 2024

ACKNOWLEDGEMENT

All praises are due to Allah for His blessings and make everything possible for me. I would like to convey gratitude to my supervisor, Associate Professor Dr Chin Suk-Fun and co-supervisors, Associate Professor Dr Mohd Effendi bin Wasli for their valuable guidance, supervision, supports, and encouragement throughout this project and in the completion of this thesis. My sincere appreciation to Dr Cindy Soo Yun Tan and Mr. Zaki Musa for their support and guidance at times needed.

I wish to express my deep sense of gratitude and dedicating this success for my beloved parents, Hajijah binti Abang Gapor and Haji Abang Ahmad bin Haji Abang Dahlan for their unconditional loves, prayers, endless supports and encouragement through thick and thin in my whole life and made it possible for me to get the best of education and get my degrees. I am deeply thankful to my soulmate, Hafizuddin Kamil for always be the helping hand and be there for me through thick and thin, throughout this journey. My special gratitude as well goes to Dr Abang Nawawi bin Haji Abang Dahlan for being generous with supports and encouragement. My warmest siblings, Dr Dayang Hafiza, Abang Nazeri, and Abang Azizul Hakimi, thank you for the good times.

This study could not happen without the financial support from Sarawak Research and Development Council (SRDC) (Grant No. RDCRG/CAT/2019/26; GL/F07/SRDC/02/2020).

Finally, my sincere appreciation to the Faculty of Resource Science and Technology and their staff, lab technician and others for the advice and support given during my period of study in UNIMAS. I also would like to thank Pusat Penyelidikan Tumbuhan (PPT) and their staffs for helping me in completing my works and making it possible for me to complete my study here. Thank you.

ABSTRACT

Fertilizers and irrigation are the primary components for upland rice cultivation to increase the quality and yield of the rice crops. Most farmers apply conventional fertilizers, however, low efficiency of plant uptake (<50%) is often reported due to nutrient losses through heavy leaching, surface run-off, undesirable reaction with organic compound in the soils, and vaporization and volatilization processes. A promising agricultural alternative to address these challenges is the encapsulation of fertilizers in superabsorbent hydrogels as controlled-release fertilizers to minimize fertilizer losses, extend nutrient supply for a longer period and enhance nutrient uptake efficiency. Therefore, this study fabricates an eco-friendly cellulose-based hydrogel as a controlled-release fertilizer (CRF) derives from waste papers, with a focus on evaluating the effect of the fabricated cellulose hydrogel CRF on the growth performance and production of upland rice, as well as nitrogen uptake and nitrogen use efficiency of the rice plants. To perform the study, a series of cellulose-based cellulose hydrogels were synthesized by crosslinking cellulose fibers extracted from waste papers and carboxymethylcellulose (CMC) with epichlorohydrin (ECH). Fourier transform infrared (FTIR) characterization at 400–500 cm^{-1} wavenumber using attenuated total reflectance (ATR) technique showed that cellulose fibers and CMC were successfully crosslinked with ECH to form hydrogel. Field emission scanning electron microscopy (FESEM) micrograph of 1000x-magnification displayed highly porous structures. Maximum swelling ratio of >2000% was obtained in C3 cellulose hydrogel (3% (w/v) cellulose, 1.75% (w/v) CMC, 5 mL ECH). Soil moisture retention increased in the presence of C3 cellulose hydrogel (36.5% in topsoil, 30.1% in wet clayey soil, 23.4% in sandy soil) after 7 days, relative to soil without C3 cellulose hydrogel. Urea as a model fertilizer was loaded onto the cellulose hydrogels with maximum loading capacity recorded at 0.51 g g^{-1}. The urea release profile of C3

cellulose hydrogel demonstrated gradual release in soils within 42 days (74.71% in topsoil, 73.37% in wet clayey soil, 71.84% in sandy soil) relative to conventional urea within 7 days (97.32% in topsoil, 95.09% in wet clayey soil, 98.47% in sandy soil). The effects of cellulose hydrogel as CRF in upland rice cultivation were evaluated using *Maswangi* (MRQ74) Mardi rice variety. The study was conducted at Pusat Penyelidikan Tumbuhan (PPT), University Malaysia Sarawak (UNIMAS), Kota Samarahan, Sarawak (1°28′09.3″N, 110°25′41.3″E). The application of cellulose hydrogels CRF at an optimum rate of nitrogen (N) fertilizer, T4H (790 kg N ha^{-1} = 75%) resulted in maximum grain yield, increasing by 71% relative to control. Maximum nutrient uptake of 0.25 g kg^{-1} was also observed in the rice plants treated with T4H CRF. Further analysis revealed that T4H CRF recorded the highest harvest index, HI (45.5%); nitrogen harvest index, NHI (67.9%); nutrient use efficiency, NUE (52.6%) and nutrient agronomic efficiency, NAE (12.8 kg kg^{-1}), respectively. Observations show that CRF with only 75% N applied (T4H) in soil improved grain yield when compared to CRF with 100% N and 100% recommended dose of fertilizer (RDF) in farmers' conventional split application. This suggested that CRF with a moderate N application might produce the highest potential yield and improved N efficiencies while enhancing crop production and further increase in N supply did not increase yield and N efficiencies. The results suggest that the application of T4H CRF for upland rice would enhance HI, N efficiencies and improve the yield of upland rice. Also, all growth parameters and yield were positively influenced by the application of CRF as a basal dose compared to split application of conventional urea fertilizers.

Keywords: Controlled-release fertilizer, cellulose, upland rice, nitrogen application, nitrogen use efficiency

Hidrogel Selulosa Mesra Alam sebagai Baja PelepasanTerkawal untuk Pengeluaran Mampan Padi Tanah Tinggi di Sarawak

ABSTRAK

Baja dan pengairan merupakan komponen utama untuk penanaman padi tanah tinggi bagi meningkatkan kualiti dan hasil tanaman padi. Kebanyakan petani menggunakan baja konvensional, walau bagaimanapun, kecekapan penyerapan tumbuhan yang rendah (<50%) sering dilaporkan disebabkan oleh kehilangan zat makanan melalui larut lesap berat, air larian permukaan, tindak balas yang tidak diingini dengan sebatian organik dalam tanah, dan proses pengewapan dan volatilisasi. Pengkapsulan baja dalam hidrogel superabsorben sebagai baja pelepasan terkawal merupakan alternatif untuk mengurangkan kehilangan baja, memanjangkan bekalan zat makanan dan meningkatkan kecekapan pengambilan zat makanan. Oleh itu, kajian ini menghasilkan hidrogel berasaskan selulosa mesra alam sebagai baja pelepasan terkawal (CRF) yang diperbuat daripada kertas buangan, untuk menilai kesan hidrogel selulosa CRF terhadap prestasi pertumbuhan padi tanah tinggi. Kajian dilaksanakan melalui sintesis hidrogel selulosa dengan memaut silang gentian selulosa yang diekstrak daripada kertas buangan dan carboxymethylcellulose (CMC) dengan epiklorohidrin (ECH). Pencirian penjelmaan infra merah fourier (FTIR) pada 400–500 cm^{-1} nombor gelombang menggunakan teknik jumlah pemantulan dilemahkan (ATR) menunjukkan gentian selulosa dan CMC berjaya dirangkai silang dengan ECH untuk membentuk hidrogel. Mikrograf daripada mikroskop electron pengimbasan pelepasan medan (FESEM) pada 1000x memaparkan struktur yang sangat berliang. Nisbah pembengkakan tertinggi dalam hidrogel selulosa C3 (3% (w/v) selulosa, 1.75% (w/v) CMC, 5 mL ECH) melebihi 2000%. Pengekalan kelembapan tanah meningkat menggunakan hidrogel selulosa C3 (36.5% tanah atas, 30.1% tanah liat basah, 23.4% tanah berpasir)

selepas 7 hari, berbanding dengan tanah tanpa hidrogel selulosa C3. Urea sebagai model baja dimuatkan ke dalam hidrogel selulosa dengan kapasiti pemuatan maksimum direkodkan pada 0.51 g g^{-1}. Profil pelepasan urea hidrogel selulosa C3 secara beransur-ansur dalam tanah dalam tempoh 42 hari (74.71% tanah atas, 73.37% tanah liat basah, 71.84% tanah berpasir) berbanding urea konvensional dalam masa 7 hari (97.32% tanah atas, 95.09% tanah liat basah, 98.47% tanah berpasir). Kesan hidrogel selulosa sebagai CRF terhadap prestasi pertumbuhan padi tanah tinggi telah dinilai menggunakan varieti padi Maswangi (MRQ74) Mardi. Kajian telah dijalankan di Pusat Penyelidikan Tumbuhan (PPT), Universiti Malaysia Sarawak (UNIMAS), Kota Samarahan, Sarawak (1°28′09.3″N, 110°25′41.3″E).Penggunaan hidrogel selulosa CRF sebagai baja nitrogen (N) pada kadar optimum, T4H menghasilkan hasil bijirin tertinggi, meningkat sebanyak 71% berbanding kawalan dan serapan nutrien tertinggi sebanyak 0.25 g kg^{-}. T4H CRF juga mencatatkan kadar tertinggi dalam indeks penuaian, HI (45.5%), indeks penuaian nitrogen, NHI (67.9%), kecekapan penggunaan zat makanan, NUE (52.6%), dan kecekapan agronomik zat makanan, NAE (12.8 kg kg^{-1}). Kajian menunjukkan CRF dengan hanya 75% N digunakan (T4H) dapat meningkatkan hasil bijirin jika dibandingkan dengan CRF dengan 100% N dan 100% RDF dalam aplikasi pecahan konvensional petani. Oleh itu, CRF dengan aplikasi N sederhana mampu meningkatkan pengeluaran tanaman dengan peningkatan kecekapan N dan kenaikan kadar N tidak meningkatkan hasil dan kecekapan N. T4H CRF untuk padi tanah tinggi juga mampu meningkatkan kecekapan HI, N dan hasil padi tanah tinggi. Selain itu, semua parameter pertumbuhan dan hasil dipengaruhi secara positif oleh penggunaan CRF sebagai dos basal berbanding penggunaan berpecah baja urea konvensional.

Kata kunci: *Baja pelepasan terkawal, selulosa, padi tanah tinggi, aplikasi nitrogen, kecekapan penggunaan nitrogen*

TABLE OF CONTENT

		Page
DECLARATION		i
ACKNOWLEDEGEMNT		ii
ABSTRACT		iii
ABSTRAK		v
TABLE OF CONTENTS		vii
LIST OF TABLES		xiii
LIST OF FIGURES		xiv
LIST OF ABBREAVIATIONS		xviii
CHAPTER 1: INTRODUCTION		1
1.1	Study Background	1
1.2	Research Issues and Problem statement	7
1.3	Research Objectives and Research Questions	14
1.3.1	Research Objectives	14
1.3.2	Research Questions	14
1.4	Scope of the Study	15
1.5	Significance of the Study	16
1.6	Motivation of the Study	18
1.7	Chapter Summary	20
CHAPTER 2: LITERATURE REVIEW		21
2.1	Overview	21
2.2	Cellulose-based Hydrogels	21

2.3 Synthesis of Cellulose-based Hydrogels 22
2.3.1 Physical Crosslinking 23
2.3.2 Chemical Crosslinking 25
2.3.3 Dual-network Polymer 27
2.4 Key Characteristics of Agricultural Hydrogels 30
2.4.1 Bulk or Core Crosslinking 31
2.4.2 Surface Crosslinking 32
2.5 Categories of Cellulose-based Hydrogels 35
2.5.1 Carboxymethylcellulose (CMC)-based Hydrogels 35
2.5.2 Hydroxymethyl Cellulose (HEC)-based Hydrogels 37
2.5.3 Cellulose-Alginate-based Hydrogels 39
2.5.4 Cellulose-Starch-based Hydrogels 41
2.5.5 Cellulose-Chitosan-based Hydrogels 43
2.6 Cellulose-based Hydrogels as a Controlled-released Fertilizer 44
2.6.1 Controlled-release Fertilizer 44
2.6.2 Mathematical Models for Nutrient Release Profile 47
2.6.2.1 Nutrient Release Profile from Hydrogels 48
2.6.2.2 Nutrient Release Profile from Polymer Granules 51
2.7 Applications of Hydrogels in Agriculture 53
2.7.1 Controlled-release Fertilizer 53
2.7.2 Water Reservoir 56
2.7.3 Potting Medium 59
2.7.4 Pesticide Carriers 62
2.7.5 Hydrogel Baits 65

2.8 Rice 68

2.8.1 *Maswangi* (MRQ74) Mardi Rice Variety 69

2.8.2 Performance Evaluation of Cellulose Hydrogels CRF on the Rice Plants 70

2.8.2.1 Effects of Cellulose Hydrogels CRF on Growth Parameters 70

2.8.2.2 Effects of Cellulose Hydrogels CRF on Yield and Yield Component Data 70

2.8.2.3 Effects of Hydrogel CRF on Nutrient (N) Uptake and Nutrient Use Efficiency (NUE) 72

2.8.2.4 Correlation Regression Study 72

2.8.3 Nitrogen (N) 75

2.8.3.1. Nitrogen (N) in soils 75

2.8.3.2. The Importance of Nitrogen (N) in Rice Cultivation 77

2.8.2.3. Influencing Factors of Soil N Availability for the Rice Plants 78

2.9 Chapter Summary 80

CHAPTER 3: MATERIALS AND METHODS 82

3.1 Introduction 82

3.2 Summary of Methods Involved in the Research 83

3.3 Fabrication of Urea-loaded Cellulose Hydrogels 85

3.3.1 Chemical Reagents and Materials 85

3.3.2 Soil Properties 85

3.3.3 Extraction of Cellulose Fibers 86

3.3.4 Preparation of Cellulose Hydrogels 87
3.3.5 Sample Characterization 88
3.3.6 Swelling Ratio 89
3.3.7 The Soil Moisture Properties 89
3.3.8 Loading of Urea Determination 90
3.3.9 Release of Urea in Water and Soils 91
3.3.10 Release Kinetics of Cellulose Hydrogels 92
3.4 Greenhouse Experiments 92
3.4.1 Materials 92
3.4.2 Experimental Details 93
3.4.3 Rice Growth Performance 97
3.4.4 Yield and Yield Component Data 97
3.5 Analyses of Nitrogen (N) Uptake and Nitrogen Efficiency Estimation (NUE) 98
3.5.1 N Uptake and NUE 98
3.5.2 Correlation Regression Study 99
3.5.3 Degradation of Cellulose Hydrogels CRF 101
3.6 Statistical Analysis 101
3.7 Chapter Summary 101
CHAPTER 4: RESULTS AND DISCUSSION 103
4.1 Fabrication of Urea-loaded Cellulose Hydrogels as a Controlled Release Fertilizer 103
4.1.1 Fourier Transform Infrared Spectroscopy (FTIR): Spectra Analysis 103

4.1.2 Differential Scanning Calorimetry (DSC) 107
4.1.3 Morphology and Swelling Behaviors of Cellulose Hydrogels 108
4.1.3.1 Effects of Cellulose Concentrations 108
4.1.3.2 Effects of Various Concentrations of CMC 112
4.1.4 Effects of Cellulose Hydrogels on the Soil Moisture 116
4.1.5 Loading of Urea in Water and Soils 118
4.1.6 Release of Urea Water and Soils 119
4.1.7 Kinetic Studies of Urea Release 122
4.2 Evaluation and Fine-tuning the Loading Capacity and Release Rate of Fertilizer to Match the Needs of the Rice Plants 124
4.2.1 Rice Growth Performance 124
4.2.1.1 Plant Height (cm) 124
4.2.1.2 Number of Tillers 126
4.2.1.3 Leaf Chlorophyll Content (SPAD) 127
4.2.2 Yield and Yield Component Data 128
4.2.3 Harvest Index (HI) 132
4.3 Analyses of Nitrogen (N) Uptake and Nitrogen Efficiency Estimation (NUE) 133
4.3.1 N Uptake of the Rice Plants 133
4.3.2 Nitrogen Harvest Index (NHI) 135
4.3.3 Nitrogen Use Efficiency (NUE) 136
4.3.4 Agronomic Nitrogen Efficiency (NAE) 137
4.3.5 Dry Matter Partitioning 139

4.3.6 Correlation Regression Analysis 142

4.3.7 Degradation of Cellulose Hydrogels CRF 147

4.4 Chapter Summary 149

CHAPTER 5: CONCLUSIONS AND RECOMMENDATIONS 151

5.1 Conclusion 151

5.2 Recommendations for Future Research 154

REFERENCES 156

LIST OF PUBLICATIONS 215

APPENDICES 217

LIST OF TABLES

		Page
Table 1.1	Rice production by states, 2021 (Zainol Abidin, 2023)	8
Table 1.2	Land area and rice production in Sarawak	9
Table 2.1	Summary of the applications of chitosan-based hydrogels in agriculture	44
Table 2.2	Summary of hydrogel CRF applications on crops	71
Table 3.1	Composition of cellulose-based hydrogels	88
Table 3.2	List of treatments with different N fertilizers doses	96
Table 4.1	The parameters of diffusion Korsmeyer and Peppas model for urea release from C3 cellulose hydrogels in water and soil	122
Table 4.2	1000-grain weight (g) and percentage filled grain (% F) of different N treatments	131

LIST OF FIGURES

		Page
Figure 1.1	(a) Molecular structure of cellulose, and (b) intermolecular and intramolecular hydrogen bonding in cellulose (Acharya et al., 2021)	3
Figure 2.1	Graphical representation of physical crosslinking in hydrogel network (Xu et al., 2018)	2
Figure 2.2	Graphical representation of chemical crosslinking in hydrogel in hydrogel network (Xu et al., 2018)	25
Figure 2.3	Schematic representation of bulk or core crosslinking within materials (Behera & Mahanwar, 2019)	31
Figure 2.4	Schematic representation of the swelling and flow of solutions through the (a) un-crosslinked and (b) surface crosslinked hydrogel particles (Jockusch et al., 2009)	33
Figure 2.5	Graphical representation of CMC-based hydrogel crosslinked by PEDGE (Xiao et al., 2014)	36
Figure 2.6	Graphical representation of cellulose-based hydrogels using CMC/HEC and citric acid as crosslinker (Das et al., 2023)	38
Figure 2.7	Graphical representation on the fabrication of cellulose-alginate-based hydrogels (Martínez-Cano et al., 2022)	40
Figure 2.8	Graphical representation of starch-based superabsorbent hydrogel composite reinforces with cellulose nanocrystals (Olad et al., 2020)	42

Figure 2.9	Graphical representation on the formation of cellulose-chitosan-based hydrogel (Peers et al., 2020)	43
Figure 2.10	Classification of controlled-release fertilizers (CRF)	45
Figure 2.11	Schematic representation of encapsulated urea fertilizer system absorbing water and releasing nutrients to soil	47
Figure 2.12	Schematic representation of applying hydrogels CRF in soil	54
Figure 2.13	Hydrogels as water reservoir system for agricultural applications (Das et al., 2020)	57
Figure 2.14	Hydrogels as potting medium (Bashir et al., 2020)	60
Figure 2.15	Argentine ants feed from alginate hydrogel bead filled with toxic liquid bait (Merill et al., 2018)	66
Figure 3.1	Experimental design involved throughout the research	84
Figure 3.2	Graphical representation of pot experiments indicating pots were arranged in a block design	93
Figure 3.3	A group of the rice plants in pots	94
Figure 3.4	Locality map of experimental site at UNIMAS, Kota Samarahan (Google maps, n.d)	94
Figure 4.1	An ECH crosslinked cellulose hydrogel with CMC	105
Figure 4.2	FTIR spectra of (a) cellulose, and (b) an ECH-crosslinked cellulose hydrogel	106
Figure 4.3	DSC curve of C3 cellulose hydrogel	100
Figure 4.4	FESEM images of (a) cellulose and cellulose hydrogels at various cellulose concentrations (b) C1, (c) C2, (d) C3, (e) C4,	111

and (f) C5 cellulose hydrogels, and 1.75 % (w/v) CMC at 1000x magnifications

Figure 4.5 Maximum swelling percentage of cellulose hydrogels at varied concentrations (% w/v) of cellulose fibers. Different letters indicate significant differences ($p \leq 0.05$) between hydrogels. Error bars represent the standard deviations from triplicates (n=3) 112

Figure 4.6 FESEM images of cellulose hydrogels at various CMC concentrations (a) 1.75, (b) CMC2.0, (c) CMC2.5, (d) CMC3.0, (e) CMC3.5, (f) CMC4.0, and (g) CMC5.0 cellulose hydrogels, and 3.0 % (w/v) cellulose at 1000x magnification 115

Figure 4.7 Maximum swelling percentage of cellulose hydrogels consisted of various CMC concentrations (% w/v). Different letters indicate significant differences ($p \leq 0.05$) between hydrogels. Error bars represent the standard deviations from triplicates (n=3) 116

Figure 4.8 Soil moisture in different types of soils using C3 cellulose hydrogel. Different letters indicate significant differences ($p \leq 0.05$) between soils. Error bars represents the standard deviations from triplicates (n=3) 117

Figure 4.9 Loading capacity of C3 cellulose hydrogel. Error bars show the standard deviations from triplicates (n=3) 118

Figure 4.10	Release behavior of C3 cellulose hydrogel and free urea in water. Different letters indicate significant differences. Error bars show the standard deviations from triplicates (n=3)	121
Figure 4.11	Release behavior of C3 cellulose hydrogel and free urea in soils. Different letters indicate significant differences. Error bars show the standard deviations from triplicates (n=3)	121
Figure 4.12	Korsmeyer and Peppas model of urea release from C3 cellulose hydrogel in (a) water, and (b) soils	123
Figure 4.13	The rice plant growth (treated with T4H) from day 15 to 130	125
Figure 4.14	The effect of N level on the plant height (cm). Different letters indicate significant differences. Error bars represent the standard deviation from 5 replications (n=5)	125
Figure 4.15	The effect of N level on the number of tillers per plant. Different letters indicate significant differences. Error bars represent the standard deviation from 5 replications (n=5)	126
Figure 4.16	The effect of N level on the leaf chlorophyll content (SPAD) of the rice plant. Different letters indicate significant differences. Error bars represent the standard deviation from 5 replications (n=5)	128
Figure 4.17	The effect of N treatments on the number of panicles per plant, number of grains per panicle, grain, and straw yield. Different letters indicate significant differences ($p \leq 0.05$). Error bars represent the standard deviation from 5 replications (n=5)	131

Figure 4.18	Harvest index of rice with different N treatments. Different letters indicate significant differences ($p \leq 0.05$)	133
Figure 4.19	The effect of N levels on the N uptake of the rice plants. Different letters indicate significant differences ($p \leq 0.05$). Error bars represent the standard deviation from 5 replications (n=5)	134
Figure 4.20	The effect of N levels on Nitrogen Harvest Index (NHI) of the rice plants. Different letters indicate significant differences ($p \leq 0.05$). Error bars represent the standard deviation from 5 replications (n=5)	135
Figure 4.21	The effect of N levels on Nitrogen Use Efficiency (NUE) of the rice plants. Different letters indicate significant differences ($p \leq 0.05$). Error bars represent the standard deviation from 5 replications (n=5)	137
Figure 4.22	The effect of N levels on the Agronomic Nitrogen Efficiency (NAE) of the rice plants. Different letters indicate significant differences ($p \leq 0.05$). Error bars represent the standard deviation from 5 replications (n=5)	138
Figure 4.23	Dry matter accumulation in rice as influenced by N rates application over the crop growth stages.	140
Figure 4.24	Pattern of dry matter partitioning to different parts of rice as influenced by time course and nitrogen levels.	141
Figure 4.25	Linear relationship of grain yield with (a) number of grains per panicle, (b) panicle number/pot, (c) harvest index (HI) and	146

linear relationship of N uptake with (e) panicle number and (f) number of grains per panicle at $p < 0.05$**

Figure 4.26 Weight loss of cellulose hydrogels CRF during the degradation time throughout the rice cultivation period. Error bars show the standard deviation from 5 replications (n=5) 147

LIST OF ABBREVIATIONS

AGU	Anhydro-D-glucopyranose ring unit
%	Percentage
% F	Percentage filled
°C	Degree Celsius
3D	Three-dimensional
AAm	Acryl amide
AUL	Absorbency under load
AW	Alginate–waste papers
CA	Citric acid
CEN	European Standardization Committee
cm	Centimeter
cm^{-1}	Per centimeter
CMC	Carboxymethylcellulose
$CONH_2$	Amide
COOH	Carboxylic acid
CRF	Controlled-release fertilizer
CRP	Controlled-release pesticide
Cu	Copper
DAS	Days after sowing
DMSO	Dimethyl sulfoxide
DP	Degree of polymerization
DSC	Differential Scanning Calorimetry

ECH	Epichlorohydrin
ESFA	Extended Substance Flow Analysis
Fe	Iron
FESEM	Field Emission Scanning Electron Microscope
FTIR	Fourier Transform Infrared Spectrometer
g	Gram
g Kg^{-1}	Gram per kilogram
g pot^{-1}	Gram per pot
g/g	Gram per gram
h	Hour
ha	Hectare
HEC	Hydroxyethyl cellulose
HI	Harvest Index
HPMC	Hydroxypropyl methylcellulose
Kg	Kilogram
Kg Kg^{-1}	Kilogram per kilogram
m^3	Cubic meter
MARDI	Malaysian Agricultural Research and Development Institute
MBA	*N*, *N*, -methylene bis-acrylamide
MCA	Monochloroacetic acid
mg/Kg	Milligram per kilogram
mL	Milliliter
mm	Millimeter
Mn	Manganese

MRQ74	*Maswangi* MARDI Rice Variety
N	Nitrogen
N_2H_4CO	Urea
Na-CMC	Sodium carboxymethylcellulose
NaCl	Sodium chloride
NAE	Nitrogen Agronomic Efficiency
NaOH	Sodium hydroxide
NH_2	Ammonia gas (amino group)
NHI	Nitrogen Harvest Index
NPK	Nitrogen-Potassium-Phosphorus
NPS	Non-point source
NU	NaOH/urea
NUE	Nutrient/Nitrogen use efficiencies
OH	Hydroxyl group
P4VP	4-vinylpyridine
PAM	Polyacrylamide
PEGDE	polyethylene glycol di-glycidyl ether
PLA	Poly lactic acid
PPK	Area Farmers Organization
PVA	Polyvinyl alcohol
R^2	Coefficient of determination
RC	Regenerated cellulose
RDF	Recommended dose of fertilizers
rpm	Rotation per minute

SAH	Superabsorbent hydrogel
SFA	Substance Flow Analysis
SO_3H	Sulfonic acid
SRF	Slow-released fertilizer
T	Temperature
w/v	Weight per volume
wt %	Weight percent
Zn	Zinc

CHAPTER 1

INTRODUCTION

1.1 Study Background

Consumers, industry, and government have growing demand for products derived from renewable and sustainable resources that are biodegradable (Ahmed et al., 2022; Song et al., 2022), environmentally friendly (Luo & Zhang, 2013; Zainal et al., 2019), non-petroleum based (Dalmazzo et al. 2019), carbon neutral, and generate low environmental impacts and minimum human health and safety hazards (Bao et al., 2020; Arun et al., 2021). Cellulose, which is a highly biodegradable substance and nature's most abundant biopolymer, has promising potential as an alternative functional material for a variety of applications (Chang & Zhang, 2011; Etale et al., 2023).

Cellulose was first introduced by Anselme Payen in 1838 when he found a residue obtained from the acids and ammonia treatments on plant tissues and water extraction process (Khan et al., 2022). Cellulose is the primary component of plants and is found in the protective cell walls of plants, including stalks, stems, trunks, and all organic parts (Kabir et al., 2018; Dutta et al., 2019). In addition, animals, fungi, and a few bacteria also can produce cellulose (Dutta et al., 2019). Cellulose can be utilized in numerous forms including woods, natural textile fibers, panels, papers, packaging materials, and other industries (Alam et al., 2021). Further, cellulose is a stable polysaccharide that is resistant to hydrolysis by weak acids and bases, as well as the hydrolytic activity of enzymes, because the glycosidic linkages are not readily accessible from microorganisms and fungi.

For the past few years, new advanced materials derived from cellulose have been developed due to increasing demand for environmentally friendly and biocompatible materials (Kashmitha & Sunil, 2022). For instance, the modern-day agriculture system has evolved to employ cellulose-based materials as an effective approach to greener fertilizers. This is because, conventional agriculture is deemed as non-sustainable due to common farmers' fertilizer practices that use synthetic fertilizers which may intensify environmental pollution (Shennan et al., 2017; Kiliç et al., 2021). Therefore, ensuring a sustainable world from the agricultural perspective has motivated the usage of sustainable and biodegradable materials as an alternative. For this reason, much research has been focused on cellulose which offers veritable prospects for future survival.

The utilization of cellulose, a naturally occurring resource that is cheap and widely accessible, will be efficient and have greater economic appeal in practical ways, especially in the sustainable fertilizer industry. However, despite their promising potential for many applications, dissolution is a major concern when using cellulose due to their insolubility in water and other common solvents (Acharya et al., 2021). This is mainly attributed to their structural architecture which makes cellulose challenging to be processed (Figure 1.1).

Cellulose is a hydrophilic linear homopolymer and is made up of anhydro-D-glucopyranose ring unit (AGU) (Gupta et al., 2016; Dutta et al., 2019). Each unit is bonded via *ß*-1,4-glycosidic bonds between C_1 of one glucose ring and C_4 of another glucose ring (Sorieul et al., 2016; Baharin et al., 2019). Each AGU in the cellulose chains contains three reactive hydroxyl groups (-OH) per AGU, except at the terminal ends (Baharin et al., 2019). Within the cellulose chain, intermolecular and intramolecular hydrogen bonds held the -OH group of the AGU, the oxygen atom of AGU ring, and the glycosidic linkage to one another

(Gupta et al., 2016; Baharin et al., 2019). The cellulose molecule is stabilized by hydrogen bonds, which allow it to be functionally active biomolecule (Kamel et al., 2008; Sannino et al., 2009).

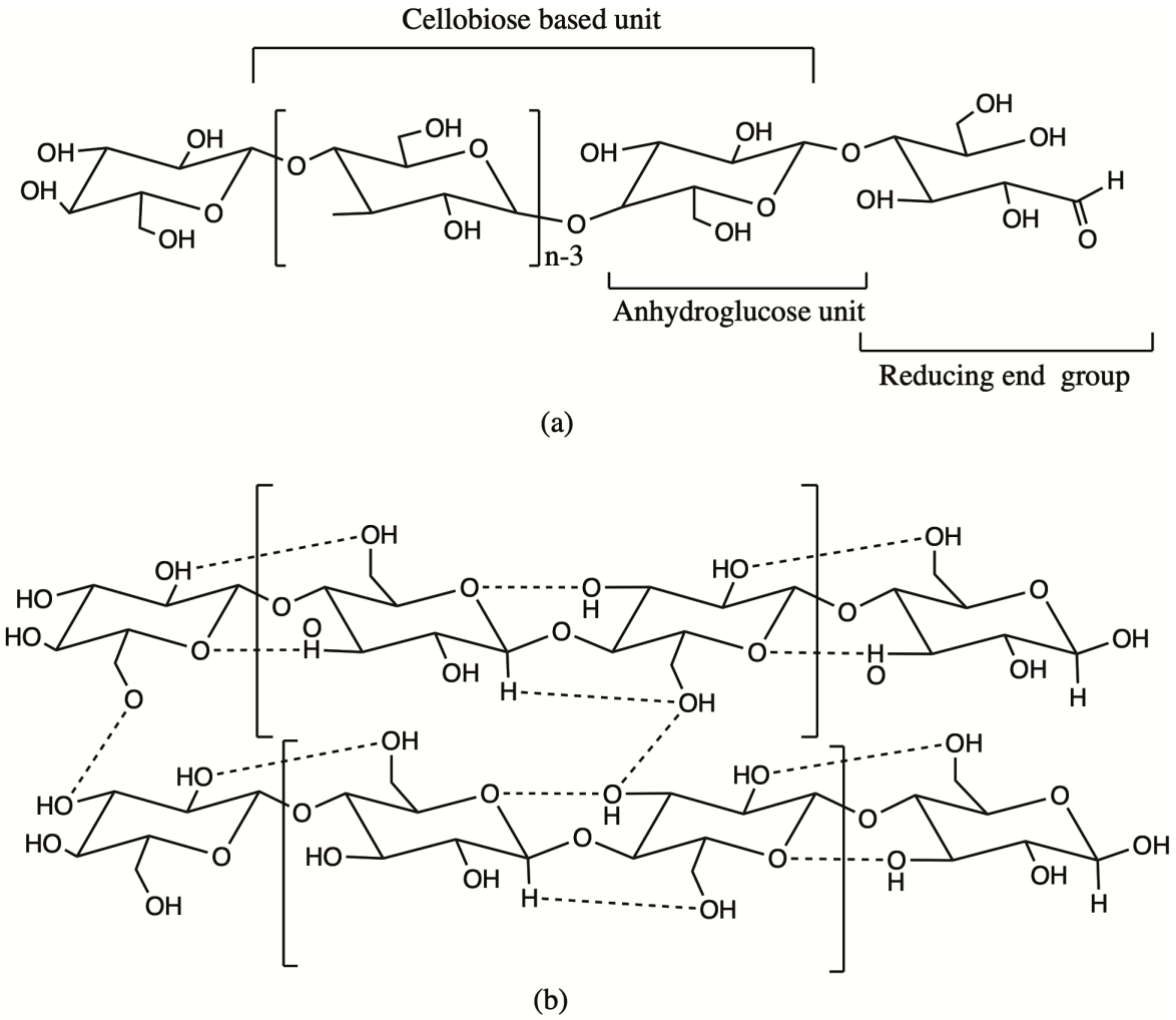


Figure 1.1: (a) Molecular structure of cellulose, and (b) intermolecular and intramolecular hydrogen bonding in cellulose (Acharya et al., 2021)

Furthermore, cellulose I or native cellulose is the natural form of crystalline cellulose and exists as cellulose I_α and cellulose I_β allomorphs (Poletto et al., 2014; Hindi, 2017). One of the main factors affecting the behavior of cellulose structure was the hydrogen bonding that existed within the repeating units of molecules. Besides, cellulose is densely packed due to the greater intermolecular and intramolecular hydrogen bonding which resulted in higher

crystallinity, thermal stability, and inhibition of thermal expansion (Hidaka et al., 2010; Poletto et al., 2014; Hangasky et al., 2020; Jospeh et al., 2022). Also, the cellulose behavior is significantly associated with different molecular weights resulting from their various resources (Qi et al., 2008).

In other words, higher molecular weight of cellulose will cause lower solubility in water and common solvents and lower the activation energy during cellulose dissolution (Shrotri et al., 2013; Chen et al., 2019; Acharya et al., 2021). In addition, cellulose is a highly crystalline polymer which reduces the accessibility of solvent into their networks (Acharya et al., 2021). Therefore, cellulose solubility is also influenced by the cellulose crystallinity which affects cellulose dissolution for high molecular weight cellulose (Lindman et al., 2010; Park et al., 2010; Parviainen et al., 2014). De-crystallization of cellulose might make it more soluble, facilitating solvent entry into their network and enabling cellulose dissolution (Park et al., 2010; Ghasemi et al., 2018).

Additionally, cellulose dissolution is attainable through non-derivatizing process by dissolving cellulose in the aqueous NaOH/urea solution and form a regenerated cellulose (RC), which is also known as cellulose-based hydrogel (Dutta et al., 2019; Zainal et al., 2019; Wang et al., 2021). The RC-based hydrogel is a green and sustainable material owing to its biocompatibility and biodegradability for better alternative in agriculture. For instance, controlled-release and slow-release media, water reservoir, seed germination medium, enhanced soil properties, and biosensors for agricultural purposes (Treesuppharat et al., 2017; Mohamed et al., 2022).

Furthermore, RC-based hydrogel is conveniently prepared because they are compatible with a wide range of polar and nonpolar solvents as well as compatible with other materials to increase the fabricated products (De France et al., 2020). The preparation of RC-based hydrogel may include a few steps including native cellulose dissolution, cellulose regeneration, crosslinking and drying. RC-based hydrogel can be prepared by two methods which are physical crosslinking and chemical crosslinking (Kabir et al., 2018; Fatima et al., 2021; Ul-Islam et al., 2021).

Generally, upon contact with water, RC-based hydrogels may absorb and retain a huge amount of water in their polymeric networks (Behera & Mahanwar, 2019; Wei et al., 2021; Ahmad et al., 2023). Their significant properties are exceptional physicochemical and hydrophilic properties, high swelling ratio and high compatibility (Thivya et al., 2022). Their compatibility with natural polymers is even more promising (Sun et al., 2020; Zhang & Huang, 2020; Amiri et al., 2021). In addition, the RC-based hydrogel will maintain their shapes even after swelling and absorbing a huge amount of water (Maitra & Shukla, 2014; Kundu et al., 2022; Thivya et al., 2022). Also, the RC-based hydrogel conserves their shape due to the intermolecular crosslinks which inhibit movement of polymer chains (Kundu et al., 2022; Thivya et al., 2022). For this reason, previous studies suggested that the absorbed water by RC cellulose-based hydrogel can be made readily accessible for plants especially in water-scarce region (Sanchita et al., 2010; Abd El-Wahid & Ali, 2013; Deshmukh & Hardaha, 2014; Maitra & Shukla, 2014).

Further, extensive research has shown the use of RC-based hydrogels as water reservoir in agriculture (Montesano et al., 2015; Abobatta, 2018; Saini et al., 2020). This is significant given that agriculture consumes over 70% of fresh water (Doungmanee, 2016;

D'Odorico et al., 2020; Heinke et al., 2020). The modern approach of water-deficit irrigation system may assist the agriculture sectors use water more efficiently. Hence, the agriculture sector can endure the rising need for fresh water. Not only that, but certain water-scarce area may be able to survive by incorporating cellulose hydrogels into their agricultural activities. RC-based hydrogels are also employed in agriculture as agrochemical releasers (Ranganathan et al., 2018; Hao et al., 2020; Ahmad et al., 2023).

As a result, cellulose hydrogels may facilitate plants obtaining sufficient nutrients according to their requirement (Kabir et al., 2018; Ahmad et al., 2023). Subsequently, excess nutrients and potential agrochemical waste could be minimized. Therefore, RC-based hydrogel is a green and sustainable alternative and might be suitable for potential use in agriculture. For these reasons, RC-based hydrogel could be potentially used as controlled-release fertilizer (CRF) as an advanced alternative to conventional fertilizers in modern agriculture.

Controlled-release fertilizer (CRF) contains plant nutrients encapsulated in their polymer networks which delay their availability for plant absorption and post-application usage (Trenkel, 2010). They allow sustained availability of nutrients to the plants significantly longer than 'rapidly available nutrient fertilizer', for instance, ammonium nitrate or urea, ammonium phosphate, or potassium chloride (Trenkel, 2010). The release of nutrients is controlled by the coating materials that encapsulate the nutrients (Lawrencia et al., 2021). Besides, CRF permits the release of nutrients in a controlled pattern and duration (Sempeho et al., 2014), which would be a huge advantage in agricultural applications.

In this study, a series of cellulose-based hydrogels were fabricated by crosslinking cellulose fibers extracted from waste papers and carboxymethyl cellulose (CMC) with epichlorohydrin (ECH). The fabrication process used NaOH/urea aqueous solution, eco-friendly, catalyst free and does not need any energy-intensive post-purification step rather than a simple water washing of the cellulose hydrogel. The cellulose fibers were derived from waste papers, because waste papers are readily available precursor materials, abundant and cheap, biocompatible, and non-toxic (Ahmad et al., 2023; Riseh et al., 2023).

Crosslinking of cellulose is essential to enhance the non-solubility, increase mechanical strength, stability, and rigidity of cellulose hydrogel. Cellulose-based hydrogels were developed and optimized for potential use as a controlled-release fertilizer for upland rice. After, the optimized cellulose-based controlled-release fertilizers hydrogels (CRF) were evaluated and fine-tuned to match the needs of the rice plants. The effects of cellulose based CRF hydrogels on the growth performance and yield of upland rice was studied extensively. Also, the effect of cellulose based CRF hydrogels on the nitrogen uptake and nitrogen use efficiencies (NUE) on upland rice was determined.

1.2 Research Issues and Problem Statement

In Malaysia, rice is normally cultivated either as wet paddy (Peninsular Malaysia) or upland rice (Sabah and Sarawak). Under wet paddy cultivation, rice production has been reduced from 1.80 million tons in 2017 to 1.51 million tons in 2021 (Zainol Abidin, 2023). As shown in Table 1.1, the largest production area for paddy cultivation is in Kedah, followed by Sarawak, Kelantan, and Perak (Zainol Abidin, 2023).

Sarawak state opened more than 83,143 hectares of land for paddy cultivation (Table 1). However, Table 1.1 shows that the rice production in Sarawak is the lowest, amounting

to only 1.79 ton ha^{-1}. The low rice production in Sarawak has reduced the national average of rice production in Malaysia (Zainol Abidin, 2023).

Table 1.1: Rice production by states, 2021 (Zainol Abidin, 2023)

States	Production area (ha)	Production (tons)	Productivity (ton/ha)
Johor	2505.00	9,031.00	3.61
Kedah	214,945.00	907,076.00	4.22
Kelantan	74,972.00	333,829.00	4.45
Melaka	3,462.00	10,287.00	2.97
N. Sembilan	1,480.00	4,662.00	3.15
Pahang	13,497.00	37,817.00	2.80
Perak	74,949.00	244,397.00	3.26
Perlis	60,478.00	256,034.00	4.23
Pulau Pinang	24,210.00	136,919.00	5.66
Selangor	35,885.00	155,631.00	4.34
Terengganu	19,601.00	72,023.00	3.67
Peninsular Malaysia	**525,984.00**	**2,167,706.00**	**4.12**
Sabah	38,732.00	112,284.00	2.90
Sarawak	83,143.00	148,903.00	1.79
Malaysia	**647,859.00**	**2,428,893.00**	**3.75**

Upland rice cultivation is generally performed by rural communities, particularly in Sarawak (Sinton 1t al., 2019). It is still a significant agricultural activity for household consumption, and farmers occasionally sell their surplus to generate income (Hanafi et al., 2009; Sinton et al., 2019). Table 1.2 shows land area the upland rice production in Sarawak, located at Batang Lupar, in Sri Aman Sarawak. Batang Lupar is one of the twelve granary areas in Malaysia (Zainol Abidin, 2023). It can be observed that, between 2017 and 2021, upland rice production did not differ significantly. The upland rice cultivation area was the same from 2017 to 2021 at 1,121 ha, but there was 10.5% increase in production in 2021compared to the previous year. The upland rice production is slightly increase from 2,252 tons in 2017 to 3,220 tons in 2021. However, the upland rice production is still below the target of 6 ton/ha (Zainol Abidin, 2023).

Table 1.2: Land area and rice production in Sarawak

Year	2017	2018	2019	2020	2021
Land area (ton ha^{-1})	1,121	1,121	1,121	1,121	1,131
Rice production (ton ha^{-1})	2,252	2,794	3,087	2,913	3,220

Upland rice cultivation system is perceived as non-sustainable due to how the system is being governed and common farmers' fertilizers practices (Wang et al., 2021). Upland rice varieties have not been largely commercialized due to their low grain yields (Wang et al., 2021). However, the low grain yields upland rice is caused by the poor management of farmer during the cultivation period, weed infestation, insect-pest attack, lack water availability and lack mineral supply (Wang et al., 2021).

Chemical fertilizers, herbicides, and insecticides are currently used in upland rice cultivation (Hu et al., 2016; Shennan et al., 2017). Chemical fertilizers are most preferred by farmers to increase agricultural productivity (Ali et al., 2021; Zhu et al., 2020). However, the long-term use and excessive usage of chemical fertilizer has generated non-point source (NPS) contamination, environmental degradation, and ecosystem disruption (Shen et al., 2012; Chen et al., 2018; Li et al., 2019; Kiliç et al., 2021).

Moreover, water quality has also been degraded because of fertilizers leaching from common farmers' practices (Shennan et al., 2017; Tal, 2018; Alcamo, 2019; Cueff et al., 2020). Water of irrigation from any sources will be supplied to the crops which concurrently hoisting the contaminants and chemicals elicited from fertilizers (Alcamo, 2019). Following that, the water from the irrigated cropland will drain back to the stream and freshwater bodies, bringing with it the elicited chemical fertilizers and contaminants (Gil-Ortiz et al., 2020; Messiga et al., 2020; Ahmad et al., 2023).

Whereas nitrogen (N) is a critical component that influences upland rice growth and productivity (Kichey et al., 2007; Momesso et al., 2020). Urea is the most often used nitrogen (N)-based fertilizer due to its high N content and low cost (Xiaoyu et al., 2013; Versino et al., 2019; Gil-Ortiz et al., 2020). Farmers used a lot of N to increase rice output. However, less than 33% of N absorbed by plants, indicating that nearly two-thirds of the inputs are lost to the environment as carbon dioxide and due to poor plant absorption, heavy leaching, and surface run-off (Tang et al., 2019; Li et al., 2019; Zhu et al., 2020; Ahmad et al., 2023).

Other studies found that farmers' fertilizer practices in rice cultivation resulted in low nutrient use efficiency and approximately 50% of nutrients loss to the environment due to heavy leaching, surface run-off, volatilization, denitrification, and undesirable organic

compounds in the soil (Li et al., 2019; Versino et al., 2019; Lawrencia et al., 2021; Ahmad et al., 2023). Fertilizer losses not only have substantial environmental repercussions, but they may also result in poor harvests and significant financial losses (Cameron et al., 2013). Furthermore, fertilizer split application and frequent dosage may induce concentration fluctuations between ineffective and toxicity levels, affecting the growth of the rice plants (Lawrencia et al., 2021). Therefore, there is an urgent need to prevent fertilizer loss by increasing fertilizer utilization efficiency. A promising approach to addressing the aforementioned challenges is the encapsulation of fertilizers in superabsorbent hydrogels as controlled-release fertilizers (CRF) to improved fertilizer efficiency by minimizing fertilizer loss by leaching, frequent dosing, cost effectiveness, extending nutrient supply for a longer period, and minimize pollution for the environment.

However, there is another prominent issue with the CRF that is currently accessible on the market. The available CRF is costly due to the high cost of coating materials and the complex manufacturing process (Abobatta et al., 2018; Lawrencia et al., 2021). The costs of these CRF are around 3-8 times higher than the cost of common fertilizers, limiting their broad application in agriculture (Zhao et al., 2013). As a result, their prospective application is limited to high-value crops to minimize fertilizer loss due to leaching, dosing frequency and irrigation frequency (Naruetharadhol et al., 2022; Roth et al., 2023). Unless and until the expenses are significantly reduced, CRF applications are limited to the government and other well-funded organizations, leaving out the individual farmers and agriculturists who could gain from its prudent usage.

In addition, the currently available CRF in the market are made of petroleum based-synthetic polymers such as starch-polyacrylonitrile based materials, vinyl-alcohol acrylic

acid-based materials, and acrylamide-based materials (Abobatta, 2018; Li et al., 2020; Lawrencia et al., 2021). Therefore, their application in agriculture may have major environmental repercussions due to their toxicity (Elsayed, 2019; Sennakesavan et al., 2020; El Sayed, 2023). After the fertilizers are released, their carriers may be hazardous to the environment since they are not easily biodegradable and may accumulate in the soil over time (Lawrencia et al., 2021; El Sayed, 2023). Consequently, soil deterioration and contamination of surface water by agrochemicals due to surface run-off or transfer of undesired contaminants on eroded soil may occur (Cueff et al., 2020). Furthermore, the release characteristics of CRF developed by other countries might not work best under our local soil and weather conditions. Thus, there is an urgent need to develop cost-effective and eco-friendly CRF from our locally available cellulosic waste and could meet the growing needs for our local paddy under the local soil and weather conditions.

Further, waste papers are critically seen as a prominent issue with serious environmental repercussions. According to data suggest, Malaysian produce more than 55,000 tons of paper and waste papers every month, which can occupy 456,000 m^3 of landfill space (Zainal et al., 2019). Waste papers are thought to constitute most of the municipal solid waste produced each year (Yong et al., 2019; Zainal et al., 2019). This may increase environmental problems including flash floods and stagnant pools where mosquitoes thrive due to winding up in drains and water ways (Yong et al., 2019). Consequently, various issues such as sickness, landslides, and traffic congestion may occur.

One feasible strategy to reduce the number of waste papers discarded at landfill is by increasing paper recovery rate, which is still low in Malaysia (less than 40%) (Zainal et al., 2019). Waste papers have received a lot of attention as an important part of solid waste.

Further, the growing demand for cellulosic substances, the concerns about deforestation, the development of environmental laws and policies, and the interest in lowering production costs have made waste papers recycling more appealing (Monte et al., 2008; Sabazoodkhiz et al., 2017; Amiri et al., 2019).

Waste papers are recycled by passing them through a paper recycling mill machine, which produces various recycled paper grades (Scheel et al., 2019). However, when the number of recycling times increased, this method could damage lignocellulosic or cellulose fibers by reducing their length (Kermanian et al., 2013) and increase the fines content of fibers. Consequently, the large fines of fibers would impair the structure of the paper by lowering interlocking of the paper web, decreasing the drainage of water from paper web, and therefore increasing production costs (Min et al., 2015; Scheel et al., 2019). Generally, most paper recycling mills segregate fiber fines residues from the process and wastewater to improve the process and product quality (Min et al., 2015; Scheel et al., 2019). These segregated fiber fines residues are considered waste, and their disposal is a serious environmental concern (Min et al., 2015). Given the concerns, it could be more advantageous to use waste papers to generate value-added cellulosic products that are both inexpensive and environmentally friendly. Due to available resources, waste papers containing cellulose can be used as a starting precursor to fabricate cellulose-based hydrogel for agricultural usage, potentially reducing environmental issue (Ahmad et al., 2023).

1.3 Research Objectives and Research Questions

Considering the discussion in the preceding parts, this section presents the research objectives and research questions for this study. Research objectives are divided into main objective and specific objectives, followed by the formulation of main research questions and specific research questions.

1.3.1 Research Objectives

The main objective of this study is to fabricate and develop an eco-friendly cellulose-based hydrogels from waste papers for agricultural application. The specific objectives of this study are as follows:

1. To synthesize and characterize cellulose-based hydrogels CRF from waste papers.
2. To investigate the loading and release capacity, as well as the release kinetics of urea-loaded cellulose-based hydrogels in water and soils.
3. To analyze and optimize fertilizer loading capacity and release rates in accordance with the rice plant requirement, as well as studying the effect of cellulose hydrogels on the growth performance and yield of upland rice in Sarawak.
4. To investigate the effects of cellulose-based hydrogel CRF on nitrogen (N) uptake and nitrogen use efficiency (NUE) of upland rice in Sarawak.

1.3.2 Research Questions

Correspondingly, the following research questions have been developed:

1. Would it be possible to fabricate eco-friendly cellulose-based hydrogels CRF from waste papers as an advanced material for agricultural application?

2. What is the loading and release capacity of urea-loaded cellulose-based hydrogels in water and soils?
3. Could cellulose-based hydrogel CRF improve upland rice growing performance and yield of upland rice in Sarawak?
4. Could cellulose-based hydrogel CRF improve upland rice nitrogen uptake and nitrogen use efficiency (NUE) of the upland rice?

1.4 Scope of the Study

It is common to set the scope of the study to ensure that the objectives specified in the previous section can be achieved in examining the extend of cellulose-based hydrogel CRF performance in upland rice cultivation. To achieve the research objectives, this study has been divided into two phases – Phase 1 for the research and development of cellulose-based hydrogel CRF, and Phase 2 for the quantitative research design on upland rice cultivation. Phase 1 is conducted to achieve the first two research objectives formulated earlier. In Phase 1 of this study, it focuses on the fabrication and development of cellulose-based hydrogel CRF, i.e., an optimized cellulose-based hydrogel CRF and its influencing factors. Several parameters were evaluated including the surface morphology of cellulose-based hydrogel, the swelling capacity, soil moisture properties, and loading and release of fertilizers from cellulose-based hydrogel CRF. Further, a cellulose-based hydrogel was characterized using several instrumentation techniques including Fourier transform infrared (FTIR) spectrometer, field emission scanning electron microscope (FESEM), differential scanning calorimetry (DSC), Kjeldahl procedure and the Nessler method. The optimized cellulose-based hydrogels CRF were administered in field study for upland rice cultivation to evaluate their performance.

In Phase 2, quantitative research involving a mini field trial for growing upland rice was conducted to achieve the remaining research objectives. The field trial was conducted in a mini greenhouse using the optimized cellulose-based hydrogel CRF developed in Phase 1 for growing upland rice. Several studies provided general recommendations on the amount of N fertilizers applied to grow the rice plants according to farmers' fertilizer practices in split application. Therefore, different treatments of N fertilizers and recommended dosage fertilizers (RDF) in single basal application and in split application were applied to fine tune the loading capacity and release rates of fertilizer to match the needs of upland rice. The N uptake and N use efficiencies of upland rice were also determined.

The analysis of results and findings of this study were restricted to the application of cellulose-based hydrogel CRF for upland rice cultivation in Sarawak context. The interpretation of the results must be wisely and carefully applied in another context. It is also unreasonable to generalize the findings of this study to other cultivation in agriculture.

1.5 Significance of the Study

This study is important for the agricultural sector in various ways. First, it contributes to the body of knowledge as an additional know-how to the literature towards the understanding of the extend of cellulose-based hydrogel CRF on the agricultural sector. There were limited literatures reported on the preparation and characterization of regenerated cellulose hydrogels derived from solid municipal waste and their applications in agriculture. As far as Malaysian government is concerned, conventional agricultural sector is regarded as non-sustainable subjected to farmers' fertilizers practices and how it is being governed. As this study examines on the influencing factors determining the optimization of cellulose-based hydrogels, particularly for agricultural applications, these factors are established as a

contribution to the body of knowledge as well as agricultural sector. Therefore, this work might provide insights into the fundamental principles of utilizing abundantly available resources towards developing a feasible sustainable alternative for agricultural applications.

Second, despite the recognized application of cellulose-based hydrogel CRF in agriculture, which has been investigated in isolated research and academic papers, cellulose-based hydrogel CRF continue to struggle to find widespread applications in agriculture, particularly upland rice production. Rice production is significantly influenced by the availability of N fertilizers. A major concern evolved as only half of the recommended dose of fertilizers can be absorbed properly by the rice plants due to leaching and surface run-off. This resulted in poor growing of the rice plants, low rice production, and poor quality of rice grains due to insufficient amount of nutrient absorbed by the rice plants. This resulted in excessive use of fertilizers as most farmers tend to increase the fertilizer inputs to meet the needs of the rice plants and generate more yields and in fact, resulted in a lot more fertilizers leached from the soil. It will be costly to apply such unnecessary amounts of fertilizer to compensate for fertilizer loss that should be absorbed by the rice plants. Therefore, cellulose-based hydrogels act as a controlled-release fertilizer, which is an important strategy for improving fertilizer use efficiency by limiting nutrient loss through leaching and minimizing potential environmental repercussions. The application of developed functional materials for fertilizer use potency may become necessary throughout the time to increase fertilizer use efficiency and rice production.

Third, cellulose-based hydrogel CRF may improve growth performance of the rice plants and grains and increase rice productivity. Currently, rising food demand has led to a mass agricultural practice, whereas crops productivity and quality is one of the major

concerns for farmers. However, poor management of nutrients and ignorance of the Liebig's Law of Minimum serves as a hurdle in efforts to increase rice production. Cellulose-based hydrogels as a carrier for agricultural inputs could enhance nutrient uptake by the rice plants with sufficient nutrients availability over longer period. This promotes healthier growing of rice and improves rice grains quality and productivity. Furthermore, rice self-sufficiency in Malaysia remains a major concern, hovering around 70% from 2008 to 2017. For this reason, they may contribute and are in line with the National Agriculture Policy, from which the government intends to increase rice self-sufficiency in Malaysia up to 75% by 2025 and 60% by 2030 in Sarawak to ensure food security for people.

1.6 Motivation of the Study

This study is conducted to identify the root causes from which research designs in Phase 1 and Phase 2 were developed to find answer to uncertainties and fill in the research gaps. Studies are conducted because there are uncertainties about a phenomenon that either has or has not occurred. In this study, it is well acknowledged that farmers' fertilizer practices in rice cultivation resulted in low nutrient efficiency and approximately half of nutrients loss to the environment due to heavy leaching, surface run-off, volatilization, denitrification, and undesirable organic compounds in the soil (Li et al., 2019).

These phenomena might lead to various issues including substantial environmental problems and excessive use of conventional fertilizers which may cause spike in toxicity levels in both plants and soils (Cameron et al., 2013; Lawrencia et al., 2021). Subsequently, biodiversity might be substantially affected and may lead to biodiversity imbalance. Not only that, but conventional farmers' fertilizer practices may also result in poor harvest and

significant financial loss (Cameron et al., 2013). Therefore, there is an urgent need to minimize fertilizer loss by increasing fertilizer use efficiency.

For these reasons, this study aims to employ a systematic research method to solve problems by conducting a deep analysis and studies of relevant factors. The performance of cellulose-based hydrogel CRF in upland rice cultivation forms an important part of the evaluation to ensure that the results obtained from this study are reasonable and reliable which are supported by the quantitative and qualitative data (both in Phase 1 and Phase 2). The process also involves designing the relevant research method employed, collecting, and describing data, making data analysis and reporting data. Thus, research might find answers that resolve the uncertainties of problems as previously discussed. Further, this study is conducted to establish, by analyzing the performance of cellulose-based hydrogel CRF in upland rice cultivation, whether the CRF formulations enhanced the growth of the rice plants and met the needs of the rice plants, thus fulfilled the gaps in this study.

This study also explores the introduction of a novel approach of administering cellulose-based hydrogel CRF as a greener alternative to conventional farmers' fertilizer practices, i.e., in upland rice cultivation. This is because, how the upland rice cultivation system is being governed with conventional practices has led to many issues. For instance, non-point-source (NPS) contamination, environmental degradation, and ecosystem degradation (Li et al., 2019). For these reasons, the administration of an eco-friendly cellulose-based hydrogels CRF is a novel approach to cater the root causes, i.e., low absorption and low fertilizer use efficiency by the rice plants from conventional farmers' fertilizer practices. Therefore, fertilizer losses could be minimized, while rice production and profits for farmers could be increased. In addition, the introduction of cellulose-based

hydrogel CRF for upland rice cultivation in Sarawak is a kind of novelty in this study. This is because, no study reported any application of cellulose-based hydrogel CRF in rice cultivation in Sarawak.

1.7 Chapter Summary

This chapter began by describing the background research on the cellulosic materials used to create a value-added novel functional material, i.e., in this study, cellulose-based hydrogels for agricultural applications. It went on to suggest extracting cellulose using waste papers as precursor materials, which are inexpensive and abundantly available. Research issues and problems have been identified and thoroughly discussed.

After, research objectives and research questions have been formulated to address the issues and problems. This chapter also includes the scope of the study, significance of the study, and motivation of the study.

CHAPTER 2

LITERATURE REVIEW

2.1 Overview

The previous chapter provides insights on the introductory explanation on the background of study, research issues and problems, research objectives and research questions, as well as significance contribution of the study. This chapter reviews past literature related to the study. Section 2.2 provides an overview of cellulose-based hydrogels and section 2.3 explains the synthesis of cellulose-based hydrogels which were used to explore the method of preparation of cellulose-based hydrogels used in this study. Next, section 2.4 offers a review of prior literature which focuses on the key characteristics of agricultural hydrogels. Section 2.5 describes the categories of cellulose-based hydrogels for agricultural applications. As this study examined the nutrient release profile of cellulose-hydrogels, review of past literature related to this area is presented in section 2.6. In line with the advancement of functional hydrogels, their increasing adoption in agriculture and the insights into the use of hydrogels as advanced functional materials are presented in section 2.7. Following the review of the use of hydrogels in agriculture, section 2.8 reviews the studies of rice variety used in this study. Section 2.8 also includes prior studies on the performance evaluation of hydrogels on crops.

2.2 Cellulose-based Hydrogels

Cellulose-based hydrogels are three-dimensional (3D) network structures made of highly crosslinked linear or branched hydrophilic cellulosic polymer chains (Kabir et al., 2018; Behera & Mahanwar, 2019; Ahmad et al., 2023). Upon contact with water, cellulose hydrogels may absorb and retain large amounts of water in their polymeric networks,

swelling up to 99% (Behera & Mahanwar, 2019; Wei et al., 2021; Ahmad et al., 2023). Furthermore, cellulose hydrogels may retain their polymeric networks stable even in swollen state (Guilherme et al., 2015).

These characteristics are significantly associated with the presence of polar hydrophilic moieties, such as SO_3H, OH, NH_2, COOH and $CONH_2$ (Zainal et al., 2021; Khan et al., 2022). These characteristics also assure the stability of cellulose hydrogels in various mediums and environments due to physical or chemical entanglement in the structures of cellulose hydrogels polymer chains (Guilherme et al., 2015; Berradi et al., 2023). Many hydrogels are developed for specific applications such as transdermal drug delivery, wound dressing, and contact lenses (Berradi et al., 2023). In addition, hydrogels have been utilized in agriculture as water reservoir, soil conservation, drought stress relief, and controlled release fertilizer (Lawrencia et al., 2021; Berradi et al., 2023).

2.3 Synthesis of Cellulose-based Hydrogels

Crosslinking can be categorized as chemical crosslinking, physical crosslinking, or both, simultaneously (hybrid) (Guilherme et al., 2015; Bashir et al., 2020; Zainal et al., 2021; Liu et al., 2022). Crosslinking is a process of stabilization that allows multidimensional extension of polymeric chain, resulting in a network structure (Maitra & Shukla, 2014). In other words, crosslinking can occur by the polymerization of monomers with two or more functional groups (Maitra & Shukla 2014). Crosslinking is governed by covalent bonds, hydrogen bonding, van der Waals interactions, mechanical interlocking and other physical entanglement (Nath et al., 2023).

The crosslinking process is important for improving the solubility, stability, thermostability and glass transition temperature of polymer network, as well as increasing mechanical strength and molecular weight. Moreover, crosslinking may enhance the swelling, rigidity, elasticity, viscosity, permeability and stiffness of the polymer networks (Maitra & Shukla, 2014; Zainal et al., 2021). The resulting crosslinking structure is critical in determining the major characteristics and properties of cellulose-based hydrogels that are best suited for specific applications (Zainal et al., 2021).

In terms of synthesis method, crosslinking is of two kinds: *in-situ* crosslinking and post-crosslinking (Mane et al., 2016). *In-situ* crosslinking is a direct crosslinking method between functional monomer and crosslinker that results in a macromolecular chain of polymer. Post-crosslinking, on the other hand, is a process of crosslinking that occurs after polymerization (Niu et al., 2015, Mane et al., 2016).

2.3.1 Physical Crosslinking

Physically crosslinked hydrogels (Figure 2.1) are also known as reversible or physical gels (Konieczynska & Grinstaff, 2017). It is formed by molecular entanglement and/or secondary forces including ionic interactions, hydrophobic interactions, hydrogen bonding interactions, crystallization, stereo-complexation and supramolecular chemistry (Ullah et al., 2015; Parhi, 2017). Physical crosslinking is a reversible process that occurs as a result of conformational changes caused by physical, chemical, or biological stimuli (Ullah et al., 2015; Parhi, 2017).

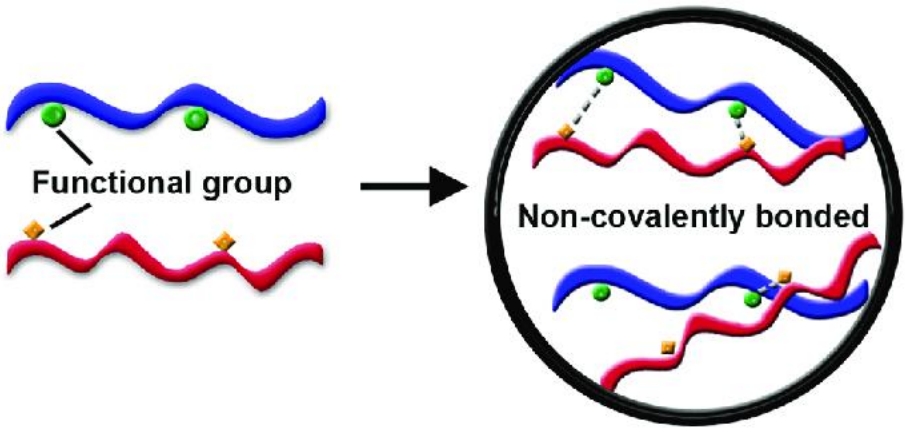


Figure 2.1: Graphical representation of physical crosslinking in hydrogel network (Xu et al., 2018)

Examples of physical stimuli include change in temperature, pressure, light intensity, electricity, magnetic field, stress and solvent composition (Mane et al., 2016). Meanwhile, chemical or biochemical stimuli include change in pH, ions and specific chemical compositions (Mane et al., 2016). This means that once the triggers are removed, physically crosslinked hydrogels may return to their initial state.

Beside, physical crosslinking may produce hydrogels that are insoluble in aqueous solutions (Maitra & Shukla, 2014). This means with physical crosslinking, solubilization is not possible because water can enter without disrupting or breaking the strong interaction that binds the polymer chains. Furthermore, dissolution is prohibited by physical interactions between different polymer chains (Kabir et al., 2018). As a result, physically crosslinked hydrogels can hold and retain an unaltered 3D polymeric network structure during swelling (Kabir et al., 2018). This can be achieved by crystallization using the freeze-thaw cycle technique (Bustamante-Torres et al., 2021; Xu et al., 2023).

In freeze-thaw cycle, cryogenic treatment is used by the association of strong hydrogen bond. The strong hydrogen bond could be formed during one of the freeze-thaw

stages, which include freezing of the initial system, storing the samples at a very low temperature, or thawing the frozen sample. Guan et al. (2014) recently reported on the preparation of novel superabsorbent cellulose-based hydrogels by repeating the freeze-thaw cycle, which produced physically chain packing in the polymer chains. Furthermore, a phase separation caused the formation of a densely packed structures from multiple freeze-thaw process, resulting in high mechanical strength and thermal stability. This technique has been reported in other studies including Dai et al. (2017) and Ahmad et al. (2023). In addition, hydrogels prepared using physical crosslinking have been reported in other studies (Chen et al., 2015; Cao et al., 2018; Yang et al., 2021; Bai et al., 2022). state.

4.3.2 Chemical Crosslinking

Chemical crosslinking (Figure 2.2) refers to intermolecular and intramolecular joining of two or more molecules through a covalent bond (simultaneously or post polymerization) in which hydrogen bonding will be replaced by a stronger and stable covalent bond (Ullah et al., 2015; Arora et al., 2017; Xu et al., 2018).

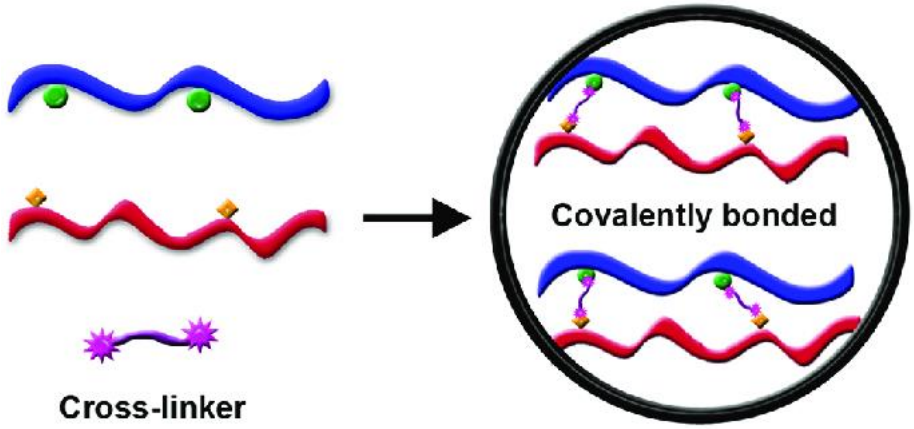


Figure 2.2: Graphical representation of chemical crosslinking in hydrogel network (Xu et al., 2018)

There are several methods that can be used to prepare chemical crosslinking, including aqueous solution polymerization, inverse-phase suspension polymerization and microwave irradiation polymerization (Guilherme et al., 2015; Bustamante-Torres et al., 2021). Chemically crosslinked hydrogels are made using both natural (i.e., cellulose, chitosan, hyaluronic acid, collagen, fibrin) and synthetic materials (i.e., polyacrylic acid, polyethylene glycol, polyvinyl alcohol, polyphosphazene, polypeptide) (Konieczynska & Grinstaff, 2017).

Moreover, chemically crosslinking produced permanent gels that are irreversible due to configurational changes (Ullah et al., 2015; Bustamante-Torres et al., 2021). Chemical crosslinking also produced hydrogels with high mechanical strength, making them more resistant to heat and pressure (Mane et al., 2016). Further, chemically crosslinked hydrogels have a better water absorption capacity than physically crosslinked hydrogels (Nasution et al., 2022; Ahmad et al., 2023). This is due to the chemical crosslinking process breaking the compact chain packing in cellulose, resulting in increased movability of macromolecules and hydrophilicity (Salleh et al., 2018).

However, it is important to note that the prepared hydrogels must be able to maintain and retain their structure without bursting upon swelling, therefore, hydrogels must have excellent strength and stability. According to studies, excessive swelling capacity may do considerable harm to the mechanical properties of hydrogels in some circumstances because they cannot withstand stress from intense swelling (Gupta & Shivakumar, 2012; Guilherme et al., 2015). This is significantly associated with permanent and irreversible damage of hydrogels due to ruptured covalent bonds when hydrogels break (Lawrencia et al., 2021). For this reason, researchers regarded this as a significant disadvantage of chemically

crosslinked hydrogels. Previous studies have reported using chemical crosslinking to make hydrogels, including Han et al. (2020), Lawrencia et al. (2021), and FitzSimons et al. (2022).

2.3.3 Dual-network Polymer

Over the past century, significant progress has been achieved in developing fancy hydrogels with better properties for the intended applications. However, there is a major concern in preparing hydrogels using solely physical crosslinking or chemical crosslinking. Chemically crosslinked hydrogels are tough but damage-irreversible, whereas physically crosslinked hydrogels are damage-recoverable, nonetheless, the resulting hydrogels have poor mechanical strength (Xin, 2022).

For this reason, researchers have devised another mechanism, namely dual-networks or double-network polymer hydrogels (Ullah et al., 2015; Ning, et al., 2022; Xin, 2022). Dual-networks polymer was developed by combining chemically-physically crosslinked hydrogels (Ullah et al., 2015), dual physically crosslinked hydrogels (Yuan et al., 2016; Xu et al., 2018) and dual chemically crosslinked hydrogels (Chen et al., 2015) with enhanced and coupled mechanical properties (Ullah et al., 2015).

According to research, dual-networks polymers are ideal for gradual drug release, drug delivery carriers, wound dressing and tissue scaffolding (Ning et al., 2022; Xin, 2022). This is because the hydrogels made from single mechanism tend to have poor strength and toughness, limiting their development (Ullah et al., 2015). Moreover, a few mechanical properties of common hydrogels are inconvenient for possible applications (Ullah et al., 2015).

One of the major problems is, the crosslinking points in their polymeric networks have soft flexibility but muscular rigidity (Ullah et al., 2015). This will cause lower buffering

effect and damage the hydrogels due to stress impact. Next, the hydrogels have a poor flexible crosslinking force, hence they may not be able to expand but retain their shape, i.e., in their swollen state, and are difficult to cover after deformation (Ullah et al., 2015). Third, hydrogels are unable to disperse energy effectively due to insufficient dissipation capacity, which may damage their networks (Ullah et al., 2015).

Therefore, researchers have focused on developing hydrogels with great mechanical strength and toughness using dual-networks polymers. They use of a dynamic covalent bond in chemical crosslinking and the stability of physical crosslinking to enhance the mechanical properties of hydrogels for various applications (Ullah et al., 2015). The idea is to use step-by-step approaches in the preparation of hydrogels (Ullah et al., 2015). The first step is highly crosslinked polymeric network but poor mechanical properties, followed by a second step of loosely crosslinked polymeric networks to fill the first structure's internal gap (Ullah et al., 2015).

The dual-networks technique will enhance the stability, strength and mechanical properties of hydrogels while preserving their original properties (Beckett et al., 2020). Hydrogels, for instance, as a controlled release fertilizer system, require long-term stability, nevertheless, hydrogel polymers often have poor strength and toughness due to chemical crosslinking (Beckett et al., 2020). Therefore, reinforcement is necessary to maintain structural stability of hydrogels for prolonged release. Hence, dual-networks crosslinking was used to prepare hydrogels with excellent mechanical properties and multifunctional capabilities (Chen et al., 2019).

For instance, Qin et al. (2019) prepared starch-based hydrogels using one-pot technique by crosslinking corn starch with polyvinyl alcohol (PVA) and borax as a

crosslinker. The first network structure of hydrogels prepared was hydrogen bonds between starch and PVA, followed by dynamic borate bond crosslinked network. The addition of borax as a crosslinker ensured the interpretation, tangling, and crosslinking of starch-PVA via covalent bonds, resulting in the formation of hydrogel suspension. Following that, a starch-PVA hydrogel was formed from the freezing-thawing cycles of the second physically crosslinked network. Hydrogels prepared show excellent stretchability and toughness, as well as good self-healing and self-recoveries capabilities, making them promising for agricultural and biomedical applications, as well as pollutant adsorbents (Qin et al., 2019).

Likewise, Ai et al. (2021) used one-pot technique by crosslinking xylan hemicellulose with PVA and borax as a crosslinker to prepare hydrogels. The hydrogen bonds and related tangles between PVA and hydroxyl groups on xylan hemicellulose were used as crosslinking points to make the first network. Following that, borax was added into the xylan-PVA, which induced chemical crosslinking networks and formed hydrogel suspension. The freeze-thaw cycles that comprise the second physically crosslinked network formed hydrogels. This dual chemical/physical crosslinking produced hydrogels with free deformation and recycling capabilities, as well as good self-healing and high mechanical properties (Ai et al., 2021).

Further, Fan et al. (2021) developed polyacrylamide/gelatin (PAM-gel) based hydrogels in a one-pot approach using dual chemical/physical crosslinking. The PAM-gel hydrogels showed high thermal stability, high swelling ratio up to 1400%, and good shape memory function under warm water (Fan et al., 2021). The PAM-gel hydrogels have the potential to be used as drug-release agents in wound dressing application. Preparation of

hydrogels using dual-networks crosslinking was also reported by Abdolmaleki et al. (2021), Guo et al. (2021), Liu et al. (2021), Chen et al. (2022) and Yang et al. (2022).

2.4 Key Characteristic of Agricultural Hydrogels

Swelling is the most important characteristics of agricultural hydrogels. The significance of hydrogels in different fields, including agricultural applications, was primarily studied through swelling and deswelling test (Hocine et al., 2023). The hydrogels swell-dry-swell multiple times depending on the external environmental condition. Furthermore, they can function effectively at temperatures ranging from 40 °C to 60 °C, making them suitable for semiarid and arid regions (Kalhapure et al., 2016). Agricultural hydrogels should have high absorbency under load (AUL) rather than a high absorption rate (Ranganathan et al., 2018).

A good superabsorbent hydrogel can absorb large and retain large amount of water or aqueous solution and gradually release it in response to the crops' need (Behera & Mahanwar, 2019; Wei et al., 2021; Ahmad et al., 2023). Conventional absorbent materials can only absorb water up to 100 times of their dry weight, but superabsorbent hydrogels increase this feature up to 1000 times (Braihi et al., 2014; Guilherme et al., 2015). The crosslinked hydrogels may retain their polymeric networks shape even in swollen state (Guilherme et al., 2015). There are two main types of crosslinking that are specifically related to the high absorption capacity and swelling ability of superabsorbent hydrogels: bulk or core crosslinking and surface crosslinking.

Moreover, they must be highly durable and stable in the swelling environment as well as during storage. High water absorption capacity and swelling rate are significantly associated with highly porous structure of polymeric networks hydrogels (Ahmad et al.,

2023). Therefore, highly porous hydrogels were also most preferred as a crucial characteristic for agricultural hydrogels (Ahmad et al., 2023).

2.4.1 Bulk or Core Crosslinking

Bulk or core crosslinking is part of chemical crosslinking which occurs during the polymerization stage of the preparation of hydrogels (Braihi et al., 2014; Behera & Mahanwar, 2019). During the polymerization step, a crosslinking agent is incorporated into the back bonds of polymer chains. For instance, polyunsaturated crosslinkers such as diacrylates or bis-acrylamides are frequently used.

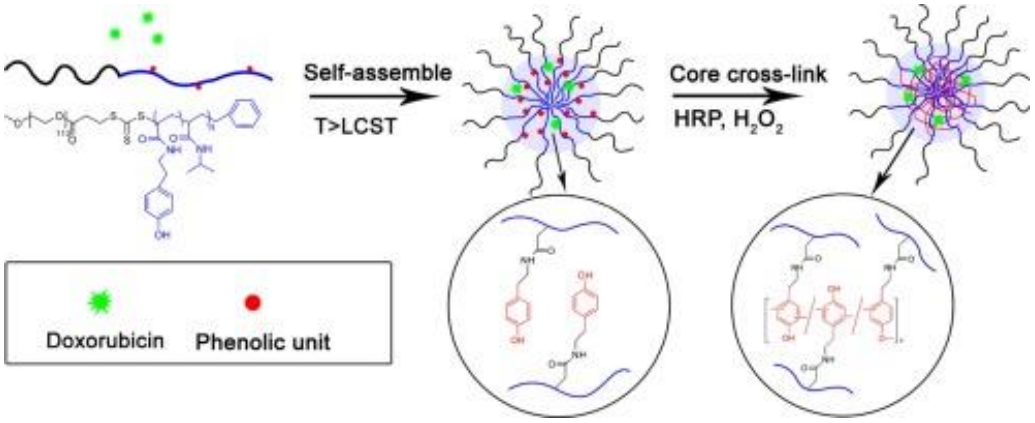


Figure 2.3: Graphical representation of bulk or core crosslinking within materials (Behera & Mahanwar, 2019)

The reactivity ratios will be determined to measure the proclivity of reaction components to react with each other (Braihi et al., 2014). High reactivity crosslinker will be consumed during the early stages of polymerization reaction (Braihi et al., 2014). Whereas any polymer chains generated later in the process are less likely to crosslinked and existed as extractable chains. Extractable chains are also known as low molecular weight polymer chains.

Low reactivity crosslinkers, on the other hand, have the opposite tendency, and the types of crosslinker used are critical in determining the final structure of polymer network (Braihi et al., 2014). This suggests that the concentration of crosslinker added has a substantial influence on the polymeric network of hydrogels formed and determines the swelling properties of hydrogels (Tholiban et al., 2019; Rico-García et al., 2020).

As reported by Das et al. (2020), cellulose-based hydrogels were prepared by crosslinking carboxymethylcellulose (CMC) and hydroxyethyl cellulose (HEC) with citric acid (CA) as the crosslinker. Various CA concentrations, i.e., 1%, 2% and 3% were added in the preparation steps. Their findings show that low crosslinker concentrations resulted in poor swelling ability due to insufficient crosslinked network formation. They also proposed that high crosslinker concentrations resulted in low swelling ability due to the formation of densely packed crosslinked networks, which reduces water permeability into the polymer network (Das et al., 2020). The optimum 2% CA crosslinker gave the highest swelling ratios of 600% due to sufficient crosslinked network formation to absorb and retain water. The as-prepared cellulose hydrogels have the potential to be used as controlled-absorb-release water materials to enhance water utilization efficiency for agricultural applications (Das et al., 2020). This finding was also reported by Salleh et al. (2018).

2.4.2 Surface Crosslinking

Surface crosslinking is a newer technique which produced hydrogels with high absorption capacity against pressure and enhanced swelling rate (Braihi et al., 2014; Behera & Mahanwar, 2019). Hydrogels with low crosslinking concentration had poor gel strength, poor absorbency under load, and the swelled particles deformed easily and clustered together under load. The capacity underload decreased as swelling underload increases. As a result,

gel blockage occurs. Therefore, post-treatment is necessary to resolve this condition. Post-treatment is normally performed on dried, milled, and sized hydrogels as the final stage of the process.

Surface crosslinking of hydrogel particles improves the flow significantly (Figure 2.4). As-prepared hydrogels have high porous structure with air pockets, allowing for high water permeability between structures (Jockusch et al., 2009; Braihi et al., 2014). Furthermore, surface crosslinking produced hydrogels with improved strength and lower core crosslinking level (Behera & Mahanwar, 2019), as well as maintaining their polymeric networks stable in a swollen state. The hard surface prevents gel blockage and allows fluid to flow freely into polymeric networks of hydrogels. Therefore, the hydrogels can absorb and retain large amounts of water into their polymeric networks while maintaining their shape.

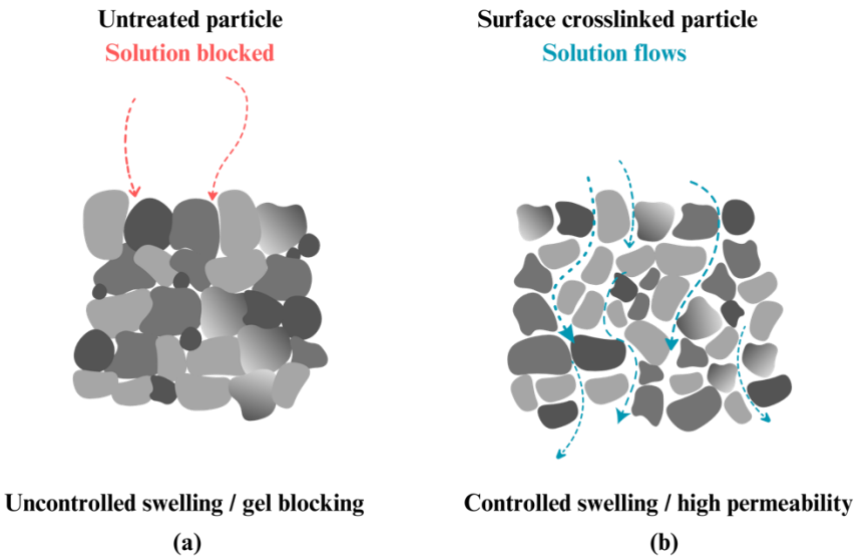


Figure 2.4: Schematic representation of the swelling and flow of solutions through the (a) un-crosslinked and (b) surface crosslinked hydrogel particles (Jockusch et al., 2009)

In agricultural application, superabsorbent hydrogels exist with neutralization (Ranganathan et al., 2018). Therefore, they do not affect nutrient availability, soil chemical composition, or the action of other agrochemicals such as fertilizers, herbicides fungicides, insecticides, and others. Furthermore, hydrogels may improve the physical properties of soils including porosity, bulk density, water retention, and local soil humidity (Ramezani et al., 2013), as well as soil permeability and aeration, thus enhanced nitrogen retention by plants (Ramos Campos et al., 2015). Moreover, hydrogels may increase biological or microbial activities in the soil, improving air availability in root zone of the plant (Ekebafe et al., 2011). Therefore, cellulose-based hydrogels could be deemed as environmentally friendly and inexpensive, as well as gradually biodegradable without the formation of toxic species (Ahmad et al., 2023).

2.5 Categories of Cellulose-based Hydrogels

Various types of hydrogels including alginate, starch, chitosan, and cellulose-ether-based hydrogels have been used for agricultural applications (Nasution et al., 2022). Crosslinkers, such as epichlorohydrin, aldehydes, aldehyde-based reagents, urea derivatives, carbodiimides, and multi-functional carboxylic acids are used in the synthesis of hydrogels (Sabbagh et al., 2018; Nasution et al., 2022). Moreover, crosslinking reactions are triggered by chemical agents and may occur in water solutions, organic solvents, or in the dry state (Guilherme et al., 2015; Bustamante-Torres, et al., 2021). As prepared cellulose hydrogels have high water absorption capacity and water retention ability, which are important features for water and nutrients release in arid and semi-arid conditions, as well as throughout growing cycle phases. Cellulose-based hydrogels with excellent properties, low toxicity and low cost are appealing for agricultural applications.

2.5.1 Carboxymethylcellulose (CMC)-based Hydrogels

CMC is made from cellulose derived from wood or cotton linters. CMC is inexpensive and soluble due to a chemical reaction between cellulose and monochloroacetic acid (MCA) and sodium hydroxide (NaOH) (Ranganathan et al., 2018). Besides, CMC has a high number of polar carboxyl groups on their backbone polymer chains, which contributes to their solubility, chemical reactivity, stability, and strong chelating properties (Ranganathan et al., 2018).

These features make CMC suitable for water absorption and retention. In addition, CMC is also easily available and often used as sodium salt, Na-CMC, which is a cellulose polyelectrolyte polysaccharide derivative (Ranganathan et al., 2018; Sabbagh et al., 2018). Therefore, they are sensitive to changes in pH and ionic strength, and have a good swelling capacity (Ranganathan et al., 2018). These advantages have led to the widespread applications of CMC-based hydrogels in agriculture.

In a study, Xiao et al. (2014) have prepared biodegradable cellulose-based hydrogels with Na-CMC as a polymer and polyethylene glycol di-glycidyl ether (PEGDE) as a crosslinker (Figure 2.5). The swelling behavior of hydrogels was influenced by crosslinker concentrations and the ratio of Na-CMC to cellulose. The ideal 9:1 Na-CMC/cellulose and 3% (w/v) PEGDE blend can swell to 230 g/g. Further increase in Na-CMC and crosslinker did not result in a higher swelling ratio. The prepared hydrogels also have low swelling ability in sodium chloride (NaCl) solution due to decrease in osmotic pressure between the inside of hydrogels and the outer medium.

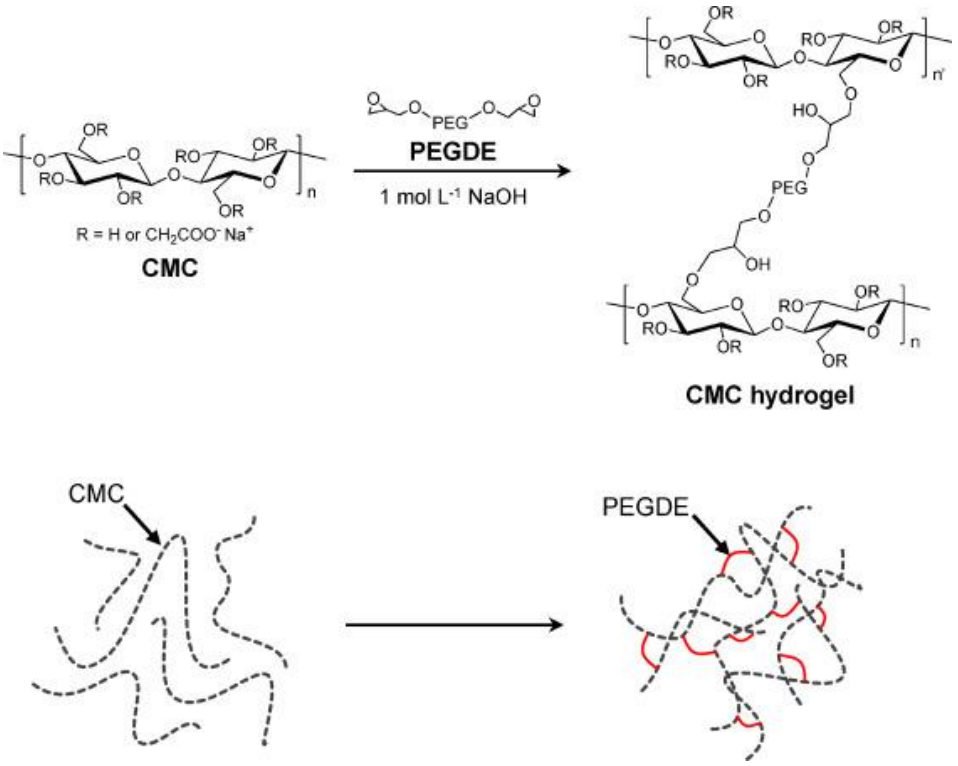


Figure 2.5: Graphical representation of CMC-based hydrogel crosslinked by PEDGE (Xiao et al., 2014)

Likewise, Ibrahim et al. (2007) also have developed cellulose-based hydrogels using Na-CMC by copolymerization with acrylamide (AAm) induced by electron beam irradiation. The optimum 9:1 CMC/AAm hydrogels have the highest swelling ability, and the swelling percentage increases with increasing temperature. Besides, higher doses of CMC did not result in higher water absorption due to dense and compact gel formations. Also, their findings suggest that the hydrogels have high thermal stability and water retention for up to 30 days. Furthermore, these hydrogels are widely acknowledged around the world due to their economic benefits and environmental friendliness.

Moreover, Mohamed et al. (2022) developed biodegradable cellulose-based hydrogels using CMC and 4-vinylpyridine (P4VP) using *N*, *N*, -methylene bis-acrylamide (MBA) as a crosslinker. These hydrogels have highly porous structures and achieve a

maximum swelling ability up to 1400%. They also have high thermal stability, which is due to the incorporation of urea into the hydrogels systems and resulted in the formation of stable cyclic compounds in hydrogels. Moreover, hydrogels have a high loading capacity (62%) of urea due to their porous structure and high-water absorption capacity. This resulted in controlled-release fertilizer effects, which were confirmed by Korsmeyer-Peppas model via the quasi Fickian.

Many studies have developed cellulose-based hydrogels using CMC for agricultural applications which have been reported by Raafat et al. (2012), Alkalin and Pulat (2019), Durpekova et al. (2020), Klein and Poverenov (2020), Bauli et al. (2021), Miljković et al. (2021), and Watcharamul et al. (2022).

2.5.2 Hydroxyethyl Cellulose (HEC)-based Hydrogels

Literature has reported that HEC is normally used in conjunction with CMC to prepare hydrogels (Durpekova et al., 2020). These combinations sought to enhance intermolecular crosslinking and stability (Ahmed, 2015; Durpekova et al., 2020). They have been used in many agricultural applications, especially for water storing. Duperkova and co-workers have developed biodegradable cellulose-based hydrogels using CMC/HEC and acid whey with citric acid as a crosslinker. The optimal 3:1 CMC/HEC ratio and citric acid (3% (w/v)) results in a high swelling ratio (1700%) as well as good thermal stability and viscoelasticity. Besides, these hydrogels also can sustainedly absorb water even after 5 drying-swelling cycles. They also have higher swelling ability at high pH and a lower swelling ability at low pH. These findings indicate that CMC/HEC hydrogels are suitable for water retention in arid and semi-arid areas and could be used as a replacement for synthetic acrylic-based hydrogels.

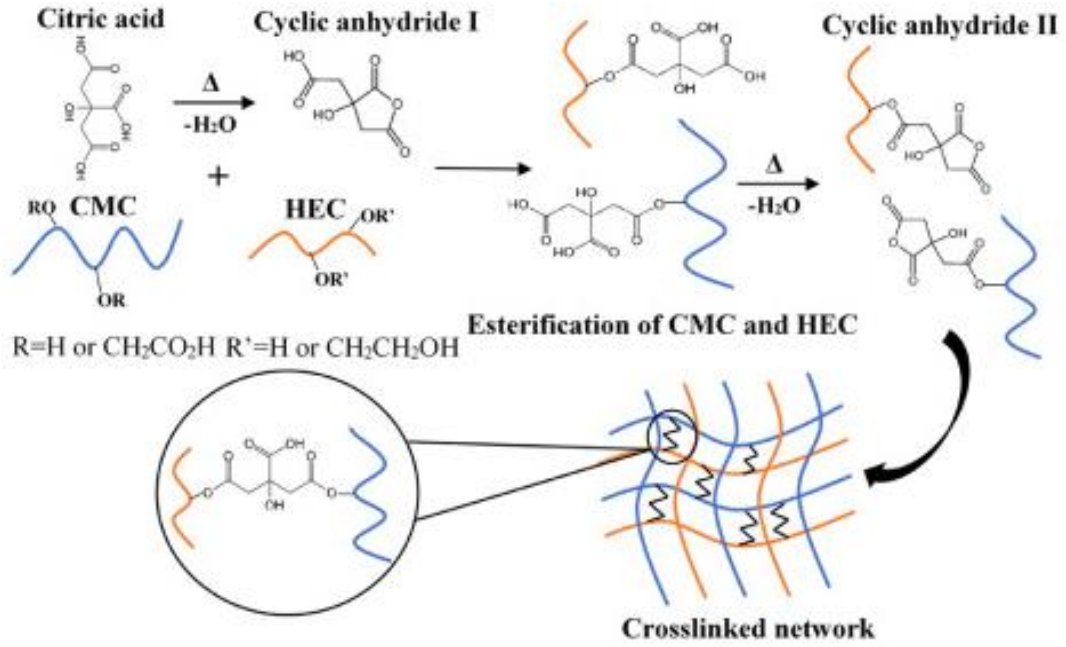


Figure 2.6: Graphical representation of cellulose-based hydrogels using CMC/HEC and citric acid as crosslinker (Das et al., 2023)

Similarly, Das et al. (2023) have prepared cellulose-based hydrogels from HEC and CMC using citric acid as a crosslinker. The ideal CMC/HEC ratio is restricted to 3:1, with a maximum swelling ability of 1070%. As-prepared hydrogels also can absorb water and soluble fertilizer without dissolution, and they also have controlled nutrients release effects. These features make CMC/HEC hydrogels suitable for arid and semi-arid acreage to preserve soil moisture and supply nutrients to crops in those areas.

Likewise, Calcagnile et al. (2019) developed biodegradable and low-cost CMC/HEC hydrogels with the addition of poly (lactic acid) (PLA) into the system for water reservoir function and fertilizer reservoir. As prepared hydrogels are effective at fine-tuning water retention capabilities in sandy soils and retain the soil moisture. Besides, the addition of PLA into the system enhanced the prolonged release effects of hydrogels. In addition, these hydrogels show high thermal stability at temperature 200 °C and degrade at 300 °C. These

findings suggest that these hydrogels have promising potential as water and fertilizer reservoir in agricultural applications.

Other studies have developed cellulose-based hydrogels using CMC/HEC with similar findings as reported by Seki et al. (2014), Montesano et al. (2015), Fekete et al. (2017), Baldino et al. (2020), Noreen et al. (2020), Das et al. (2021), Tuan Mahamood et al. (2021), Kang and Yun (2023).

2.5.3 Cellulose-Alginate-based Hydrogels

Alginate is a natural polysaccharide containing mannuronic and glucuronic acid residues as well as calcium ion crosslinking (Martínez-Cano et al., 2022). Crosslinking can occur at physiological pH and room temperature. These characteristics enable cellulose alginate hydrogels to be used in variety of industries, including the food industry, as a thickener, stabilizer, and binder (Martínez-Cano et al., 2022). In addition, alginate hydrogels offer important properties for food and products, such as water retention capacity, gelling and the ability to form capsules and films (Martínez-Cano et al., 2022). They are safe to consume because they are intoxicant, highly biodegradable, and human-degradable (Martínez-Cano et al., 2022). For these reasons, cellulose alginate hydrogels have been used in agricultural applications for healthier crops.

Gomaa and Aldaby (2023) prepared biodegradable hydrogels from alginate (A) and cellulose derived from wastepaper (W) as soil conservation and moisture retention in sunflowers. The alginate-wastepaper (AW) hydrogels prepared from this study are durable and stable, with a swelling ratio of up to 313%. Besides, the swelling ratio (424%) increases with increasing temperature (50 °C). Also, the effects of AW hydrogels on sunflower growth under drought stress conditions were studied.

This study found that sunflowers treated with AW hydrogels have higher height, increased in root length by 32% and 41% in moderate drought stress and extreme drought stress, respectively, and similar stem length under moderate drought stress compared to controls. Besides, sunflowers treated with AW hydrogels generated greater fresh roots and dry weight when compared to controls. Healthier sunflowers growth is associated with better absorption of phosphorus by sunflowers and less phosphorus loss to the environment due to leaching. Therefore, the authors suggested that AW hydrogels ameliorate drought stress by enhancing water retention in soils and minimizing phosphate leaching.

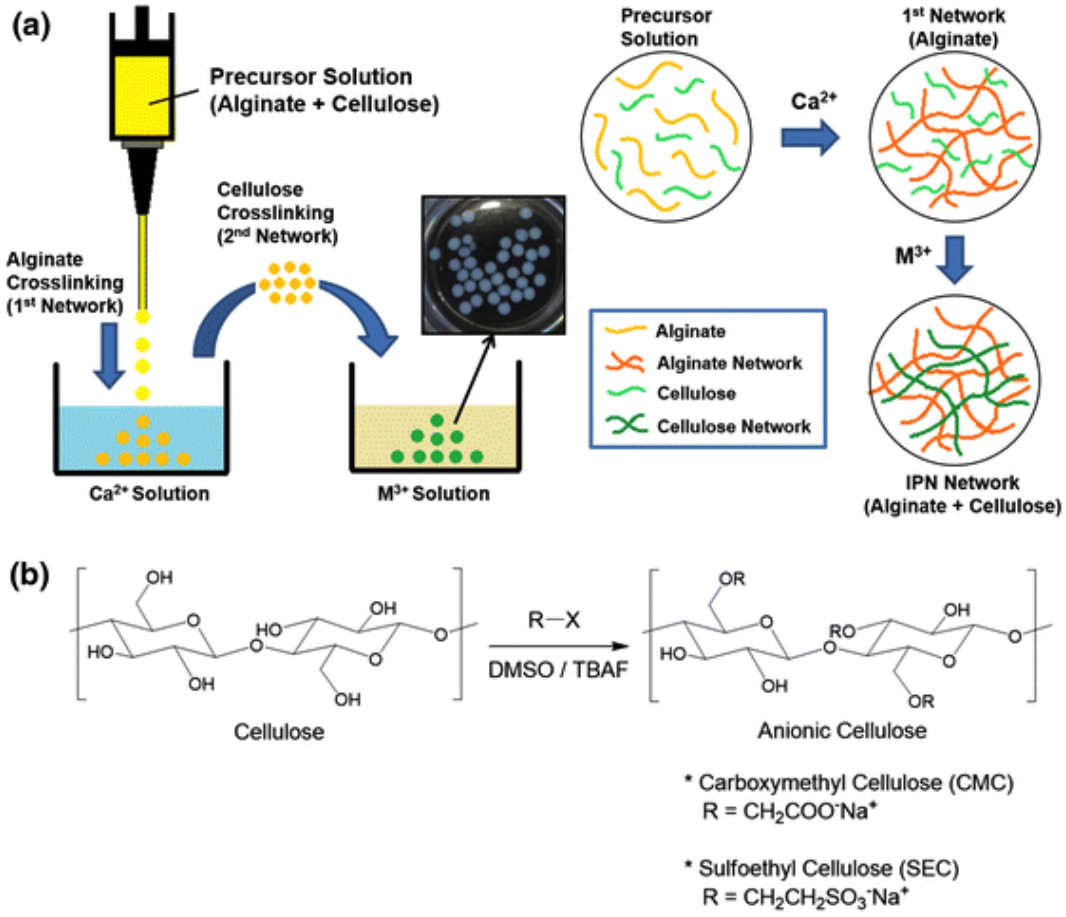


Figure 2.7: Graphical representation on the fabrication of cellulose-alginate-based hydrogels (Martínez-Cano et al., 2022)

In addition, alginate hydrogels have been used as a sustained-release fertilizer and for water retention (do Nascimento et al. 2022), primarily in wheat (Wang et al. 2021), as well as for the controlled release of nitrogen, phosphorus, potassium chemical (Liu et al., 2021), sulfur and oxygen (Ranganathan et al. 2018). Moreover, alginate/glutaraldehyde hydrogels have been investigated as a carrier and delivery device for the controlled release of liquid pesticide neem seed oil (Ranganathan et al. 2018). Further, a starch-alginate clay composite was used as a matrix for the controlled release of fungicide thiram (Singh et al. 2009). Similarly, starch-alginate crosslinked with calcium ions has been used as a matrix to controlled-release and deliver pesticide chlorpyrifos to the targeted zone (Roy et al., 2009).

2.5.4 Cellulose-Starch-based Hydrogels

Starch is one of most abundant and naturally occurring plant polysaccharides (Ranganathan et al., 2018; Qamruzzaman et al. 2021). Many hydroxyl groups in starch enable hydrogels networking (Ranganathan et al., 2018; Qamruzzaman et al., 2021). Furthermore, starch is a low-cost, non-toxic, and highly biodegradable material (Qamruzzaman et al., 2021). These features make cellulose/starch hydrogels a viable alternative to synthetic hydrogels. Moreover, microorganisms can degrade cellulose/starch hydrogels (Jiang et al., 2020; Adjuik et al., 2023). Therefore, they can potentially be used for sustainable soil conservation as a highly biodegradable matrix for nutrients carriers and controlled release (Adjuik et al., 2023).

Cellulose/starch blends can be used to prepare superabsorbent hydrogels by dissolving starch in water to form suspension, followed by modification and reinforcement with cellulose (Olad et al., 2020). Superabsorbent hydrogels have been prepared using carboxymethyl starch and CMC with high water absorption capacity, i.e., 350 g/g and 815.2

g/g (Fekete et al., 2017). Findings from both studies show potential applications of cellulose/starch hydrogels in agriculture as water reservoir and retain soil moistures. Some studies also investigated the applicability of cellulose/starch hydrogels to improve soil condition and promote healthy plants growth (Nnadi & Brave, 2011; Bai et al., 2023).

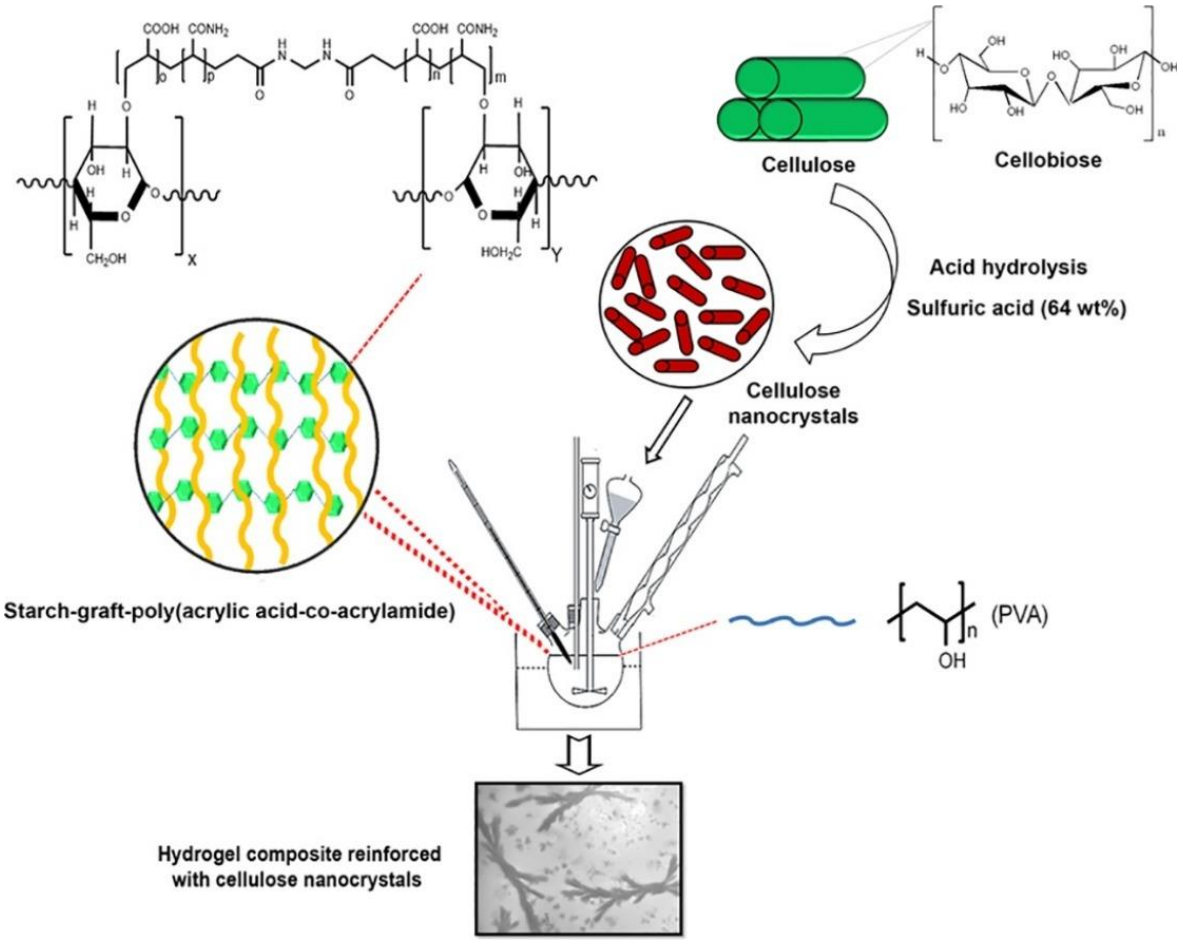


Figure 2.8: Graphical representation of starch-based superabsorbent hydrogel composite reinforced with cellulose nanocrystals (Olad et al., 2020)

Parvati et al. studied the effect of saponified cassava starch-based superabsorbent hydrogels on the physical, chemical, and biological properties of soil. Also, the effects of the same hydrogels on the growth performance of chili (*Capsicum annuum* L.) at different water irrigation intervals were studied. Their findings suggested that the water retention capacity in the soil depends on the concentration of superabsorbent hydrogels which control

the release of water to soils. Moreover, starch-based hydrogels were designed for controlled release of pesticides such as fluometuron, thiophanate, thiophanate methyl and trifluralin (Abd El-Mohdy et al., 2011).

2.5.5 Cellulose-Chitosan-based Hydrogels

Chitosan is the second most abundant polysaccharides which can be used to prepare hydrogels through non-covalent polyelectrolyte complexation and covalent Schiff-based formation (Peers et al., 2020; Duceac & Coseri, 2022). Chitosan is essential as a precursor material due to its biocompatibility, biodegradability, and antimicrobial properties. Chitosan-based hydrogels have been extensively used in biomedical applications including drug administration, wound healing, cell culture, bioimaging and others (Pella et al., 2018; Peers et al., 2020). However, there are limited chitosan-based hydrogels formulations adapted for agricultural applications (Ranganathan et al., 2018).

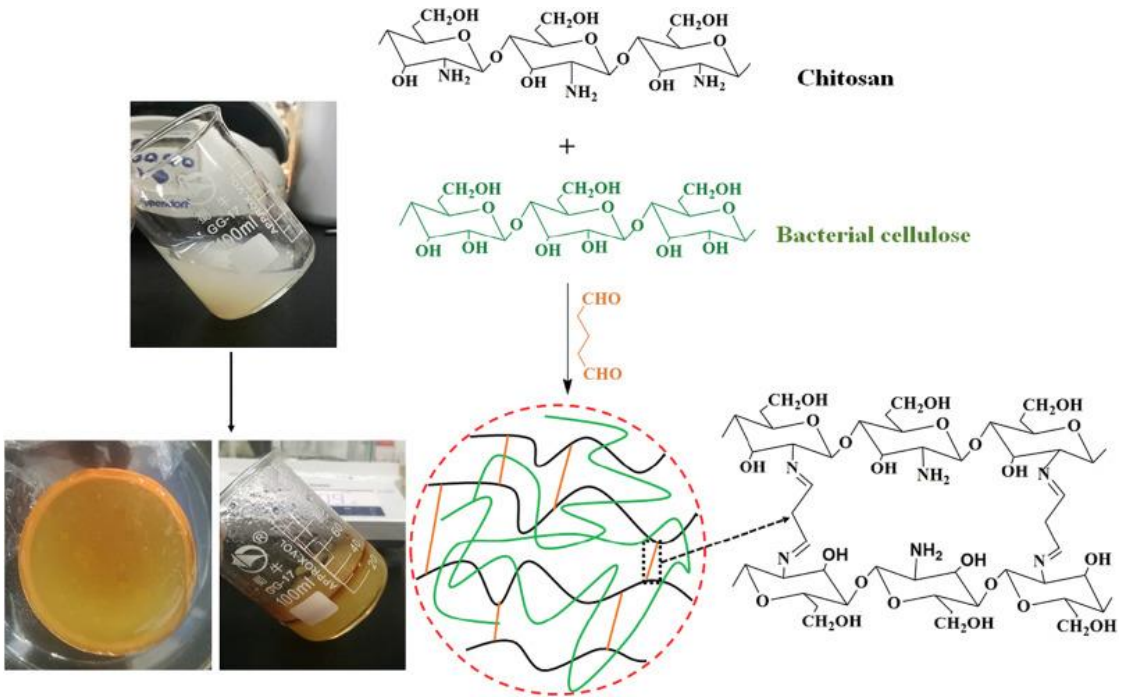


Figure 2.9: Graphical representation on the formation of cellulose-chitosan-based hydrogel (Peers et al., 2020)

Some studies have focused primarily on the applicability of chitosan-based hydrogels for agricultural uses, as shown in Table 2.1.

Table 2.1: Summary of the applications of chitosan-based hydrogels in agriculture

Agricultural applications	Previous studies involved
Water reservoir and carrier device to deliver active ingredients and fertilizers	Narayanan et al. (2018), Said et al. (2018), Iftime et al. (2019), Lopez-Vleazques et al. (2019), Perez Bravo and Francois (2020).
Growing tomato and watermelon	Juarez-Maldonado et al. (2016), Gomez et al. (2017).
Soilless plant cultivation	Zhang et al. (2023)
Seed Germination	Nayan et al. (2018), Jong et al. (2023)

2.6 Cellulose-based Hydrogels as a Controlled-release Fertilizer

2.6.1 Controlled-release Fertilizer

The terms slow-release fertilizer (SRF) and controlled-release fertilizer (CRF) are frequently used interchangeably, although there is no significant difference between SRF and CRF (Trenkel, 2010). SRF and CRF fertilizers contain plant nutrients encapsulated in their polymer networks which delay their availability for plant absorption and post-application usage (Trenkel, 2010). They allow sustained availability of nutrients to the plants significantly longer than 'rapidly available nutrient fertilizer', for instance, ammonium nitrate or urea, ammonium phosphate, or potassium chloride (Trenkel, 2010).

In the literature, different definitions of SRF and CRF are found. SRF are compounds with low solubility, high molecular weight structure that release nutrients to plants by microbial or chemical decomposition (Lawrencia et al., 2021). SRF is a system of condensation products of urea-aldehydes that can be coated, incorporated into matrix, and super granules (Trenkel, 2010; Ramli, 2019). Besides, SRF only concerns the slow release of nutrients, with no control over the release rate, durations, and patterns as influenced by environmental conditions such as soil and climate (Naz & Sulaiman, 2016).

In contrast, CRF refers to materials containing plant nutrients, the release of which is controlled by the coating materials that encapsulate the fertilizers (Lawrencia et al., 2021). CRF permits the release of fertilizer in a controlled pattern and duration (Sempeho et al., 2014). CRF is a subset of SRF and is regarded as fertilizer with a physical barrier or encapsulated products (Trenkel, 2010). Classification of CRF is shown in Figure 2.2 (Lawrencia et al., 2021). Studies suggest that the similarity of SRF and CRF is on their encapsulated polymer application as a slow-release or controlled-release fertilizer (Davidson et al., 2013; Lawrencia et al., 2021). This type of formulation is also best applied for agricultural purposes (Davidson et al., 2013; Zanin et al., 2020; Lawrencia et al., 2021).

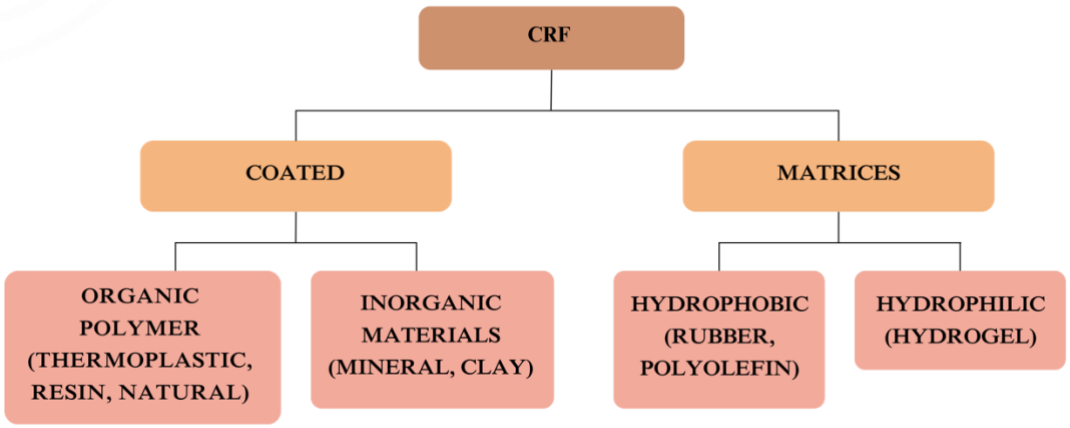


Figure 2.10: Classification of controlled-release fertilizers (CRF)

The required nutrient release rate by CRF varies for each plant depending on the metabolic requirements of the crop for a specific period. However, the European Standardization Committee (CEN) Task Force has made some recommendations on the criteria of CRF. First, the nutrient release rates must be slower than that of common fertilizers, with no more than 15% nutrient released in 24 hours, no more than 75% released in 28 days, and at least approximately 75% release within the specified released time (Trenkel, 2010).

In the preparation of SRF and CRF, the slow-release and controlled-release properties can be obtained through various processes. One of the possible ways is by modification of conventional fertilizers (Trenkel, 2010). Their solubility and release properties can be modified chemically or physically. The conventional fertilizers are encapsulated or coated using a protective polymer coating that allows water to penetrate their polymer network and dissolve the loaded fertilizers (Ahmad et al., 2023). Fertilizers will be released gradually from the surface membrane when the polymer coating swells, synchronized to the plant's requirement.

Figure 2.11 shows an illustration of urea fertilizers encapsulated in hydrogel. As hydrogel is a hydrophilic crosslinked polymer, they aid in the initial stages of water absorption and penetration, as well as the release of loaded nutrients (Guilherme et al., 2015; Li et al., 2020; Ahmad et al., 2023). Fertilizers loaded in the hydrogel will be diffused and begin to disperse due to the concentration gradient differences between inside and outside of hydrogels (Ahmad et al., 2023). Subsequently, the exchange of water in hydrogels and fertilizers occurs (Rashidzadeh & Olad, 2014). There would be steric effect present, which

inhibits the adsorption of fertilizer by dispersing fertilizer into the soil (Li et al., 2016). Therefore, the nutrients-released varied in a controlled pattern and duration (Li et al., 2016).

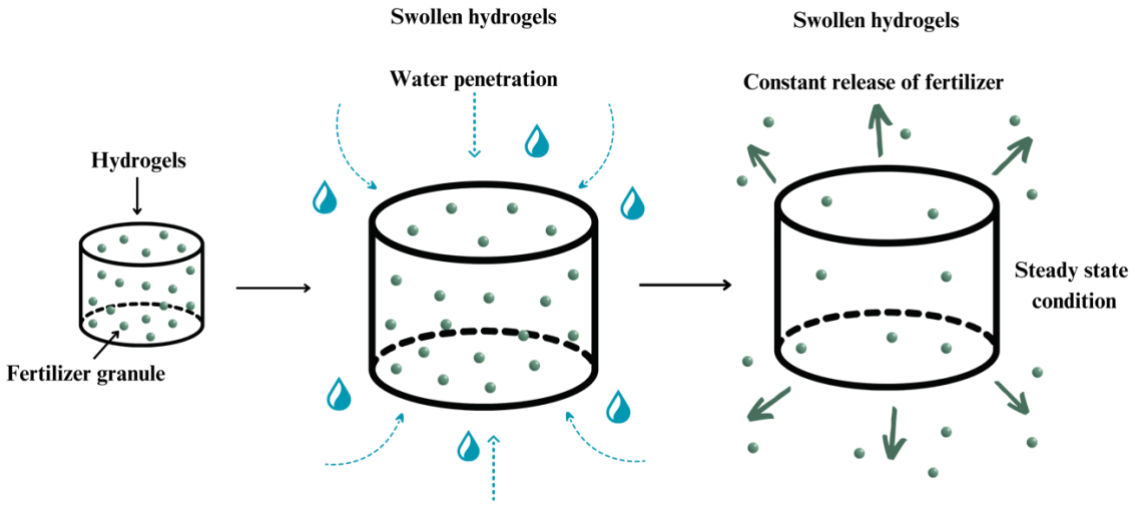


Figure 2.11: Schematic representation of encapsulated urea fertilizer system absorbing water and releasing nutrients to soil

2.6.2 Mathematical Models for Nutrient Release Profile

The dried, pre-application CRF hydrogels are typically rigid, which may influence the swelling of hydrogels and release of nutrients from hydrogels. The release rate of nutrients from CRF is determined by diffusion, swelling, erosion or a combination of these factors. When hydrophilic CRF is involved, the release occurs by diffusion, whilst when hydrophobic CRF is involved, the release is due to swelling or erosion in the matrix.

Therefore, it is crucial to select the appropriate modelling approach for each CRF formulation to obtain realistic theoretical assumptions and comprehend the transport mechanism to prepare optimal CRF designs. The following mechanisms and mathematical models for nutrients release from hydrogels were discussed, with an emphasis on agricultural applications.

2.6.2.1 Nutrient Release Profile from Hydrogels

Many mathematical models developed for controlled-release fertilizers are focused on the nutrients released from the coated polymers in the granules form as reported in previous study (Basu et al., 2010; Guilherme et al., 2015). However, those models are less suitable for controlled-release fertilizers from hydrogels due to difficulties to obtain certain parameters required in the mathematical equations, as well as relationship between the release rate and the properties of carrier materials (Zheng et al., 2009; Guilherme et al., 2015).

Fortunately, chemically crosslinked hydrogels are easily prepared and have more reliable release patterns than other nutrient carriers (Zheng et al., 2009). Their nutrient release is driven by the concentration gradients between the inside and outside of hydrogels, therefore, they respond and fine-tune precisely according to the plants' requirement (Zheng et al., 2009; Guilherme et al., 2015; Ahmad et al., 2023). The nutrients release can be best described using three methods. First, water is absorbed via diffusion through the porous structure of polymeric networks of hydrogels. Second, controlled release of nutrients via diffusion and/or convective flows (Wang et al., 2011). Third, macromolecular chain relaxation during swelling and deswelling of hydrogels.

These methods are best fit by either Fickian or non-Fickian diffusion model employing the Ritger-Peppas and Korsmeyer-Peppas model equations as follows (Guilherme et al., 2015; Lawrencia et al., 2021; Ahmad et al., 2023).

$$\frac{M_t}{M_\infty} = K_{KP} t^n \qquad \text{Equation 2.1}$$

where K_{KP}, t, and n are diffusion constant (m^2/s), time (s), and diffusion exponent of the release mechanism, respectively. M_t/M_∞ (g/g) is the fraction of fertilizer released at the time, t. The nutrient release mechanism is classified based on the values of n. The value of $n < 0.45$ indicates that the fertilizer release mechanism is a Fickian model, whilst $0.45 < n < 0.89$ indicates that the fertilizer release mechanism is a non-Fickian diffusion transport. When $n > 0.89$, the nutrient release follows the case II transport.

Fickian or non-Fickian diffusion model is the most reliable approach to improving synchronism between the nutrients release and the plants' requirement (Guilherme et al., 2015; Ahmad et al., 2023). This model would be the most useful when the release mechanism is unknown or when more than one release mechanism is involved (Lawrencia et al., 2021). Therefore, this model could aid in the development of controlled-release fertilizers for agricultural use. Other studies have used this model to describe swelling and release mechanisms (Chetouani et al., 2014; Liang et al., 2014; Wei et al., 2019; Hermida & Augustin, 2019; Bi et al., 2020; Ahmad et al., 2023).

Next, the Higuchi model describes the release mechanism of soluble or less soluble nutrients from hydrogels (Phang et al., 2020; Babadi et al., 2021). Some parameters must be considered when adopting this model. For instance, in the release environment, the initial concentration of nutrients in hydrogels must be greater than their solubility, diffusion occurs in only one direction, negligible swelling, nutrient particles must be much smaller than the thickness of coating, constant diffusivity, and perfect sink condition must be achieved (Phang et al., 2020; Babadi et al., 2021). The Higuchi model can be calculated using the following mathematical model.

$$Q = \sqrt{2C_0\xi\frac{Dt}{\tau\pi}} = K_H\sqrt{t} \qquad \text{Equation 2.2}$$

where Q is the cumulative amount of fertilizer released at time, t per unit area (g cm^{-2}), C_0 is the concentration of diffusing liquid in a porous matrix (g cm^{-3}), ξ is porosity, D is the diffusion coefficient in the matrix medium (cm^2 day^{-1}), τ is capillary tortuosity factor, t is time (day), and K_H is the release constant of Higuchi.

Further, nutrients release from hydrogels can be described using a logistic growth model using mathematical equation 2.3 (Zheng et al., 2009).

$$\frac{dC}{dt} = k_R\left(1 - \frac{C}{C_\infty}\right) \qquad \text{Equation 2.3}$$

where C_∞ is the equilibrium nutrient concentration (mol), similar to the carrying capacity of the environment in logistic growth model and k_R is the release rate.

This model was developed based on logistic growth, which describes the change in the nutrients concentration over time in given volumes of water or nutrient solution. The increase in nutrients concentration with time may be compared to the logistic growth of population in the environment with limited resources (Zheng et al., 2009).

Another diffusion-based model was developed which is related to the distribution of the solute into hydrogels and considering the mathematical development using Fick's Second Law in equation 2.4 (Reis et al., 2007).

$$\alpha = \frac{F_{max}}{1 - F_{max}}$$ Equation 2.4

where α is the physical and chemical affinities of the solute for the hydrogel matrix and for the external fluid. The diffusion of solute from hydrogel into external fluid occurs even when α > 0. The higher the α value, the higher the affinity of solute for the external fluid.

This model provides an insight on affinity of the solute for its environment and prediction of 100% in vitro release. However, this model has two main limitations: the application is limited to short release, and this model does not account for erosion. The application of this model in release mechanism has been reported in other studies (Piai et al., 2008; Valente et al., 2010; Bossoni et al., 2014).

2.6.2.2 Nutrient Release Profile from Polymer Granules

Substance Flow Analysis (SFA) is an analysis of the total flow of nutrients through a system at a specific duration (Guilherme et al., 2015). This method of analysis is commonly used in conventional agriculture to monitor nutrients in natural systems (Saruchi et al., 2013). This method, however, does not provide a systematic measurement method for nutrient release in soils, expensive, time-consuming, and simplistic (Chen et al., 2010). Therefore, this method is regarded as unreliable for quantifying the nutrient release mechanism in soil.

For this reason, another method, extended substance flow analysis (ESFA), was developed (Chen et al., 2010). The ESFA method is divided into six steps: (i) system definition, (ii) model development, (iii) database development, (iv) model validation, (v) results interpretation, and (vi) uncertainty analysis. Reports show that leaching of fertilizer,

herbicide, and pesticide contributed to eutrophication and groundwater nitrate enrichment (Basu et al., 2010). Coated fertilizer granules and crosslinked hydrogels may be used to address the issues (Basu et al., 2010; Bortolin et al., 2013). Coated fertilizer granules for the controlled-release nutrients in soils have been reported in previous studies (Trenkel, 2010; Basu et al., 2010).

The nutrients release profile from coated fertilizer granules can be classified into three stages, i.e., (i) initial stage with no nutrient release, (ii) constant release from medium at time intervals, and (iii) gradual decline of the release rate from the longer release time (Guilherme at el., 2015). Based on these release profiles, a mathematical model based on Fick's Second Law was developed to predict the release rate using a numerical solution and Fourier series expansion (Guilherme et al., 2015). The release time at the initial stage can be estimated using equation 2.5, and the second and third release profiles can be derived using equations 2.6 and 2.7, respectively.

$$t' = \frac{\gamma r l}{3 p_h \Delta P} \qquad \text{Equation 2.5}$$

$$g_t = \frac{3}{p_s r}\left(\frac{D(t-t')}{l} C_s - \frac{1}{6}\right) \text{ for } t' < t \leq Y \qquad \text{Equation 2.6}$$

$$g_t = 1 - \frac{C_s}{p_s} \exp\left(-\frac{3D}{rl}(t-y)\right) \text{ for } t > Y \qquad \text{Equation 2.7}$$

where γ is the total granule porosity, p_h is water permeability of the membrane, ΔP is the vapor pressure difference between water and saturated nutrient solution (in Pa), r is the radius of diffusion (in mm) in the coated granule, Y is the time when all solid nutrients are

dissolved, p_s is the nutrient density (kg m^{-3}), D is the constant coefficient diffusion, and C_s is the saturated concentration of nutrients (kg m^{-3}).

Various mathematical models used to describe nutrients release mechanisms have been studied and reported in previous publications. For instance, models based on mass transfer (Arkhincheev, 2019; Susanti et al., 2019; Anarbaev et al., 2021; Heyland et al., 2021), single granules (Irfan et al., 2018; Irfan et al., 2020; Vakal et al., 2020), and molecular and ionic diffusion (Guilherme et al., 2015; Tredenick et al., 2019; Griffiths & York, 2020). Other mathematical model, such as van Genuchten's equation to describe soil water retention and water transport from hydrogels to plants was reported in other studies including Ghanbarian-Alavijeh et al. (2010), Yang and You, (2013) and Pan et al. (2019).

2.7 Applications of Hydrogels in Agriculture

2.7.1 Controlled-release Fertilizer

Regenerated cellulose has attracted many researchers for developing CRF or SRF for the agriculture sector. Hydrogels as CRF are a multifunctional fertilizer that can reduce fertilizer loss due to leaching, surface run-off, volatilization, denitrification, and other chemical processes, thereby improving fertilizer use efficiencies for plant uptake (Wen et al., 2017; Versino et al., 2019; Zhang et al., 2020; Ahmad et al., 2023). Besides, hydrogels CRF are cellulose-based, therefore they are environmentally friendly and highly biodegradable (Ahmad et al., 2023). Figure 2.12 shows an illustration of the application of hydrogels as CRF in agricultural applications.

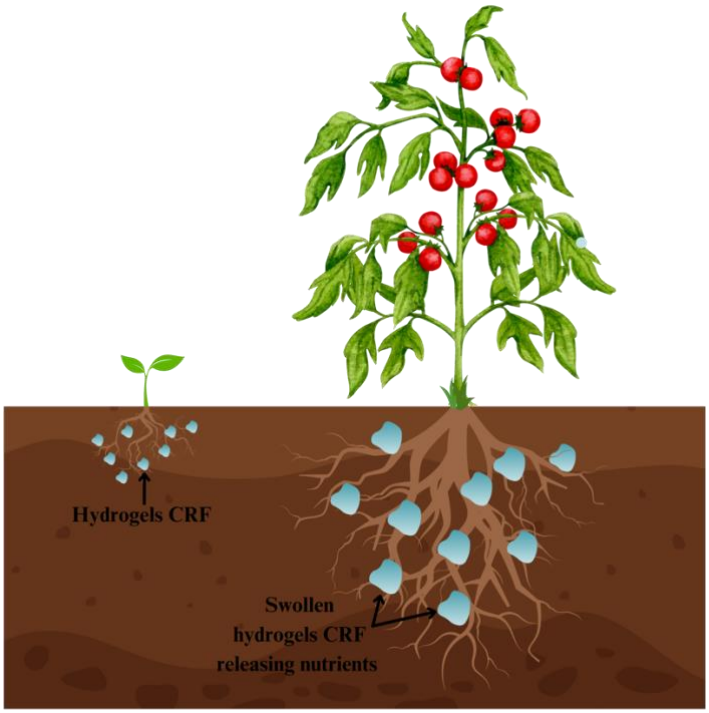


Figure 2.12: Schematic representation of applying hydrogels CRF in soil

As reported by Ramli et al. (2019), superabsorbent hydrogels SRF were prepared using cellulose derived from coco peat fiber using an *in-situ* solution polymerization technique grafted-poly (acrylic acid)/Nitrogen-Potassium-Phosphorus (NPK). The coco peat cellulose-hydrogels SRF have homogenously porous structures, thicker, smaller pore sizes, and interconnected capillaries between channels, all of which contribute to their higher mechanical strength. A maximum absorption capacity of 165 g/g was attained with a five-week slow release of fertilizer in water. The slow-release effect was due to effective encapsulation of NPK in the polymeric networks of coco peat cellulose hydrogels. In addition, as-prepared hydrogels are environmentally friendly due to significant increase in their biodegradability. The coco peat cellulose-based hydrogels have promising properties as SRF for potential use in agriculture.

Further, Zhang and others also used grafting copolymerization to prepare cellulose-based hydrogels from sawdust (Zhang et al., 2020). The sawdust cellulose-based hydrogels SRF have improved mechanical strength and achieved a maximum water absorbency of 210 g/g due to the presence of hydroxyl groups. The cumulative release rate was 82.4% within 20 days, with a release pattern characterized by slow release at the beginning, quick release in the middle, and slow release at the end, which closely matches the plant's growth requirement. As a result, the sawdust cellulose-based hydrogels SRF are potentially suitable for wide-use applications in agriculture.

Another study by Kareem et al. (2021) reported the preparation of hydrogels SRF by crosslinking cellulose derived from blended paper and hydroxypropyl methylcellulose (HPMC), polyvinyl alcohol (PVA) and glycerol. The blended paper cellulose hydrogels SRF have porous spongy-like particles in their structure which facilitate water penetration and improved water absorption capacity and water retention in soil. Further, the blended paper cellulose hydrogels SRF are highly degradable, with an effective slow-release rate of 87.01% in soil within 44 days. The prepared hydrogels are not only environmentally friendly and inexpensive, but they also have promising properties as a reliable SRF for sustainable agricultural applications.

Mohamed et al. (2022) prepared hydrogels CRF by crosslinking carboxymethylcellulose (CMC) and poly(4-vinylpyridine) (P4VP) with N, N-methylene bis-acrylamide (MBA) as a crosslinker. The CMC-P4VP-MBA-hydrogels CRF have highly porous structure that allows water to penetrate the hydrogel structures and achieve a maximum swelling capacity of 1400%. The controlled-release effect was achieved using the best-fitting super case II transport mechanism for urea and the Fickian mechanism for

calcium nitrate. The CMC-P4VP-MBA-hydrogels CRF showed significant biodegradability (50% of their initial weight), making them environmentally friendly and appropriate for agricultural applications.

Other controlled-release system using hydrogels as nutrients carrier in agriculture were reported in several studies including Elbarbary and Ghobashy (2017), Satriani et al. (2018), Suresh et al. (2018), Wróblewska et al. (2018), Kenawy et al. (2021) and Diógenes et al. (2022), compared to conventional fertilizers (Chen et al., 2017).

2.7.2 Water Reservoir

Superabsorbent hydrogels (SAH) have become the center of attention among researchers for developing water reservoir for agricultural systems (Montesano et al., 2015; Abobatta, 2018; Saini et al., 2020). This is significant given that agriculture consumes over 70% of fresh water (Doungmanee, 2016; D'Odorico et al., 2020; Heinke et al., 2020). The modern approach to water-stressed irrigation systems may assist the agriculture sectors use water more efficiently. For this reason, SAH can be utilized in agriculture to optimize water resources and reduce water usage. Hence, the agriculture sector can withstand the increasing demand for fresh water. Furthermore, certain water-stressed areas may be able to survive by introducing cellulose hydrogels into their agricultural activities.

In agriculture, SAH, as a water reservoir system, begins to ooze water, the release of which is initiated by a humidity gradient between the inside and outside SAH and is driven by a slow diffusion mechanism (Sabbagh et al., 2018; Das et al., 2020). The SAH water reservoir system works similarly to the nutrients released from hydrogels, as demonstrated in Figure 2.4. Water irrigation applied during cultivation will be absorbed by dried hydrogels, and hydrogen atoms in the polymeric networks of hydrogels will emerge as

positive ions. Following that, several negative ions were left throughout the length of the polymeric chains of hydrogels. The negative ions oppose each other, causing the polymeric networks of hydrogels to generate free passable passages, attracting water molecules, and binding them with hydrogen bonds (Kalhapure et al., 2016).

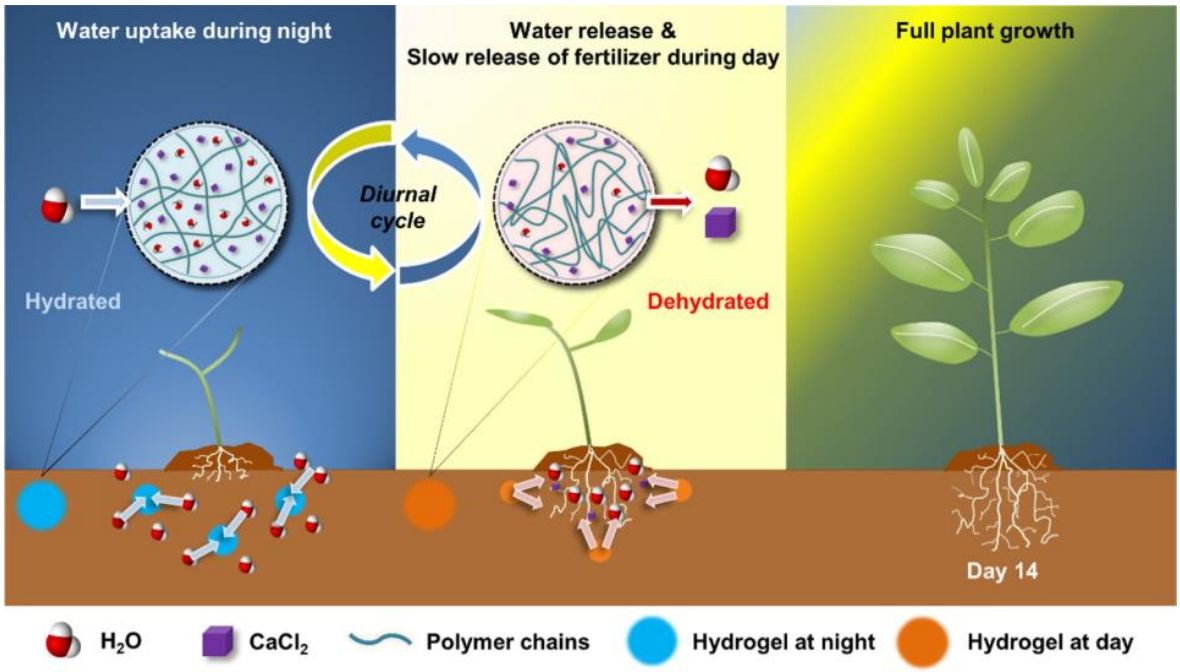


Figure 2.13: Hydrogels as water reservoir system for agricultural application (Das et al., 2020)

The hydrogels can absorb and store large amounts of water and act as a reservoir (Das et al., 2020), allowing water to be available to plants for a longer period (Akhter et al., 2011). When the root zones surrounding began to dry, the hydrogels gradually oozed up to 95% of their stored water for plant absorption (Das et al., 2020). When exposed to another watering condition, rehydration begins and the process of absorbing and storing water into hydrogels continues. This system may improve water availability and enhance water utilization efficiency, as well as maintain soil humidity for longer period (Das et al., 2020). Besides, other molecules incorporated in the polymeric network of SAH, such as fertilizer,

herbicides, and others, can be controlled-released by simple diffusion according to the plants' requirement (Sabbagh et al., 2018; Ahmad et al., 2023). These characteristics make SAH applicable for cultivation in arid and semi-arid regions (Demitri et al., 2013; Sabbagh et al., 2018; Ahmad et al., 2023).

Furthermore, SAH as water reservoir may prevent the drainage or evaporation of water immediately following irrigation (Sabbagh et al., 2018). Besides, swelling ability of SAH is a key feature that is advantageous for soil application which is significantly associated to the size of SAH before and after swelling. Upon contact with water, the dried SAH will absorb a substantial amount of water (Ahmad et al., 2023) and expand in size (Sabbagh et al., 2018). Hence, they will create porosity, as well as increase pores and air pockets in the soil which may improve oxygenation of the roots of the plant and enhance soil aerating (Abobatta, 2018). For this reason, studies found that large hydrogels are better than smaller hydrogels for cultivation (Sabbagh et al., 2018).

In the agriculture industry, cellulose-based hydrogels are most preferred over the other types of hydrogels such as acrylate-based hydrogels (Abobatta et al., 2018; Li et al., 2020; Lawrencia et al., 2021). A novelty in this new functional SAH is their ability to absorb and retain large amounts of water, as well as their stable mechanical properties (Behera & Mahanwar, 2019; Wei et al., 2021; Ahmad et al., 2023). Soils mixed with a small quantity of hydrogels can retain soil humidity for a longer time than moist soil without hydrogels (Sabbagh et al., 2018). Hydrogels can act as buffers against temporary drought stress during cultivation period in severe weather conditions.

As reported by Das et al. (2020), cellulose-based hydrogels were prepared by crosslinking carboxymethylcellulose (CMC) and hydroxyethyl cellulose (HEC) with citric

acid (CA) as a crosslinker. The CMC-HEC-CA hydrogels achieved a substantial swelling ratio of 600%. The CMC-HEC-CA hydrogels swell and release water into plants via diffusion, improving water availability to the plants during cultivation period. This shows that the prepared hydrogels have a promising potential as water reservoir for agricultural use. Similar findings have been reported by Demitri et al. (2013), Wali et al. (2019), Chin et al. (2022) and Mohamed et al. (2022).

In addition, hydrogels have been recently used in fruits and vegetables planting with a significant reduction in water irrigation frequency, such as melon, citrus, strawberry, gerbera, and others (Verma et al., 2018; Jeyabaskaran et al., 2021; Mohammad Padzil et al., 2020). farming.

2.7.3 Potting Medium

Hydrogels have been used as a potting medium in modern agriculture due to their biodegradability and lightweight (Bashir et al., 2020; Mohammad Padzil et al., 2020; Qin et al., 2022). Potting media is a material used for plants cultivation and established roots in an optimum condition (Mehmood et al., 2013; Agarwal et al., 2021). The potting medium is crucial for healthier plants growth. Soil is the most common potting medium in conventional agriculture. This is because, soils are readily available, nevertheless, there are certain drawbacks to their use, such as difficulty in handling and transportation for large-scale production, such as in glasshouses (Rollon et al., 2018).

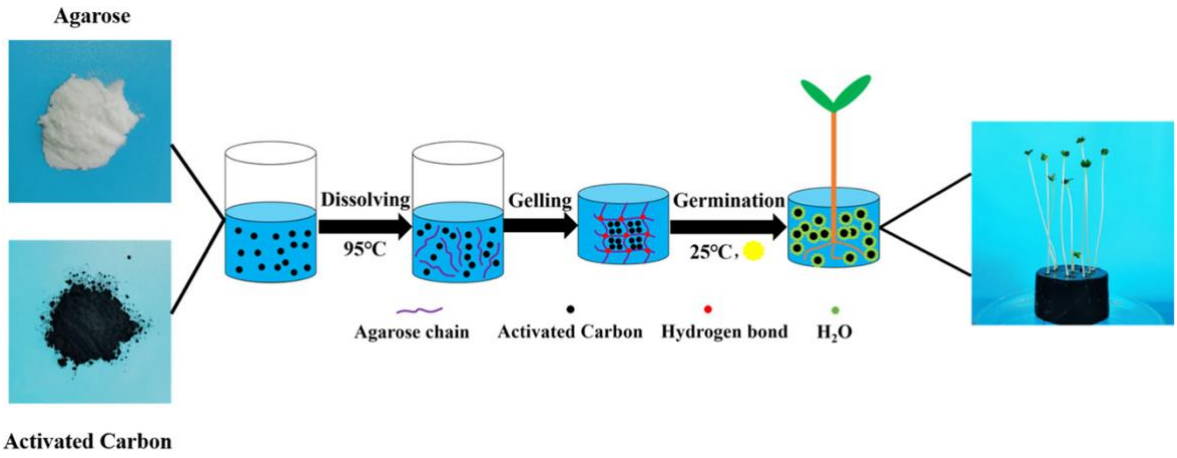


Figure 2.14: Hydrogels as potting medium (Bashir et al., 2020)

Plants in conventional agriculture are susceptible to soil-borne diseases caused by pathogens and parasites (Hayati & Lestari, 2020). Agricultural soils have poor aeration, drainage, and water retention capacity, and they may contain a wide variety of microorganisms and debris on the surface (Olubanjo & Yessoufou, 2019). Besides, soil might potentially be contaminated with heavy metals from some industrial areas (Wuana & Okieimen, 2011). Further, conventional farming is more expensive than urban farming approaches, for instance hydroponics in the long run of operation (Alshrouf, 2017). Therefore, farmers are eager to flee from the constraints of conventional soil-based farming, preferring a better alternative approach through urban farming.

A lightweight potting medium has attracted researchers for soilless modern agricultural approaches due to easy handling. Agricultural-industrial by-products such as rock wood, coco peat, sphagnum moss and perlites have been used as an alternative lightweight potting media (Tm et al., 2020; Agarwal et al., 2021; Gbollie et al., 2021). However, their applications are limited due to ecological and environmental concerns, and some are harmful to plants (Agarwal et al., 2021).

In-depth research on advanced functional materials has led to the development of hydrogels as potting medium (El-Kazzaz & El-Kazzaz, 2017; Zhang et al., 2020; Sikder et al., 2021). Hydrogels are lightweight, highly biodegradable, and environmentally friendly; therefore, they are suitable as potting media in agriculture. Some important features for an ideal potting medium are the ability to hold large amount of water (Xu et al., 2018; Dhanalakshmi et al., 2020), to provide water and nutrients sustainedly over a longer period, porosity (Verma et al., 2018), and cation exchange abilities (Giree & Shrestha, 2018). Since the 1950s, hydrogels have been utilized as a potting medium to enhance root establishment of seedlings (Abobatta, 2018). Several studies on the use of hydrogels as a potting medium have demonstrated that they have a significant positive effect on plants and seedling growth.

In a study by Peyrusson (2021), hydrogels were used as a potting medium for radish seedlings. The hydrogels increased water retention significantly in both sandy soils (27%) and clay soils (44%), compared to sandy soils (16.8%) and clay soils (37.5%) without hydrogels. These properties have led to a significant improvement for healthier radish seedlings. Radish plants increased by 110% in hydrogel-clay soils and 78% in hydrogel-sandy soils, compared to untreated soils which are 3% (clay soils) and 6% (sandy soils). Furthermore, hydrogel potting medium increased radish seeds germination by 27%, whilst radish seedlings failed to germinate in soil analogs.

As reported by Melo et al. (2019), cellulose-based hydrogels prepared have excellent water absorption capacity and have been used to grow tomato seedlings. Their data indicate that the root superficial area and root volume have increased significantly. Therewithal, de Vasconcelos et al. (2020) observed a significant improvement in melon seedlings with larger roots size. Moreover, extensive studies have been conducted on different crops with similar

findings such as chrysanthemum (Anupama et al., 2007), barley, wheat, and chickpea (Ahkter et al., 2011), cucumber (Gholamhoseini et al., 2018), black gram (Dhanalakshmi et al., 2010), Korean mint (Xu et al., 2018), gerbera (Verma et al., 2018) and marigold seeds (Giree & Shrestha, 2018).

2.7.4 Pesticides Carriers

Researchers have motivated to adopt a translational concept of hydrogels as a nutrient carrier into a delivery device for insecticides and fungicides. In agriculture, pest management is crucial to protect crops by applying pesticides (Huang et al., 2018). Statistical report analysis demonstrated that roughly 3.5 million tons of pesticides were applied to crops yearly worldwide (50-60% herbicides, 20-30% insecticides, and 10-20% fungicides) (Hayes et al., 2017; Syafrudin et al., 2021; Tudi et al., 2021). However, less than 1% of the pesticides were precisely reached the targeted pests (Huang et al., 2018; Tudi et al., 2021), and the remaining pesticides were lost to the environment through leaching, evaporation, and volatilization (Campos et al., 2015).

As a result, large number of crops productions are lost due to pests (78% fruits, 54% vegetables, and 32% grains) (Campos et al., 2015; Tudi et al., 2021). Moreover, the loss pesticides reached non-targeted plants, leached into the streams, and accumulated in the sediment soils and bodies of aquatic organisms, posing a health risk to humans, and having an environmental repercussion (Sharma et al., 2019; Syafrudin et al., 2021). Also, it has been reported that the pesticides that are lost to the environment may contaminate drinking water (Yadav et al., 2015; Sharma et al., 2019; Syafrudin et al., 2021). Therefore, there is an urgent need for effective pest management to prevent pesticides loss by increasing their utilization efficiency and ensuring that the pesticides reach the targeted pests.

One feasible approach for effective pest management is using hydrogels as a pesticide delivery matrix. Optimized formulations for pesticide delivery device should be able to provide controlled-release effects to the pesticides, large water holding capacity, prolong residual effects and enhance biological efficacy of pesticides on pest, longer applications intervals, reduce pesticides dosage, be inexpensive, easy availability and biodegradability, as well as safe for human, non-targeted organisms, and the environment (Roy et al., 2014; Campos et al., 2015; Shah et al., 2022).

Meanwhile, hydrogels can be prepared from abundantly available resources, inexpensive, highly biodegradable, high absorption capacities with controlled-release ability, and are environmentally friendly (Lawrencia et al., 2021; Ahmad et al., 2023). This is an essential industrial pesticide delivery technology, especially in agriculture. Studies show that polysaccharide-based hydrogel formulations as pesticides carriers have been extensively explored and widely used in the agriculture sector (Huang et al., 2018; Shah et al., 2022).

Hydrogels, as a controlled-release pesticides (CRP), deliver active ingredients and biocontrol agents to the specified target at an optimal release rate for a longer period (Campos et al., 2015; Huang et al., 2018; Michalik & Wandzik, 2020; Shah et al., 2022). As a result, hydrogels CRP may reduce environmental repercussions by minimizing loss due to leaching, volatilization, and vaporization (Campos et al., 2015). Therewithal, this approach has the potential to increase pesticides loading, enhance the dispersibility and stability of active ingredients, and precisely reach the designated target without affecting non-target organisms (Huang et al., 2018; He et al., 2019).

Reports suggest that the encapsulation of pesticides in the hydrogel matrix enhanced the safety and handling of pesticides (Campos et al., 2015). The more volatile and combustible pesticides were encapsulated in the hydrogel matrix for easy handling and transport, reducing the likelihood of inflammation and evaporation (Campos et al., 2015). Following this, Dailey (2004) has reported a significant reduction in vertical mobility (44.7%) of imidacloprid insecticides encapsulated in hydrogel matrix when applied to soil, compared to the initial technical products (82.3%). Moreover, the volatilization of active ingredients has decreased using hydrogel matrix system (Dailey, 2004). This is consistent with findings as reported in other studies (Wlodarczyk, 2014, Wlodarczyk & Siwek, 2016).

During seed germination, for instance, the initial release of pesticides is not desired because they may harm the germinating seeds due to residual pesticides in the soils (Campos et al., 2015). In this treatment, hydrogel matrix has been designed for controlled release of pesticides in soils. This hydrogels CRP system regulated the initial release of pesticides at a desired rate and dose, reducing the residual pesticides in soils and reduced phytotoxicity (Campos et al., 2015).

Furthermore, studies show that polysaccharide SAHs were developed for controlled release of chlorpyrifos and carbaryl insecticides for control approximately 100 species of insects in soils and several types of crops such as citrus, coffee, cotton, nuts, corn foliage, shade trees, as well as other crops including poultry, livestock, and pets (Baloch et al., 2021). Findings from these studies also highlighted that the hydrogels CRP are highly biocompatible with *Escherichia coli*, thereby resolving a biosafety concern (He et al., 2019). Therewithal, other studies have developed super sorption pesticide hydrogels for insecticides

(Shah et al., 2022), fungicides (Xiang et al., 2018; Supare & Mahanwar, 2022), and herbicides for agricultural applications (Xu et al., 2021; Supare & Mahanwar, 2022).

Further, recent development for hydrogels CRP is formulated for natural pesticide compounds (Gharbi & Tay, 2022) and bioagents (Ropek & Kulikowski, 2009) for potential applications in some organic farming systems that require biocontrol. Several studies have also discussed the applications of hydrogels CRP against pests (Stefan et al., 2020), plants root-feeding insects (Shetty & Prakash, 2020), *Phytophthora capsici* infestation in capsicum (Chang et al., 2021), and ant populations in trees (Stefan et al., 2020). Comprehensive studies have demonstrated the applicability of hydrogels as CRP and have shown encouraging results, indicating that they have a high potential for wide-area agricultural applications.

2.7.5 Hydrogel Baits

Highly porous structure of hydrogels contributes significantly to their high absorption capacity and results in high swelling ability, while preserving their stability without rupturing their shape in the swollen state (Lawrencia et al., 2021; Ahmad et al., 2023). Therefore, they can be used as a potential carrier for liquid sucrose baits (Tay et al., 2020). Their highly porous structures allow absorption of various liquids and deliver various active ingredients to specific sites (Tay et al., 2020). This system is an advanced alternative for ant baiting (Tay et al., 2020). For instance, optimized hydrogels can be immersed in conditioning liquids containing active ingredients and sucrose solution bait, which can be controlled-released to invasive ants (Rust et al., 2015; Tay et al., 2020).



Figure 2.15: Argentine ants feed from alginate hydrogel bead filled with toxic liquid bait (Merill et al., 2018)

As reported in previous studies, hydrogels have been used to deliver liquid bait to control several sugar-fed ant species for fruit crops (Rust et al., 2015; Tay et al., 2017; Cooper et al., 2019). Conventional liquid baiting requires the use of a bait station to store and dispense the sucrose bait (Hogg et al., 2018). Hydrogels, on the other hand, do not require bait stations and dispensers (Rust et al., 2015; Tay et al., 2017; Cooper et al., 2019). Hydrogels could controlled-release the liquid sucrose bait and may sustain the bait palatable for longer period by retaining water (Rust et al., 2015). The liquid sucrose that oozed from the hydrogel matrix triggers ants and attracts them to feed on the liquid sucrose from the surface of the hydrogels without consuming the hydrogel matrix. Liquid sucrose-fed ants will then share the liquid bait with the rest of the colony (Rust et al., 2015). Hydrogels may lose water over time, but they will be rehydrated by irrigation or rainfall, thus resuming their insecticidal activity, and attracting urban pests (Tay et al., 2020; Shah et al., 2022).

Hydrogels as a liquid sucrose bait delivery device is still unrecognized as compared to pesticides carrier (Tay et al., 2020), therefore, only few research on the usage of such applications have been reported. However, according to certain studies, hydrogel baits have been practiced in agricultural fields for almost a decade (Tay et al., 2020). For instance, spherical shapes hydrogels and irregular shapes hydrogels have been used to deliver liquid baits to several ant species including argentine ants (Rust et al., 2015, Cooper et al., 2019), yellow crazy ants (Peck et al., 2017), and western yellow jackets (Rust et al., 2017; Choe et al., 2018).

In a massive scale practice in the conservation areas of the Californian Channel Islands (Rust et al., 2015; Boser et al., 2017; Merill et al., 2018), hydrogels containing liquid sucrose bait and insecticides thiamethoxam were manually hand-spread, as well as using farm fertilizer spreaders and all-terrain vehicles with a motorized hopper. Moreover, a plane carrying hundreds of kilograms of hydrogels baits and insecticides, released and dispersed the hydrogels to inaccessible wild areas. Argentine ant activity was significantly reduced over 74 hectares (Boser et al., 2017) and 177 hectares (Merill et al., 2018).

As reported by Tay et al. (2017), hydrogel baits containing sucrose solution and 0.0001% thiamethoxam insecticide reduced ant activity by 79% over 24 hours. This demonstrates that hydrogels baits have the potential for area-wide applications. Several studies have demonstrated encouraging results in the elimination of invasive ant populations using hydrogels baits in urban, agricultural, and environmental areas such as in Hawaiian Islands (Krushelnycky, 2019), California (Schall et al., 2018; McCalla et al., 2020), and Florida (Tay et al., 2020).

The application of hydrogels not only for ants, but also have been evaluated for control of other pests such as wasp (Choe et al., 2018; Tay et al., 2020; Shah et al., 2022) and cockroaches (Oladipupo et al., 2020; Shah et al., 2022). Most of the research used alginate hydrogels and polyacrylamide hydrogels as ant baits, with encouraging results in wide-area applications. This could serve as a steppingstone to creating natural hydrogels from different polysaccharide sources, which could become a novelty as a new functional ant baiting strategy.

2.8 Rice

Rice is a basic essential food for over 3 billion people globally. More than two billion Asians consume rice-derived goods for 60-70% of their energy needs (Mohd Fairulnizal et al., 2015; Tan et al., 2023). Malaysians of all socioeconomic backgrounds eat rice as part of their daily diet. In Malaysia, rice is the primary food crop, occupying an area of 685,548 hectares and producing roughly 2.57 million tons in 2017 and decreased to 2.34 million tons in 2020 (Abu Bakar et al., 2020; Zakaria et al., 2022).

At the same time, the rice self-sufficiency level in Malaysia remained around 62.6% in 2022 (Yiau, 2023). In accordance with the National Agricultural Policy, the government intends to raise the rice self-sufficiency to 75% by 2025, 80% by 2030 to ensure food security for people (Radin et al., 2022; Yiau, 2023). Meanwhile, Sarawak has just 38% rice self-sufficiency, with the rest imported from other countries (Aubrey, 2022). The rice self-sufficiency level is significantly low that the Sarawak government has targeted increasing it to 60% by 2030 (Aubrey, 2022; Tawie, 2023).

Meanwhile, as mentioned in the previous section, Sarawak is the second largest production area (83,143 ha) for upland rice cultivation (Zainol Abidin, 2023). However, the

average yield of upland rice in Sarawak is the lowest in 2021, amounting to 1.79 ton ha^{-1}, compared to Sabah (2.90 ton ha^{-1}) (Zainol Abidin, 2023). The low upland rice production in Sarawak has reduced the national yield average of rice production in Malaysia (Yiau, 2023; Zainol Abidin, 2023).

Upland rice varieties have not been largely commercialized due to their low grain yields (Radin et al., 2022). However, the low grain yields upland rice is caused by the poor management of farmer during the cultivation period, weed infestation, insect-pest attack, lack water availability and lack mineral supply (Radin et al., 2022; Zainol Abidin, 2023).

2.8.1 *Maswangi* (MRQ74) MARDI Rice Variety

Maswangi, also known as MRQ74, is a Malaysian Agricultural Research and Development Institute (MARDI) specialty rice variety that was first introduced in February 2005. MRQ74 rice was characterized with long and thin rice shape, a high amylose content, a moderate soft gel consistency, a moderate alkali spreading value, and a high gamma-amino butyric acid (Suhaimee et al., 2009; Mohd Yusof et al., 2014). Furthermore, local consumers favored MRQ74 rice as they are flaky, non-sticky, and aromatic rice, with a low glycemic index (Suhaimee et al., 2009; Mohd Yusof, et al., 2014; Abd Rahman et al., 2021).

In 2005, the Area Farmers Organization (PPK) Kangkong, Kelantan, and PPK Langkawi, Kedah were granted licenses for MRQ74 rice. This licensing allows local farmers to plant, process, pack, and sell rice while MARDI provides technical supports and pure seeds for agricultural exposition and promotion to local society purpose (Suhaimee et al., 2009). Residences from small-sized households were the target consumers for MRQ74 rice (Suhaimee et al., 2009). Commercialization of MRQ74 rice may increase the rice self-

sufficiency level and provide an alternative to other specialty rice from Pakistan, such as Ponny and Basmathi rice (Suhaimee et al., 2009; Mohd Yusof et al., 2014). 2022).

2.8.2 Performance Evaluation of Cellulose Hydrogels CRF on the Rice Plants

2.8.2.1 Effect of Cellulose Hydrogels CRF on Growth Parameters

Rice growth is dependent on cell division and cell expansion, which require enough water and fertilizer inputs (Guo et al., 2017; Hashim et al., 2017) and are regularly hampered by low soil moisture and water levels, especially in upland rice cultivation. Hydrogels CRF might improve rice growth by delivering uniform and adequate nutrients supply and extending it until maturity and harvest. Moreover, improved growth is associated with higher plant height (Ahmad et al., 2023). This is because the incorporation of hydrogels CRF in the soil may enhance nutrients uptake by the rice plants near the root zone, hence increasing the accessible nutrients for the rice plants and enhancing the rice growth (Ransom et al., 2020; Leite et al., 2021; Ayadi et al., 2022).

In order to study the effect of hydrogels CRF on the rice growth, growth performance parameters were evaluated including the height (cm) of the rice plants, number of tillers, and the SPAD reading on leaf chlorophyl content (Ho et al., 2009; Hashim et al., 2017; Rea et al., 2019). The data must be collected at specific time intervals (15, 35, 55, 75, 90, 115 and 130 days after days of sowing (DAS)) throughout the rice growing cycle (Ahmad et al., 2023).

2.8.2.2 Effect of Cellulose Hydrogels CRF on Yield and Yield Component Data

In rice cultivation, higher N rates may be related to greater N availability during the tillering stage, which is crucial for cell division (Wang et al., 2018). N-induced cell division promotes panicle formation during reproductive phases of the rice crops (Jahan et al., 2022).

Also, the increased number of grains with increasing N rates could be attributed to a high number of panicles, resulting in a high rice yield (Koutrubas & Ntanos, 2003). During harvest, the number of panicles, number of grains per panicle, grain yield, straw yield, 1000-grain weight, and percentage (%) filled grains were collected to study the effect of hydrogels CRF on yield and yield component.

Several findings have shown positive effects on yield and yield component data of various crops with the applications of hydrogels CRF (Table 2.2). This includes pearl millet seed (Singh 2012), sunflower seed (Nazarli et al., 2010) and chrysanthemum seed (Allahdadi et al. 2005), orange trees (Bey et al., 2021), and parsley (Karipcin, 2023).

Table 2.2: Summary of hydrogel CRF applications on crops

Crops	Yield component and yield		
	Effective tillers /stem shoot	Yield (ton ha^{-1})	Harvest index (%)
Pearl millet seed (Singh, 2012)	3.09	1.98	30.79
Sunflower seed (Nazarli et al., 2010)	4.0	0.25	19.53
Parsley (Karipcin, 2023)	3.3	ns	ns
'Maltaise Ballerin' orange trees (Bey et al., 2021)	ns	24.1	ns
Chrysanthemum (Allahdadi et al., 2005)	15	11.96	ns

2.8.2.3 Effect of Cellulose Hydrogels CRF on Nutrient (N) Uptake and Nutrient Use Efficiency (NUE)

Hydrogels CRF acts as a nutrients carrier which can control the release of nutrients in soils near the root zone and thus better matching the rice needs (Lawrencia et al., 2021). In comparison to conventional farmers' fertilizer practices, hydrogels CRF may prevent nutrients loss to the environment through leaching and surface run-off by encapsulating nutrients in their polymeric networks (Lawrencia et al., 2021). Hydrogels CRF will control the release of nutrients according to the requirements of the rice plants and sustainedly supply nutrients throughout the rice growing cycle. Therefore, rice may absorb sufficient nutrients for better N uptake, increased nutrient use efficiency, healthier rice growth, and increase rice output (Lawrencia et al., 2021).

In order to study the effect of hydrogels on nutrient uptake and NUE in rice, the vegetative parts and rice grains will be collected to determine their nutrient content. The nutrient content of rice plant materials will be determined by the modified Kjeldahl acid-digestion method using concentrated sulfuric acid (Ho et al., 2009; Sarfraz et al., 2017; Hanafi et al., 2009). Formulae to calculate nutrient uptake, NUE and NAE indices will be discussed in Chapter 3.

2.8.2.4 Correlation Regression Study

In regression analysis study, the independent variable has a significant relationship with the dependent variables, assessing the relative intensity of the effect of independent variables on the dependent variable and making predictions (Hastini et al., 2019). The coefficient of determination (R^2) is a measure of the accuracy or deviation of prediction in regression analysis. The coefficient of determination (R^2) indicates the size of the model

corresponds to the dependent variable in comparison to the mean. The measure R^2 can be determined using the following equation:

$$R^2 = \frac{SS_R}{SS_T} \qquad \text{Equation 2.8}$$

where SS_T (total variation or sum of squares) is the total number of all square difference of between each observation and the average. Whereas SS_R (sum of squared regression) is the variation in the data described using regression analysis R^2 and has a value between 0 and 1. When the value of R^2 approaches 1 (i.e, $R^2 = 0.998$), it shows the best fit to the model, hence it can be assumed that more variation in *y* can be explained by variation in *x*.

In addition, R^2 is used to measure the magnitude of the regression equation strength. R^2 value indicated the variability percentage of the dependent variable that was explained by the model. R^2 or coefficient of determination gave the information on how high the dependent variable variation was due to the independent or predictor variable (Hastini et al., 2019).

To execute correlation regression analysis, it is assumed that the dependent and independent variables have a mathematical relationship. The relationship can be described as either a straight line (linear regression), a polynomial curve (polynomial regression), or a non-linear relationship (non-linear regression) (Badaruzaman & Tiong, 2022). Following that, a scatter plot of the dependent and independent variables was plotted, and the most likely values for the coefficient of determination (R^2) were obtained (Putri et al., 2020; Han et al., 2022). The relationship between two or more variables is established using regression

analysis. Besides, regression analysis demonstrates how the standard value of the dependent variable varies with the change of any independent variables while the other independent variables remain constant (Kang et al., 2021). Linear regression is one of the most commonly used mathematical modelling techniques.

In other words, correlation and regression analysis were the common techniques used to elucidate the relationship between two quantitative variables. How strong the relationship between two quantitative characters could be analysed using correlation, while regression analysis gave the information about the direction and causal-effect relationship in the equation form (Hastini et al., 2019).

The common issues in the correlation relationship of the rice agronomical characters were grain yield, plant height, number of tillers per plant, panicle length, number of grains per panicle, 1000-grains weight, and number of filled grains per panicle (Hastini et al., 2019). Number of grains per panicle usually had a positive correlation with the panicle length, and number of filled grain per panicle (Hastini et al., 2019).

As many studies had shown that the grain yield showed a positive and significant correlation with the number of grains per panicle, then the number of grains per panicle could be used as the dependent variable in a regression with other traits (Hastini et al., 2019).

This study aimed to understand the correlation and regression relationship between the number of grains per panicle with other traits of rice panicle branching. The other traits would be used as a predictor in the regression analysis. Furthermore, this study could give the information on the panicle branching traits contribution to the total grains number per panicle.

Previous study by Sun et al. (2017) on the correlation and regression of rice reported that, rice traits being studied showed the striking positive correlations among the panicle length, grains number per panicle, primary panicle branch, and secondary panicle branch. Moreover, Bagheri et al. (2011) and Norain et al. (2014) reinforced the statement that there was a high significant and positive correlation between the number of grains per panicle and panicle length.

Meanwhile, Karim et al. (2014) reported that the number of primary panicle branches per panicle had a highly significant and positive correlation with the number of filled grains per panicle. The total number of grains per panicle was used as the main trait as it is expected to reflect the potential yield of tested rice genotypes.

In line with this expectation, Devi et al. (2016) found that the relationship between the number of grains per panicle and the grain yield per plant was positively and highly significantly correlated. In the other case, the filled grains per panicle indicated positive and highly significant indirect correlation with the yield per ha in phenotypic and genotypic level (Oladosu et al. (2018).

2.8.3 Nitrogen (N)

2.8.3.1 Nitrogen (N) in Soils

Nitrogen (N) is an important nutrient that plants need to grow. It helps them make proteins and chlorophyll, which are necessary for their growth and health. The nitrogen cycle is a repeating cycle of processes during which nitrogen moves through both living and non-living things: the atmosphere, soil, water, plants, animals and bacteria. In order to move through the different parts of the cycle, nitrogen must change forms. In the atmosphere,

nitrogen exists as a gas (N_2), but in soil, N comes in different forms, such as organic nitrogen, inorganic nitrogen, ammonium (NH_4^+), and nitrate (NO_3^-).

Organic nitrogen comes from dead plants and animals. Plants are unable to use the organic nitrogen until it is broken down by tiny organisms in the soil. In comparison, inorganic nitrogen comes in two forms that plants can use immediately when available. Whereas, ammonium (NH_4^+) is a form of nitrogen that plants may absorb easily, while nitrate (NO_3^-) is another form of nitrogen that plants can absorb, however it can easily be washed away by water.

N moves through the soil in a cycle, involving several key steps including nitrogen fixation, mineralization, nitrification, denitrification, leaching and volatilization. Nitrogen fixation occurs when some plants, such as beans and peas, have bacteria that could turn N from the air into a form that plants can use. Mineralization occurs when tiny organisms in the soil break down dead plants and animals, releasing nitrogen as ammonium. Meanwhile, nitrification occurs when ammonium changes into nitrate, which is another form that plants can use. Other cycle such as denitrification which may occur in areas without much oxygen (like waterlogged soil), some bacteria turn nitrate back into nitrogen gas, which escapes into the air. Other process involves leaching and volatilization, which means that N could be lost from the soil to the environment when nitrate gets washed away by water or when nitrogen gas escapes into the air.

Nitrogen often used as a source of fertilizer. Farmers often add N fertilizers to soil to help crops grow. These fertilizers include things like urea or ammonium nitrate. However, using too much N fertilizer can lead to problems, such as pollution of rivers and lakes, or the release of gases that contribute to climate change. However, N deficiency may occur,

especially when plants receive insufficient N fertilizers. Symptoms such as plants that turn yellow (especially the older leaves), grow slowly, and produce fewer fruits or vegetables could be observed. This may happen if there is insufficient N available in the soil due to poor fertilization, excessive water which may wash N fertilizer away, or not insufficient organic matter. However, excessive use of N fertilizers may also cause harm to the environment as discussed in the previous section. Therefore, it is important to apply the right amount of N fertilizers to soils, according to the needs of the crops to prevent wasting N fertilizers and harming the environment, thus increasing the crops production.

2.8.3.2 The Importance of Nitrogen (N) in Rice Cultivation

N fertilizer is crucial for rice cultivation because which influences the growth, yield, and quality of the rice plants. Sufficient supply of N fertilizer to the rice plants may boost growth and development of the rice plants, thus producing taller rice plants. Besides, taller rice plants is associated with sufficient N availability to make enough proteins for the rice plants growth. Besides, the rice plant may grew stronger and develop more tillers, panicles and leaves. Moreover, N is essential for making proteins to promote the formation of enough chlorophyll on the rice leaves, which allows them to perform photosynthesis. Further, sufficient N availability helps the rice plants to produce proteins and enzymes, which are important for cell growth and overall rice plant health. In addition, N promotes the initiation of more tillers, which means more rice-producing stems or panicles, thus more space for the formation of grains per rice panicle (the cluster where grains form) and improves grain size, leading to higher yields. Therefore, this may increase the rice yield and better quality harvest.

As reported in other studies, the rice plants need different amounts of N at different stages of growth. Proper management ensures that N is applied at the right time to maximize

the rice plants development. Excessive use of N may lead to excessive leaf growth, making the rice plants more vulnerable to pests and diseases, while also wasting resources and causing environmental issues like water pollution. Therefore, in rice cultivation, N is key for healthy plant growth, higher yields, and better-quality grains. Proper nitrogen management ensures that rice gets what it needs without harming the environment.

2.8.3.3 Influencing Factors of Soil N Availability for the Rice Plants

Soil nitrogen (N) availability is influenced by several factors that affect how nitrogen is cycled, retained, or lost in soils. These factors determine how much N is available for the rice plants to absorb and use for growth. The N availability in soils can be influenced by soil organic matter. Organic matter is a primary source of N in soils. As soil organisms break down organic material, such as dead plants and animals, N is released in a process called mineralization. Mineralization occurs when organic N is converted into ammonium (NH_4^+) and nitrate (NO_3^-), which are forms that the rice plants can absorb.

Next, soil N availability can be influenced by the soil temperature. Temperature influences microbial activity, which is crucial for N cycling. Warmer temperatures accelerate the breakdown of organic matter and may increase mineralization rates, producing more N, thus increasing N availability in soils. In contrast, cold temperatures may slow down these processes, thus reducing N availability in soils.

Further, soil moisture may affect the N availability in soils. The presence of water in the soils affects N dynamics. In other words, optimal soil moisture enhances microbial activity and the mineralization of organic N. Whereas, excess soil moisture may lead to N loss through leaching or denitrification.

Another common condition that may influence soil N availability is drought. Drought conditions limit N availability by reducing microbial activity and N movement to the rice plants roots. For this reason, many farmers have to apply N fertilizers multiple times to cover the loss N fertilizer throughout the rice cultivation period.

Soil pH may affect N availability in soils because soil pH will directly affect the chemical form of N and any microbial activity in soils. For instance, in acidic soils, ammonium (NH_4^+) tends to be the dominant form of N. Whereas, in neutral or alkaline soils, nitrate (NO_3^-) tends to be the dominant form of N. Another condition such as extremely acidic or alkaline, this condition may inhibit microbial processes, such as nitrification, thus limiting N availability.

Furthermore, human factor such as fertilization and manure application will inevitably affect soil N availability. For example, N fertilizers such as urea, ammonium nitrate, and organic materials such as manure and compost will increase soil N levels. However, poor application timing or excessive use of N fertilizer may lead to N losses through leaching, surface run-off, volatilization, and denitrification.

Other factor such as soil texture may also influence soil N availability. Soil texture, or the proportion of sand, silt, and clay, influences N retention. In other words, sandy soils tend to have higher drainage, thus would not be able to hold and retain N in soils. Thus, this will cause faster N loss through leaching. Soils such as clay-rich soils which have denser texture, this type of soil may hold and retain water and nutrients more effectively, reducing N loss, thus improving N availability to the rice plants.

In summary, factors like soil organic matter, temperature, moisture, pH, fertilization, texture, biological fixation, and soil management practices play important roles in determining how much nitrogen is available in soils for plant uptake.

2.9 Chapter Summary

This chapter provides an in-depth review of past literature related to this study. Firstly, the earlier studies on cellulose-based hydrogels and their methods of synthesis were reviewed to gain a better understanding of the concept of hydrogels formulations. It was then followed by the discussion of prior literature focusing on the key characteristics of agricultural hydrogels, where crucial factors determining their characteristics and optimum formulations for agricultural applications were identified.

This chapter also reviewed the categories of cellulose-based hydrogels which have been extensively studied primarily for agricultural applications. As nutrient release from cellulose-based hydrogels is the unit of analysis of this study, this study also provides the review of literature on the definition of controlled-release fertilizer, as well as possible mathematical models for nutrient release profile from hydrogel and polymer granules context.

As a respond to the increasing use of hydrogels for agricultural applications, this chapter was then presented the review of several studies that investigated the use of hydrogels in agriculture. Review of literature on rice variety and the variables used in this study were also provided in this chapter. The review of literature on responsive variable – the effects of hydrogels CRF on rice growth performance was discussed.

The following chapter – Chapter 3 explains research methodology used in this study. Discussion on both quantitative and qualitative research design will be presented. This

chapter presents all parameters used to develop and achieve research objectives. The development of measurements of each variable used in this study will be discussed in more detail. The chapter also includes the discussion of data collection and data analysis for both quantitative and qualitative phases.

CHAPTER 3

MATERIALS AND METHODS

3.1 Introduction

The purpose of this chapter is to introduce the research methodology and techniques applied for the fabrications of cellulose hydrogel CRF for upland rice cultivations in Sarawak. This approach allows for a more in-depth understanding on the optimal formulations to meet the key characteristics of cellulose hydrogel CRF for rice cultivation, as well as simulating the real field trials to develop theory from data to understand how hydrogel CRF affects growth performance and yield of rice. The applicability of cellulose hydrogel CRF and a constructivist approach for this study are discussed in-depth in this chapter.

The research framework, research methodology, and analysis method used in this study are also primary components of this chapter. This chapter consists of four sections. The first (Section 3.2) described the summary of various methods and analyses involved in this study. In section 3.3, optimum urea-loaded cellulose-based hydrogels as a controlled release fertilizer is fabricated. The following section (3.4) is about conducting greenhouse experiments. The experiments were conducted to evaluate and fine-tune fertilizer loading capacity and release rates to match the needs of the rice plants, as well as studying the effect of cellulose hydrogels on the growth performance and yield of upland rice in Sarawak. Finally, Section 3.5 studies the nitrogen (N) uptake and nitrogen use efficiency (NUE) estimation of rice cultivation using hydrogel CRF. This section also includes determining the dry matter accumulation and dry matter partitioning of the rice plants. Additionally,

correlation regression analysis was studied to determine the relationship between dependent and independent variables which affect the rice growth performance and production.

3.2 Summary of Methods Involved in the Research

In this study, three materials of interest; wastepaper, sodium carboxymethyl cellulose (CMC) and epichlorohydrin (ECH) were used to synthesize urea-loaded cellulose hydrogels. Procedures and tests employed in this study were summarized as in Figure 3.1. Firstly, the synthesis of cellulose hydrogel of various cellulose and CMC concentrations were conducted via crosslinking reaction. After, the synthesized cellulose hydrogels underwent various characterization techniques to identify the optimum formulation to be used as CRF.

Thirdly, the optimum formulation of cellulose hydrogel was selected for further analysis to make cellulose hydrogel CRF such as soil moisture test, loading and release of urea, and kinetic release of urea in water and soil. Subsequently, the cellulose hydrogel CRFs were employed in upland rice cultivation to fine-tuning and evaluate their performance in rice cultivation. Various analyses throughout the growing stages of rice cultivation were conducted as depicted in Figure 3.1.

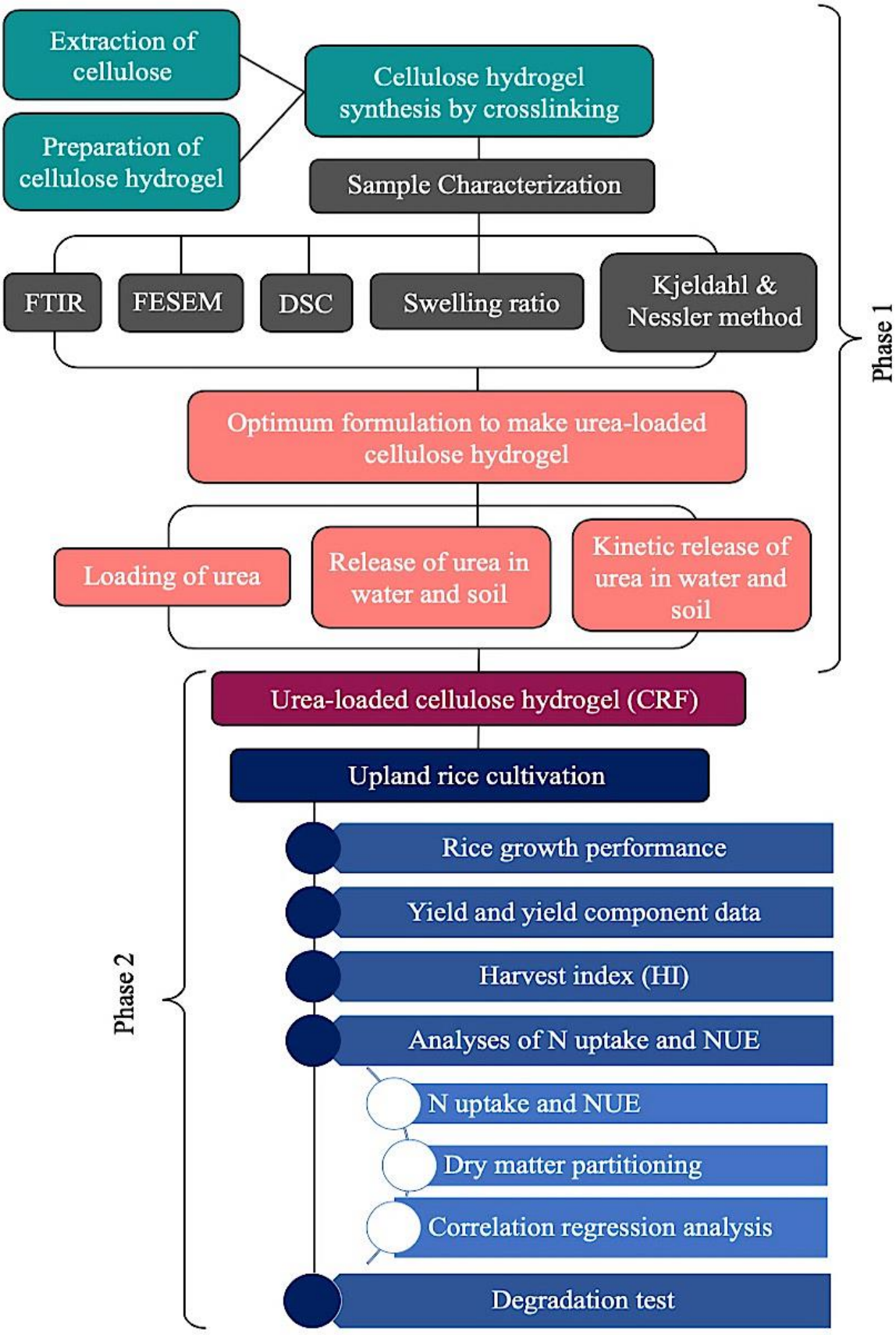


Figure 3.1: Experimental design involved throughout the research

3.3 Fabrication of Urea-loaded Cellulose Hydrogels

3.3.1 Chemical Reagents and Materials

Cellulose fibers extracted from wastepaper (sorted office papers) were used as a precursor material which was collected from the Faculty of Resource Science and Technology (FRST), at University Malaysia Sarawak (UNIMAS). Sodium carboxymethyl cellulose (CMC, molecular weight = 262.9) was supplied by Sigma Aldrich (Wisconsin, United States of America). Epichlorohydrin (ECH, ≥ 99% GC, molecular weight = 92.52) was supplied by R&M Chemicals (Essex, United Kingdom). Sodium hydroxide (NaOH, molecular weight = 40) was supplied by Sigma Aldrich, while urea (N_2H_4CO, molecular weight = 60) was supplied by HmbG Chemicals (Hamburg, Germany). Reagent solution for the Kjeldahl procedure and the Nessler method was purchased from Hach Company/Hach Lange GmbH (United States of America). All chemicals were used without further purification (Ahmad et al., 2023).

The upland rice seeds were provided by the Malaysian Agricultural Research and Development Institute (MARDI). Soils (topsoil, wet clayey soils and sandy soils) were collected from Plant Research Centre (PRC), UNIMAS.

3.2.3 Soil Properties

Topsoil is characterized as red or yellow podzolic soil (as defined by the Sarawak Soil Classification System). The soil is acidic (pH 4 – 5) and sandy clay-like (30 – 50% clay) (Tanaka et al., 2009; Sellan et al., 2021). The cation exchange capacity (CEC) clay value of topsoil is greater than 24 cmol kg^{-1} (Tanaka et al., 2009; Sellan et al., 2021).

Wet clayey soil is classified as gley soil (as defined by the Sarawak Soil Classification System) (Perumal et al., 2015). The soil is alkaline (pH 8 – 10) and contains clay minerals, with the gleied layer occurring within the reach of the root systems or cultivated plants, i.e., the gleied horizon or 50% gleiing within 50 cm below O horizon (top of the soil structure which made up of mostly organic matter) (Perumal et al., 2015). Wet clayey soil is sticky and has a plastic texture when wet, can become hard, brittle, and non-plastic when dried (Perumal et al., 2015).

Sandy soil is classified as arenaceous soil (as defined by the Sarawak Soil Classification System) and has pH levels ranging from 5.8 to 6.3 (Ho et al., 2009). Mineral soil content with a sandy particle-size class is present in the upper 50 cm or more of the profile (Ho et al., 2009).

3.3.3 Extraction of Cellulose Fibers

Shredded waste papers (250 g) were pulverized, soaked in distilled water (2000 mL) in a 2000 mL beaker (HmbG borosilicate glass beaker) with continuous stirring at 2000 rpm for 2 h. Following that, the filtered waste papers were treated with 12% (w/v) NaOH under constant stirring for 12 h (Chin et al., 2018). After, the extracted cellulose pulps were rinsed with distilled water multiple times to eliminate excess NaOH before drying in an oven at 60 °C in 3 – 5 days or to a constant weight. The dried cellulose fibers were ground and sieved through a 60 mesh.

3.3.4 Preparation of Cellulose Hydrogels

Cellulose hydrogel was prepared by adopting the procedure used by Chin et al. (2018) and Alam et al. (2019). Prior to usage, a 7:12% (w/v) NaOH/urea (NU) solvent was prepared (using a 500 mL HmbG borosilicate glass beaker) and precooled (–20 ºC). Cellulose fibers (obtained from 3.3.3) were dissolved in the NU solution and agitated at 2000 rpm for 1 h. Different concentrations of cellulose fibers (wt%) and CMC (Table 3.1) were added to the NU solvent to form a suspension. For instance, to make a C1 cellulose hydrogel, 1% (w/v) cellulose was dissolved in the NU solvent for 1 h before adding 1.75% (w/v) CMC.

The suspension was well agitated until the CMC had completely dissolved (until there is no more clumping CMC powder observed in the beaker). Following that, 5 mL of 99% ECH was gently added to the mixture and agitated at 1800 rpm for 15-25 min at room temperature, until the mixture formed a highly viscous gel (Muharam et al., 2017). The viscous gel was then frozen at -20 °C overnight to facilitate crosslinking and the formation of hydrogels (Chin et al., 2018). After that, the hydrogel was retrieved by thawing at room temperature, soaked in excess distilled water, and thoroughly washed to remove excess ECH. Finally, the hydrogel was oven dried at 50-60 °C to a constant weight, stored in a closed vials and placed in a humidity control dry cabinet (Hengkai 250 L) for further analysis.

Table 3.1: Composition of cellulose-based hydrogels

Composition	Cellulose concentration (% w/v)	CMC concentration (% w/v)
C1	1.0	1.75
C2	2.0	1.75
C3	3.0	1.75
C4	4.0	1.75
C5	5.0	1.75
CMC2.0	3.0	2.0
CMC2.5	3.0	2.5
CMC3.0	3.0	3.0
CMC3.5	3.0	3.5
CMC4.0	3.0	4.0
CMC4.5	3.0	4.5
CMC5.0	3.0	5.0

3.3.5 Sample Characterization

Dried cellulose hydrogel was analysed using Fourier Transform Infrared (FTIR) Spectrometer (Thermo Scientific Nicolet iS10) with a wavenumber range of 400 to 500 cm^{-1} using ATR technique. The surface morphology of the specimen was examined using a 1000x magnification Field Emission Scanning Electron Microscope (FESEM) (JEOL JSM-IT500HR). Differential Scanning Calorimetry (DSC) (Netzsch-Geratebau GmbH-DSC 200 F3 Maia Thermal Analyzer) was used to assess the thermal stability of the specimen in the temperature range of -150 °C to 600 °C. VELP Scientifica Kjeldahl equipment was used for

Kjeldahl nitrogen determination throughout this study. The Nessler method (method 8075 reagent solution) using Hach (an EPA approved method for TKN following the sTKN method using TNT880) was used to analyze data.

3.3.6 Swelling Ratio

The swelling behavior of cellulose hydrogels was examined using an immersion technique in distilled water at room temperature. A pre-weighed, dried regular-shaped hydrogel specimen was immersed in a 250 mL distilled water (using 500 mL beaker) in a controlled condition. Mass of the hydrogel were recorded until they were constant. The swelling ratio (%) was calculated using Equation 3.1 (Kirchmajer et al., 2013).

$$\text{Swelling ratio} = \frac{\text{M}-\text{Mf}}{\text{Mf}} \times 100 \qquad \text{Equation 3.1}$$

where M and Mf are mass (g) of the swollen and dried specimens, respectively.

3.3.7 The Soil Moisture Properties

The soil moisture properties were determined by adopting procedure used by Panescu et al. (2022) and Jong et al. (2023). Soil moisture was measured using an Extech Instruments-MO750 digital soil moisture meter. A 200 g sample of each type of soil was placed in a 90 mm petri dish borosilicate glass and dried to a constant weight in the oven at 60 °C. After, the dried soils were collected and transferred into a 200 mL beaker. A 0.25g, 15 mm optimized cellulose hydrogel (i.e., hydrogels selected from previous test with the highest porosity on their morphological structure and the highest swelling percentage) was then buried in dried soils. The hydrogel was placed approximately 5 cm beneath the dried soil surface. Right after, initial soil moisture content was measured. The moisture content of each

soil was measured again after 1 week to determine the moisture properties of cellulose hydrogels in soils. A control treatment involving soils without cellulose hydrogel was also included.

The moisture content of each soil was determined again after 1 week period, because most soils should take about 1 week to dry out after normal watering (Panescu et al., 2022). If soils are still wet for more than a week, without outside contributing factors, such as rain or flooding, there might be a waterlogging or drainage problem (Panescu et al., 2022). Therefore, in this study, control treatments without hydrogels were conducted to ensure that there will be no outside factors affecting the soil moisture contents. Whereas the presence of hydrogels in each type of soil are expected to increase and retain the soil moisture content after 1 week.

3.3.8 Loading of Urea Determination

The optimized cellulose hydrogel was selected for the fabrication of urea-loaded cellulose hydrogels as a controlled-release fertilizer (CRF). The selection criteria were based on their porosity, swelling and soil moisture properties.

Urea-loaded cellulose hydrogel was fabricated by adopting the method used by Li et al. (2016). A pre-weighed, dried regular shape hydrogel sample was soaked in a 2.5% (w/v) urea solution for 48 h in a controlled condition. The swollen urea-loaded hydrogels were dried in an oven (60 °C) to a constant weight. The loading capacity (g/g) of fertilizers was computed using the following equation.

$$\text{Loading capacity } \left(\frac{\text{g}}{\text{g}}\right) = \frac{(\text{Total amount of urea}) - (\text{Nonbound urea})}{\text{Weight of hydrogel}} \quad \text{Equation 3.2}$$

The total N in the solution was measured using Kjeldahl procedure and the Nessler method (Li et al., 2016) (Appendix 1). This method was conducted by adopting the methods from Hach et al. (1987) and Rossi et al. (2004).

3.3.9 Release of Urea in Water and Soils

The release of urea in water and soil was established by adopting the procedure used by Li et al. (2016) and Liu et al. (2019). The urea-loaded, dried hydrogel was immersed in 100 mL distilled water (using a 250 mL beaker) and incubated at 20 °C to estimate the nitrogen release. Solution (2 mL) was collected (using a 5 mL syringe) at intervals 1, 3, 5, 7, 11, 14, 22, and 30 days, or the time when the total release of the fertilizers reached over 80%. Following that, 2 mL of fresh distilled water was added to maintain the total liquid volume at 100 mL. A control treatment involving free urea was also conducted. The total N concentrations of the collected solution were measured using Kjeldahl procedure and the Nessler method (Rossi et al., 2004) (Appendix 1).

To investigate the release of urea from cellulose hydrogel in soils, the dried, urea-loaded, cellulose hydrogel was placed in non-woven plastic mesh bags and buried 5 cm beneath the surface of the soil in a beaker containing 200 g of dried soil. Water (70 mL) was irrigated to the soil twice daily as control, and to allow urea oozes from cellulose hydrogel. A small amount of soil specimen (0.25 – 0.30 g) were collected at 1, 3, 5, 7, 11, 14, 22, 30 and 42 days. A control treatment involving the release of free urea in the soils was also included. The N content in the soil was determined using Kjeldahl procedure and the Nessler method (Rossi et al., 2004) (Appendix 1). Each treatment was performed in triplicates. To study the release behavior of the cellulose hydrogels in different soils, three types of soils were used: topsoil, wet clayey soil, and sandy soil.

3.3.10 Release Kinetics of Cellulose Hydrogels

The release behavior of urea from cellulose hydrogels in water and soils was analyzed using the Korsmeyer-Peppas equation (Korsmeyer et al., 1983) given in Equation 3.3:

$$\frac{M_t}{M_\infty} = K_{KP} t^n \qquad \text{Equation 3.3}$$

where K_{KP}, t, and n are diffusion constant, time, and exponent of the release mechanism, respectively. M_t/M_∞ is the fraction of fertilizer released at the time, t. The nutrient release mechanism is categorized based on the value of n. The value of $n < 0.45$ indicates that the fertilizer release mechanism is a Fickian model, whereas $0.45 < n < 0.89$ indicates that the fertilizer release mechanism is a non-Fickian diffusion transport. When $n > 0.89$, nutrient release follows case II transport (Korsmeyer et al., 1983).

3.4 Greenhouse Experiments

3.4.1 Materials

In this study, the Mardi rice variety (MRQ74) was used. Malaysian Agricultural Research and Development Institute (MARDI) provided the MRQ74 rice seeds for this study, which allows the use of the rice seeds for rice cultivation and collection of seeds and vegetative parts of the rice plants for analysis, reports, publications, and other purposes, as well as agricultural exposition and promotion to local society. The experiment was conducted in accordance with corresponding institutional, national, and international rules and legislation.

3.4.2 Experimental Details

A pot experiment (Figure 3.2 and 3.3) was used to examine the effects of urea-loaded cellulose hydrogels-controlled release fertilizer on rice growth and yield. The experiment was conducted during the year of 2022 (June–December) in a mini greenhouse located at Pusat Penyelidikan Tumbuhan (PPT), Universiti Malaysia Sarawak (UNIMAS), Kota Samarahan, Sarawak (1°28′09.3″N, 110°25′41.3″E) (Figure 3.4). The climate was tropical rainforest characterized by high temperature (31–33 °C) and rainfall (which may vary from nearly nothing to 70 mm) during the entire rice growth period.

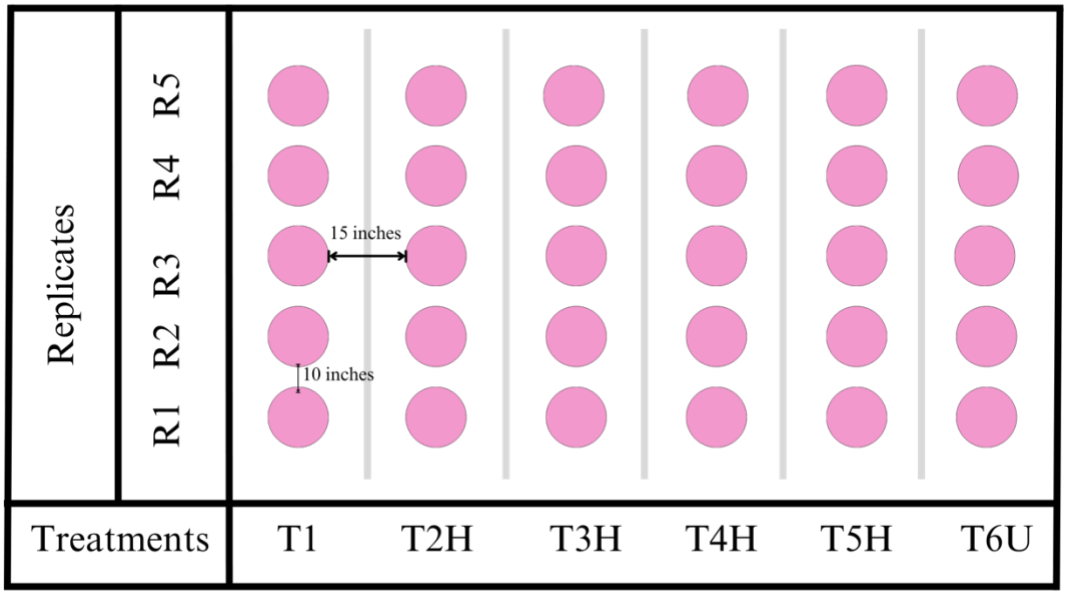


Figure 3.2: Graphical representation of pot experiment indicating pots were arranged in a block design



Figure 3.3: A group of the rice plants in pots

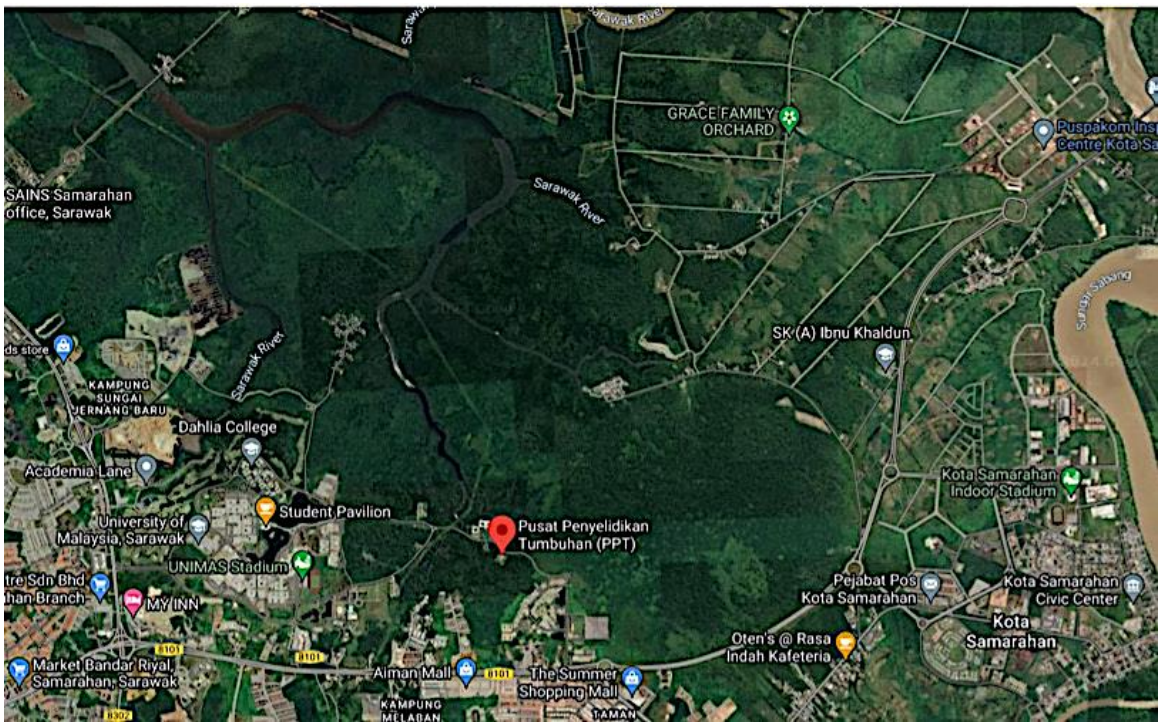


Figure 3.4: Locality map of experimental site at UNIMAS, Kota Samarahan (Google Maps, n.d)

Topsoil (0–30 cm depth) was collected from the same location, air-dried, ground, and sieved through a 0.2 mm mesh for soil analysis (Ho et al., 2009). Soil pH and available total N in topsoil of the experimental site were measured (Rea et al., 2019, Chen et al., 2018). Total N in topsoil was 0.141%, with 0.6% P, 0.83% K, 1.5 mg kg^{-1} Zn, 23.7 mg kg^{-1} Fe, 2.7 mg kg^{-1} Mn, and 1.36 mg kg^{-1} Cu (Lawrencia et al., 2021). Soil pH was 4.83 and measured using Sonkir Soil pH meter MS02.

Planting pots with an inside top diameter of 30.5 cm, a bottom diameter of 26.6 cm, and a height of 30 cm were used. Each pot was filled with 12 kg of uniform topsoil. The experiment comprised of 6 treatments (Table 3.2), each with 5 replications to account for variance amongst the rice plants in a completely randomized block design. Each treatment was arranged in a separate block of pots at different coordinates in the greenhouse. The experiment was executed with different treatments to minimize the effect of variation from the experiment occurring at different periods.

In addition, treatments consisted of the recommended dose of fertilizers (RDF) according to the nutrient requirement for upland rice cultivation in previous studies (Ho et al., 2009; Munda et al., 2016; Hashim et al., 2017; Karki et al., 2018). Therefore, a series of RDF was selected, including T1 with no fertilizer applied as a control, 30 kg N ha^{-1} in T2H (25% RDF), 60 kg N ha^{-1} in T3H (50% RDF), 90 kg N ha^{-1} in T4H (75% RDF) and 120 kg N ha^{-1} in T5H (100% RDF). As an initial study, RDF for 12 kg of soil in pots was computed using equation 3.4 (Sarfraz et al., 2017) and applied as in Table 3.2. Urea (46% N) was used as a source of fertilizer.

Paddy seeds were soaked in water to remove unfilled seeds floating on the surface of water, while the filled seeds were collected and dried. After, 6 filled seeds were inserted to

247 a soil depth of 5 cm in the pots. Before rice sowing, dried urea-loaded cellulose hydrogels
248 were placed in a pail of topsoil (8-10 cm soil depth), for T2H, T3H, T4H, and T5H treatment.
249 The urea-loaded cellulose hydrogels were covered with topsoil, and the soils in the pots were
250 hydrated with water.

251 The rice plants growth experiment lasted for 130 days. Throughout the study, there
252 was no standing water observed during the entire growing period of the rice plants to
253 simulate the actual field conditions. Water irrigation was applied 10 days after sowing and
254 at 2-day intervals to reduce water scarcity on the rice plants and allow the rice plants to reach
255 the maturity stage (Elbarbary & Ghobashy, 2006; Davidson et al., 2013). Manual weeding
256 and insect, pest, and disease management practices were executed to minimize crop losses.
257

$$\text{Amount of Fertilizer per pot} = (\text{Recommended Dose of Fertilizer (RDF) / 1 ha)} \times \text{weight of soil in a pot} \quad \text{Equation 3.4}$$

258

259 **Table 3.2:** List of treatments with different N fertilizers doses

Treatment	Amount of N fertilizers
T1	0 N (control)
T2H	1.6 g N pot^{-1} hydrogels = 25 % RDF
T3H	3.2 g N pot^{-1} hydrogels = 50 % RDF
T4H	4.8 g N pot^{-1} hydrogels = 75 % RDF
T5H	6.4 g N pot^{-1} hydrogels = 100 % RDF
T6U	6.4 g N pot^{-1} urea (100 % RDF) applied with three split applications at 15, 35 and 55 DAS

260

3.4.3 Rice Growth Performance

Plant heights (cm), number of tillers, and SPAD meter readings were collected as the components of rice growth performance data. Data were collected at 15, 35, 55, 75, 90, 115 and 130 days after sowing (DAS) (Ho et al., 2009; Munda et al., 2016; Hashim et al., 2017, Karki et al., 2018). At 90 DAS, culm height was measured, and panicle numbers were counted. The height of seedlings or young plants was measured from the ground to the tip of the tallest leaf. The height of the mature plants was measured as the distance from the ground level to the tip of the tallest panicle. Culm height was measured from the ground to the node of the tallest panicle. Panicle length at harvest was determined by subtracting the plant and culm heights.

Furthermore, the number of tillers was manually counted, and tiller with at least one visible leaf were included until harvesting time. The number of unproductive tillers (if any) and panicles at maturity (before harvest) were also counted. The chlorophyll levels in leaves were measured using a SPAD meter (Minolta SPAD-502DL model, Minolta, Japan), a probe that provides a quick and non-destructive approach that allows for in situ assessment (Halim et al., 2018). The SPAD measurements were taken in the center of each leaf and averaged. All growth data were collected in compliance with the treatments, replicates, and measurement times.

3.4.4 Yield and Yield Component Data

At maturity, panicles from each plant within each sampling were plucked, kept in different bags, and labelled appropriately for the determination of yield components. The filled and empty grains were separated accordingly and counted. Total filled grains and 1000-grains weight, as well as its moisture content were determined. Grain yields for each

treatment were adjusted to a standard moisture content of 14% of fresh weight. This can be done by drying rice grains in an oven (60 °C) to 12-14 % moisture content, which was determined using a digital moisture meter.

Following that, the harvested samples were oven-dried at 70 °C for three to five days and recorded as a total biomass. The percentage (%) of filled spikelet was estimated by multiplying the number of filled spikelet per panicle by a factor of 100 over the total number of spikelets per panicle (Wiangsamut et al., 2013). The following equation was used to calculate the grain harvest index (HI) (Wiangsamut et al., 2013).

Harvest Index (HI) = [Grain yield / (Grain yield + Biomass)] Equation 3.5

3.5 Analyses of Nitrogen (N) Uptake and Nitrogen Efficiency Estimation (NUE)

3.5.1 N Uptake and NUE

The N content of plant materials was measured by the modified Kjeldahl acid-digestion method using concentrated sulfuric acid (Hanafi et al., 2009; Ho et al., 2009; Sarfraz et al., 2017) (Appendix 1). After collecting final growth performance and harvesting the panicles, each plant from each sampling pot was cut at the ground for the determination of N content. Leaves were removed from the stem and placed in different plastic zip lock bags (with tiny holes) according to the treatments. The fresh weight of the leaves and stems were recorded prior to drying.

After, all samples were oven-dried for three to five days at 70 °C to a constant weight. Each sample was weighed and pulverized with a mechanical grinder before subsamples were taken for N determination. The N content of the vegetative parts and grains was measured by the Kjeldahl method (Appendix 1). Total N uptake in grain and straw was estimated by

multiplying the N concentration (%) in grain and straw by their respective yields (Hammad et al., 2017). The following equations were used to determine the N harvest index (NHI), N use efficiency (NUE), and N agronomic efficiency (NAE) (Abbasi et al., 2012).

$$NHI = \text{N uptake in grain} / \text{N uptake in plant} \quad \text{Equation 3.6}$$

$$NUE = [\text{N uptake (added)} - \text{N uptake (control)}] / \text{Total N applied} \times 100 \quad \text{Equation 3.7}$$

$$NAE = (Yn - Yo) / N \quad \text{Equation 3.8}$$

where N is nitrogen (g pot^{-1}, N uptake is nitrogen uptake (g kg^{-1}), Yn is grain yield (g pot^{-1}) at N = x, and Yo is grain yield (g pot^{-1}) at N = 0.

In addition, plant samples of rice were collected for dry matter estimation at different growth stages (tillering, panicle initiation, heading, flowering and grain filling, dough, and maturity stages) from different N treatments. Dried plant samples were weighed to determine the dry matter accumulation and dry matter partitioning.

3.5.2 Correlation Regression Study

Correlation regression study was conducted by adopting a method designed in previous research including Putri et al. (2020), Varghese et al. (2020), Kang et al. (2021), Badaruzaman & Tiong (2022), and Han et al. (2022). In this study, correlation regression analysis was performed using GraphPad Prism 9 v9.4.1 (2022), which analysed the relationship between variables and fit mathematical models to the data.

To execute correlation regression analysis, it is assumed that the dependent and independent variables have a mathematical relationship. The relationship can be described as either a straight line (linear regression), a polynomial curve (polynomial regression), or a

non-linear relationship (non-linear regression) (Badaruzaman & Tiong, 2022). Following that, a scatter plot of the dependent and independent variables was plotted, and the most likely values for the coefficient of determination (R^2) were obtained (Putri et al., 2020; Han et al., 2022). The relationship between two or more variables is established using regression analysis. Regression analysis demonstrates how the standard value of the dependent variable varies with the change of any independent variables while the other independent variables remain constant (Kang et al., 2021). Linear regression is one of the most commonly used mathematical modelling techniques.

In regression analysis study, the independent variable has a significant relationship with the dependent variables, assessing the relative intensity of the effect of independent variables on the dependent variable and making predictions. The coefficient of determination (R^2) is a measure of the accuracy or deviation of prediction in regression analysis. The coefficient of determination (R^2) indicates the size of the model corresponds to the dependent variable in comparison to the mean. The measure R^2 can be determined using the following equation:

$$R^2 = \frac{SS_R}{SS_T} \qquad \text{Equation 3.9}$$

where SS_T (total variation or sum of squares) is the total number of all square difference of between each observation and the average. Whereas SS_R (sum of squared regression) is the variation in the data described using regression analysis R^2 and has a value between 0 and 1. When the value of R^2 approaches 1 (i.e, R^2 = 0.998), it shows the best fit to the model, hence it can be assumed that more variation in *y* can be explained by variation in *x*.

3.5.3 Degradation of Cellulose Hydrogels CRF

After harvest, the degraded hydrogels CRF fragments were retrieved from the soils and washed with distilled water to remove excess soils (Cui et al., 2019). The weight of the degraded hydrogels CRF fragments was measured using a weighing balance.

3.6 Statistical Analysis

ANOVA was used to analyze significant differences in the mean, as well as the correlation regression analysis, and the differences presented throughout are significant at $p \leq 0.05$ or 0.01 using SAS software package 9.2. All diagrams were generated using the software GraphPad Prism 9 v9.4.1 (2022).

3.7 Chapter Summary

This chapter discussed the research design and technical approach underlying the research methodology in relation to achieving research objectives. The optimum formulation of cellulose hydrogel CRF was influenced by porosity in their structure, water absorption capacity and swelling ratio, moisture retention ability, loading capacity of fertilizer and release profiles in water and soils. In addition, extensive studies were conducted to demonstrate the applicability of cellulose hydrogels CRF, i.e., fine-tuning the application rates of N fertilizers to match the needs of rice plants, thus improving the growth performance and yield of rice. The growth performance of the rice plants was recorded (plant height, number of tillers, SPAD values), rice grain yield and yield component data were calculated including 1000-grain weight, percentage of filled grains, panicle number, number of grains per panicle and straw yield. In addition, dry matter accumulation and dry matter partitioning of the rice plants throughout the growing period were computed.

Furthermore, studies on the nutrient uptake and NUE by the rice plants treated with cellulose hydrogel CRF were also included. Degradation rates of cellulose hydrogel CRF were determined at the end of the growing period. After, the correlation regression study was conducted to assess the relationship between dependent and independent variables involved in this study, as well as to predict the relative strength between those variables. Similar previous studies that employed the research approach for agricultural applications have been identified. Data collection method, measurement of parameters and data analysis have been identified. The next chapter presents the results and discusses the findings of the study.

CHAPTER 4

RESULTS AND DISCUSSION

4.1 Fabrication of Urea-loaded Cellulose Hydrogels as a Controlled Release Fertilizer

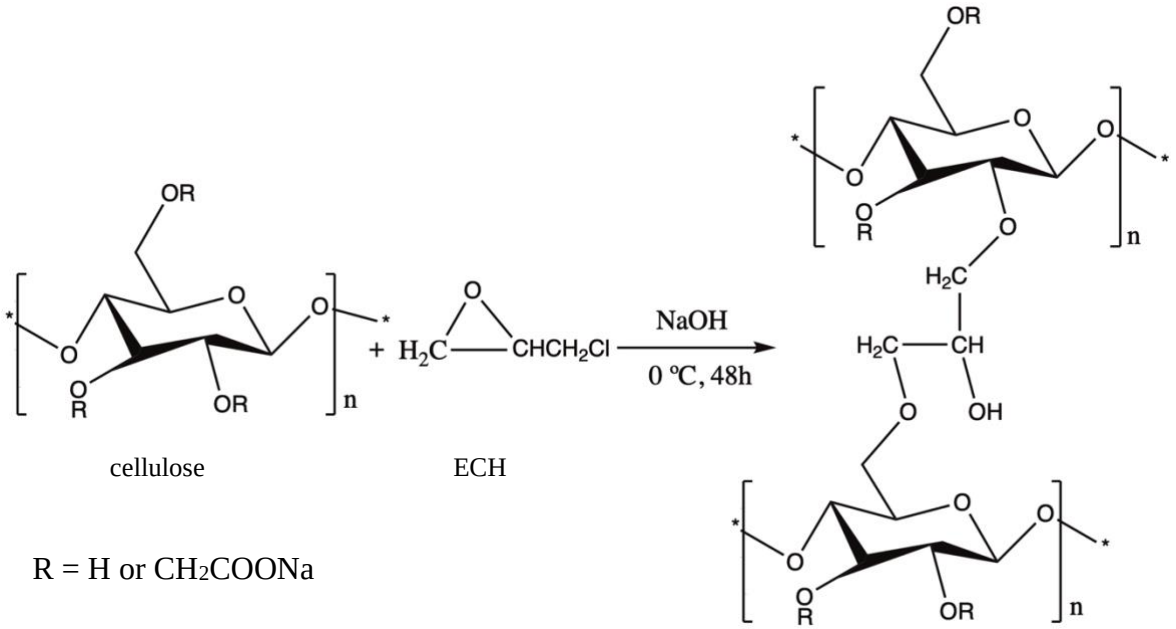
4.1.1 Fourier Transform Infrared Spectroscopy (FTIR): Spectra Analysis

The preparation of ECH crosslinked cellulose hydrogel with CMC is presented in Figure 4.1. The FTIR spectra of (a) cellulose fibres, (b) CMC, and (c) an ECH-crosslinked cellulose hydrogel are presented in Figure 4.2. The wavenumber ranges 3360 cm^{-1} and 2900 cm^{-1} were assigned to polysaccharides -OH and C-H bonds (Figure 4.2a) (Lawrencia et al., 2021). The large peak at 3335 cm^{-1} was caused by the hydroxyl group stretching vibration in polysaccharides, which also included intermolecular and intramolecular hydrogen bond vibration in cellulose (Lawrencia et al., 2021). Meanwhile, the peak at 2920 cm^{-1} was attributed to the -CH stretching vibration of all polysaccharide hydrocarbon constituents (Lawrencia et al., 2021).

Further, cellulose bands were identified in the range of 1630 cm^{-1} to 900 cm^{-1} (Figure 4.1a). The vibration of water molecules absorbed in cellulose caused the peak at roughly 1633 cm^{-1} which was due to vibration of water molecules absorbed in cellulose. In addition, the absorption bands at 1428 cm^{-1}, 1367 cm^{-1}, 1334 cm^{-1}, 1027 cm^{-1}, and 896 cm^{-1} correspond to the stretching and bending vibrations of $-CH_2$, -CH, -OH and C-O bonds in cellulose (Salleh et al., 2018). The vibration bands at 1420 cm^{-1} to 1430 cm^{-1}, also known as the crystallinity band, were associated with the amount of the crystalline structure of the cellulose (Salleh et al., 2018). The band at 897 cm^{-1}, on the other hand was attributed to the amorphous region in cellulose (Salleh et al., 2018).

Figure 4.2 (b) shows the FTIR spectrum of CMC. The characteristic transmission band at 3202 cm^{-1} shows the hydrogen bonding -OH stretching region (Salleh et al., 2018). The small hump at 2922 cm^{-1} and 2872 cm^{-1} were associated to -CH stretching vibration (Salleh et al., 2018). The sharp peak observed at 1587 cm^{-1} confirms the presence of COO^- was due to stretching vibration of carboxyl group (Salleh et val., 2018). This band is important in determining the complexation between polymer and salt and this is expected to shift or otherwise if complexes occur (Zhang et al., 2017; Salleh et al., 2018). The band around 1410 cm^{-1} and 1319 cm^{-1} were assigned to -OH stretching in-plane and -CH stretching in symmetric of CMC (Salleh et al., 2018). The IR spectrum of CMC polymer which appeared at 1107 cm^{-1} and 1039 cm^{-1} were assigned to C-O stretching on polysaccharide skeleton (Zhang et al., 2017; Salleh et al., 2018).

Figure 4.2 (c) depicts the crosslinking reaction in the cellulose hydrogels, with the transmittance peak at 1060 cm^{-1} due to the stretching vibration of C-O-C which formed from the reaction component ECH and CMC (Zhang et al., 2017). Furthermore, the presence of the carbonyl group (C=O) at 1720 cm^{-1} confirms the successful incorporation of the carbonyl group in the structures (Zhang et al., 2017). This result also confirms the presence of COOH groups in CMC and hydrogels. Meanwhile, a new peak at 1328 cm^{-1} in the crosslinked hydrogel showed the presence of crosslinking (Zhang et al., 2017). Finally, the intended product, a chemically crosslinked cellulose hydrogel, was successfully formed.



422

423 **Figure 4.1:** An ECH crosslinked cellulose hydrogel with CMC.

424

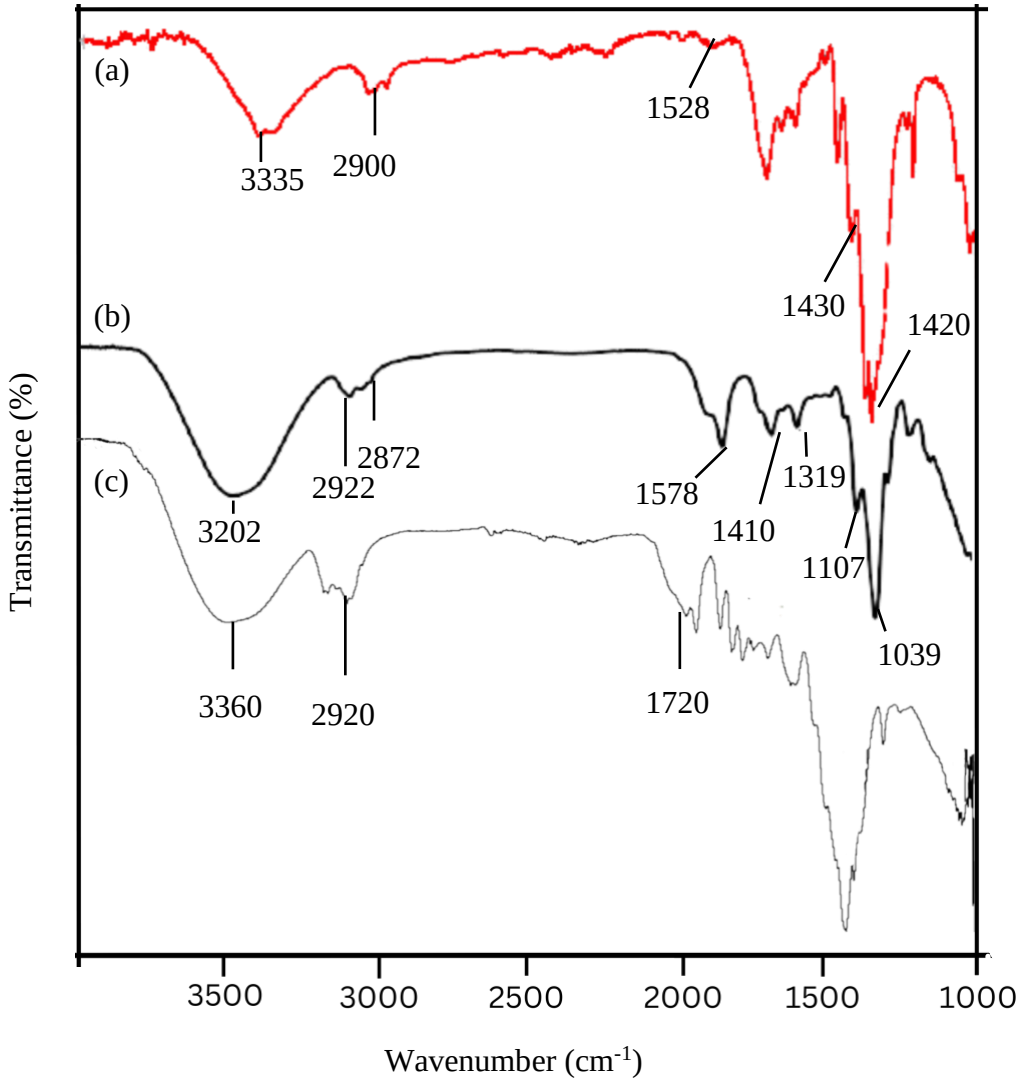


Figure 4.2: FTIR spectra of (a) cellulose fibers, (b) CMC, and (c) ECH-crosslinked cellulose hydrogel

4.1.2 Differential Scanning Calorimetry (DSC)

The DSC curve of C3 cellulose hydrogel is shown in Figure 4.3. The phase transformation of C3 cellulose hydrogel occurs in two steps: (i) melting or fusion, and (ii) formation or crystallization. Correspondingly, one endotherm and one exotherm were observed in the DSC curve.

The endotherm dip in the temperature region 90–100 °C is melting or fusion of cellulose hydrogel, which corresponds to loss of absorbing water or solvent. Also, the molecules in the cellulose hydrogel polymeric network are randomly oriented. Second, the exothermic peak can be observed in the temperature range of 130–170 °C due to crystallization of cellulose hydrogel. In other words, exothermic peak corresponds to heat release due to conformational energy, i.e., crystallization of cellulose hydrogel. At low temperature, the molecules in the hydrogel polymeric network are randomly oriented. At high temperature where crystallization occurred, molecules in the hydrogel polymeric network release excess free energy because the molecules are no longer in random configuration. This means that heat flows out of the hydrogel specimen crystallized or semi-crystallized amorphous molecules in hydrogel polymeric network formed.

Further, the exothermic peak continued to drop (T = 290 °C) and translated to an endothermic peak from which the crystallized amorphous molecules in hydrogel polymeric network melts (with random-oriented molecules again). This means that energy flows into the hydrogel specimen to generate a phase change from crystalline to amorphous molecules (melting). In this case, possibly the hydrogel specimen has melted.

Additionally, the DSC curve analysis as evidence for transformation behaviors of hydrogels have been reported in other studies (Yang et al., 2010; Jayaramudu et al., 2016;

Liu et al., 2017; Treesuppharat et al., 2017; Dai et al., 2018; Butylina et al., 2020; de Lima et al., 2020; Harada et al., 2021).

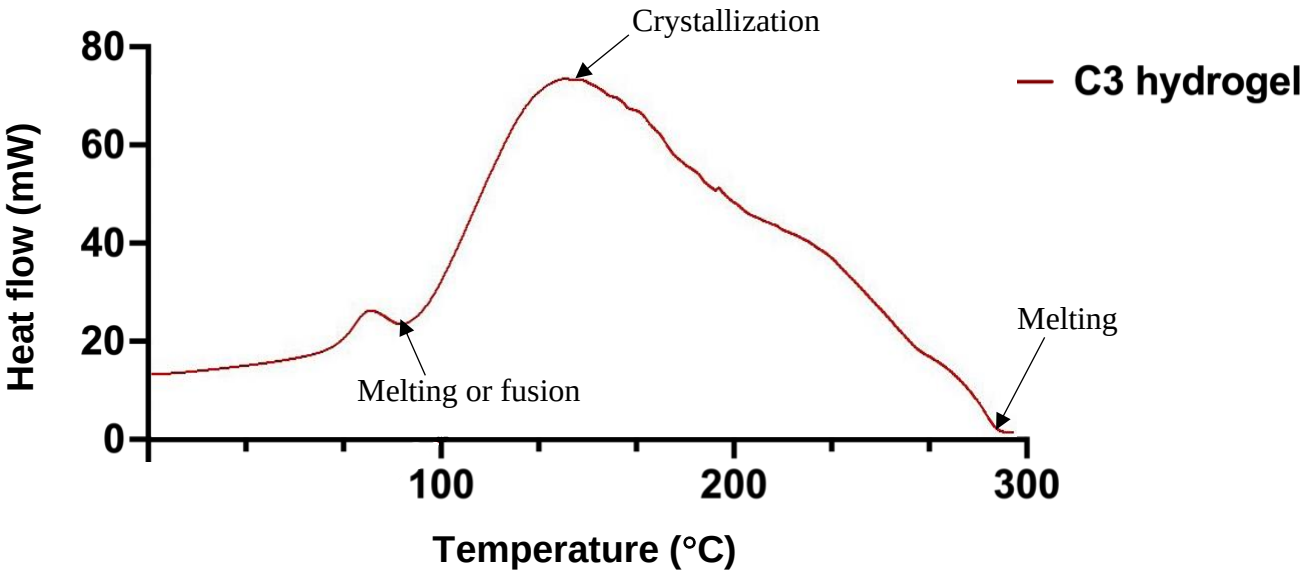


Figure 4.3: DSC curve of C3 cellulose hydrogel

4.1.3 Morphology and Swelling Behaviors of Cellulose Hydrogels

4.1.3.1 Effects of Cellulose Concentrations

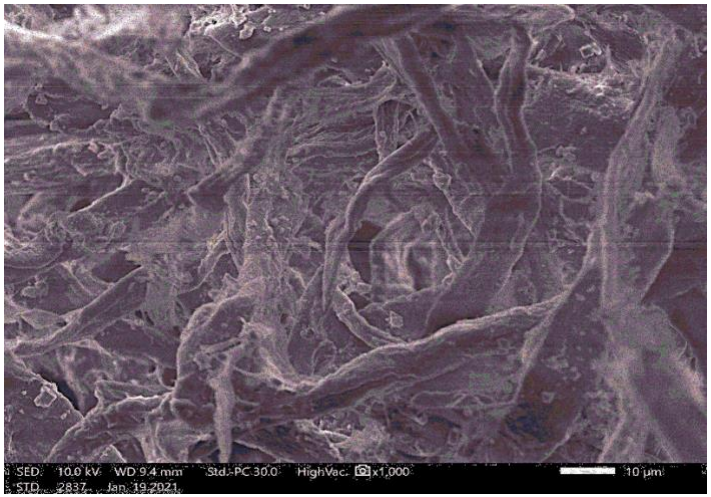
The FESEM images of cellulose fibers (Figure 4.4a) appeared as long fibers, flattened shapes. Figure 4.4 (b)-(f) depicts and compares the microstructures of successfully synthesized cellulose hydrogels at various cellulose concentrations (% (w/v)).

The swelling behaviors of dried cellulose hydrogels of various cellulose compositions were studied (Figures 4.5) (Appendix 2). Among all formulations, the C3 cellulose hydrogel with 3% (w/v) cellulose and 1.75% (w/v) CMC demonstrated the highest swelling percentage of 2055% (Figure 4.5). The high swelling percentage of C3 cellulose hydrogel could be due to their highly porous microstructure with many channels and interconnected capillaries (Figure 4.4d), which allows water molecules to diffuse into the

cellulose hydrogel network (Chetouani et al., 2014; Voon et al., 2016). Phase separation in the polymer solution formed during the freeze-thaw preparative multiple cycles, allowing the formation of porous C3 assembles (Jampi et al., 2021; Kareem et al., 2021).

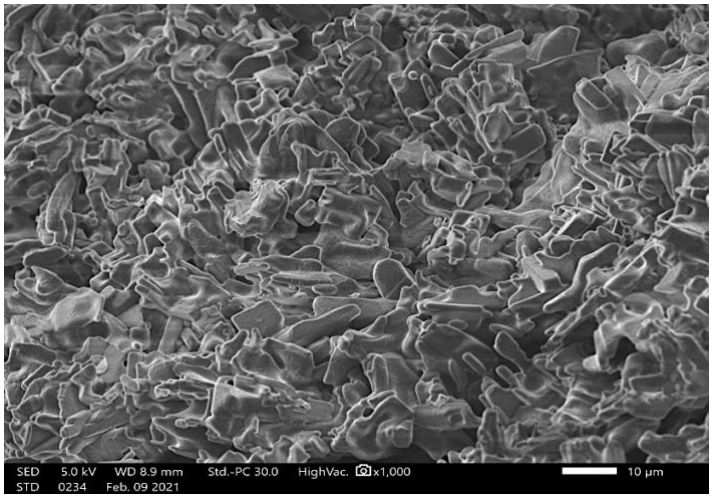
Lower swelling ratios were observed for C4 and C5 cellulose hydrogels, implying that increased cellulose content in the hydrogels contributes to stronger polymer chain entanglement via intra and intermolecular hydrogen interactions (Jampi et al., 2021). Furthermore, low swelling percentages in distilled water were identified in C1 and C2 hydrogels, owing to the weaker hydrogels formed from lower cellulose concentrations, which displayed uneven granular surfaces and rod-like morphology in FESEM micrographs (Figure 4.4 b and c).

(a)



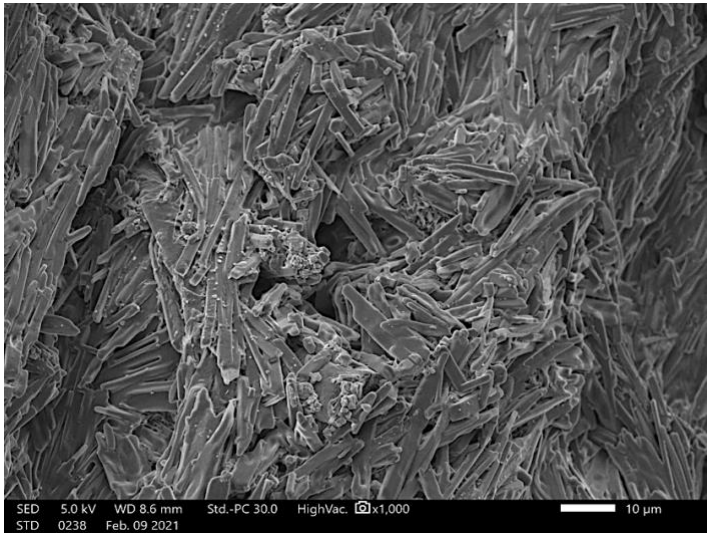
Cellulose

(b)



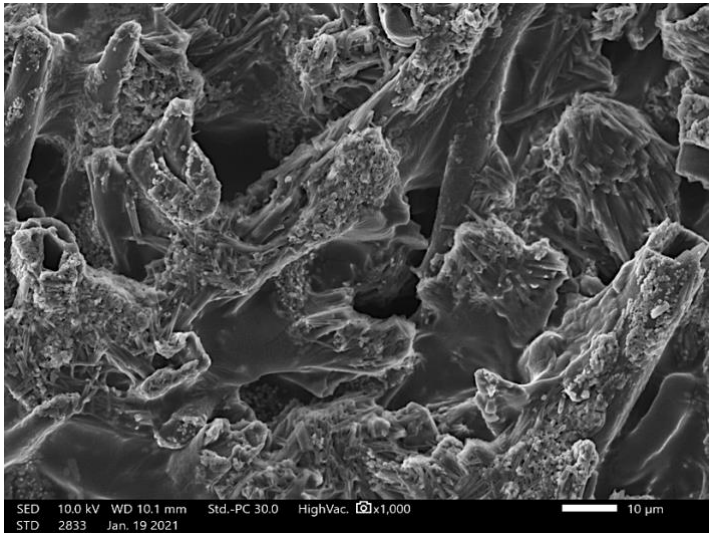
C1 (1.0 % w/v cellulose, 1.75 % w/v CMC)

(c)



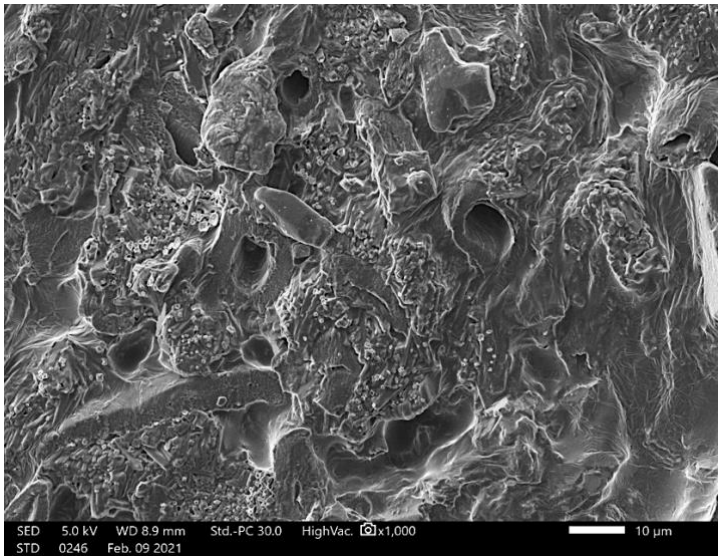
C2 (2.0 % w/v cellulose, 1.75 % w/v CMC)

(d)



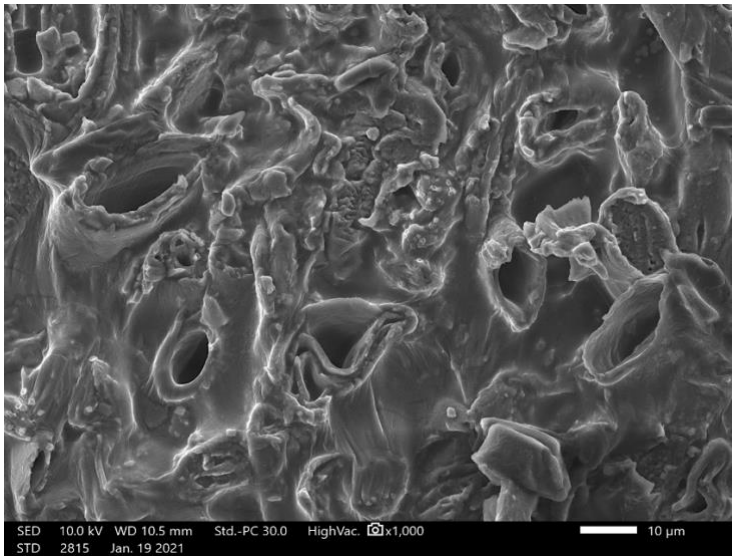
C3 (3.0 % w/v cellulose, 1.75 % w/v CMC)

(e)



C4 (4 % w/v cellulose, 1.75 % w/v CMC)

(f)



C5 (5 % w/v cellulose, 1.75 % w/v CMC)

Figure 4.4: FESEM image of (a) cellulose fibers, and cellulose hydrogels at various cellulose concentrations (b) C1, (c) C2, (d) C3, (e) C4, and (f) C5 cellulose hydrogels, and 1.75 % (w/v) CMC at 1000x magnification

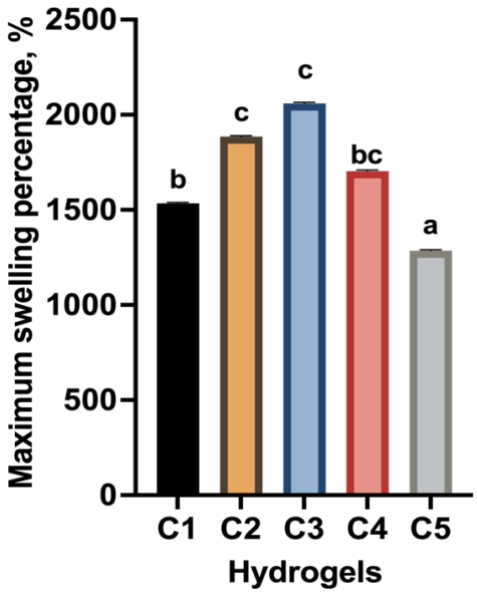


Figure 4.5: Maximum swelling percentage of cellulose hydrogels varied concentrations (% w/v) of cellulose fibers. Different letters indicate significant differences ($p \leq 0.05$) between hydrogels. Error bars represent the standard deviations from triplicates (n=3)

4.1.3.2 Effects of Various Concentrations of CMC

FESEM images of cellulose hydrogels at various CMC concentrations are shown in Figure 4.6. Figure 4.6(a)-(f) depicts and compares the microstructures of the successfully synthesized cellulose hydrogels at various CMC concentrations.

Also, the swelling behaviors of cellulose hydrogels at various CMC compositions were further characterized (Figures 4.7) (Appendix 3). Figure 4.6 shows the maximum swelling percentage of cellulose hydrogels synthesized at various concentrations of CMC. The highest swelling percentage (2038%) was observed in CMC5.0 cellulose hydrogels, followed by CMC4.5 cellulose hydrogels (2023%).

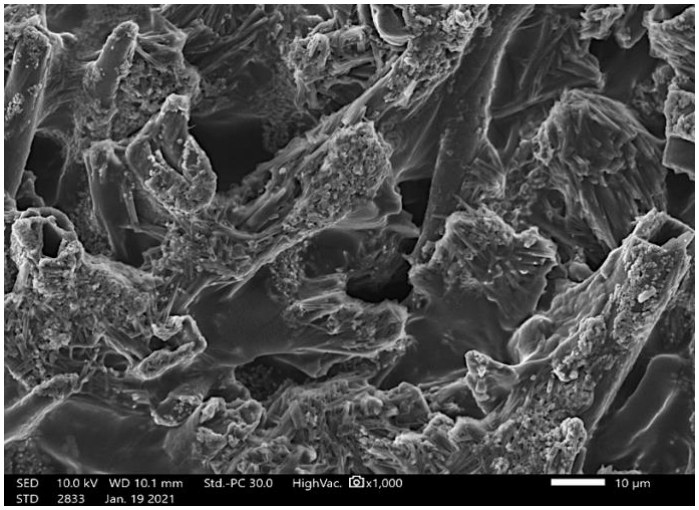
Generally, the swelling percentage increases with CMC concentrations due to its polyelectrolyte properties (Wei et al., 2019). This can be observed from the increasing

swelling percentage from lower to higher CMC concentrations, i.e., from CMC2.0 (1073%) to CMC4.0 (1685%) as shown in Figure 4.7. This is due to their high hydrophilic nature, as well as the wide and flat thread-like interconnecting capillaries and channels in their structure (Figure 4.6 b-g). These structures increase the contact surface area of cellulose hydrogels polymeric networks and may absorb more water into their structures (Olad et al. 2018).

However, the presence of ions in the system (i.e., Na^+), which may withhold water absorption could potentially influence hydrogel swelling. In other words, due to the increasing amount of Na^+ ions at high CMC concentrations (i.e., CMC4.5 and CMC5.0), no significant changes in water absorption were observed (Figure 4.6) (Quesada-Perez et al., 2011). This indicates that further increase in CMC concentration would not increase the swelling percentage, as reported in other studies (Ibrahim et al. 2007; Mohamed et al. 2022).

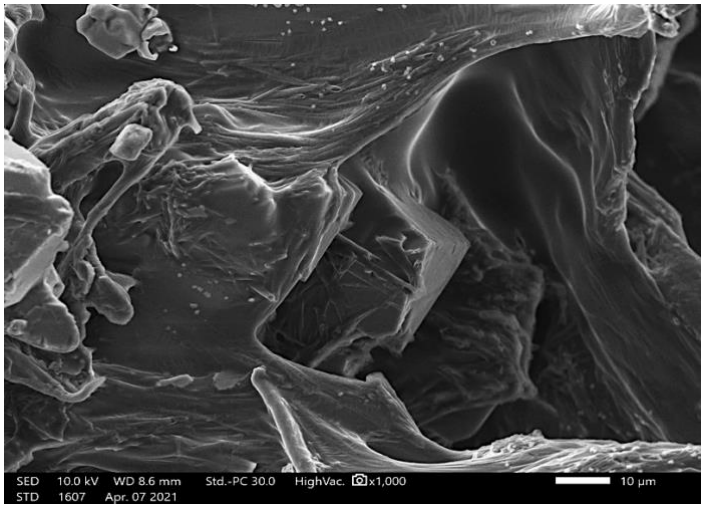
Herein, the swelling behavior in cellulose hydrogels could be described using the Flory-Rehner theory, which states that the equilibrium volume of the cellulose hydrogel networks is determined by the balance of osmotic pressure and elastic restorative force (Brandt et al., 2017). Previous studies that demonstrated findings in accordance with the presence results include Sannino et al. (2009), Raafat et al. (2012), Raucci et al. (2012), Xiao et al. (2014), Ranganathan et al. (2018) and Kareem et al. (2021).

(a)



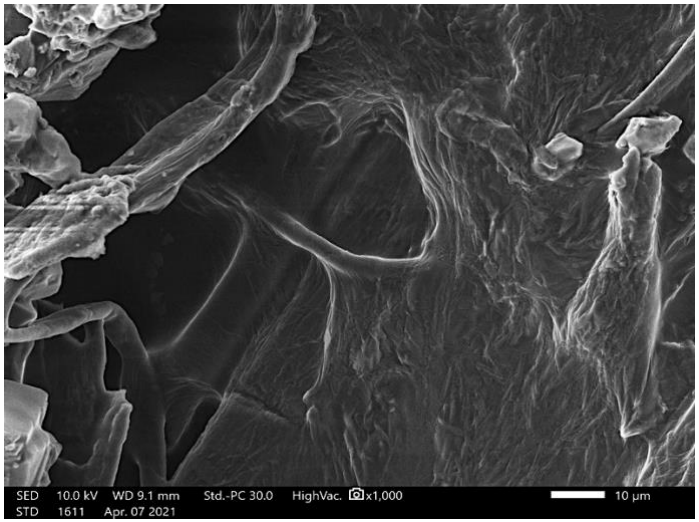
C3/CMC1.75 (1.75 % w/v CMC, 3.0 % w/v cellulose)

(b)



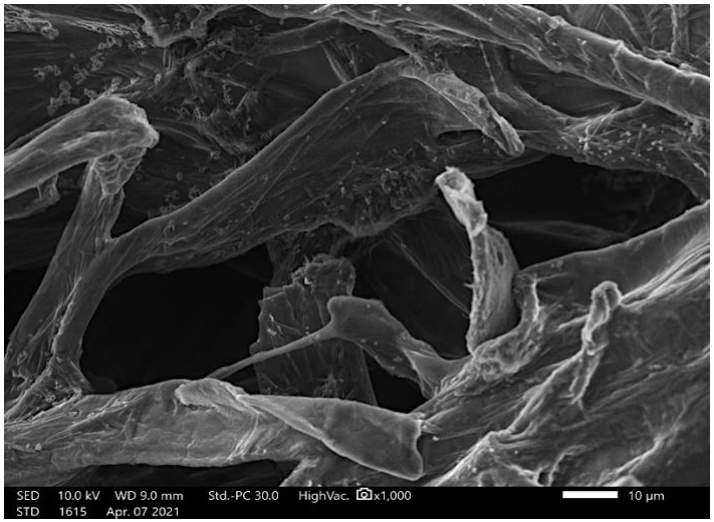
CMC2.0 (2.0 % w/v CMC, 3.0 % w/v cellulose)

(c)



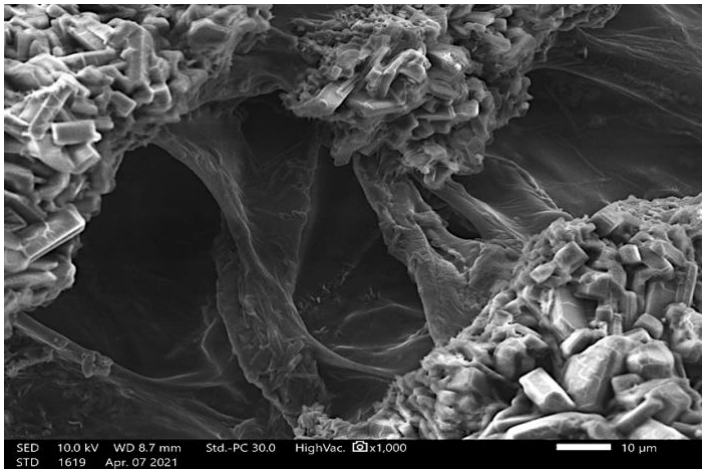
CMC2.5 (2.5 % w/v CMC, 3.0 % w/v cellulose)

(d)



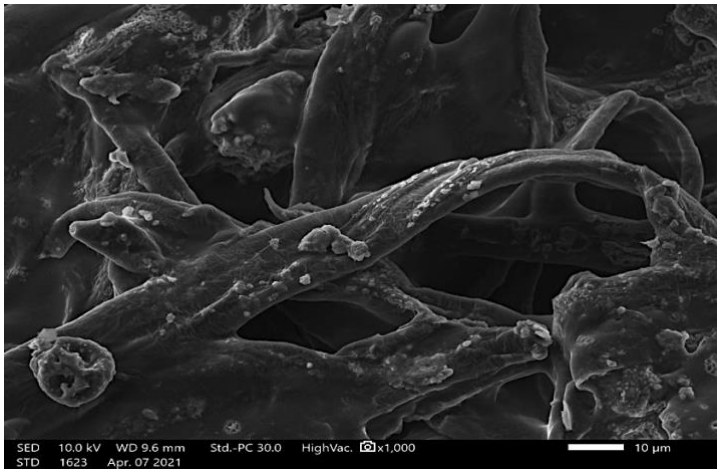
CMC3.0 (3.0 % w/v CMC, 3.0 % w/v cellulose)

(e)



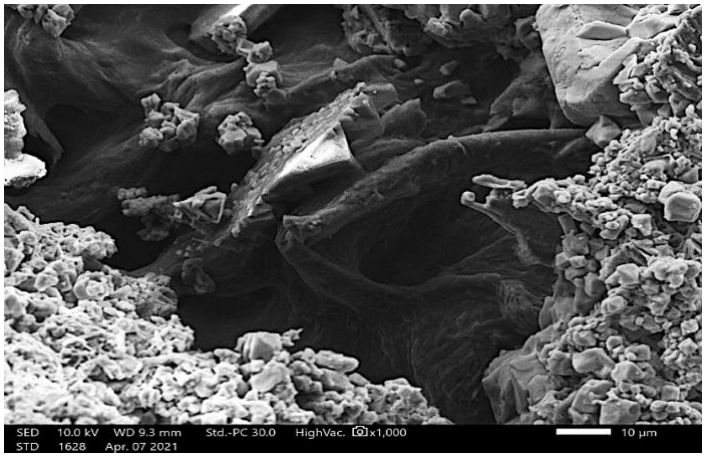
CMC3.5 (3.5 % w/v CMC, 3.0 % w/v cellulose)

(f)



CMC4.0 (4.0 % w/v CMC, 3.0 % w/v cellulose)

(g)



CMC5.0 (5.0 % w/v CMC, 3.0 % w/v cellulose)

Figure 4.6: FESEM image of cellulose hydrogels at various CMC concentrations (a) 1.75, (b) CMC2.0, (c) CMC2.5, (d) CMC3.0, (e) CMC3.5, (f) CMC4.0, and (g). CMC5.0 cellulose hydrogels, and 3.0 % (w/v) cellulose at 1000x magnification

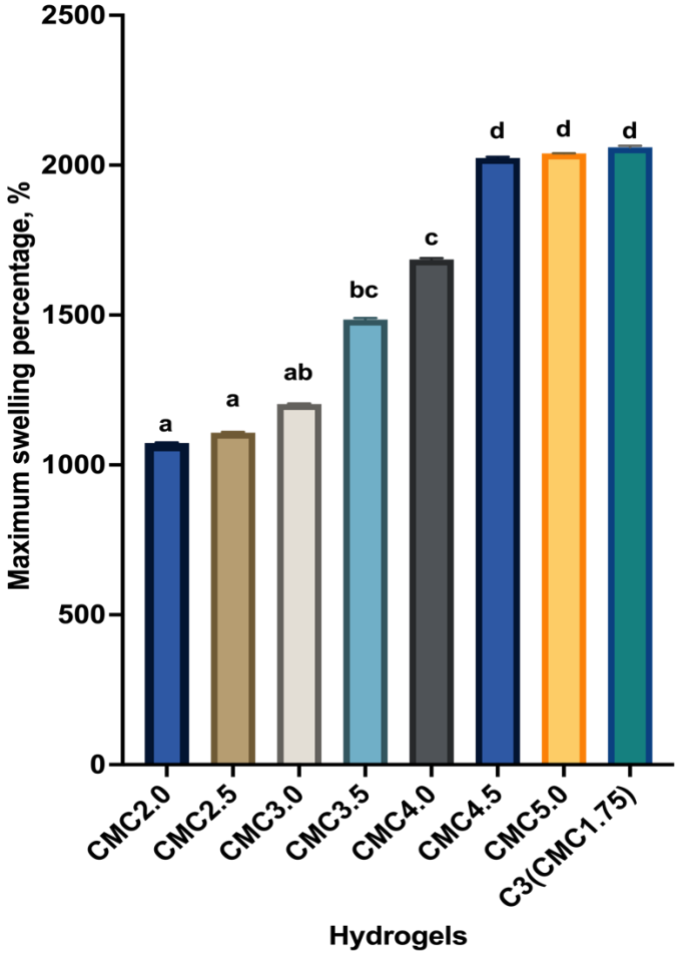


Figure 4.7: Maximum swelling percentage of cellulose hydrogels consisted of various CMC concentrations (% w/v). Different letters indicate significant differences ($p \leq 0.05$) between hydrogels. Error bars represent the standard deviations from triplicates (n=3)

4.1.4 Effects of Cellulose Hydrogels on the Soil Moisture

Soil moisture of three different types of soil is shown in Figure 4.8 (Appendix 4). The addition of the C3 cellulose hydrogel to the dry soils increased the moisture content significantly and retained the moisture for 7 days before the hydrogel dried out. Topsoil had the maximum soil moisture of up to 36.5% after 7 days, followed by wet clayey soil (30.1%) and sandy soil (23.4%). Also, the moisture of topsoil was 26.62% higher with C3 cellulose hydrogel than without C3 cellulose hydrogel, whereas wet clayey soil and sandy soil were 22.13% and 23.6% higher, respectively.

Compared to the topsoil, the decreased moisture content in the wet clayey soil might potentially be due to the sluggish infiltration of water from cellulose hydrogel through the compact soil profile of clayey soil with small particle size. In the presence of C3 cellulose hydrogel, the soil moisture content in the sandy soil was 23.4%, which is higher than the threshold moisture value of sandy soil, which ranges between 3% to 10% from the driest condition to the wettest condition (Khoo et al., 2016).

These results suggest that the presence of C3 cellulose hydrogel increases the soil moisture content while decreasing water transpiration. The application of C3 cellulose hydrogel in soil may reduce water irrigation frequencies in farming while increasing plant survival and crop yield during dry seasons.

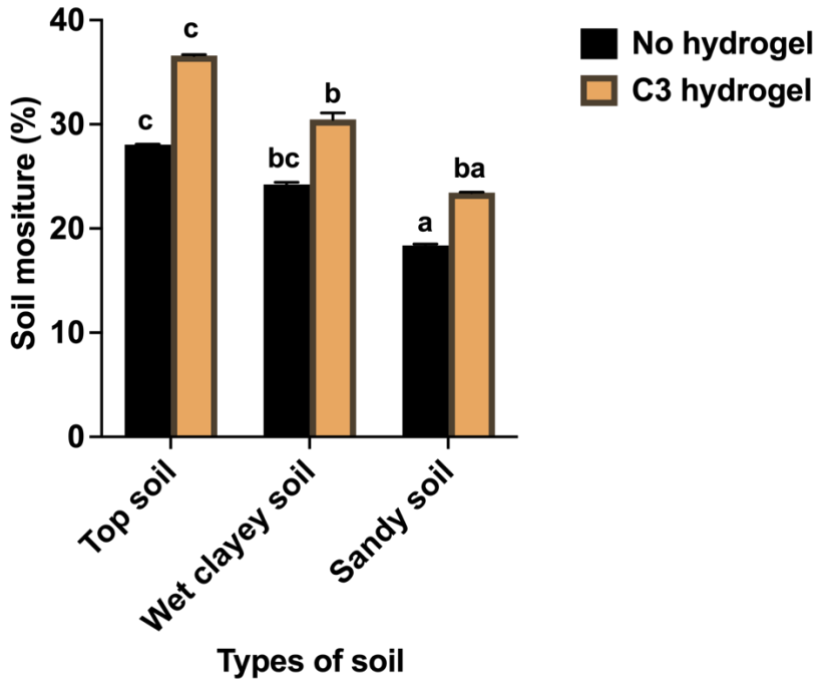


Figure 4.8: Soil moisture in different types of soils using C3 cellulose hydrogel. Different letters indicate significant differences ($p \leq 0.05$) between soils. Error bars represents the standard deviations from triplicates (n=3)

4.1.5 Loading of Urea in Water and Soils

Based on the analysis reported in this study and included in the previous section, the ideal formulation to prepare cellulose hydrogel was observed in C3 composition. Hence, C3 cellulose hydrogel composition was selected for the fabrication of urea-loaded cellulose hydrogels as a controlled release of fertilizers.

Figure 4.9 (Appendix 5) depicts the urea loading capacity of C3 cellulose hydrogel. The urea loading for C3 cellulose hydrogel was rapid, and equilibrium was attained in 48 h. The maximum loading capacity of urea (nutrient content) of C3 cellulose hydrogel was 0.51 g g^{-1}. The rapid encapsulation of urea by C3 cellulose hydrogel was induced by the high initial concentration gradient of urea in the water as well as the easy diffusion of urea into the porous structures of C3 cellulose hydrogel (Liang et al., 2014).

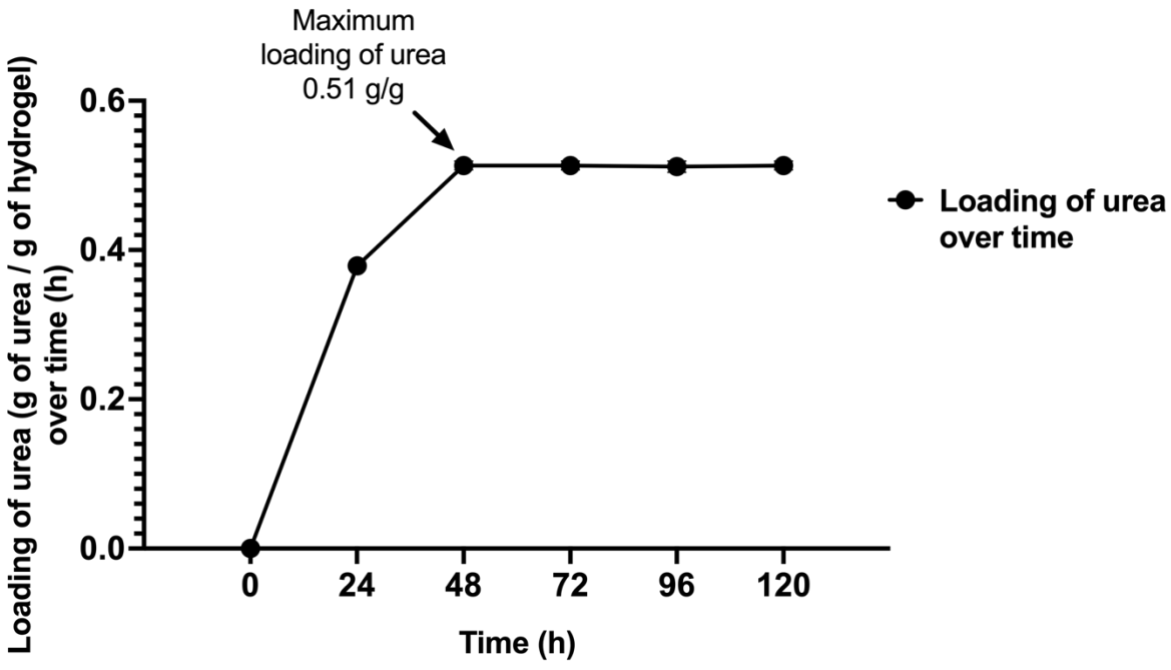


Figure 4.9: Loading capacity of C3 cellulose hydrogel. Error bars show the standard deviations from triplicates (n=3)

4.1.6 Release of Urea in Water and Soils

Urea release profiles of C3 cellulose hydrogel in water and soils are shown in Figure 4.10 (Appendix 6) and 4.11 (Appendix 7), respectively. In control studies, 98.7% free urea was released in water within 1 day (Figure 4.10). In comparison, urea release from C3 cellulose hydrogel in water in a controlled and slower pattern, with only 50.77%, 71.26%, and 80.46% release after 1 day, 1 week and 1 month, respectively. Furthermore, "burst release" can be observed at the initial stage of the studies (within 1 h) for all types of fertilizer due to the high initial concentration gradient of loaded urea in the cellulose hydrogels and the release of urea towards the surface (Ding et al., 2016). The term "burst release" is uncontrolled release which occurs when a large proportion of urea is rapidly release in the first few minutes or hours (Lawrencia et al., 2021). Following burst release, a more constant, controlled, or slow release is then achieved (Lawrencia et al., 2021).

The controlled-release behaviors of free urea and C3 cellulose hydrogel in various soils were evaluated to assess the possible applicability of C3 cellulose hydrogel for precision agriculture (Figure 4.11). Free urea (control) release was more than 95% in topsoil, wet clayey soil, and sandy soil within 1 week. In comparison, the urea release by C3 cellulose hydrogels in those soil samples was significantly reduced to less than 60% after 7 days. For the wet clayey soils, the N-nutrient content released was 42.14% (1 day), 56.32% (1 week) and 73.37% (1 month). Meanwhile, N-nutrient release in C3 cellulose hydrogels in topsoil was 47.70%, 56.34% and 74.71% within 1 day, 1 week and 1 month, respectively. C3 cellulose hydrogels in sandy soils showed a similar urea release trend, with 45.98%, 55.17%, and 71.84% urea release in the soils at 1 day, 1 week and 1 month, respectively.

The possible release mechanism of C3 cellulose hydrogels may involve a combination of absorption, dissolution, and diffusion (Trenkel, 2020; Ding et al., 2016). High urea release (>70%) from C3 cellulose hydrogels within 1 month could be induced by the excellent hydrophilic properties of the extracted cellulose from blended wastepaper and CMC polyelectrolyte (Kareem et al., 2021). These features facilitate water diffusion and penetration into the hydrogel networks from the soils, causing the hydrogels to swell. The dynamic exchange of free water is anticipated between the cellulose hydrogels and the urea solution (Arbona et al., 2005; Chin et al., 2018).

Hence, this gradually improves urea solubility within the hydrogels and accelerates urea diffusion from the porous hydrogels to the surroundings. The main driving force of the nutrient release from cellulose hydrogels are differences in the osmotic pressure between the cellulose hydrogels and their surroundings (Kareem et al., 2021). Based on these preliminary findings, the release profiles of urea from C3 cellulose hydrogels in water and various soil conditions (<80%) within 30 days demonstrate promising compliance with the Committee of European Normalization (CEN) requirements for controlled release of fertilizer (Trenkel, 2010; Olad et al., 2018).

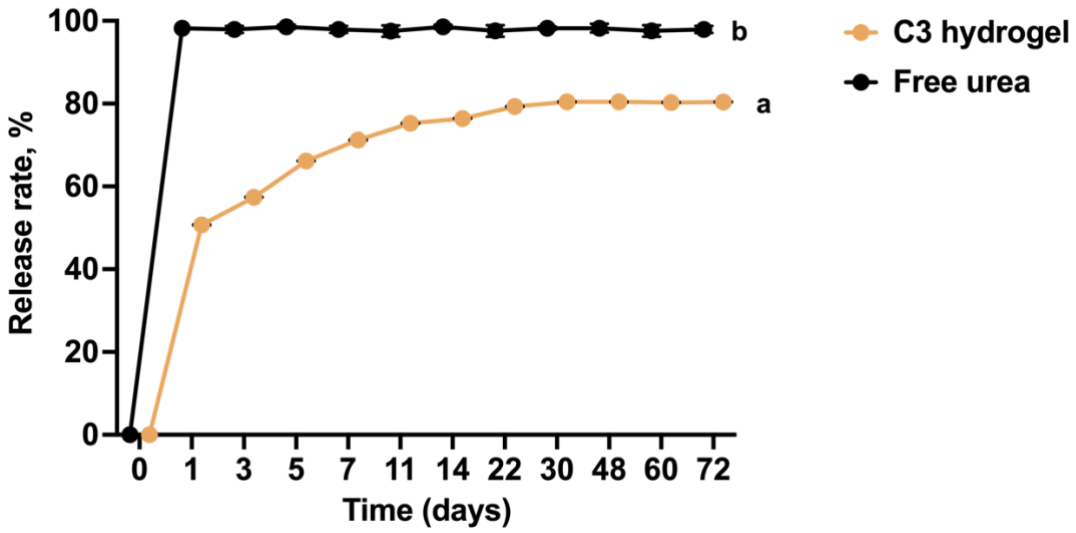


Figure 4.10: Release behavior of C3 cellulose hydrogel and free urea in water. Different letters indicate significant differences. Error bars show the standard deviations from triplicates (n=3)

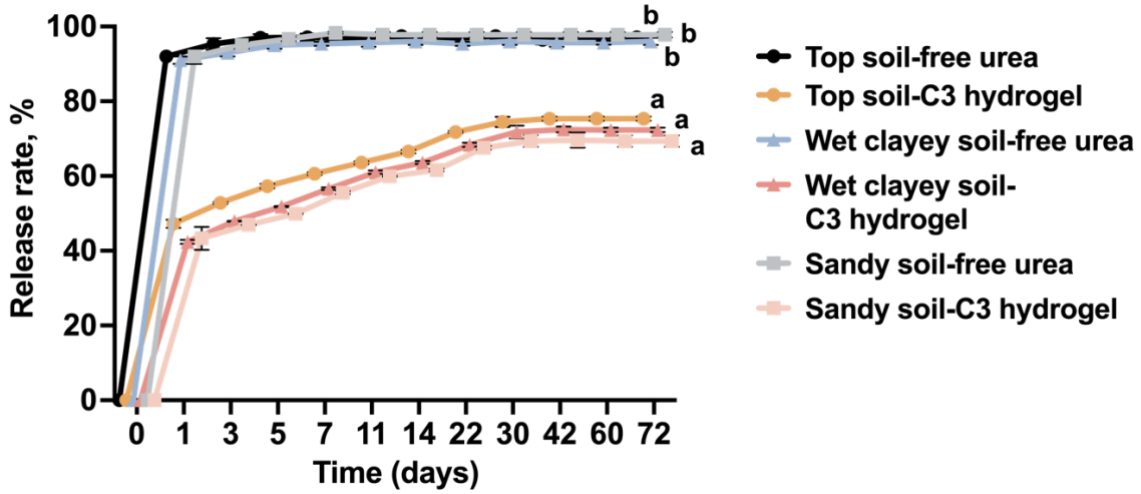


Figure 4.11: Release behavior of C3 cellulose hydrogel and free urea in soils. Different letters indicate significant differences. Error bars show the standard deviations from triplicates (n=3)

4.1.7 Kinetic Studies of Urea Release

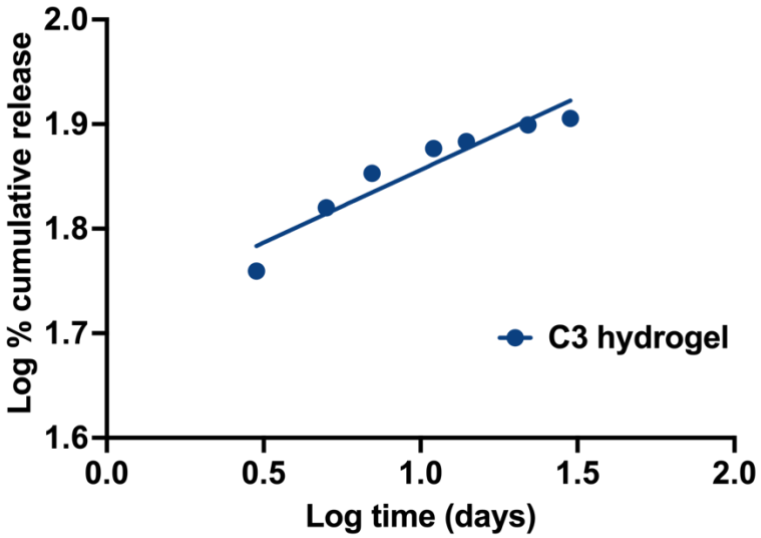
In the Korsmeyer-Peppas (Fickian, non-Fickian diffusion) model, the mechanism of urea release from C3 cellulose hydrogels in both water and soils was indicated by the value of the release exponent 'n' (Chetouani et al., 2014; Liang et al., 2014). Table 4.1 shows the kinetics release parameters in water and soils, which are represented in Figure 4.12 (a) and (b), respectively.

Table 4.1 shows that, among all diffusion types in the Korsmeyer-Peppas model, the Fickian diffusion is most suited to describe the control-release mechanism of fertilizer in water and soils ($R^2 > 0.85$ and $n < 0.45$). This suggests that the fertilizer release of C3 cellulose hydrogels was driven by diffusion through their pores and channels, which was regulated by the concentration gradient and degree of swelling of the hydrogels (Hermida et al., 2019; Wei et al., 2019; Bi et al., 2020).

Table 4.1: The parameters of Fickian diffusion in the Korsmeyer and Peppas model for urea release from C3 cellulose hydrogels in water and soil

Kinetic model	Parameter	Water	Topsoil	Wet clayey Soil	Sandy soil
Korsmeyer-Peppas model (Fickian diffusion)	R^2	0.9565	0.9734	0.9935	0.9575
	n	0.1452	0.1284	0.1245	0.2574
	K_{KP}	1.7103	1.653	1.6727	1.3608

(a)



(b)

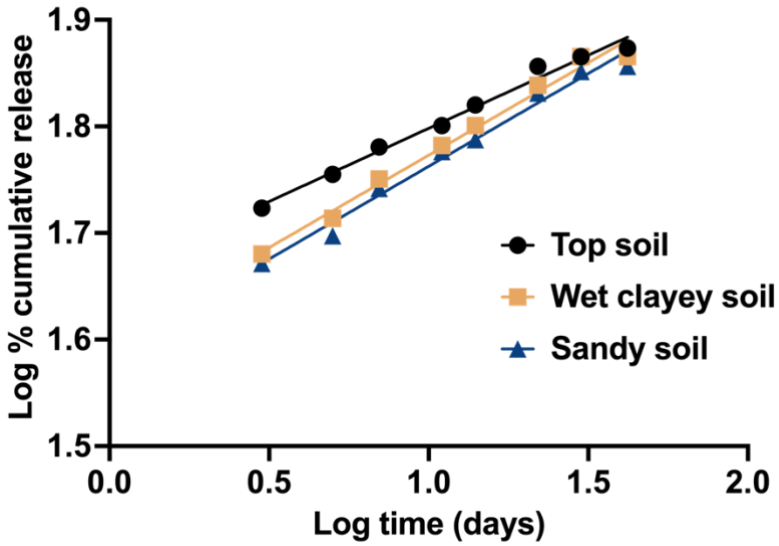


Figure 4.12: Korsmeyer and Peppas model of urea release from C3 cellulose hydrogel in (a) water, and (b) soils

4.2 Evaluation and Fine-tuning the Loading Capacity and Release Rate of Fertilizer to Match the Needs of the Rice Plants

4.2.1 Rice Growth Performance

4.2.1.1 Plant Height (cm)

Plant height increased with time in all treatments until maturity was reached at 130 DAS (Figure 4.13 and 4.14) (Appendix 8). Treatment T4H (4.8 N g pot^{-1} = 75% RDF) had the highest rice plant height (129.6 cm) compared to the treatment with common urea dosage (T6U, 122.4 cm) and control treatment (T1, 86.1 cm). Plant height using T5H (120.7 cm) was comparable to the treatment T6U (122.4 cm). Whereas plant heights in other treatments were 109.4 cm (T3H) and 94.1 cm (T2H).

The curve (Figure 4.14) shows that the growth of the rice plants in T4H initially delayed behind those given common urea (T6U) and higher dose of N (T5H). Nevertheless, from 30 to 45 DAS, the rice plants were almost of the same height, and after this point, the rice plants in T4H outpaced the rice plants in T6U and T5H. Besides, T4H was able to sustain the plant height, however T5H did not show a significant improvement in the plant height. These findings indicate that CRF with 75% N (T4H) has a more sustained fertilizer release in soil than common urea (T6U).

In general, N increases the protein content in plants (Dellero, 2020; Leite et al., 2021; Ayadi et al., 2022). When the plants receive an adequate amount of N, protein may be available at an optimal level to establish metabolic processes, which increases the vegetative and reproductive growth of the plant and the plant yield (Lawlor, 2002; Masclaux-Deubresse et al., 2010; Ransom et al., 2020). Higher plant height is significantly related to improved growth. Similar findings have been reported with rice using encapsulated urea, which results

in higher plant height than rice treated with common urea (Davidson et al., 2013; Fazlina et al., 2014; Hashim et al., 2017).

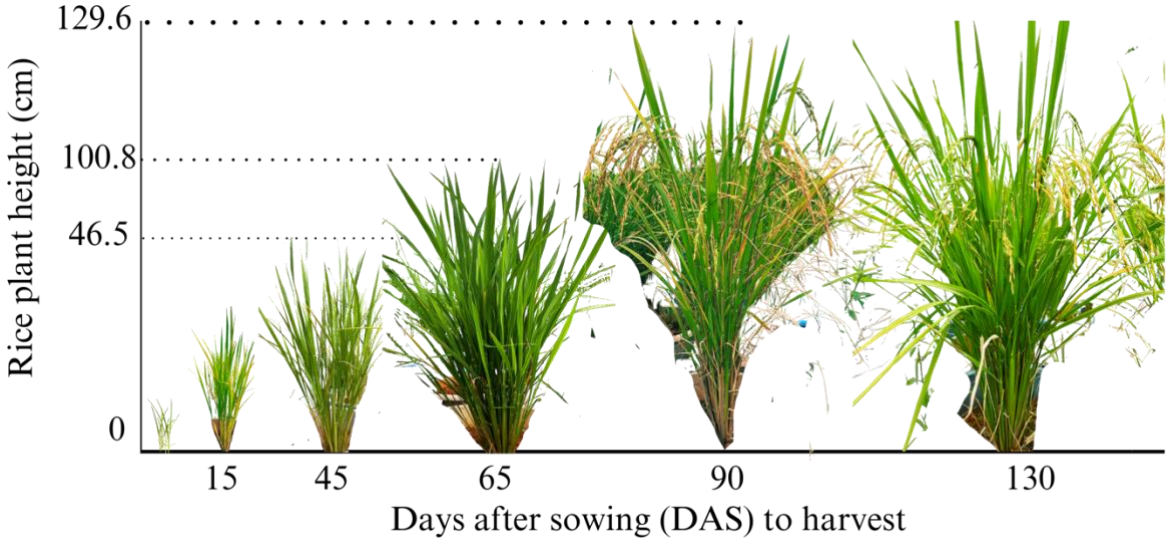


Figure 4.13: The rice plants growth (treated with T4H) from day 15 to 130.

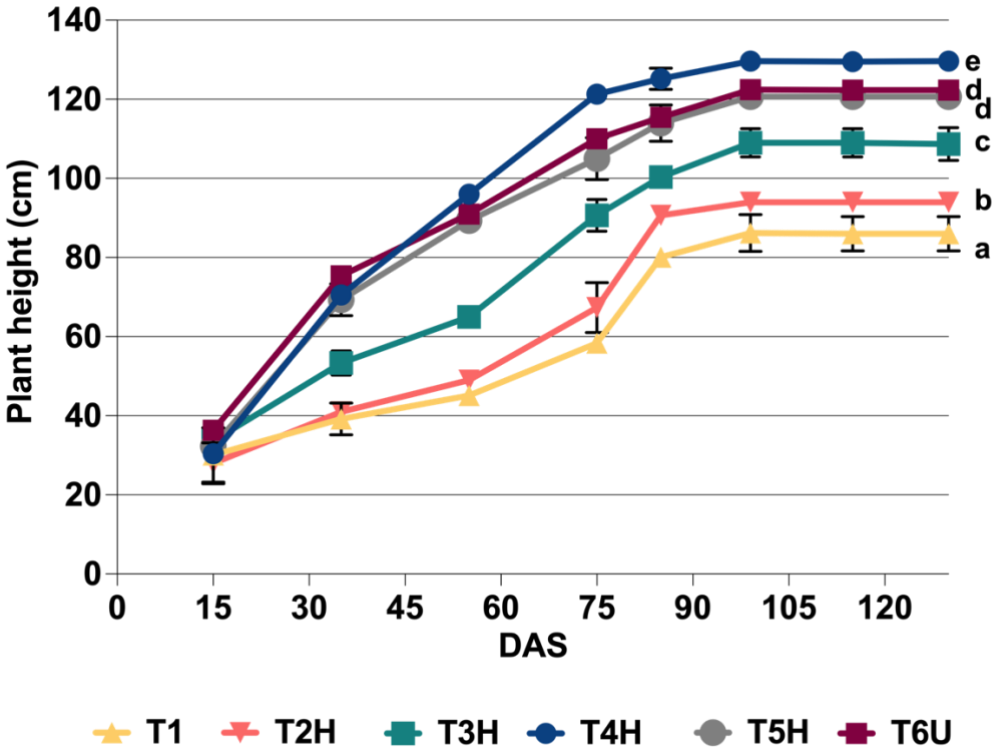


Figure 4.14: The effect of N level on the plant height (cm). Different letters indicate significant differences. Error bars represent the standard deviations from 5 replications (n=5)

4.2.1.2 Number of Tillers

Following that, treatment T4H (4.8 N g pot^{-1} = 75% RDF) generated the most tillers per plant (12) compared to the treatment given common urea dosage (T6U, 9 tiller per plant) and control treatment (T1, 5 tillers per plant) (Figure 4.15). Other treatments have 11 tillers (T5H), 9 tillers (T3H), and 6 tillers per plant (T2H). The higher number of tillers in CRF confirmed the findings of another study, which found that the application of CRF may improve the number of tillers in rice compared to conventional urea (Hashim et al., 2017; Ghosh et al., 2020). This is most likely owing to prolonged release and sufficient N availability to the rice plants (Hashim et al., 2017; Ghosh et al., 2020).

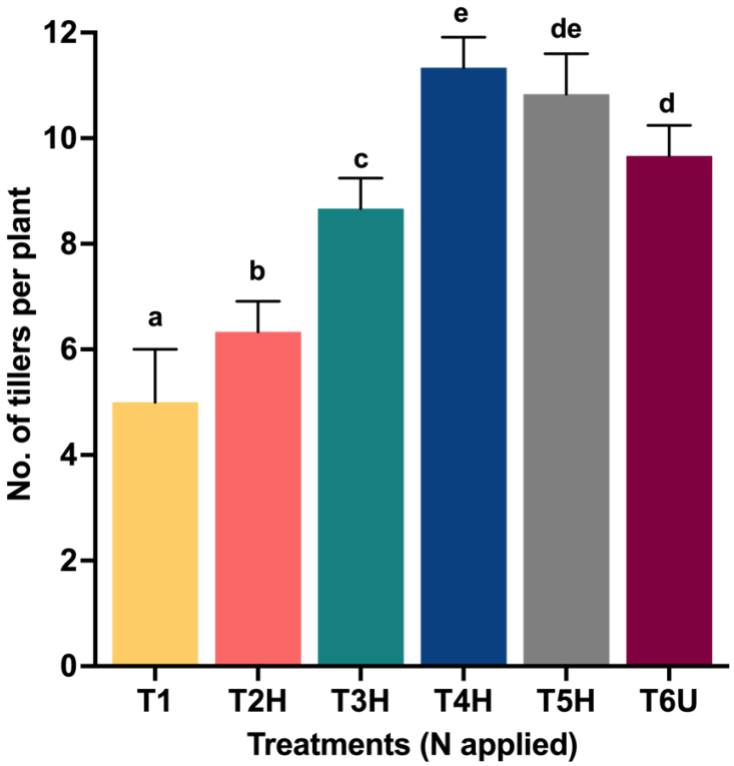


Figure 4.15: The effect of N level on the number of tillers per plant. Different letters indicate significant differences. Error bars represent the standard deviations from 5 replications (n=5)

4.2.1.3 Leaf Chlorophyll Content (SPAD)

Additionally, measurement of leaf chlorophyll content is an important parameter for assessing overall plant health and enhancing NUE (Cortazar et al., 2015). It denotes the physiological states of the rice plants as indicated by photosynthetic pigment and leaf N content (Zhang et al., 2022). Furthermore, N availability in soil has a substantial effect on the chlorophyll level of leaf tissue (Li et al., 2017; Zhang et al., 2022). In this study, maximum SPAD reading was 39.5 in T4H (4.8 N g pot^{-1} = 75% RDF) and the order was T4H>T5H>T3H>T2H>T6U>T1 (Figure 4.16) (Appendix 9). CRF at 75% N (T4H) and 100% N (T5H) led to a significant improvement in the leaf photosynthetic rate compared to the rice plants given common urea dosage (T6U) and control treatment (T1).

This indicates that SPAD readings were related to and linearly correlated with the chlorophyll and N levels in the plants (Loh et al., 2002; Xiong et al., 2015). A greater SPAD value suggests a higher chlorophyll content due to improved N uptake. Increased N uptake by the rice plant increases the protein content in the plant (Ayadi et al., 2022), which supports better photosynthetic rates and subsequently improves the plant growth (Masclaux-Deubresse et al., 2010).

According to Dobermann and Fairhurst (2010), the optimal SPAD threshold for the rice plants is between 29 and 32. In this study, T4H (39.5) and T5H (38.1) elevated the SPAD values in rice plants above the optimum SPAD threshold. Meanwhile, the rice plants given common urea dosage (T6U) resulted in a SPAD reading of 31.7 which is still within the optimal threshold range. Increased SPAD readings suggest that the application of CRF, i.e., T4H and T5H improved N uptake by the rice plants while minimizing N loss to the

environment (Ransom et al., 2020). Similar results have been reported in other studies (Yang et al., 2012; Geng et al., 2015; Li et al., 2017; Chen et al., 2020; Zhao et al., 2023).

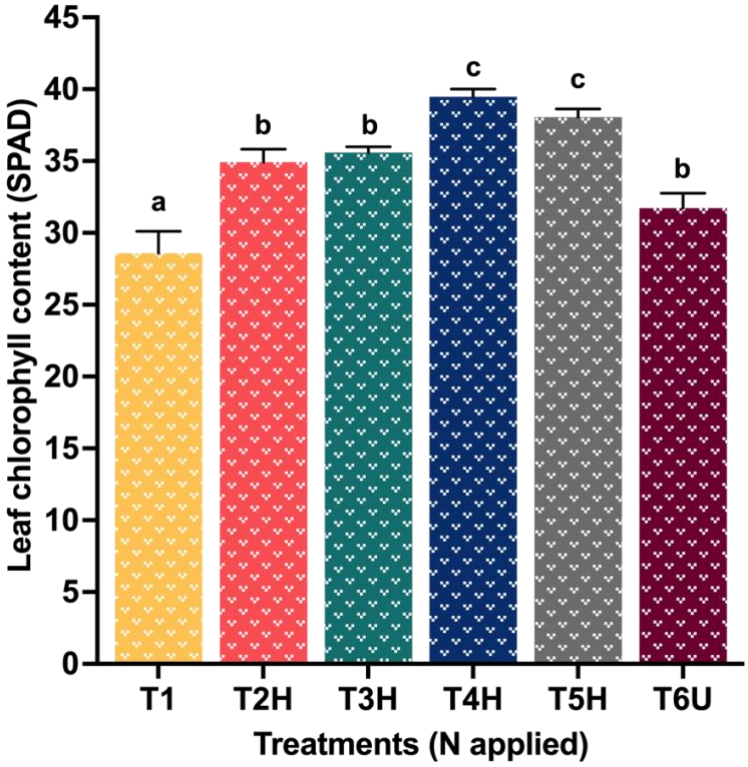


Figure 4.16: The effect of N level on the leaf chlorophyll content (SPAD) of the rice plants. Different letters indicate significant differences. Error bars represent the standard deviations from 5 replications (n=5)

4.2.2 Yield and Yield Component Data

The N treatments had a significant effect on the yield and yield parameters of rice plants (Table 4.2 and Figure 4.17 (Appendix 10)). Grain yields were estimated using yield components such as 1000-grain weight, percentage filled grains (PFG), panicle number, and number of grains per panicle.

The highest 1000-grain weight was 24.85 g in T4H (4.8 N g pot^{-1} = 75% RDF), but it did not differ substantially from other treatments (T3H, T5H and T6U) (Table 4.2). Previous studies found that N management has no significant effect on 1000-grain weight

(Mauad et al., 2003; Kamara et al., 2010; Alam et al., 2021). Furthermore, further increases in N may decrease 1000-grain weight, most likely due to inadequate carbohydrates to support the increased number of grains produced. PFG varied with N treatments, with T4H having the highest PFG, followed by T5H and T6U, and T1 having the lowest.

Figure 4.15 shows that the number of panicles in each pot ranged from 6 to 12 panicle pot^{-1}. The most panicles were produced by T4H (12 panicles pot^{-1}), followed by T5H (10 panicles pot^{-1}). The rice plants given common urea dosage, T6U, and T3H (CRF 50% N) produced the same number of panicles (8 panicles pot^{-1}) and T1 produced the fewest panicles (6 panicles pot^{-1}). These results corroborated with previous research which found increased panicle number with increased N rates (Manzoor et al., 2006; Zhang et al., 2020). Furthermore, increased N rates may imply greater N availability during the tillering stage, which is crucial for cell division (Wang et al., 2018). During the reproductive stages of the rice crops, sufficient N availability could induce cell division and stimulate the formation of panicles (Jahan et al., 2022).

The highest number of grains was observed in T4H (134 grains) compared to the rice plants given common urea dosage (T6U, 123 grains) and control treatment (T1, 110 grains). The number of grains in other treatments was 128 grains (T5H), 118 grains (T3H), and 116 grains (T2H). The increased number of grains with increasing N rates could be attributed to a greater number of panicles, resulting in high grain yield in rice (Parida et al., 2022; Ye et al., 2022; Wang et al., 2023).

In terms of grain yields, T3H, T4H, T5H, and T6U all showed significant improvements in rice grain yield as depicted in Figure 4.15. T4H increased rice grain yield by 71.1% when compared to the control treatment, T1. Furthermore, T4H increased rice

grain yield (%) significantly greater than in other treatments, with T2H increasing by 14.5%, T3H increasing by 31.1%, T5H increasing by 57.9%, and T6U increasing by 46.7 %.

In this study, CRF with only 75% N (T4H) application in soil increased the rice grain yield when compared to the CRF with 100% N (T5H) and 100% RDF, i.e., common urea dosage (T6U) by farmers' fertilizer practices. This suggested that the application of CRF to soil may minimize N fertilizer consumption and frequency of dosing while increasing crop yield (Hashim et al., 2015; Ke et al., 2017; Li et al., 2017).

Moreover, these results were comparable with those of other studies (Qiao et al., 2012; Yao et al., 2012; Wu et al., 2013), indicating that a moderate N application, i.e., T4H in this study, may produce the highest rice grain yield potential, and that further increasing N supply did not increase rice grain yield. Furthermore, observations indicate that CRF may provide a prolonged N supply to the rice plants through sustained N release, which is crucial for improving N uptake at late growth stages of rice, hence increasing rice grain yields (Wang et al., 2018; Pratiwi et al., 2021).

This was further supported by Zhang et al. (2020) who found that increasing N rates significantly increased rice grain yields; nonetheless, this increase in rice grain yield is restricted to a particular range of N rates. Thus, the favorable effects of CRF on the yield and yield-attributing factors compared to that of T6U (common urea) were consistent with earlier findings (Qiao et al., 2012; Wu et al., 2013; Hashim et al., 2017; Ke et al., 2017; Li et al., 2017; Liu et al., 2019; Gil-Ortiz et al., 2020; Alemu, 2021; Yuan et al., 2021; Yan et al., 2022).

Table 4.2: 1000-grain weight (g) and percentage filled grain (% F) of different N treatments

Treatment	1000-grain weight (g)	Percentage filled grains (% F)
T1	20.46[a]	71.74[a]
T2H	20.52[a]	73.36[a]
T3H	21.76[ab]	77.69[b]
T4H	24.85[b]	89.59[c]
T5H	24.06[b]	87.9[c]
T6U	23.25[b]	72.38[a]

Different letters indicate significant differences ($p \leq 0.05$)

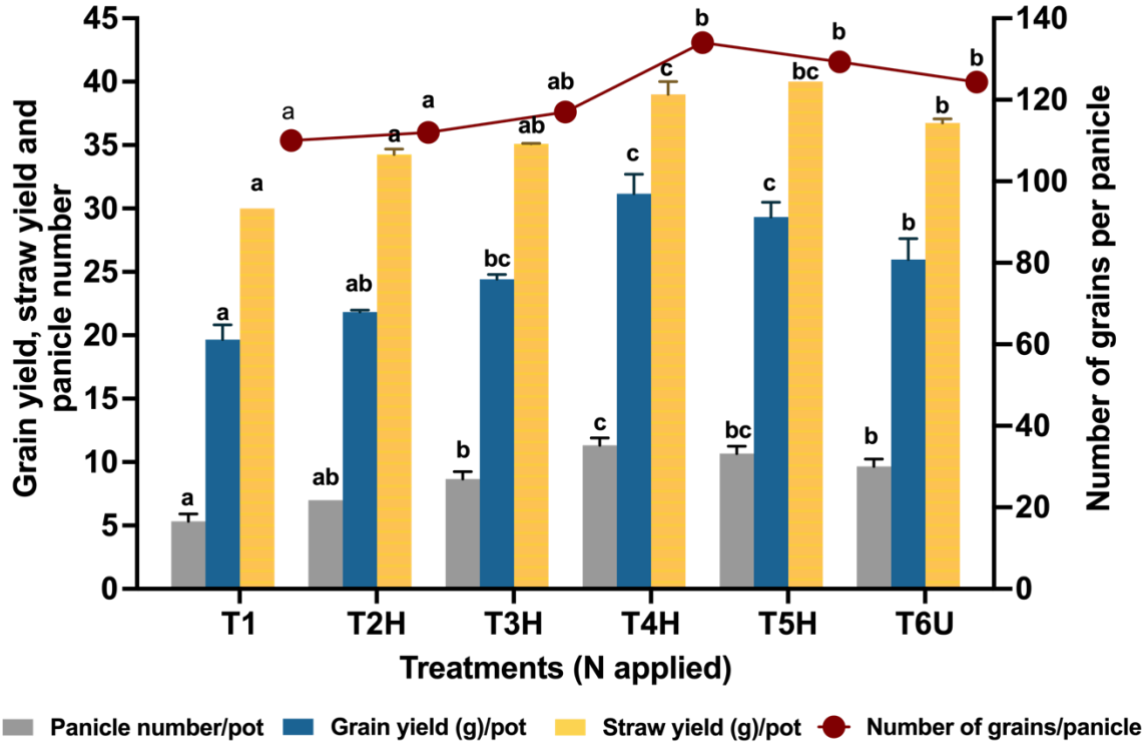


Figure 4.17: The effect of N treatments on the number of panicles per plant, number of grains per panicle, grain, and straw yield. Different letters indicate significant differences ($p \leq 0.05$). Error bars represent the standard deviation from 5 replications (n=5)

4.2.3 Harvest Index (HI)

Higher HI implies that more of the aboveground components of rice collected were grains (Jiang et al., 2018). For this reason, higher HI is preferable when CRF is applied to the paddy field as the grain yield is the most significant aspect of rice farming. Figure 4.18 (Appendix 11) depicts that all CRF treatments improved rice HI, with T4H attaining the highest HI (45.5%). T5H demonstrated a slight improvement in HI, however not substantially different from T4H and other treatments.

The rise in HI for T4H could be related to an increase in total N uptake in the rice plants, which peaked during the 11th week of grain formation (Oikeh et al., 2008; Hashim et al., 2015). After the 11th week, during the grain filling and maturity stage, most of the N required for rice emerges from the culm, leaves, and panicles rather than from the soil (Hashim et al., 2015; Shrestha et al., 2020). This shows that N uptake from the soil was minimal (Shrestha et al., 2020). This is most likely the most significant component that improves HI. Since the rice plants received sufficient N before the 11th week, more N is likely be transmitted to the grains, thus increasing HI and grain yield over biomass.

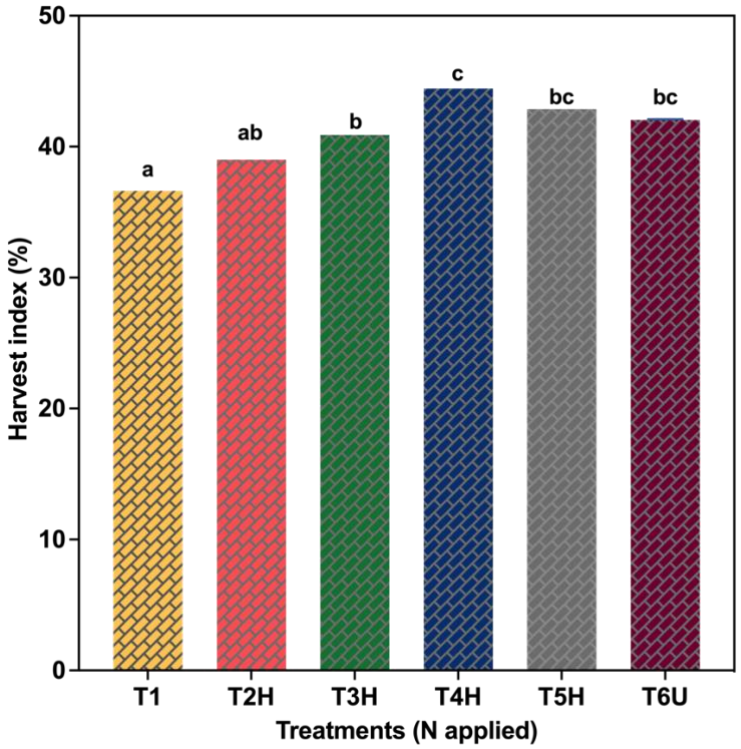


Figure 4.18: Harvest index of rice with different N treatments. Different letters indicate significant differences ($p \leq 0.05$)

4.3 Analyses of Nitrogen (N) Uptake and Nitrogen Efficiency Estimation (NUE)

4.3.1 N Uptake of the Rice Plants

Figure 4.19 (Appendix 12) shows the effect of N treatments on the rice N uptake and N use efficiencies over field studies. The optimum N uptake rate was shown in the presence CRF hydrogels at different N rates (%). The rice N uptake in different treatments showed significant differences at $p < 0.05$. The highest N uptake of rice was observed in T4H (0.25 g kg^{-1}) compared to rice given common urea dosage (T6U, 0.19 g kg^{-1}) and control treatment (T1, 0.03 g kg^{-1}). The second highest N uptake of rice was 0.22 g kg^{-1} (T5H). Observations from this study shows that the CRF applications, i.e., T4H and T5H significantly improved the rice N uptakes compared to those treated with conventional urea (T6U) at higher N applied. However, crop N uptake was relatively lower in T2H (0.88 g kg^{-1}) and T3H (0.09 g kg^{-1}).

The trend of rice N uptake is comparable with the findings by Hashim et al. (2015). In general, increasing N uptake is directly correlated with increasing aboveground yield (Figure 4.17) because the crop N uptake followed a similar trend as plant biomass. According to Nong et al. (2020), an increase in N uptake with CRF application could be attributed to N translocation from vegetative parts of the rice plants to grain during the final phases of the rice plant growth. Furthermore, urea-loaded hydrogels were observed to facilitate the gradual release of nutrients that closely matched the N requirements of the rice crops, resulting in improved N use efficiencies. These findings were consistent with those reported by Fazlina et al. (2014), Liu et al. (2019), Gil-Ortiz et al. (2020), Yuan et al. (2021), Yan et al. (2022).

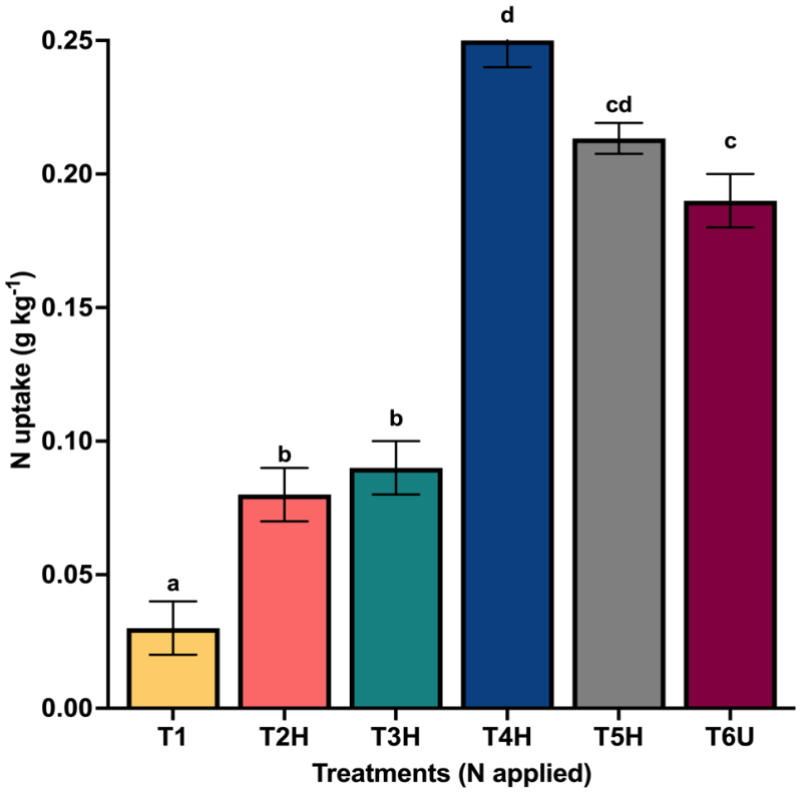


Figure 4.19: The effect of N levels on the N uptake of the rice plants. Different letters indicate significant differences ($p \leq 0.05$). Error bars show the standard deviation from 5 replications (n=5)

4.3.2 Nitrogen Harvest Index (NHI)

In Figure 4.20 (Appendix13), the highest NHI was observed in T4H (67.9%) of all N treatments. T5H had the second highest NHI (61.3%), followed by T6U (60.5%). The NHI values for T2H, T3H and T1 were estimated to be 53.0%, 58.9% and 50.4%, respectively. These findings suggest that the highest NHI in T4H indicates positive synchronization between improved rice grain yield (Figure 4.16) and HI (Figure 4.17). Further, higher NHI was positively correlated with total N uptake of the rice plants (Padhan et al., 2023). Higher NHI resulted in higher N uptake (Padhan et al., 2023). Besides, other treatments demonstrated positive synchronization with NHI patterns comparable to T4H.

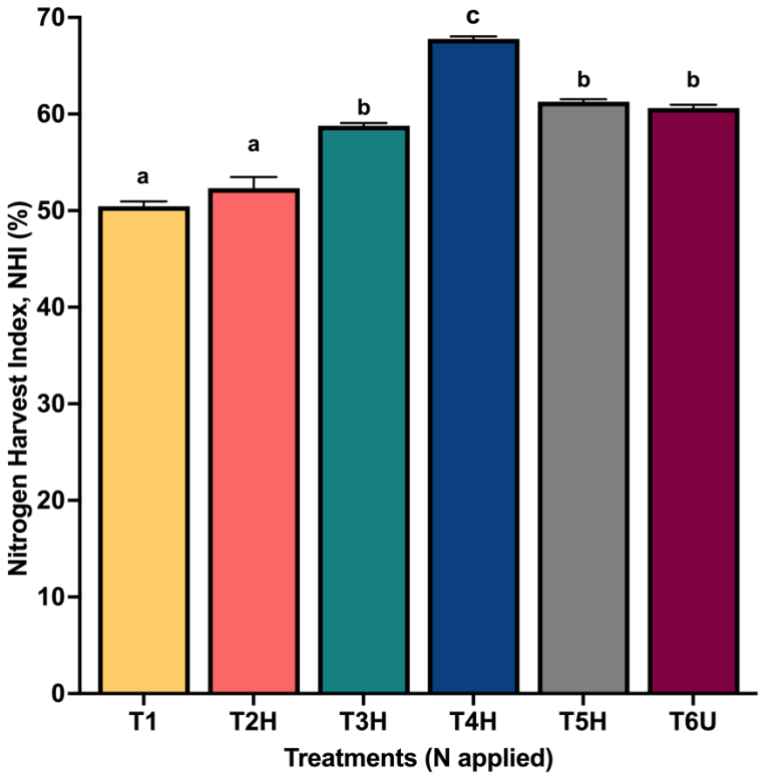


Figure 4.20: The effect of N levels on Nitrogen Harvest Index (NHI) of the rice plants. Different letters indicate significant differences ($p \leq 0.05$). Error bars show the standard deviation from 5 replications (n=5)

A preliminary study from Wang et al. (2017) showed an increase in NHI of the rice plants at average of 73.3% when 75% of N fertilizer encapsulated in CRF was applied. In

addition, their findings reported that NHI declined with increasing N rates; 68.9% NHI (165 kg ha^{-1} N/100%) and 65.1% NHI (247.5 kg ha^{-1} N/120%). Also, their findings found that the highest number of grains was observed in 75% N fertilizer treatment. This suggests that the highest NHI in their study indicates positive synchronization with improved rice grain yield.

Other study by Padhan et al. (2023) reported an increase in NHI values of the rice plants ranging from 45% to 89% using N fertilizer encapsulated in CRF hydrogel. In their study, the highest NHI (89%) was recorded at 120% N rate, meanwhile 75% N rates recorded 64.6% NHI. Their findings also showed a positive synchronization between increased NHI values with that of higher grain yield and harvest index.

4.3.3 Nitrogen Use Efficiency (NUE)

In Figure 4.21 (Appendix 14), treatment T4H (4.8 N g pot^{-1} = 75% RDF) had the highest NUE (52.6%), while treatment T6U had the lowest NUE (31.2%). In general, the NUE of CRF treatment increased with increasing N application rate up to 4.8 N g pot^{-1} (T4H), after which NUE began to decrease with increasing N rate (6.4 N g pot^{-1} in T5H and 6.4 N g pot^{-1} in T6U). This is consistent with prior research demonstrating that a moderate N rate may lead to higher NUE potential because further increase in N rate may not further increase the NUE levels (Qiao et al., 2012; Yao et al., 2012).

Furthermore, investigations have revealed that conventional urea used in farmers' practices has resulted in a low NUE (Chen et al., 2015), resulting in poor synchronization of N supply and crop demand. In other words, this is associated with the main contributing issues, i.e., over 50% fertilizer loss to the environment due to leaching and surface run-off (Lawrencia et al., 2021; Ahmad et al., 2023). This was confirmed in current study, in which T6U exhibited the lowest NUE of all N treatments.

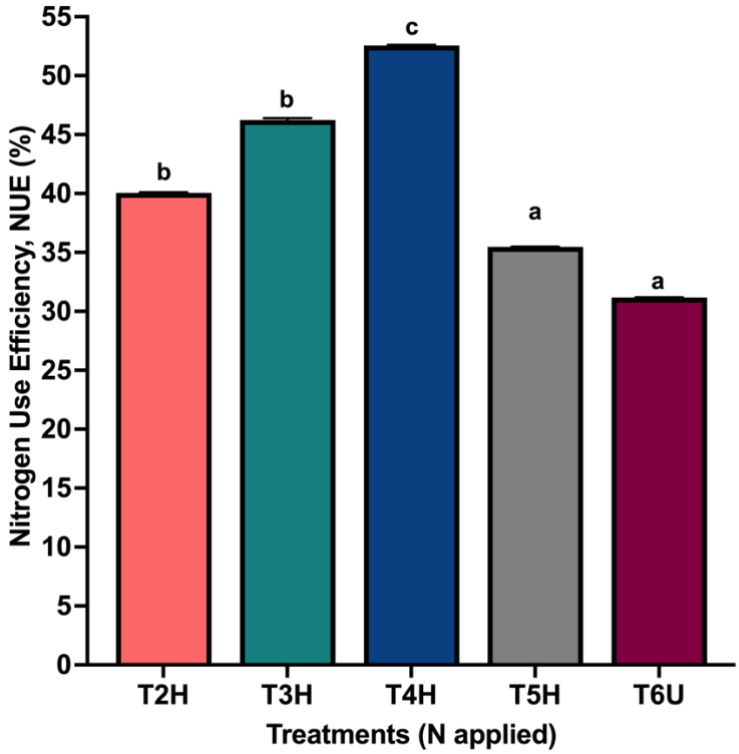


Figure 4.21: The effect of N level on Nitrogen Use Efficiency (NUE) of the rice plants. Different letters indicate significant differences ($p \leq 0.05$). Error bars show the standard deviation from 5 replications (n=5)

4.3.4 Agronomic Nitrogen Efficiency (NAE)

Figure 4.22 (Appendix 15) shows the influence of N treatments on NAE. NAE ranged from 3.33 kg kg^{-1} to 12.78 kg kg^{-1} for various N rates. The highest NAE was observed in T4H (12.78 kg kg^{-1}) compared to rice given common urea dosage (T6U, 5.73 kg kg^{-1}). NAE increased with increasing N rate for CRF up to 4.8 N g pot^{-1} in T4H (90 kg N ha^{-1}), but after that decline with increasing N rates in T5H and T6U. The NAE values in T5H and T6U were still higher than in T2H (3.33 kg kg^{-1}) and T3H (6.15 kg kg^{-1}) because of greater rice grain yields in T5H and T6U (Figure 4.14). Similar findings were observed by Barbieri et al. (2008), with NAE declining as the N application rates increased.

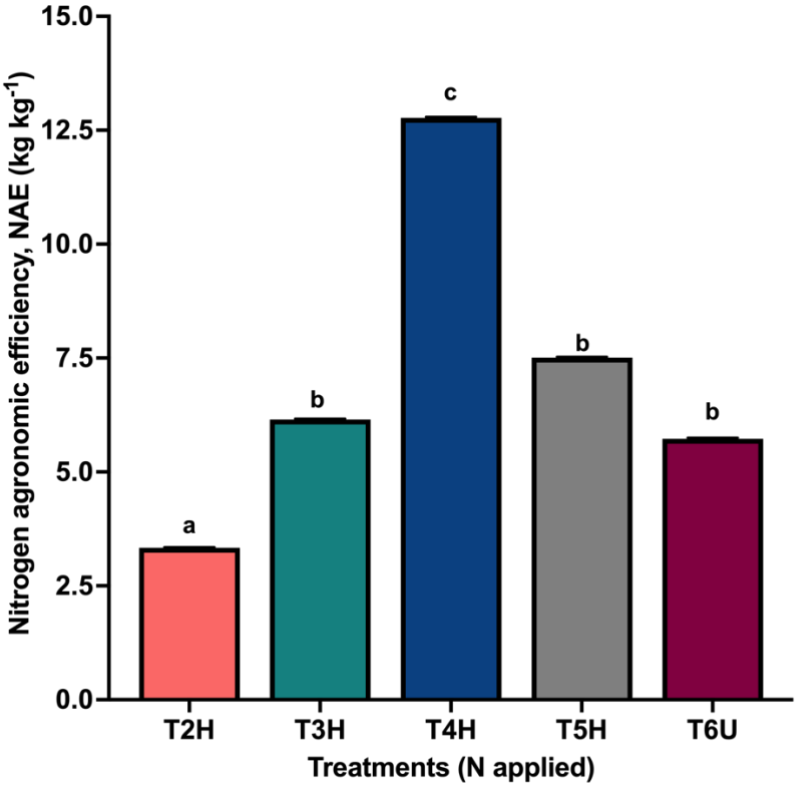


Figure 4.22: The effect of N levels on Agronomic Nitrogen Efficiency (NAE) of the rice plants. Different letters indicate significant differences ($p \leq 0.05$). Error bars show the standard deviation from 5 replications (n=5)

One of the primary objectives of N fertilization is to improved N uptake and efficiencies in upland rice cultivations by the application of cellulose-based hydrogels as controlled release fertilizers. In this study, rice plants given with CRF at 4.8 g N pot^{-1} (T4H; 75% RDF) recorded the highest N efficiency when compared to the traditional farmers' nitrogen fertilization practices and 100% N CRF application. This could be explained by the level of N rate in T4H which corresponds to the optimal crop N requirement. This also indicates that the application of CRF to soil may minimize N losses to the environment, reduce fertilizer consumption as well as frequency of dosing while increasing crop yield and N efficiency (Hashim et al., 2015; Ke et al., 2017; Li et al., 2017).

Additionally, findings from this study are consistent with data from other studies, including Wang et al. (2018), Gil-Ortiz et al. (2020), Qi et al. (2020), Pratiwi et al. (2021), Yuan et al. (2021), Tian et al. (2022), Yan et al. (2022).

4.3.5 Dry Matter Partitioning

Dry matter progression in the rice plants increased steadily throughout the growth phases and peaked at maturity (Figure 4.23) (Appendix 16). The dry accumulation pattern in the rice plants demonstrated a modest exponential growth, period of linear growth, and a period of constant weight. The highest dry matter (109.9 g pot^{-1}) was obtained in T4H, while the lowest (62.3 g pot^{-1}) dry matter was obtained in control treatment, T1. Dry matter in T5H and T6U was 107.9 g pot^{-1} and 107.1 g pot^{-1}, respectively. Results thus indicate that response was more pronounced with higher N rate applications than lower N rate applications.

Higher N rates can increase dry matter content due to higher protein content in the rice plants, which promotes higher photosynthetic rates on leaves (Leite et al., 2021; Ayadi et al., 2022). This enhanced the rice plants growth during vegetative stage and later distribution of assimilates to the reproductive organs (Leite et al., 2021; Ayadi et al., 2022). Furthermore, dry matter production is profoundly associated with intercept photosynthetically active radiation (Xiong et al., 2015).

Low N supply in the rice plants have been identified as a limiting factor in alleviating radiation usage efficiency and biomass productivity, resulting in lower dry matter yield (Loh et al., 2002; Xiong et al., 2015). Information on dry matter production and partitioning between different plant sections as influenced by N rates application is crucial to develop rice growth models (Loh et al., 2002; Xiong et al., 2015; Leite et al., 2021; Ayadi et al.,

2022). Dry matter partitioning to the reproductive organs depends on number, capacity, and activity of physiological sinks (Loh et al., 2002).

The distribution of dry matter into leaf, leaf sheath, stem and panicles of the rice plants was nearly identical across the treatment levels (Figure 4.24) (Appendix 17). The portioning of dry matter into leaf, leaf sheath, and stem increased up to 65 DAS, while panicle dry weight rose until 75 DAS.

After 65 DAS, dry matter partitioning into vegetative parts reduced, indicating remobilization of assimilates from vegetative parts towards flowering stages and forming grains (Xiong et al., 2015). N fertilization induced a considerable variation in the pattern of dry matter partitioning of the rice plants at all growth stages, where low N rates stimulate allocation of least dry matter to all plant sections.

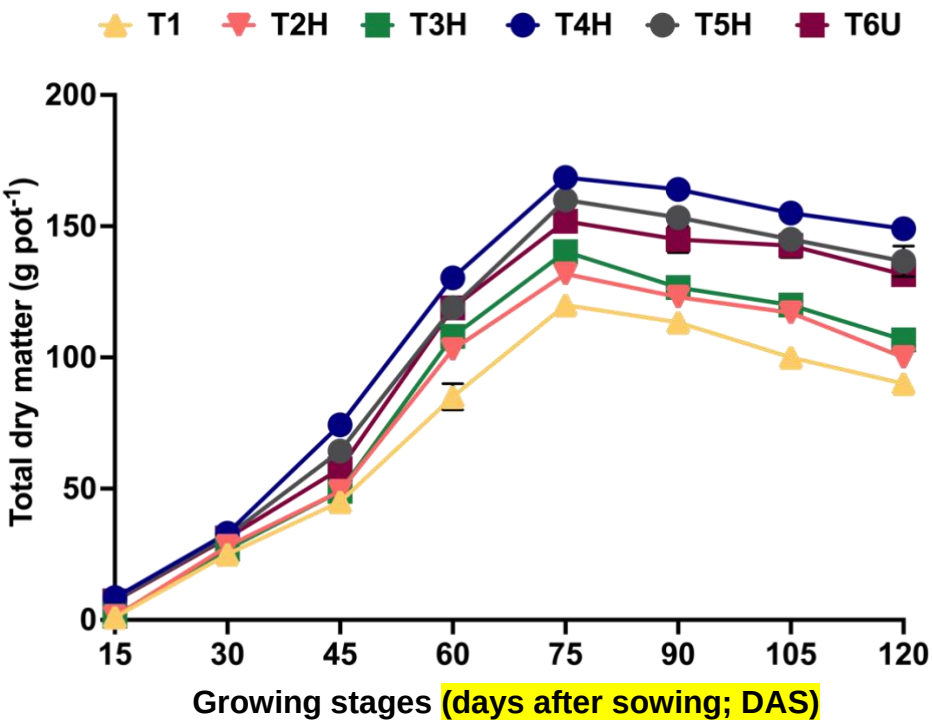


Figure 4.23: Dry matter accumulation in rice as influenced by N rates application over the crop growth stages.

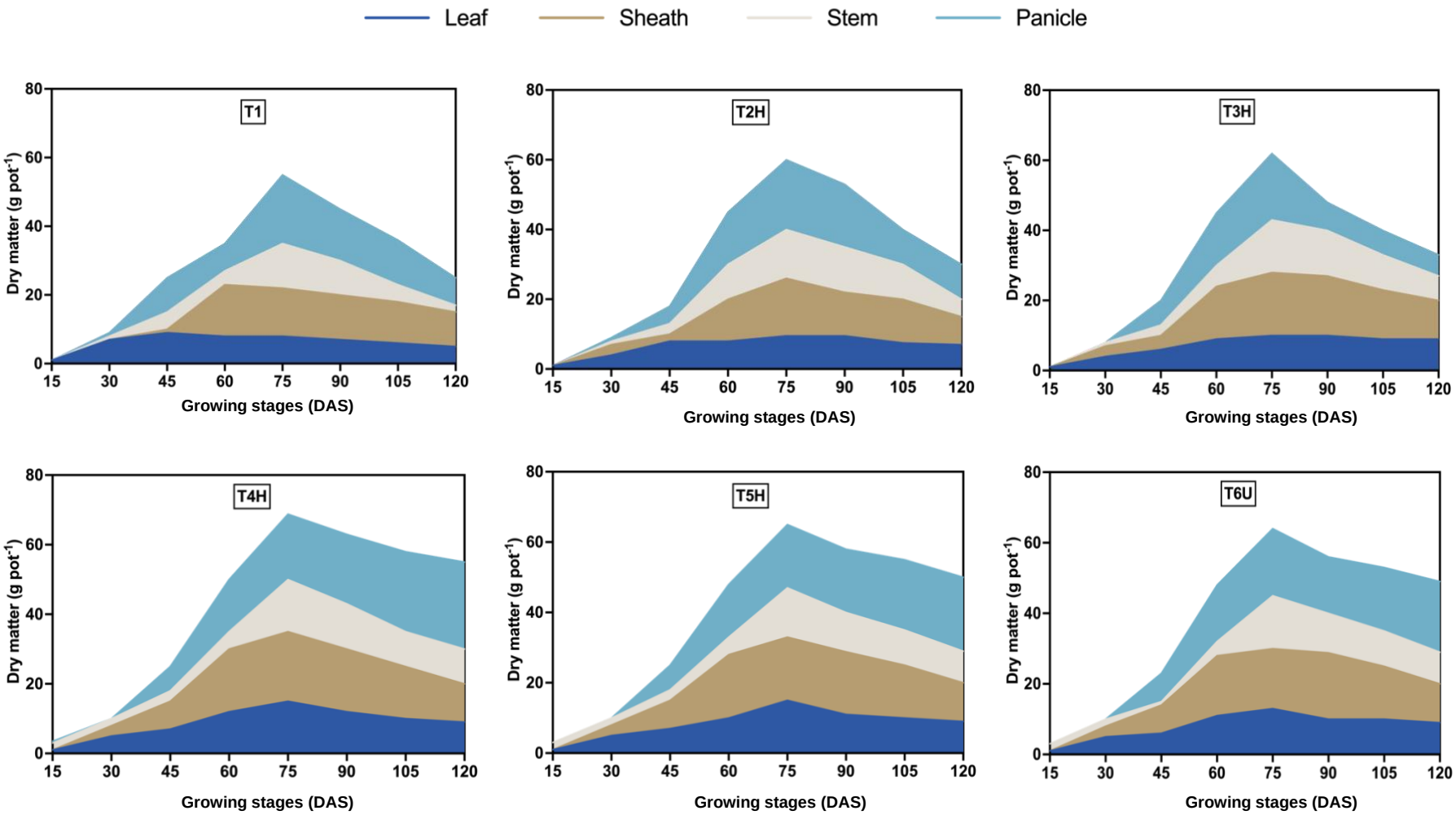


Figure 4.24: Pattern of dry matter partitioning to different parts of rice as influenced by time course and nitrogen level

4.3.6 Correlation Regression Analysis

Grain yield is determined by yield-attributing components such as the number of panicle and number of grains per panicle. The relationship between growth characteristics, yield-attributing factors, and grain yield was evaluated using a simple correlation coefficient ($p < 0.05$) (Figure 4.25) (Appendix 18).

Figure 4.25 (a) and (b) illustrate that there is a positive relationship between the grain yield and yield-attributing components. Similarly, as illustrated in Figure 4.25 (c), the associated between the grain yield and HI was both positive and significant ($R^2 = 0.7881$, $P < 0.001$). Grain yield accounted for 78.8% of the increase in HI, with other variables accounting for the remaining 21.2% of the increase in rice grain yield.

Sui et al. (2013) demonstrated that the increase in grain yield was attributable with the increased panicle number and number of grains per panicle, which corresponds with findings from this study that the panicle number and number of grains per panicle were the most variable yield components identified (Figure 4.17). The highest rice grain yield for T4H could be associated with the increased panicle number and number of grains. This was further confirmed by a substantial and positive relationship between grain yield and both the number of grains per panicle ($R^2 = 0.9607$, $P < 0.05$) and panicle number ($R^2 = 0.9722$, $P < 0.05$), as illustrated in Figures 4.25 (a) and (b).

Further, similar study by Karki et al. (2018) demonstrated a positive correlation between number of grains per panicle with yield attributing factors such as panicle number, number of tillers and test weight. Similarly, their findings suggest that the relationship between grain yield and harvest index was positively correlated and significant ($R^2 = 0.453$). The number of tillers/m^2 contribute approximately 25.4% ($R^2 = 0.254$) on the grain yield.

Whereas the remaining 74.60% increase in grain yield may be due to variable other than number of tillers. Similarly, approximately 31.5% (R^2 = 0.315) contribution was given by number of filled grains per panicles on grain yield. And the remaining 68.50% part was contributed by the variables other than filled grains per panicle. Again, test weight input about 7.1% (R^2 = 0.071) share on grain yield and left over 92.9% increase in grain yield was due to other variables except test weight. Whereas grain yield contributed about 45.3% (R^2 = 0.453) towards increase in the harvest index. And the remaining 54.70% contribution for increasing yield was given by the variable other than harvest index.

Previous study by Sun et al. (2017) on the correlation and regression of rice reported that, rice traits being studied showed the striking positive correlations among the panicle length, grains number per panicle, primary panicle branch, and secondary panicle branch. Moreover, Bagheri et al. (2011) and Norain et al. (2014) reinforced the statement that there was a high significant and positive correlation between the number of grains per panicle and panicle length.

Meanwhile, Karim et al. (2014) reported that the number of primary panicle branches per panicle had a highly significant and positive correlation with the number of filled grains per panicle. The total number of grains per panicle was used as the main trait as it is expected to reflect the potential yield of tested rice genotypes.

In line with this expectation, Devi et al. (2016) found that the relationship between the number of grains per panicle and the grain yield per plant was positively and highly significantly correlated. In the other case, the filled grains per panicle indicated positive and highly significant indirect correlation with the yield per ha in phenotypic and genotypic level (Oladosu et al. (2018).

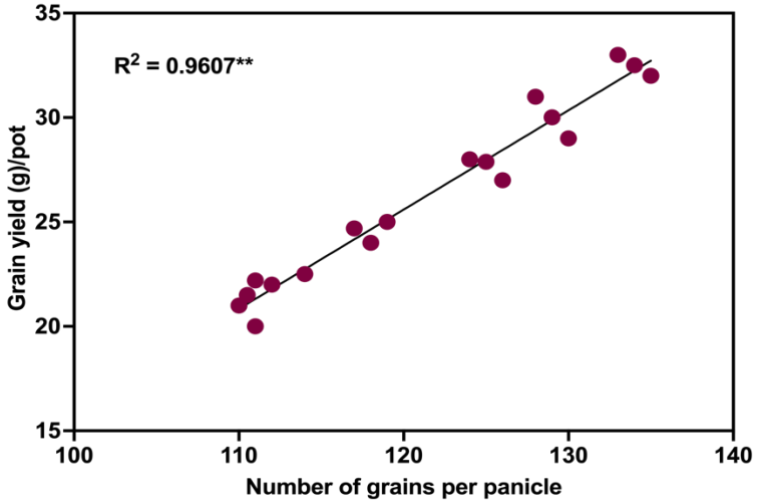
The common issues in the correlation relationship of the rice agronomical characters were grain yield, plant height, number of tillers per plant, panicle length, number of grains per panicle, 1000-grains weight, and number of filled grains per panicle (Hastini et al., 2019). Number of grains per panicle usually had a positive correlation with the panicle length, and number of filled grain per panicle (Hastini et al., 2019).

As many studies had shown that the grain yield showed a positive and significant correlation with the number of grains per panicle, then the number of grains per panicle could be used as the dependent variable in a regression with other traits (Hastini et al., 2019).

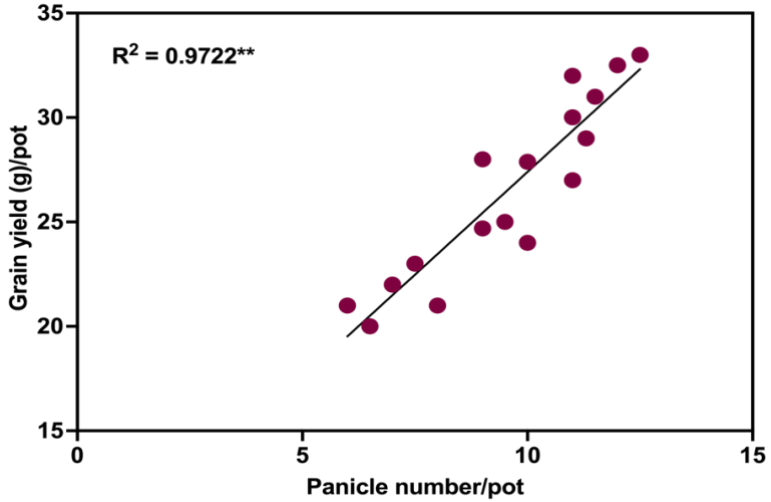
Moreover, panicle number is one of the determining components that influence rice grain yield. This is because increasing the number of panicles has a similar effect as increasing grain yield (Lee et al., 2010; Jahan et al., 2022). Furthermore, current findings revealed that the number of panicles and the number of grains per panicle were both positively correlated with N uptake (Figure 4.25 d, e). This demonstrates that greater N uptake improved grain formation, resulting in higher grain yield.

This study aimed to understand the correlation and regression relationship between the number of grains per panicle with other traits of rice panicle branching. The other traits would be used as a predictor in the regression analysis. Furthermore, this study could give the information on the panicle branching traits contribution to the total grains number per panicle.

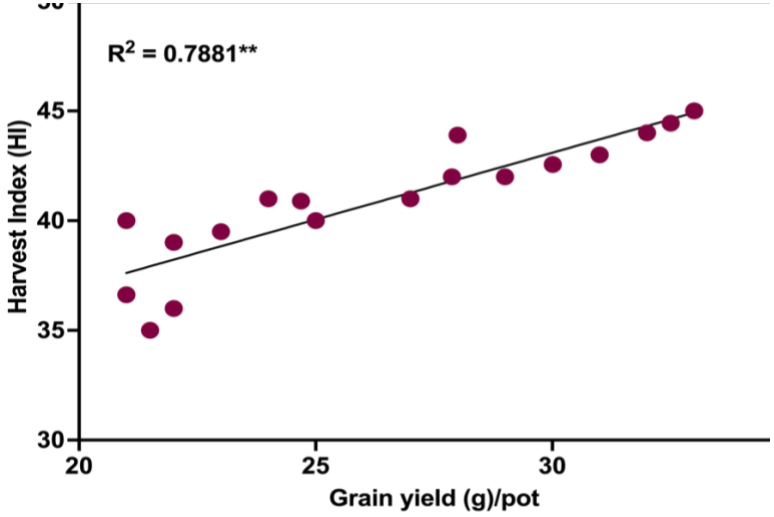
(a)


R² = 0.9607**
Grain yield (g)/pot
Number of grains per panicle
35
30
25
20
15
100
110
120
130
140

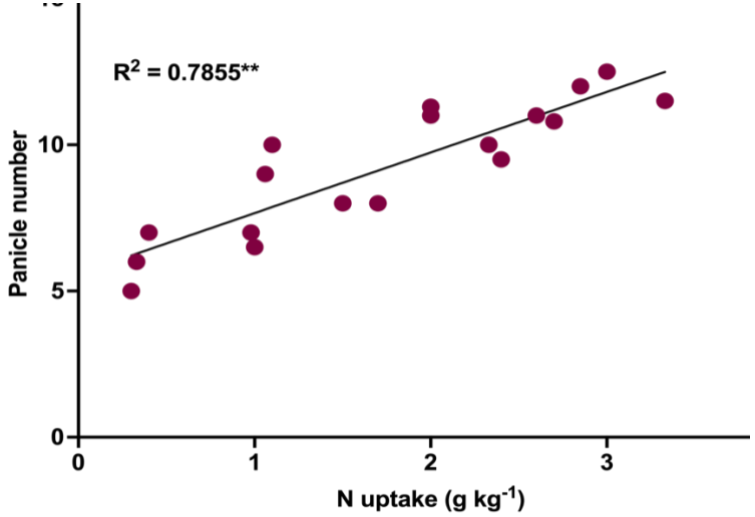
(b)


R² = 0.9722**
Grain yield (g)/pot
Panicle number/pot
35
30
25
20
15
0
5
10
15

(c)


R² = 0.7881**
Harvest Index (HI)
Grain yield (g)/pot
45
40
35
30
20
25
30

(d)


R² = 0.7855**
Panicle number
N uptake (g kg-1)
10
5
0
0
1
2
3

(e)

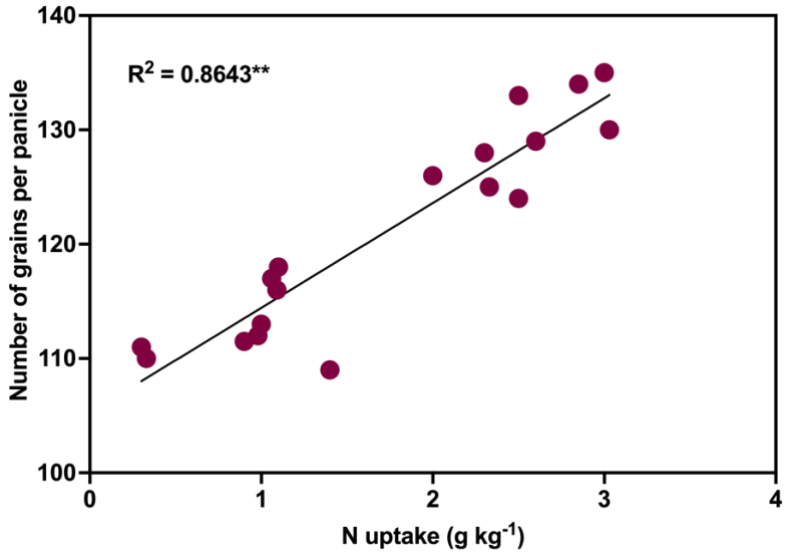


Figure 4.25: Linear relationship of grain yield with (a) number of grains per panicle, (b) panicle number/pot, (c) harvest index (HI) and linear relationship of N uptake with (e) panicle number and (f) number of grains per panicle at $p < 0.05$*

4.3.7 Degradation of Cellulose Hydrogels CRF

The soil test was used to assess the biodegradability of cellulose hydrogels CRF throughout the rice cultivation period. The weight of cellulose hydrogels CRF lost during the degradation time throughout the rice cultivation period is shown in Figure 4.26 (Appendix 19). The graph shows that the weight of cellulose hydrogels CRF gradually decreasing over time (a decreasing linear function), indicating that biodegradation of cellulose hydrogels CRF occurs in soils. Following harvest, only small fragment of cellulose hydrogels could be found, and weight loss reached up to 97% of their initial weight. This shows that the cellulose hydrogels CRF had nearly 100% degraded after 135 days.

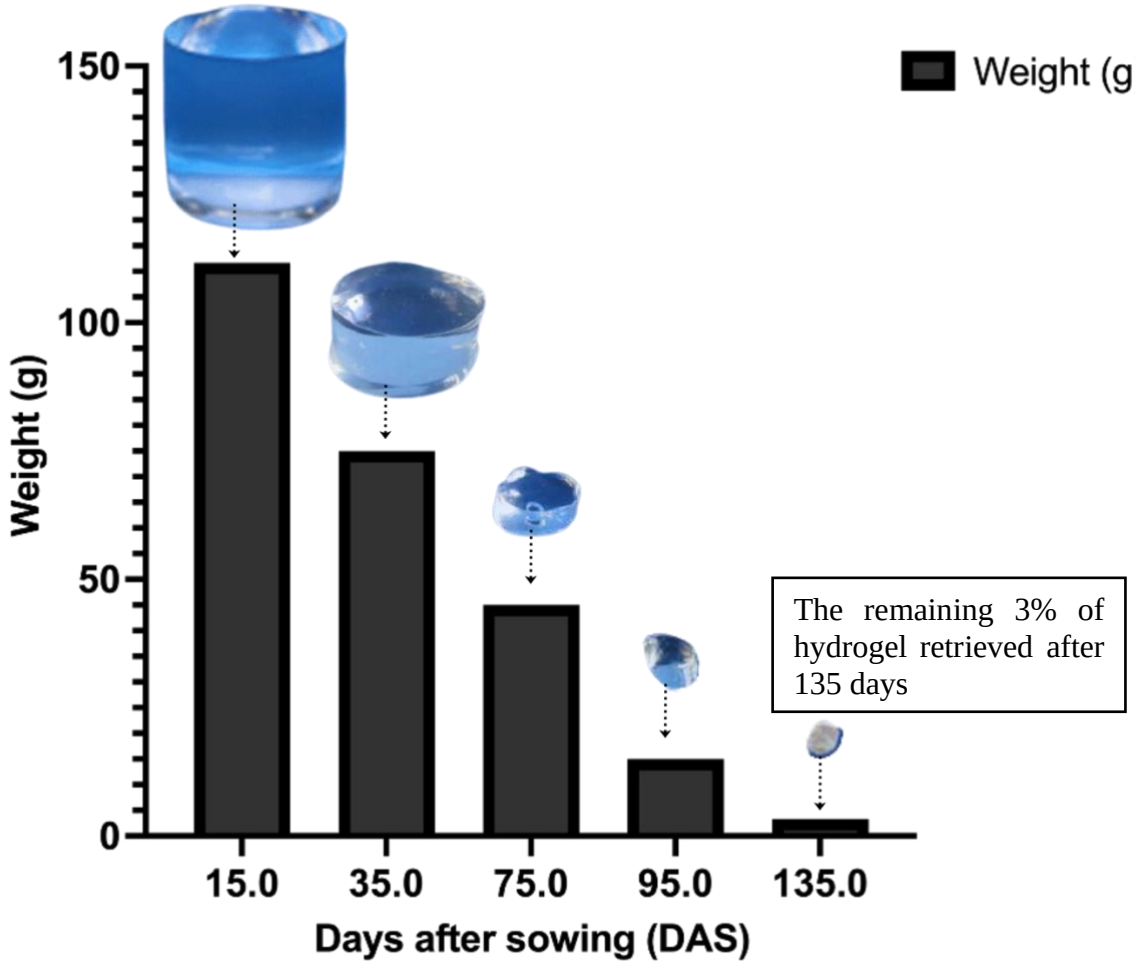


Figure 4.26: Mass loss of cellulose hydrogels CRF (with images of hydrogels retrieved accordingly) during the degradation time throughout the rice cultivation period.

In conclusion, CRF treatments have significantly increased rice yields, which was also observed in the current study, particularly in T4H (4.8 N g pot^{-1} = 75% RDF). A possible explanation for this might be due to sufficient N supply from the sustained release of hydrogels CRF closely matched the N requirements of the rice crop. Urea fertilizers encapsulated in cellulose hydrogels were observed to facilitate gradual and uniform N release over the growing cycle, allowing rice plants to absorb adequate N efficiently while minimizing N losses through leaching, surface run-off, and ammonium volatilization (Lawrencia et al., 2021; Ahmad et al., 2023).

A single basal application of CRF significantly reduced N leaching compared to split application of the traditional farmers' nitrogen fertilization practices, with no loss of crop yield. Yang et al. (2012) and Ni et al. (2011) also reported that CRF delivered controlled N release over time to better met crop N requirements throughout the growing season. Therefore, CRF could be an advanced alternative to ameliorate environmental N losses in rice cultivation, thus improving N efficiencies compared to rice given conventional urea (Giroto et al., 2019).

According to Cao et al. (2018) and Yi et al. (2019), increased N efficiencies in rice were attributed to higher N assimilatory activity. Furthermore, an important element of N assimilatory enzyme, glutamine synthetase activity is highly favorable in order to enhance N utilization of rice crops (Masclaux-Deubresse et al., 2010; Wang et al., 2022). These findings further support the results from this study that CRF treatment, i.e., urea-loaded cellulose-based hydrogels increased grain yield and enhanced N efficiencies.

It is noted that although T2H and T3H were both CRF, both treatments did not give considerably higher yields unlike T4H, presumably due to insufficient N application rate to

meet the N requirements of the rice crop. Another factor that may have contributed to the excellent performance of T4H was that the urea-loaded cellulose hydrogels (CRF) remained longer in soil at high enough N content and existed in the N form that the rice plants could absorb throughout the cultivation period. This could potentially be related to the rate of N in the soil before and after rice cultivation. In this study, the rate of N release in the soil prior to rice cultivation was 75% (Ahmad et al., 2023), whereas the rate of N release after rice cultivation was 87%. The remaining 13 % N existed in CRF, where it was retained in the soil and degraded over time.

Following rice cultivation, small fragments of CRF hydrogels were retrieved and the CRF weight decrease (up to 97%) relative to their initial weight. This shows that CRF hydrogels had nearly 100% degraded after 135 days. Thus, CRF with this ability could be highly advantageous for upland rice cultivations, such as reduced N losses and frequent dosing, resulting in healthier rice growths, higher rice yields, and greater N efficiency (Lawrencia et al., 2021). Furthermore, CRF can be applied as a single basal dose, making it convenient for farmers to implement in their farming practices, owing to less frequent dosing and hence lower labor cost.

4.5 Chapter Summary

This chapter presented the results for the optimized urea-loaded cellulose hydrogels as a controlled release fertilizer and their effects on the growth performance of upland rice. Results presented in this chapter were used to achieve all four research objectives. For the fabrication of urea-loaded cellulose hydrogels, the results were first presented from which it was observed that the extent of nutrients released from hydrogels in soils were 74.7% release in topsoil, 73.37% release in wet clayey soil, and 71.84% release in sandy soil within 42

days compared to common urea which was about 97.32% release in topsoil, 95.09% release in wet clayey soil, and 98.47% release in sandy soil. The optimized urea-loaded cellulose hydrogels achieved a maximum swelling capacity of 2000%.

Urea-loaded cellulose hydrogels as a controlled release fertilizer (hydrogels CRF), were administered in upland rice cultivation and their effect on the rice growth performance were discussed. Biometric observations on the rice plants shows healthier rice growth with hydrogels CRF at an optimal N rate (T4H: 4.8 g N pot^{-1} hydrogels = 75% RDF) compared to the rice plants treated with conventional fertilizer. Rice yield and yield attributing components, as well as harvest index increased significantly with the N application of only 75% RDF compared to the rice plants treated with. conventional fertilizer. Furthermore, significant increase in N uptake by the rice plants and enhanced NUE were observed. Lastly, correlation regression analysis confirmed the positive correlation between the growth parameters, yield attributing factors and grain yield.

This chapter provides the results which could potentially be evidence of the positive effects of cellulose hydrogels as CRF, which the novelty lies in their application in upland rice cultivation in Sarawak. Biodegradability test after harvest shows that hydrogels CRF have nearly 100% degraded after 135 days. This proves that these hydrogels CRF are environmentally friendly and safe as an advanced functional CRF for upland rice cultivation.

CHAPTER 5

CONCLUSIONS AND RECOMMENDATIONS

5.1 Conclusion

This study is aimed to achieve four research objectives through two phases of research design – Phase 1 for the research and development of cellulose-based hydrogel CRF, and Phase 2 for the quantitative research design on upland rice cultivation.

The first research objective was achieved through the fabrication and development of optimized formulation of cellulose-based hydrogels as a controlled release fertilizer (CRF). Cellulose-based hydrogel CRF was successfully synthesized by crosslinking cellulose fibers extracted from waste papers and carboxymethyl cellulose (CMC) with epichlorohydrin (ECH). The fabrication process is aqueous based using pre-cooled NaOH/urea solution, eco-friendly, catalyst free and does not need any energy-intensive post-purification step rather than a simple water washing of the cellulose hydrogel. The physical, chemical, and thermal properties of synthesized cellulose hydrogel were analyzed using several instrumentation techniques including Fourier Transform Infrared (FTIR) Spectrometer, Field Emission Scanning Electron Microscope (FESEM), and Differential Scanning Calorimetry (DSC). The chemical characterization of synthesized cellulose hydrogel was performed via FTIR spectrometer, whereby the formation of crosslinking in the synthesized cellulose hydrogel was detected at 1060 cm^{-1} due to the stretching vibration of C-O-C which formed from the reaction component ECH and CMC. A new peak at 1328 cm^{-1} in the crosslinked hydrogel showed the presence of crosslinking. The presence of the carbonyl group (C=O) at 1720 cm^{-1} confirms the successful incorporation of the carbonyl group in the structures. Moreover, the DSC analysis of synthesized cellulose hydrogel CRF

showed a drastic heat loss (T > 290 °C) due to dehydration or decomposition of cellulose. This means that the synthesized cellulose hydrogel may endure high temperature and decompose at temperature of more than 290°C.Besides, the FESEM analysis indicated that the synthesized cellulose hydrogel had highly porous microstructure with many channels and interconnected capillaries in their structure. This allowed water molecules to diffuse into the cellulose hydrogel network. Therefore, the highest swelling percentage of 2055% was achieved, i.e., from the optimum formulation of cellulose hydrogel, C3 (3% (w/v) cellulose fibers, 1.75% (w/v) CMC). Moreover, the effects of the optimum formulation of cellulose hydrogel, C3 on the soil moisture were successfully determined using soil burial method. Result shows that in the presence of C3, maximum soil moisture contents reported at 36.5% in topsoil, followed by 30.1% in wet clayey soil and 23.4% in sandy soil after 7 days compared to soils without C3 hydrogel (27.1% in topsoil, 24.9% in wet clayey soil, 18.9% in sandy soil).

The second objective was achieved by conducting further analysis on the loading capacity and release behavior of fertilizer from cellulose hydrogels in water and soil (topsoil, wet clayey soil, sandy soil). The optimized formulation, C3 cellulose hydrogel was selected for the rest of analysis throughout this study. Urea as a model fertilizer was loaded onto the C3 cellulose hydrogel. The loading and release of urea from C3 cellulose hydrogel was successfully determined using Kjeldahl procedure and the Nessler method. C3 cellulose hydrogel obtained its highest loading capacity (0.5 g/g) at contact time of 48 h and at room temperature. Furthermore, C3 cellulose hydrogel was observed to facilitate gradual released of urea in topsoil (74.71%), wet clayey soil (73.37%), and sandy soil (71.84%) within 42 days relative to the free urea (control) which was about 97.32%, 95.09%, and 98.47% release in topsoil, wet clayey soil, and sandy soil. Furthermore, analysis on kinetic model to study

the release mechanism of urea from C3 cellulose hydrogel revealed that the Fickian diffusion model was most suited to describe control-release mechanism of urea in water and soil (R^2 > 0.85 and n < 0.45). This suggests that the fertilizer release of C3 cellulose hydrogels was driven by diffusion through their pores and channels, which was regulated by the concentration gradient and degree of swelling of the hydrogels.

The third research objective of this study was to evaluate and fine-tune fertilizer loading capacity and release rates to match the needs of the rice plants, as well as studying the effect of cellulose hydrogels on the growth performance and yield of upland rice in Sarawak. As with the initial research, nitrogen (N) treatments were applied as CRF treatments; T2H (30 kg N ha^{-1}), T3H (60 kg N ha^{-1}), T4H (90 kg N ha^{-1}), T5H (120 kg N ha^{-1}) and recommended dose of fertilizer (RDF) at 120 kg N ha^{-1} RDF (T6U) in split application and T1 (0 N) as control. Study found that the application of N fertilizer at an optimum rate, T4H resulted in the highest rice plant height (129.6 cm), most tillers per plant (12 tillers), and maximum SPAD reading (39.5). Further analysis revealed that T4H treatment resulted in maximum grain yield, increasing by 71% relative to control treatment. Moreover, the rice plants in T4H treatment had the highest 1000-grain weight (24.85 g), most panicles per plant (12 panicles) and grains (134).

Finally, the fourth research objective was to study the effects of cellulose-based hydrogel CRF on nitrogen (N) uptake and nitrogen use efficiency (NUE) of upland rice in Sarawak. N uptake and NUE were determined using Kjeldahl procedure and the Nessler method. From the analysis, study shows that the rice plant in T4H treatment resulted in the highest N uptake at 0.25 g kg^{-1}, harvest index (HI) at 45.5% and nitrogen harvest index (NHI) at 67.9%. The application of T4H also recorded the highest N use efficiency (NUE) at 52.6%

and N agronomic efficiency (NAE) at 12.8 kg kg^{-1}. Further analysis on correlation regression study revealed that N uptake was positively correlated with panicle number (78.6% correlated) and the number of grains per panicle (86.4% correlated) which contributed to increased grain yields. Therefore, this study suggests that the panicle number and number of grains per panicle were the most variable yield components identified.

In addition, degradation of cellulose hydrogel CRF (T4H) was successfully determined using analytical and precision weighing method. Result shows that T4H displayed a significant weight loss (up to 97%) relative to their initial weight. This shows that the cellulose hydrogel CRF had nearly degraded after 135 days. In conclusion, the advancement of cellulose-based hydrogel CRF as a greener alternative to conventional farmers' fertilizer practices in upland rice cultivation system plays a crucial and promising role in a sustainable agriculture.

5.2 Recommendations for Future Research

Despite valuable results and findings on the cellulose hydrogel CRF in this study, it is yet subjected to several limitations. Recommendations for future research are also addressed pertaining to those limitations. First, this study only examined on the cellulose hydrogels as CRF in relative to conventional urea and control treatment, thus ignoring the potential differences of cellulose hydrogel CRF formulated in this study and other reported CRFs. For future research, it would be meaningful if both CRFs could be incorporated and administered during the upland rice cultivation. Furthermore, comparison of results generated in this study and potential future studies can be made.

The second limitation of this study is that this study examined on N content only. Therefore, only urea as a model fertilizer was loaded onto the cellulose hydrogel network as

a source of N. Although N is the primary component and the most essential element which contributes to the rice growth performance, however, nutrients such as phosphorus (P) and potassium (K) might have affected the rice plants growth. For instance, K is essential for early flowering stage (1-3 days) and might aid in reducing the severity of common diseases in the rice plants (i.e., spot on the rice leaves and stem rot). Whereas P might stimulate root growth of the rice plant. Hence, it is suggested that the future research incorporates the loading of NPK fertilizer onto cellulose hydrogel CRF, and their utilization and effects on the rice growth performance.

Third, analysis on the rice growth performance, N uptake and efficiencies was conducted in a mini greenhouse during the year of 2022 (June–December). The study was conducted by following the existing recommendations which are the legitimate protocols for pot experiments to simulate the actual fields. In addition, the transferability of the experimental results to natural conditions is not restricted and may represent the actual results. However, there are broader range of parameters that might influence the rice growth performance in the actual field. For instance, the growing season, different types of soils, mineral content in soil, soil pH, weather conditions, pesticides and insecticides and others. Although the results and findings are considered reliable, however, they represent the rice growth performance, N uptake and efficiencies during the period when it is under study in a mini greenhouse. Hence, cannot be generalized to represent overall rice growth performance in agricultural sector. It is recommended that for future research, this study can be replicated to examine the rice growth performance in actual field and future period, so that potential similarities or comparison between the effects of cellulose hydrogels CRFs on upland rice cultivation in a mini greenhouse and actual field can be observed.

REFERENCES

Abbasi, M.K., Tahir, M.M., Sadiq, A., Iqbal, M., & Zafar, M. (2012). Yield and nitrogen use efficiency of rainfed maize response to splitting and nitrogen rates in Kashmir, Pakistan. *Agronomy Journal*, *104*, 448-457.

Abd El-Mohdy, H. L., Hegazy, E. A., El-Nesr, E. M., & Abd El-Wahab, M. (2011). Control release of some pesticides from starch/(ethylene glycol-co-methacrylic acid) copolymers prepared by γ-irradiation. *Journal of Polymer Research*, *18*, 1605-1615.

Abd El-Rehim, H.A. (2006). Characterization and possible agricultural application of polyacrylamide/sodium alginate crosslinked hydrogels prepared by ionizing radiation. *Journal of Applied Polymer Science*, *101*, 3572-3580.

Abd El-Wahid, M. H., & Ali, E. A. (2013). Effect of irrigation system, amount of irrigation water and mulching on corn yield, water use efficiency and net profit. *Agricultural Water Management*, *120*, 64-71.

Abd Rahman, S. N. B., Abd Razak, M. S. F. B., Mohamed Hamim, N., Othman, M. R. B., Abd, Rahim, N. I. B. (2021). Identification of drought tolerant among MARDI rice varieties based on morpho-agronomic traits and drought grain yield QTLs. *International Journal of Current Microbiology and Applied Sciences*, *10*, 471-493.

Abdolmaleki, A., Gharibi, H., Molavia, M. R., Narouzi, M. R., & Asefifeyzabadi, N. (2021). Physicochemical modification of hydroxylated polymers to develop thermosensitive double network hydrogels. *Journal of Applied Polymer Science*, *138*, 50778-50795.

Abobatta, W. (2018). Impact of hydrogel polymer in agricultural sector. *Advances in Agriculture and Environmental Science*, *1*, 59, 64.

Abu Bakar, B. H., Abdul Rahman, M. S., Rahim, H., Abd Rani, M. N. F., Ghazali, M. S. S., Mohd. Bookeri, M. A., Ahmad, M. T., Teoh, C. C., Bujang, A. S., Abdullah, M. Z. K., & Ismail, R. (2020). Saving fertilizer in Malaysia's large-scale paddy production through precision farming. *FFTC Agricultural Policy Platform*, 1-7.

Acharya, S., Liyanage, S., Parajuli, P., Rumi, S. S., Shamshina, J. L., & Abidi, N. (2021). Utilization of cellulose to its full potential: a review on cellulose dissolution, regeneration, and application. *Polymer(Basel), 13*, 4344-4381.

Adjuik, T. A., Nokes, S. E., & Montross, M. D. (2023). Biodegradability bio-based and synthetic hydrogels as sustainable soil amendments: A review. *Journal of Applied Polymer Science*, *140*, e53655.

Agarwal, P., Saha, S., & Hariprasad, P. (2021). Agro-industrial-residues as potting media: physicochemical and biological characters and their influence on plant growth. *Biomass Conversion and Biorefinery*. Doi: https://doi.org/10.1007/s13399-021-01998-6

Ahmad, D. F. B. A., Wasli, M. E., Tan, C. S. Y., Zaki, M., & Chin, S. F. (2023). Eco-friendly cellulose-based hydrogels derived from wastepapers as a controlled-release fertilizer. *Chemical and Biological Technologies in Agriculture*, *10*, 36-45.

Ahmed, M. E. (2015). Hydrogel: preparation, characterization, and applications: a review. *Journal of Advanced Research*, *6*, 105-121.

Ahmed, R., Siddiqui, S. I., Al Alwan, B., Almesfer, M., Khanna, M. K., Fatima, B., Mishra, R., Ansari, M. A., & Oh, S. (2022). Biodegradable acid based nanocomposite-CuO-ZnO-$Ni(OH)_2$/PA: a novel material for water cleansing. *Journal of Cleaner Production*, *341*, 130860-130870.

Ai, J., Li, K., Li, J., Yu, F., & Ma, J. (2021). Super flexible, fatigue resistant, self-healing PVA/xylan/borax hydrogel with dual-crosslinked network. *International Journal of Biological Macromolecules*, *172*, 66-73.

Akhter, J., Mahmood, K., Malik, K., Amrdan, A., Ahmad, M., & Iqbal, M. (2011). Effects of hydrogel amendment on water storage of sandy loam and loam soils and seedling growth of barley, wheat and chickpea. *Plant, Soil and Environment*, *50*, 463-469.

Alam, I, Kumar, J., & Sharma, C. (2021). Preparation of regenerated cellulose from rice straw lignocellulosic waste and its use for reinforced paper products. *Tappi Journal*, *20*, 439-451.

Alam, M.N., Islam, M.S., & Christopher, L.P. (2019). Sustainable production of cellulose-based hydrogels with superb absorbing potential in physiological saline. *The Journal of Physical Chemistry Letters*, *4*, 9419-9426.

Alcamo, J. (2019). Water quality and its interlinkages with the sustainable development goals. *Current Opinion in Environmental Sustainability*, *36*, 126-140.

Alemu, G. A. (2021). The role of harvest index in improving crop productivity: A review. *Journal of Natural Sciences Research*, *9*, 24-28.

Ali, S. S., Kornaros, M., Manni, A., Al-Tohamy, R., El-Shanshoury, A. E. R., Matter, I. M., Elsamahy, T., Sobhy, M., & Sun, J. (2021). Chapter 28-advances in microorganism-based biofertilizers: major mechanisms and applications. *Biofertilizers*, *1*, 371-385.

Alkalin, G. O., & Pulat, M. (2019). Controlled release behaviour of zinc-loaded carboxymethyl cellulose and carrageenan hydrogels and their effects on wheatgrass growth. *Journal of Polymer Research*, *27*, 6.

Allahdadi, I., Yazdani, F., Akbari, G. A., & Behbahani, S. M. (2005). Evaluation of the effects of different rates of superabsorbent polymer (superab a200) on soybean yield

and yield component (*Glycine max* L.). In: *Third specialized training course and seminar on the application of superabsorbent hydrogels in agriculture*. pp. 20-32.

Alshrouf, A. (2017). Hydroponics, aeroponics and aquaponic as compared with conventional farming. *American Scientific Research Journal for Engineering, 27,* 247-255.

Amiri, E., Rahmaninia, M., & Khosravani, A. (2019). Effect of chitosan molecular weight on the performance of chitosan-silica nanoparticle system in recycled pulp. *Bioresources, 14,* 7687-7701.

Amiri, M., Khazaeli, P., Salehabadi, A., & Salavati-Niasari, M. (2021). Hydrogel beads-based nanocomposites in novel drug delivery platforms: recent trend and developments. *Advances in Colloid and Interface Science, 288,* 102316.

Anarbaev, A., Tursonov, O., Kodirov, D., Allenova, I., Nazaraliev, D., & Obidjanov, D. (2021). Determination of model parameters of water-nutritional process in soil for nitrogen compounds. *Earth and Environmental Science, 939,* 1-7.

Anupama, K. R., Singh, R., Kumar, A., & Parmar, B. S. (2007). Performance of a new superabsorbent polymer on seedling and post planting growth and water use pattern of chrysanthemum grown under controlled environment. *Acta Horticulturae, 724,* 43-50.

Arbona, V., Iglesias, D.J., Jacas, J., Primo-Millo, E., Talon, M., & Gomez-Cadenas, A. (2005). Hydrogel substrate amendment alleviates drought effects on young citrus plant. *Plant Soil, 270,* 73-82.

Arkhincheev, V. E. (2019). Acceleration of mass transfer processes in plants due to the geometric structure: a fractional order equation of mass transfer and its application. *Scientific Reports, 9,* 15269.

Arora, B., Tandon, R., Attri, P., & Bhatia, R. (2017). Chemical crosslinking: role in protein and peptide science. *Current Protein and Peptide Science*, *18*, 946-955.

Arun, R., Shruthy, R., Preeta R., & Sreejit, V. (2021). Biodegradable nano composite reinforced with cellulose nano fiber from coconut industry waste for replacing synthetic plastic for food packaging. *Chemosphere*, *291*, 132786

Aubrey, S. (2022, July 20). State hopes to achieve 60 pct rice self-sufficiency by 2030, says Deputy Minister. *The Borneo Post*. https://www.theborneopost.com/2022/07/20/state-hopes-to-achieve-60-pct-rice-self-sufficiency-by-2030-says-deputy-minister/

Ayadi, S., Jallouli, S., Chamekh, Z., Zouari, I., Landi, S., Hammami, Z., Azaiez, F. E. B., Baraket, M., Esposito, S., & Trifa, Y. (2022). Variation of grain yield, grain protein content and nitrogen use efficiency components under different nitrogen rates in Mediterranean durum wheat genotypes. *Agriculture*, *12(7)*, 916-928.

Babadi, F. E., Yunus, R., Soltani, S. M., & Shotipruk, A. (2021). Release mechanisms and kinetic models of gypsum-sulfur-zeolite-coated urea sealed with microcrystalline wax for regulated dissolution. *ACS Omega*, *6*, 11144-11154.

Badaruzaman, M. F., & Tiong, O. C. (2022). Crop yield prediction with multiple linear regression in Malaysia. *Proceedings of Science and Mathematics*, *9*, 211-221.

Bagheri, N., Babaelan-Jelodar, N., Pasha, A. (2011). Path coefficient analysis for yield and yield components in diverse rice (*Oryza sativa* L.) genotypes. *Biharean Biologist*, *5*, 32-35.

Baharin, K. W., Zakaria, S., Ellis, A. V., Talip, N., Kaco, H., Gan, S., Zailan, F. D., & Hashim, S. N. A. S. (2019). Factors affecting cellulose dissolution of oil plam empty fruit bunch and kenaf pulp in NaOH/urea solvent. *Sains Malaysiana*, *47*, 377-386.

Bai, H., Zhang, Z., Huo, Y., Shen, Y., Qin, M., & Feng, W. (2022). Tetradic double-network physical cross-linking hydrogels with synergistic high stretchable, self-healing, self-adhesive, and self-strain properties. *Journal of Material Science and Technology*, *98*, 169-176.

Bai, W., Ji, B., Fan, L., Peng, Q., Liu, Q., & Song, J. (2023). Preparation and characterization of a novel cassava starch-based phosphorus releasing super-absorbent polymer, and optimization of the performance of water absorption and phosphorus release. *Polymers*, *15*, 1233.

Baldino, L., Zuppolini, S., Cardea, S., Diodato, L., Borriello, A., Reverchon, E., & Nicolais, L. (2020). Production of biodegradable superabsorbent aerogels using supercritical CO_2 assisted drying. *The Journal of Supercritical Fluids*, *156*, 104681.

Baloch, F. E., Afzali, D., & Fathirad, F. (2021). Design of acrylic acid/nanoclay grafted polysaccharide hydrogels as superabsorbent for controlled release of chlorpyrifos. *Applied Clay Science*, *211*, 106194.

Bao, X., Dong, F., Yu, Y., Wang, Q., Wang, P., Fan, X., & Yuan, J. (2020). Green modification of cellulose-based natural materials by HRP-initiated controlled “graft from” polymerization. *International Journal of Biological Macromolecules*, *164*, 1237-1245.

Barbieri, P.A., Echeverría, H.E., Saínz Rozas, H.R., & Andrade, F.H. (2008). Nitrogen use efficiency in maize as affected by nitrogen availability and row spacing. *Journal of Agronomy*, *100*,1094-1100.

Bashir, S., Hina, M., Iqbal, J., Rajpar, A. H., Mujtaba, M. A., Alghamdi, N. A., Wageh, S., Ramesh, K., & Ramesh, S. (2020). Fundamental concepts of hydrogels: synthesis, properties, and their applications. *Polymers (Basel)*, *12*, 2702-2761.

Basu, S. K., Kumar, N., & Srivastava, J. P. (2010). Modelling NPK release from spherically coated fertilizer granules. *Simulation Modelling Practice and Theory*, *18*, 820-835.

Bauli, C. R., Lima, G. F., de Souza, A. G., Ferreira, R. R., & Rosa, D. S. (2021). Eco-friendly carboxymethyl cellulose hydrogels filled with nanocellulose or nanoclays for agriculture applications as soil conditioning and nutrient carrier and their impact on cucumber growing. *Colloid and Surfaces A: Physicochemical and Engineering Aspects*, *623*, 126771.

Beckett, L. E., Lewis, J. T., Tonge, T. K., Korley, L. T. J. (2020). Enhancement of the mechanical properties of hydrogels with continuous fibrous reinforcement. *ACS Biomaterials Science & Engineering*, *6*, 5453-5473.

Behera, S., & Mahanwar, P. A. (2019). Superabsorbent polymers in agriculture and other applications: a review. *Polymer-Plastic Technology and Materials*, *59*, 341-56.

Berradi, A., Aziz, F., El Achaby, M., Ouazzani, N., & Mandi, L. (2023). A comprehensive review of polysaccharide-based hydrogels as promising biomaterials. *Polymers*, *15*, 2908-2956.

Bey, N. E., Aounallah, M. K., Chammam, M. R., & Bettaieb, T. (2021). Effect of controlled-release fertilizers (CRF) on vegetative growth, nutritional status, fruit yield and quality of ‘Maltaise Ballerin’ orange trees. *Plant Physiology Report*, *26*, 1-10.

Bi, S., Barinelli, V., & Sobkowicz, M. J. (2020). Degradable controlled release fertilizer composite prepared via extrusion: fabrication, characterization and release mechanism. *Polymers*, *12*, 301-315.

Bortolin, A., Aouada, F. A., Mattoso, L. H. C., & Ribeiro, C. (2013). Nanocomposite/PAAm/methylcellulose/montmorillonite hydrogel: evidence of

synergistic effects for the slow release of fertilizer. *Journal of Agricultural and Food Chemistry*, *61*, 7431-7439.

Boser, C. L., Hanna, C., Holway, D. A., Faulkner, K. R., Naughton, I., Randall, J. M., Cory, C., Choe, D. H., & Morrison, S. A. (2017). Protocols for argentine ant eradication in conservation areas. *Journal of Applied Entomology*, *141*, 540-550.

Bossoni, R., Riul, A., Valente, A. J. M., Rubira, A. F., & Muniz, E. C (2014). release of vitamin B12 and diclofenac potassium from N,N-dimethylacrylamide-modified arabic gum hydrogels – the partition-diffusion model. *Journal of the Brazilian Chemical Society*, *25*, 1124-1134.

Braihi, A. J., Salih, S. I., Hashem, F. A., Ahmed, J. K. (2014). Proposed cross-linking model for carboxymethyl cellulose/starch superabsorbent polymer blend. *International Journal of Materials Science and Applications*, *3*, 363-369.

Brandt, M.J., Johnson, K.M., Elphinston, A.J., & Ratnayaka, D.D. (2017). Hydrology and Surface Supplies. Twort's Water Supply. 7th edn. Butterworth Heinemann:IWA publishing.

Bustamante-Torres, M., Romarro-Fierro, D., Arcentales-Vera, B., Palomino, K., Magana, H., & Bucio, E. (2021). Hydrogels classification according to the physical or chemical interactions and as stimuli-sensitive materials. *Gels*, *7*, 182-206.

Butylina, S., Geng, S., Laatikainen,K., & Oksman, K. (2020). Cellulose nanocomposite hydrogels: from formulation to material properties. *Frontiers in Chemistry*, *8*, 1-11.

Cai, J., & Zhang, L. (2005). Rapid dissolution of cellulose in LiOH/urea and NaOH/urea aqueous solutions. *Macromolecular Bioscience*, *5*, 539-548.

Calcagnile, P., Sibillano, T., Giannini, C., Sannino, A., & Demitri, C. (2019). Biodegradable poly (lactic acid)/cellulose-based superabsorbent hydrogel composite material as

water and fertilizer reservoir in agricultural applications. *Journal of Applied Polymer Science*, *136*, 47546-47556.

Cameron, K. C., Di, H. J., & Moir, J. L. (2013). Nitrogen losses from the soil/plant system: A review. *Annals of Applied Biology*, *162*, 145-173.

Campos, E. V. R., de Oliveira, J. L., Fraceto, L. F., & Singh, B. (2015). Polysaccharides as safer release system for agrochemicals. *Agronomy for Sustainable Development*, *35*, 47-66.

Cao, J., Li, J., Chen, Y., Zhang, L., & Zhou, J. (2018). Dual physical crosslinking strategy to construct moldable hydrogels with ultrahigh strength and toughness. *Advanced Functional Materials*, *28*, 1-9.

Chang, C., & Zhang, L. (2011). Cellulose-based hydrogels: present status and application prospects. *Carbohydrate Polymers*, *84*, 40-53.

Chang, L., Xu, L., Liu, Y., & Qiu, D. (2021). Superabsorbent polymers used for agricultural water retention. *Polymer Testing*, *94*, 107021.

Chen, G., Cao, H., Liang, J., Ma, W., Guo, L., Zhang, S., Jiang, R., Zhang, H., & Goulding, K.W.T. (2018). Factors affecting nitrogen use efficiency and grain yield of summer maize on smallholder farms in the North China plain. *Sustainability*, *10*, 1-18.

Chen, G., Tang, W., Wang, X., Zhao, X., Chen, C., & Zhu, Z. (2019). Applications of hydrogels with special physical properties in biomedicine. *Polymers*, *11*, 1420-1436.

Chen, H., Chen, Q., Hu, R., Wang, H., Newby, B. M. Z., Chang, Y., & Zheng, J. (2015). Mechanically strong hybrid double network hydrogels with antifouling properties. *Journal of Materials Chemistry B*, *3*, 5426-5435.

Chen, J., Lü, S., Zhang, Z., Zhao, X., Li, X., Ning, P., & Liu, M. (2018). Environmentally friendly fertilizers: a review of materials used and their effects and the environment. *Science of The Total Environment*, *613-614*, 829-839.

Chen, L., Shao, J., Yu, Q., & Wang, S. (2022). High strength, anti-fatigue, stretchable self-healing polyvinyl alcohol hydrogel based on borate bonds and hydrogen bonds. *Journal of Dispersion Science and Technology*, *43*, 690-703.

Chen, M., Chen, J., & Sun, F. (2010). Estimating nutrient releases from agriculture in China: an extended substance flow analysis framework and a modelling tool. *Science of the Total Environment*, *408*, 5123-5136.

Chen, Q., Zhu, L., Chen, H., Yan, H., Huang, L., Yang, J., & Zheng, J. (2015). A novel design strategy for fully physically crosslinked double networks hydrogels with tough, fatigue resistant, and self-healing. *Advanced Functional Materials*, *25*, 1598-1607.

Chen, X., Huang, L., Mao, X., Liao, Z., & He, Z. (2017). A comparative study of the cellular microscopic characteristics and mechanisms of maize seedling damage from superabsorbent hydrogels. *Pedosphere*, *27*, 274-282.

Chen, Y. L., Zhang, X., You, T. T., & Su, F. (2019). Deep eutectic solvents (DESs) for cellulose dissolution: a mini-review. *Cellulose*, *26*, 205-213.

Chen, Y., Peng, J., Wang, J., Fu, P., Hou, Y., Zhang, C., Fahad, S., Peng, S., Cui, K., Nie, L., & Huang, J. (2015). Crop management based on multi-split topdressing enhances grain yield and nitrogen used efficiency in irrigated rice in China. *Field Crop Research*, *184*, 50-57.

Chen, Z., Wang, Q., Ma, J., Zou, P., & Jiang, L. (2020). Impact of controlled-release urea on rice yield, nitrogen use efficiency and soil fertility in as single rice copping system. *Science Reports*, *10*, 1-10.

Chetouani, A., Elkolli, M., Bounekhel, M., & Benachour, D. (2014). Physicochemical characterization of gelatin-cmc composite edibles films from polyion-complex hydrogels. *Journal of Chilean Chemical Society*, *59*,2279-2283.

Chin, S. F., Jong, S. J., & Yeo, Y. J. (2022). Optimization of cellulose-based hydrogel synthesis using response surface methodology. *Biointerface Research in Applied Chemistry*, *12*, 7136-7146.

Chin, S.F., Jimmy, F.B., & Pang, S.C. (2018). Size controlled fabrication of cellulose nanoparticles for drug delivery applications. *Journal of Drug Delivery Science and Technology*, *43*, 262-266.

Choe, D. H., Campbell, K., Hoddle, M. S., Kabashima, J., Dimson, M., & Rust, M. K. (2018). Evaluation of a hydrogel matrix for baiting western yellow jacket (Vespidae: Hymenoptera). *Journal of Economic Entomology*, *111*, 1799-1805.

Cooper, M. L., Hobbs, M. B., Boser, C. L., & Varela, L. G. (2019). Argentine ant management: using toxin-laced polyacrylamide crystals to target ant colonies in vineyards. *Catalyst Discovery Practice*, *3*, 23-30.

Cortazar, B., Koydemir, H. C., Tseng, D., Feng, F., & Ozcan, A. (2015). Quantification of plant chlorophyll content using google glass. *Lab Chip*, *15*, 1708-1716.

Cueff, S., Aletto, L., Bourdat-Deschamps, M., Benoit, P., & Pot, V. (2020). Water and pesticide transfers in undisturbed soil columns sampled from a Stagnic Luvisol and a Vermic Umbrisol both cultivated under conventional and conservation agriculture. *Geoderma*, *377*, 114590-114602.

Cui, X., Lee, J. J. L., & Chen, W. N. (2019). Eco-friendly and biodegradable cellulose hydrogels produced from low cost okara: towards non-toxic flexible electronics. *Scientific Reports*, *9*, 1-9.

D'Odorico, P., Chiarelli, D. D., Rosa, L., & Rulli, M. C. (2020). The global value of water in agriculture. *PNAS*, *117*, 21985-21993.

Dai, H., Huang, Y., & Huang, H. (2018). Eco-friendly polyvinyl alcohol /carboxymethyl cellulose hydrogels reinforced with graphene oxide and bentonite or enhanced adsorption of methylene blue. *Carbohydrate Polymers*, *185*, 1-11.

Dai, H., Ou, S., Liu, Z., & Huang, H. (2017). Pineapple peel carboxymethyl cellulose/polyvinyl alcohol/mesoporous silica SBA-15 hydrogel composites for papain immobilization. *Carbohydrate Polymers*, *169*, 504-514.

Dailey, O. D. (2004). Volatilization of alachlor from polymeric formulations. *Journal of Agricultural and Food Chemistry*, *52*, 6742-6746.

Dalmazzo, D, Carrión, A. J. D. B., Tsantilis, L., Presti, D. L., & Santaga, E. (2019). Non-petroleum based binders for paving applications: rheological and chemical investigation on ageing effects. *Proceeding of the 5th International Symposium on Asphalt Pavements & Environment (APE)*, *48*, 67-76.

Das, D., Bhattacharjee, S., & Bhaladhare, S. (2023). Preparation of cellulose hydrogels and hydrogel nanocomposites reinforced by crystalline cellulose nanofibers (CNF) as a water reservoir for agricultural use. *ACS Applied Polymer Materials*, *5*, 2895-2904.

Das, D., Prakash, P., Rout, P. K., & Baladhare, S. (2020). Synthesis and characterization of cellulose-based hydrogels for agricultural application. *Starch-Stärke*, *73*, 1-10.

Das, D., Prakash, P., Rout, P. K., & Bhaladhare, S. (2021). Synthesis and characterization cellulose-based hydrogel for agricultural application. *Starch*, *73*, 1900284.

Davidson, D. W., Verma, M. S., & Gu, F. V. (2013). Controlled root targeted delivery of fertilizer using an ionically crosslinked carboxymethyl cellulose hydrogel matrix. *SpringerPlus*, *2*, 318.

De France, K., D'Emilio, E., Cranston, E. D., Geiger, T., Nyström, G. (2020). Dual physically and chemically crosslinked regenerated cellulose – gelatin composite hydrogels towards art restoration. *Carbohydrate Polymers*, *234*, 115885.

de Lima, G. F., de Souza, A. G., & Rosa, D. D. S. (2020). Nanocellulose as reinforcement in carboxymethylcellulose superabsorbent nanocomposite hydrogels. *Macromolecular Symposia*, *394*, 1-9.

de Vasconcelos, M. C., Gomes, R. F., Sousa, A. A. L., Moreira, F. J. C., Rodrigues, F. H. A., Fajardo, A. R., & Neto, L. G. P. (2020). Superabsorbent hydrogel composite based on starch/rice husk ash as a soil conditioner in melon (*Cucumis Melo*, L.) Seedling Culture. *Journal of Polymers and the Environment*, *28*, 131-140.

Dellero, Y. (2020). Manipulating amino acid metabolism to improve crop nitrogen use efficiency for a sustainable agriculture. *Frontiers Plant Science*, *11*, 1-14.

Demitri, C., Scalera, F., Madaghiele, M., Sannino, A., & Mafezzoli, A. (2013). Potential of cellulose based superabsorbent hydrogels as water reservoir in agriculture. International *Journal of Polymer Science*, *2013*, 1-6.

Deshmukh, G., & Hardaha, M. K. (2014). Effect of irrigation and fertigation scheduling under drip irrigation in papaya. *Journal of AgriSearch*, *1*, 216-220.

Devi, K. R., Parimala, K., Srinivas, G., & Cheralu, C. (2016). Variability and association of yield components and quality traits in upland rice (*Oryza sativa* L.). *Journal of Environment and Ecology*, *34*, 2306-2310.

Dhanalakshmi, A., Vijayakumari, K. K., Marimuthu, S., & Surendran, U. (2020). Evaluation of different soil textures in combination with growing media on growth, yield, and water productivity of blackgram. *Communications in Soil Science and Plant Analysis*, *51*, 2670-2682.

Ding, H., Zhang, Y.S., Li, W.H., Zhen, X.Z., Wang, M.K., Tang, L.N., & Chen. D.L. (2016). Nutrients release from a novel gel-based slow/controlled release fertilizer. *Applied Environmental Soil Science, 2016*, 1-13.

Diógenes, M.F.S., Mendonça, V., De Medeiros Mendonça, L.F., De Moura, E.A., Da Silva Lima Reges, K., De Oliveira, L.M., & De Oliveira, A.M.F. (2022). Use of hydrogel in the irrigation management of white pitaya (*Hylocereus undatus*) seedlings: Biometrics and accumulation of organic and inorganic solutes. *Semina-Ciencias Agrarias*, *43*, 491-508.

do Nascimento, D. M., Nunes, Y. L., Feitosa, J. P. A., Dufresne, A., & Rosa, M. D. F. (2022). Cellulose nanocrystals-reinforced core-shell hydrogels for sustained release of fertilizer and water retention. *International Journal of Biological Macromolecules*, *216*, 24-31.

Doungmanee, P. (2016). The nexus of agriculture water use and economic development level. *Kasetsart Journal of Social Science*, *37*, 38-45.

Duceac, I. A., & Coseri, S. (2022). Chitosan Schiff-base hydrogels – a critical perspective review. *Gels*, *8*, 779.

Durpekova, S., Filatova, K., Cisar, J., Ronzova, A., Kutalkova, E., & Sedlarik, V. (2020). A novel hydrogel based on renewable materials for agricultural application. *International Journal of Polymer Science*, *2020*, 1-13.

Dutta, S. D., Patel, D. K., & Lim, K. T. (2019). Functional cellulose-based hydrogels as extracellular matrices for tissue engineering. *Journal of Biological Engineering*, *13*, 1-19.

Ekebafe, L. O., Ogbeifun, D. E., Okieimen, F. E. (2011). Polymer applications in agriculture. *Biokemistri*, *23*, 81-89.

El Sayed, M. M. (2019). Hydrogel preparation technologies: relevant kinetics, thermodynamics and scaling up aspects. *Journal of Polymers and the Environment*, *27*, 871-891.

El Sayed, M. M. (2023). Production of polymer hydrogel composites and their applications. *Journal of Polymers and the Environment, 31*, 2855-2879.

El-Kazzaz, K. A., & El-Kazzaz, A. A. (2017). Soilless agriculture a new and advanced method for agriculture development: an introduction. *Agricultural Research & Technology Open Access Journal*, *3*, 1-10.

El-Sakhawy, M., Tohamy, H.A.S, Salama, A., & Kamel, S. (2019). Thermal properties of carboxymethyl cellulose acetate butyrate. *Cellulose Chemistry and Technology*, *53*, 667-675.

El-Sherbiny, I.M., Salama, A., & Sarhan, A.A. (2009). Grafting study and antifungal activity of a carboxymethyl cellulose derivative. *International Journal of Polymer Materials*, *58*, 453-467.

Elbarbary, A. M., & Ghobashy, M. M. (2017). Controlled released fertilizers using superabsorbent hydrogel prepared by gamma radiation. *Radiochimica Acta*, *105*, 865-876.

Etale, A., Onyianta, A. J., Turner, S. R., Eichhorn, S. J. (2023). Cellulose: a review of water interaction, applications in composite, and water treatment. *American Chemical Society*, *123*, 2016-2048.

Fan, W., Zhang, Z., Liu, Y., Wang, J., Li, Z., & Wang, M. (2021). Shape memory polyacrylamide/gelatin hydrogel with controllable mechanical and drug release properties potential for wound dressing application. *Polymer*, *226*, 123786-123795.

Fatima, A., Yasir, S., Khan, M. S., Manan, S., Ullah, M., & Ul-Islam, M. (2021). Plant extract-loaded bacterial cellulose composite membrane for potential biomedical applications. *Journal of Bioresources and Bioproducts*, *6*, 26-32.

Fazlina, N.S., Khanif, Y.M., & Oad, F.C. (2014). Nutrient uptake pH changes and yield of rice under slow release sulfur coated urea fertilizers. *Australian Journal of Crop Science*, *8*, 1359-1366.

Fekete, T., Borsa, J., Takács, E., & Wojnárovits, L. (2017). Synthesis and characterization of superabsorbent hydrogels based on hydroxyethylcellulose and acrylic acid. *Carbohydrate Polymers*, *166*, 300-308.

FitzSimons, T. M., Anslyn, E. V., & Rosales, A. M. (2022). Effect of pH on the properties of hydrogels cross-linked via dynamic thia-michael addition bonds. *ACS Polymers Au*, 2, 129-136.

Gbollie, S. N., Mwonga, S. M., & Kibe, A. M. (2021). Effects of calcium nitrate levels and soaking duration on cocopeat nutrient content. *Journal of Agricultural Chemistry and Environment*, *10*, 372-388.

Geng, J., Sun, Y., Zhang, M., Li, C., Yang, Y., Liu, Z., & Li, S. (2015). Long-term effects of controlled release urea applications on crop yields and soil fertility under rice-oilseed rape rotation system. *Field Crops Research*, *184*, 65-73.

Ghanbarian-Alavijeh, B., Liaghat, A., Guan-Hua, H., & Van Genuchten, M. T. (2010). Estimation of the van genuchten soil water retention properties from soil textural data. *Pedosphere*, *20*, 456-465.

Gharbi, K., & Tay, J. W. (2022). Fumigant toxicity of essential oils against *Frankliniella occidentalis* and *F. insularis* (Thysanoptera: Thripidae) as affected by polymer release and adjuvants. *Insects*, *13*, 493-507.

Ghasemi, M., Alexandridis, P., & Tsianou, M. (2018). Dissolution of cellulose fibers: impact of crystallinity and fiber diameter. *Biomacromolecules*, *19*, 640-651.

Ghasemi, M., Tsianou, M., & Alexandridis, P. (2017). Assessments of solvents for cellulose dissolution. *Bioresource Technology*, *228*, 330-338.

Gholamhoseini, M., Habibzadeh, F., Ataei, R., Hemmati, P., & Ebrahimian, E. (2018). Zeolite and hydrogel improve yield of greenhouse cucumber in soil-less medium under water limitation. *Rhizosphere*, *6*, 7-10.

Ghosh, M., Swain, D.P., Jha, M.K., Tewari, V.K., &. Bohra, A. (2020). Optimizing chlorophyll meter (SPAD) reading to allow efficient nitrogen use in rice and wheat under rice-wheat cropping system in Eastern India. *Plant Production Science*, *23*, 270-285.

Gil-Ortiz, R., Naranjo, M. A., Ruiz-Navarro, A., Cabalerro-Molada, M., Atares, S., García, C., & Vicento, O. (2020). New eco-friendly polymeric-coated urea fertilizers enhanced crop yield in wheat. *Agronomy*, *10*, 438-452.

Giree, S., & Shrestha, G. (2018). Comparative study of marigolds in soil and soilless media. *Nepalese Journal of Agricultural Sciences*, *16*, 73.

Giroto, A.S., Guimarães, G.G., Colnago, L.A., Klamczynski, A., Glenn, G., & Ribeiro, C. (2019). Controlled release of nitrogen using urea-melamine-starch composite. *Journal of Cleaner Production*, *217*, 448-455.

Gomaa, M., & Aldaby, E. S. E. (2023). Macroalgal-derived alginate/wastepaper hydrogel to alleviate sunflower drought stress. *Planta*. Doi: https://doi.org/10.1007/s00425-023-04152-w

Gomez, H. G., Godina, F. R., Ortiz, H. O., Mendoza, A. B., Torres, V. R., & De La Fuente, F. C. (2017). Use of chitosan-PVA hydrogels with cooper nanoparticles to improve the growth of grafted watermelon. *Molecules*, *22*, 1031-1040.

Griffiths, M., & York, L. M. (2020). Targeting root ion uptake kinetics to increase plant productivity and nutrient use efficiency. *Plant Physiology*, *182*, 1854-1868.

Guan, Y., Bian, J., Peng, F., Zhang, X. M., & Sun, R. C. (2014). High strength of hemicelluloses based hydrogels by freeze/thaw technique. *Carbohydrate Polymers*, *101*, 272-280.

Guilherme, M. R., Aouada, F. A., Fajardo, A. R., Martins, A. F., Paulino, A. T., Davi, M. F. T., Rubira, A. F., & Muniz, E. C. (2015). Superabsorbent hydrogels based on polysaccharides for application in agriculture as soil conditioner and nutrient carrier: a review. *European Polymer Journal*, *72*, 365-385.

Guo, C., Zheng, Z., Yu, S., Zhou, X., Liu, Q., Pei, D., Lu, D., & Geng, Z. (2021). Highly stretchable, compressible, adhesive hydrogels with double network. *Journal of Polymer Research*, *28*, 1-9.

Guo, J., Hu, X., Gao, L., Xie, K., Ling, N., Shen, Q., Hu, S., & Guo, S. (2017). The rice production practices of high yield and high nitrogen use efficiency in Jiangsu, China. *Scientific Reports*, *7(1)*, 2101-2110.

Gupta, N. V., & Shivakumar, H. G. (2012). Investigation of swelling behaviour and mechanical properties of a pH-sensitive superporous hydrogel composite. *Iran Journal of Pharmaceutical Research*, *11*, 481-493.

Gupta, V. K., Carrott, P. J. M., Singh, R., Chaudhary, M., & Kushwaha, S. (2016). Cellulose: a review as natural, modified and activated carbon adsorbent. *Bioresource Technology*, *216*, 1066-1076.

Hach, C. C., Bowden, B. K., Kopelove, A. B., & Brayton, S. V. (1987). More powerful peroxide Kjeldahl Digestion Method. *Journal of the Association of the Official Analytical Chemist*, *70*, 783-787.

Halim, N. S. A., Abdullah, R., Karsani, S. A., Osman, N., Panhwar, Q. A., & Ishak, C. F. (2018). Influence of soil amendments on the growth and yield of rice in acidic soil. *Agronomy*, *8*, 165-175.

Hammad, H.M., Farhad, W., Abbas, F., Fahad, S., Saeed, S., Nasim, W., & Bakhat, H.F. (2017). Maize plant nitrogen uptake dynamics at limited irrigation water and nitrogen. *Environmental Science and Pollution Research*, *24*, 2549-2557.

Han, X., Liu, F., He, X., & Ling, F. (2022). Research on rice yield prediction model based on deep learning. *Computational Intelligence and Neuroscience*, *10*, 1-10.

Hanafi, M. M., Hartinie, A., Shukor, J., & Mahmud, T. M. M. (2009). Upland rice varieties in Malaysia: agronomic and soil physico-chemical characteristics. *Pertanika Journal of Tropical Agricultural Science*, *32*, 225-246.

Hangasky, J. A., Detomasi, T, C., Lemon, C. M., & Marletta, M. A. (2020). 5.12-Glycosidic bond oxidation: the structure, function, and mechanism of polysaccharides monooxygenase. *Comprehensive Natural Products III (Third Edition) Chemistry and Biology*, *5*, 298-331.

Hao, L., Lin, G., Lian, J., Chen, L., Zhou, H., Chen, H., Xu, H., & Zhou, X. (2020). Carboxymethyl cellulose capsulated zein as pesticide nano-delivery system for improving adhesion and anti-uv properties. *Carbohydrate Polymers*, *231*, 115725.

Harada, N., Mitsukami, Y., & Uyama, Y. (2021). Preparation and characterization of water-swellable hydrogel-forming porous cellulose beads. *Polymer*, *215*, 123381.

Hashim, M. M., Yusop, M. K., Othman, R., & Samsuri, A. W. (2015). Characterization of nitrogen uptake pattern in Malaysian rice MR219 at different growth stages using 15N isotope. *Rice Science*, *22*, 250-254.

Hashim, M.M., Yusop, M.K., Othman, R., & Wahid, S.A. (2017). Field evaluation of newly-developed controlled release fertilizer on rice production and nitrogen uptake. *Sains Malaysiana*, *46*, 925-932.

Hayati, N., & Lestari, M. (2020). The influence of growing media and buds source on growth and results of strawberries (*Fragaria Ananassa Duchesne*). *International Journal of Advanced Science and Technology*, *29*, 4961-4967.

Hayes, T. B., Hansen, M., Kapuscinski, A. R., Locke, K. A., & Barnosky, A. (2017). From silent spring to silent night. Agrochemicals and the anthropocene. *Elementa: Science of the Anthropocene*, *5*, 1-24.

He, F., Zhou, Q., Wang, L., Yu, G., Li, J., & Feng, Y. (2019). Fabrication of a sustained release delivery system for pesticides using interpenetrating polyacrylamide/alginate/montmorillonite nanocomposite hydrogels. *Applied Clay Science*, *183*, 105347-105357.

Heinke, J., Lannerstad, M., Gerten, D., Havlík, P., Herrero, M., Notenbaert, A. M. O., Hoff, H., & Müller, C. (2020). Water use in global livestock production- opportunities and constraints for increasing water productivity. *Water Resources Research*, *56*, 1-16.

Hermida, L., & Agustian, J. (2019). Slow release urea fertilizer synthesized through recrystallization of urea incorporating natural bentonite using various binders. *Environmental Technology & Innovation*, *13*, 113-121.

Heyland, A., Roszell, J., Chau, J., Chai, K., Eaton, A., Nolan, K., Madden, K., & Ahmed, W. H. (2021). Mass transfer and flow characterization of novel algae-based nutrient removal system. *Biotechnology for Biofuels*, *14*, 104-114.

Hidaka, H., Kim, U. J., & Wada, M. (2010). Synchrotron X-ray fiber diffraction study on the thermal expansion behaviour of cellulose crystals in tension wood of Japanese poplar in the low-temperature region. *Holzforschung*, *64*, 167-171.

Hindi, S. S. Z. (2017). The inconvertibility of cellulose's allomorphs. *International Journal of Innovative Research in Science, Engineering and Technology*, *6*, 715-722.

Ho, S. Y., Wasli, M. E., & Perumal, M. (2009). Evaluation of physicochemical properties of sandy-textured soils under smallholder agricultural land use practices in Sarawak, East Malaysia. *Applied and Environmental Soil Science*, *2019*, 1-14.

Hocine, S., Ghemati, D., & Aliouche, D. (2023). Synthesis, characterization and swelling behaviour of pH-sensitive polyvinylalcohol grafted poly(acrylic acid-co-2-acrylamido-2-methylpropane sulfonic acid) hydrogels for protein delivery. Polymer Bulletin. Doi: https://doi.org/10.1007/s00289-022-04664-7.

Hogg, B. N., Nelson, E. H., Hagler, J. R., Daane, K. M. (2018). Foraging distance of the argentine ant in California vineyards. *Journal of Economic Entomology*, *111*, 672-679.

Hu, X. F., Cheng, C., Luo, F., Chang, Y. Y., Teng, Q., Men, D. Y., Liu, L., & Yang, M. Y. (2016). Effects of different fertilization practices on the incident of rice pest and

diseases: a three year case study in Shanghai in subtropical southeastern China. *Field Crops Research*, *196*, 33-50.

Huang, B., Chen, F., Shen, Y., Qian, K., Wang, Y., Sun, C., Zhao, X., Cui, B., Gao, F., Zeng, Z., & Cui, H. (2018). Advances in targeted pesticides with environmentally responsive controlled release by nanotechnology. *Nanomaterials*, *8*, 102-119.

Ibrahim, S. M., El Samawi, K. M., & Zahran, A. H. (2007). Synthesis of crosslinked superabsorbent carboxymethyl cellulose/acrylamide hydrogels through electron-beam irradiation. *Journal of Applied Polymer Science*, *104*, 2003-2008.

Iftime, M. M., Ailiesei, G. L., Ungureanu, E., & Marin, L. (2019). Designing chitosan based eco-friendly multifunctional soil conditioner systems with urea controlled release and ater retention. *Carbohydrate Polymers*, *223*, 115040-115050.

Inoue, Y., Moran, M. S., & Horie, T. (2015). Analysis of spectral measurements in paddy field for predicting rice growth and yield based on a simple crop simulation model. *Plant Production Science*, *1*, 269-279.

Irfan, A. S., Azeem, B., Irshad, K., Algarni, S., KuShaari, K., Islam, S., & Abdelmohimen, M. A. H. (2020). Machine learning model for nutrient release from biopolymers coated controlled-release fertilizer. *Agriculture*, *10*, 538-551.

Irfan, S. A., Razali, R., KuShaari, K., Mansor, M., Azeem, B., & Versypt, A. N. F. (2018). A review of mathematical modelling and simulation of controlled-released fertilizers. *Journal of Controlled Release*, *271*, 45-54.

Jahan, A., Islam, A., Sarkar, M. I. U., Iqbal, M., Ahmed, M. N., & Islam, M. R. (2022). Nitrogen response of two high yielding rice varieties as influenced by nitrogen levels and growing seasons. *Geology, Ecology, and Landscapes*, *6(1)*, 24-31.

Jampi, A. L. W., Chin, S. F., Wasli, M. E., & Chia, C. H. (2021). Preparation of cellulose hydrogel from sago pith waste as a medium for seed germination. *Journal of Physical Science*, *32*, 13-26.

Jayaramudu, T., Ko, H., Zhai, L., Li, Y., & Kim, J. (2016). Preparation and characterization of hydrogels from polyvinyl alcohol and cellulose and their electroactive behavior. *Soft Materials*, *5*, 64-72.

Jeyabaskaran, K. J., Shirgure, P. S., Pandey, V., Srivastava, A. K., & Uma, S. (2021). Fertigation in horticulture: a guarantee to economized quality production. *Indian Journal of Fertilizer*, *17*, 364-383.

Jiang, T., Duan, Q., Zhu, J., Liu, H., & Yu, L. (2020). Starch-based biodegradable materials: challenges and opportunities. *Advanced Industrial and Engineering Polymer Research*, *3*, 8-18.

Jiang, Y., Qian, H., Wang, L., Feng, J., Huang, S., Hungate, B.A., Van Kessel, C., Horwath, W.R., Zhang, X., Qin, X., Li, Y., Feng, X., Zhang, J., Deng, A., Zheng, C., Song, Z., Hu, S., Van Groenigen, K.J., & Zhang, W. (2018). Limited potential of harvest index improvement to reduce methane emissions from rice paddies. *Global Change Biology*, *25*, 686-698.

Jockusch, S., Turro, N. J., Mitsukami, Y., Matsumoto, M., Iwamura, T., Lindner, T., Flohr, A., Massimo, G. (2009). Photoinduced surface crosslinking of superabsorbent polymer particles. *Journal of Applied Polymer Science*, *111*, 2163-2170.

Jong, S. J., KarunaKaran, K., Wasli, M. E., Musa, Z., & Chin, S. F. (2023). Cellulose-based hydrogel as a natural medium for paddy seed germination. *Starch*, *76*, 1-13.

Joseph, B., Sagarika, V. K., Sabu, C., Kalarikkal, N., & Thomas, S. (2022). Cellulose nanocomposite: fabrication and biomedical applications. *Journal of Bioresources and Bioproducts*, *5*, 223-237.

Juarez-Maldonado, A., Ortega-Ortiz, H., Perez-Labrada, F., Cadenaz-Pliego, G., & Benavides-Mendoza, A. (2016). Cu nanoparticles absorbed on chitosan hydrogels positively alter morphological, production, and quality characteristics of tomato. *Journal of Applied Botany and Food Quality*, *89*, 183-189.

Kabir, S. M. F., Sikdar, P. P., Haque, B., Bhuiyan, M. A. R., Ali, A., & Islam, M. N. (2018). Cellulose-based hydrogel materials: chemistry, properties and their perspective applications. *Progress in Biomaterials*, *7*, 153-174.

Kalhapure, A., Kumar, R., Singh, V. P., & Pandey, D. S. (2016). Hydrogels: a boon for increasing agricultural productivity in water stress-environment. *Current Science*, *111*, 1773-1779.

Kamara, A.Y., Ekeleme, F., Omoigui, L.O., Oikeh, S.O., Chikoye, D., & Tegbaru, A. (2010). Response of upland rice cultivars to nitrogen fertilizer in the Savannas of Nigeria. *Journal of Agronomy*, *102*, 333-339.

Kamel, S., Ali, N., Jahangir, K., Shah, S. M., & El-Gendy, A. A. (2008). Pharmaceutical significance of cellulose: a review. *eXPRESS Polymer Letters*, *2*, 758-778.

Kang, J. & Yun, S. (2023). Double-network hydrogel films based on cellulose derivatives and k-carrageenan with enhanced mechanical strength and superabsorbent properties. *Gels*, *9*, 20-34.

Kang, Y., Nam, J., Kim, Y., Lee, S., Seong, D., Jang, S., & Ryu, C. (2021). Assessment of regression models for predicting rice yield and protein content using unmanned aerial vehicle-based multispectral imagery. *Remote Sensing*, *13*, 1508-1528.

Kareem, S.A., Dere, I., Gungula, D.T., Andrew, F.P., Saddiq, A.M., Adebayo, E.F., Tame, V.T., Kefas, H.M., Joseph, J., & Patrick, D.O. (2021). Synthesis and characterization of slow-release fertilizer hydrogel based on hydroxy propyl methyl cellulose, polyvinyl alcohol, glycerol and blended paper. *Gel, 7*, 262-278.

Karim, D., Siddique, M. N. A., Sarkar, U., Hasnat, M. Z., & Sultana, J. (2014). Phenotypic and genotypic correlation co-efficient of quantitative characters and character association of aromatic rice. *Journal of Bioscience and Agriculture Research, 1*, 34-46.

Karipcin, M. Z. (2023). Hydrogels improved parsley (*Petroselinium crispum*(Mill.) Nyman) growth and development under water deficit stress. *PeerJ, 11*, e15105.

Karki, S., Poudel, N.S., Bhusal, G., Simkhada, S., Regmi, B.R., Adhikari, B., & Poudel, S. (2018). Growth parameter and yield attributes of rice (*Oryza sativa*) as influenced by different combination of nitrogen sources. *World Journal of Agricultural Research, 6*, 58-64.

Kashmitha, M., & Sunil, D. (2022). Cellulose as and eco-friendly and sustainable material for optical anticounterfeiting applications: an up-to-date appraisal. *ACS Publications, 7*, 42681-42699.

Ke, J., Xing, X., Li, G., Ding, Y., Dou, F., Wang, S., Liu, Z., Tang, S., Ding, C., & Chen, L. (2017). Effects of different controlled-release nitrogen fertilisers on ammonia volatilization, nitrogen use efficiency and yield of blanket-seedling machine-transplanted rice. *Field Crops Research, 205*, 147-156.

Kenawy, E. R., Hosny, A., & Saad-Allah, K. (2021). Reducing nitrogen while enhancing growth, yield performance and physiological traits of rice by the application of controlled-release urea fertilizer. *Paddy and Water Environment, 19*, 173-188.

Kermanian, H., Razmpour, Z., Ramezani, O., Mahdavi, S., & Rahmaninia, M. (2013). The influence of refining history of waste NSSC paper on its recyclability. *BioResources*, *8*, 5424-5434.

Khan, F., Atif, M., Haseen, M., Kamal, S., Khan, M. S., Shahid, S., & Nami, S. A. A. (2022). Synthesis, classification and properties of hydrogels: their application in drug delivery and agriculture. *Journal of Material Chemistry B*, *10*, 170-203.

Khan, R., Jolly, R., Fatima, T., & Shakir, M. (2022). Extraction processes for delivering cellulose: a comprehensive review on green approaches. *Polymers for Advanced Technologies*, *33*, 2069-2090.

Khoo, S.M., Moghaddam, P.N., Fareghi, A.R., & Movagharnezhad, N. (2016). Synthesis of a cellulose-based hydrogel network: characterization and study of urea fertilizer slow release. *Journal of Applied Polymer Science*, *133*, 42935-42944.

Kichey, T., Hirel, B., Heumez, E., Dubois, F., & Le Gouis, J. (2007). In winter wheat (*Triticum aestivum* L.), post-anthesis nitrogen uptake and remobilisation to the grain correlates with agronomic traits and nitrogen physiological markers. *Field Crops Research*, *102*, 22-32.

Kiliç, O., Boz, I., & Eryilmaz, G. A. (2021). Comparison of conventional and good agricultural practices farms: a socio-economic and technical perspective. *Journal of Cleaner Production*, *258*, 120666-120676.

Kirchmajer, D.M., Watson, C.A., Ranson, M., & Panhuis, M.I.H. (2013). Gelapin, a degradable genipin cross-linked gelatin hydrogel. *RSC Advances*, *3*, 1073-1081.

Klein, M., & Poverenov, E. (2020). Natural biopolymer-based hydrogels for use in food and agriculture. *Journal of the Science Food and Agriculture*, *100*, 2337-2347.

Konieczynska, M. D., & Grinstaff, M. W. (2017). On-demand dissolution of chemically crosslinked hydrogels. *Accounts of Chemical Research*, *50*, 151-160.

Korsmeyer, R.W., Gurny, R., Doelker, E., Buri, P., & Peppas, N,A. (1983). Mechanism of soliute release from porous hydrophilic polymers. *International Journal of Pharmaceutics*, *15*, 25-35.

Koutroubas, S. D., & Ntanos, D. A. (2003). Genotypic differences for grain yield and nitrogen utilization in Indica and Japonica rice under Mediterranean conditions. *Field Crops Research*, *96*, 37-47.

Krushelnycky, P. (2019). Evaluation of water-storing granules as promising new baiting tool for the control of invasive ants in Hawaii. Report of 1 year activities to the Hawaii invasive species council. Available from https://dlnr.hawaii.gov/hisc/files/2019/07/UH-CTAHR-KrushelnyckyP-Ant-Bait_FY18_Final-Report.pdf.

Kundu, R., Mahada, P., Chhirang, B., & Das, B. (2022). Cellulose hydrogels: green and sustainable soft biomaterials. *Current Research in Green and Sustainable Chemistry*, *5*, 100252-100262.

Lawlor, D.W. (2002). Carbon and nitrogen assimilation in relation to yield: mechanisms are the key to understanding production systems. *Journal of Experimental Botany*, *53*, 773-787.

Lawrencia, D., Wong, S. K., Low, D. Y. S., Goh, B. H., Goh, J. K., Ruktanonchai, U. R., Soottitantawat, A., Lee, L. H., Tang, S. Y. (2021). Controlled release rertilizers: a review on coating materials and mechanism of release. *Plants*, *10*, 238-263.

Lee, J. H., Kang, C. S., Roh, A. S., Park, K. Y., & Lee, H. J. (2010). Assessment of N topdressing rate at panicle initiation stage with chlorophyll meter-based diagnosis in rice. *Journal of Crop Science and Biotechnology*, *12*, 195-200.

Leite, R. G., Cardosa, A. D. S., Fonseca, N. V. B., Silva, M. L. C., Tedeschi, L. O., Delevatti, L. M., Ruggieri, A. C., & Reis, R. A. (2021). Effects of nitrogen fertilization on protein and carbohydrates fractions of Marandu palisadegrass. *Scientific Reports*, *11(14786)*, 1-8.

Li, P., Lu, J., Hou, W., Pan, Y., Wang, Y., Khan, M.R., Ren, T., Cong, R., & Li, X. (2017). Reducing nitrogen losses through ammonia volatilization and surface runoff to improve apparent nitrogen recovery of double cropping of late rice using controlled release urea. *Environmental Science and Pollution Research*, *24*, 11722-11733.

Li, Q., Li, S., Xiao, Y., Zhao, B., Wang, C., Li, B., Gao, X., Li, Y., Bai, G., Wang, Y., & Yuan, D. (2019). Soil acidifications and its influencing factors in the purple hilly area of southwest China from 1981 to 2012. *CATENA*, *175*, 278-285.

Li, X., Li, Q., Xu, X., Su, Y., Yue, Q., & Gao, B. (2016). Characterization, swelling and slow-release properties of a new controlled release fertilizer based on wheat straw cellulose hydrogel. *Journal of the Taiwan Institute of Chemical Engineers*, *60*, 564-572.

Liang, Y., Cao, X., Zhao, L., Xu, X., & Harris, W. (2014). Phosphorus release from dairy manure, the manure-derived biochar, and their amended soil: effects of phosphorus nature and soil property. *Journal of Environmental Quality*, *43*, 1504-1509.

Lindman, B., Karlstromm, G., & Stiggson, L. (2010). On the mechanism of dissolution of cellulose. *Journal of Molecular Liquids, 156*, 76-81.

Liu, S., Wang, X., Peng, Y., Wang, Z., & Ran, R. (2021). Highly stretchable, strain-sensitive, and antifreezing macromolecular microsphere composite starch-based hydrogel. *Macromolecular Materials and Engineering*, *306*, 2100198-2100207.

Liu, S., Wu, Q., Sun, X., Yue, Y., Tubana, B., Yang, R., & Cheng, H. N. (2021). Novel alginate-cellulose nanofiber-poly(vinyl alcohol) hydrogels for carrying and delivering nitrogen, phosphorus, and potassium chemicals. *International Journal of Biological Macromolecules*, *172*, 330-340.

Liu, W., Liu, S., Liu, T., Liu, T., Zhang, J., & Liu, H. (2019). Eco-friendly post-consumer cotton waste recycling for regenerated cellulose fibers. *Carbohydrate Polymers*, *206*, 141-148.

Liu, X., Liao, J., Song, H., Yang, Y., Guan, C., Zhang, Z. (2019). A biochar-based route for environmentally friendly controlled release of nitrogen: Urea-loaded biochar and bentonite composite. *Scientific Report*, *9*, 1-12.

Liu, Y., Wang, J., Chen, H., & Cheng, D. (2022). Environmentally friendly hydrogel: a review of classification, preparation and application in agriculture. *Science of The Total Environment*, *846*, 157303-157313.

Liu, Z., Li, D., Dai, H., & Huang, H. (2017). Preparation and characterization of papain embedded in magnetic cellulose hydrogels prepared from tea residue. *Journal of Molecular Liquids*, *232*, 449-456.

Loh, C.W.F., Grabosky, J.C., & Bassuk, N.L. (2002). Using the SPAD 502 meter to access chlorophyll and nitrogen content of Benjamin fig and cottonwood leaves. *HortTechnology*, *12*, 682-686.

Lopez-Velazquez, J. C., Rodriguez-Rodriguez, R., Espinosa-Andrews, H., Qui-Zapata, J. A., Garcia-Morales, S., Navarro-Lopez, D. E., Luna-Barcenas, G., Vassalo-Brigneti, E.

C., & Garcia-Carvajal, Z. Y. (2019). Gelatin-chitosan-PVA hydrogels and their applications in agriculture. *Journal of Chemical Technology and Biotechnology*, *94*, 3495-3504.

Luo, X., & Zhang, L. (2013). New solvents and functional materials prepared from cellulose solutions in alkali/urea aqueous system. *Food Research International*, *52*, 387-400.

Maitra, J., & Shukla, V. K. (2014). Cross-linking in hydrogels - a review. *American Journal of Polymer Science*, *4*, 25-31.

Mane, S., Ponrathnam, S., & Chavan, N. (2016). Effect of chemical cross-linking on properties of polymer microbeads: a review. *Canadian Chemical Transaction Year 2015*, *3*, 473-485.

Manzoor, Z., Awan, T.H., Zahid, M.A., & Faiz, F.A. (2006). Response of rice crop (Super Basmati) to different nitrogen levels. *Journal of Animal and Plant Science*, *16*, 52-55.

Martínez-Cano, B., Mendoza-Meneses, C. J., García-Trejo, J. F., Marcías-Bobadilla, G., Aguirre-Becerra, H., Soto-Zarazúa, G. M., & Feregrino-Pérez, A. A. (2022). Review and perspectives of the use of alginate as a polymer matrix for microorganisms applied in agro-industry. *Molecules*, *27*, 4248-4258.

Masclaux-Deubresse, C., Daniel-Vedele, F., Dechorgnat, J., Chardon, F., Gaufichon, L., & Suzuki, A. (2010). Nitrogen uptake, assimilation and remobilization in plants: challenges for sustainable and productive agriculture. *Annals of Botany*, *105*, 1141-1157.

Mauad, M., Alexandre, C., Crusciol, C., Filho, H.G., & Corrêa, J.C. (2003). Nitrogen and silicon fertilization of upland rice. *Agricultural Science*, *60*, 1-8.

McCalla, K., Tay, J. W., Mulchandani, A., Choe, D. H., & Hoddle, M. (2020). Biodegradable alginate hydrogel bait delivery system effectively controls high-density populations of argentine ant in commercial citrus. *Journal of Pest Science, 93*, 1031-1042.

Mehmood, T., Ahmad, W., Ahmad, K. S., Shafi, J., Shehzad, M. A., & Sarwar, M. A. (2013). Comparative effect of different potting media on vegetative and reproductive growth of floral shower (*Antirrhinum majus* L.). *Universal Journal of Plant Science, 1*, 104-111.

Melo, R. A. C., Jorge, M. H. A., Bortolin, A., Boiteux, L. S., Ribeiro, C., & Marconcini, J. M. (2019). Growth of tomato seedlings in substrates containing a nanocomposite hydrogel with calcium montmorillonite (NC-MMT). *Horticultura Brasileira, 37*, 199-203.

Merill, K., Boser, C. L., Hanna, C., Holway, D. A., Naughton, I., Choe, D. H., & Wilson-Rankin, E. (2018). Argentine ant (*Linepithema humile*, Mayr) eradication efforts on San Clemente Island, California, USA. *Western North American Naturalist, 78*, 829-836.

Messiga, A. J., Dyck, K., Ronda, K., Van Baar, K., Haak, D., Yu, S., & Dorais, M. (2020). Nutrients leaching in response to long-term fertigation and broadcast nitrogen in blueberry production. *Plants, 9*, 1530-1550.

Michalik, R., & Wandzik, I. (2020). A mini-review on chitosan based hydrogels with potential for sustainable agricultural applications. *Polymers, 12*, 2425-2441.

Miljković, V., Gajić, I., & Nikolić, L. (2021). Waste materials as a resource for production of CMC superabsorbent hydrogel for sustainable agriculture. *Polymer (Basel), 13*, 4115-4127.

Min, B. C., Bhayani, B. V., Jampana, V. S., & Ramao, B. V. (2015). Enhancement of the enzymatic hydrolysis of fines from recycled paper mill waste rejects. *Bioresources and Bioprocessing*, *2*, 1-10.

Mohamed, R. R., Fahim, M. E., & Soliman, S. M. A. (2022). Development of hydrogel based on carboxymethyl cellulose/poly(4-vinylpridine) for controlled releasing of fertilizers. *BMC Chemistry*, *16*, 1-12.

Mohammad Padzil, F. N., Lee, S. H., Ainun, Z. M. A. A., Lee, C. H., & Abdullah, L. C. (2020). Potential of oil palm empty fruit bunch resources in nanocellulose hydrogel production for versatile applications. *Materials*, *13*, 1245-1271.

Mohd Fairulnizal, M. N., Norhayati, M. K., Zaiton, A., Norliza, A. H., Rusidah, S., Aswir, A. R., Suraiami, M., Mohd Naeem, M. N., Jo-Lyn, A., Mohd Azerulazree, J., Vimala B., & Mohd Zainuldin, T. (2015). Nutrient content in selected commercial rice in Malaysia: an update of Malaysian food composition database. *International Food Research Journal*, *22(2)*, 768-776.

Mohd Yusof, M. N., Zawawi, N. Z., Mansor, H., Mohamad Saad, M., Ramli, A., Ibrahim, I. Z., Malik, Z., & Abu Bakar, M. (2014). Penilaian potensi baja organik yang diperkaya terhadap hasil varieti Padi Wangi MRQ74. *Jurnal Teknologi*, *70*, 49-51.

Momesso, L., Cruscio, C. A. C., Soratto, R. P., Tanaka, K. S., Costa, C. H. M., Cantarella, H., & Kurame, E. E. (2020). Upland rice yield enhanced by early nitrogen fertilization on previous palisade grass. *Nutrient Cycling in Agroecosystems*, *118*, 115-131.

Monte, M. C., Fuente, E., Blanco, A., & Negro, C. (2008). Waste management from pulp and paper production in the European union. *Waste Management*, *29*, 293-308.

Montesano, F. F., Parente, A., Santamaria, P., Sannino, A., & Serio, F. (2015). Biodegradable superabsorbent hydrogel increases water retention properties of growing media and plant growth. *Agriculture and Agricultural Science Procedia*, *4*, 451-458.

Munda, S., Nayak, A.K., Mishra, P.N., Bhattacharyya, P., Mohanty, S., Kumar, A., Kumar, U., Baig, M.J., Tripathi, R., Shahid, M., Adak, T., & Thilagam, V.K. (2016). Combined application of rice husk biochar and flyash improved the yield of lowland rice. *Soil Research*, *54*, 1-9.

Narayanan, A., Kartik, R., Sangeetha, E., & Dhamodharan, R. (2018). Super water absorbing polymeric gel rom chitosan, citric acid and urea: synthesis and mechanism of water absorption. *Carbohydrate Polymers*, *191*, 152-160.

Naruetharadhol, P., Ketkaew, C., & Srisathan, W. A. (2022). Innovative price-setting approaches to high value product: a pricing method for agribusiness farmers. *Heliyon*, *8*, 1-15.

Nasution, H., Harahap, H., Dalimunthe, N. F., Ginting, M. H. S., Jaafar, M., Tan, O. O. H., Aruan, H. K., Herfananda, A. L. (2022). Hydrogels and effect of crosslinking agent on cellulose-based hydrogels: a review. *Gels*, *8*, 568-598.

Nath, P. C., Debnath, S., Sharma, M., Sridhar, K., Nayak, P. K., & Inbaraj, B. S. (2023). Recent advances in cellulose-based hydrogels: food applications. *Foods*, *12*, 350-377.

Nayan, N. H., Hamzah, M. S., Tahir, A., Rajali, A. A., Muslih, E. F., & Mazlan, R. (2018). Development of polyvinyl alcohol/chitosan hydrogel loaded with fertilizer compound: preparation, properties and effect on seed germination. *Journal of Science and Technology*, *10*, 21-27.

Naz, M. Y., & Sulaiman, S. A. (2016). Slow release coating remedy for nitrogen loss from conventional urea: a review. *Journal of Controlled Release*, *225*, 109-120.

Nazarli, H., Zardashti, M. R., Darvishzadeh, R., & Najafi, S. (2010). The effect of water stress and polymer on water use efficiency, yield and several morphological traits of sunflower under greenhouse condition. *Note Science Biology*, *2*, 53-58.

Ni, B., Liu, M., Lu, S., & Xie, L. (2011). Environmentally friendly slow-release nitrogen fertilizer. *Journal of Agricultural and Food Chemistry*, *59*, 10169-10175.

Ning, X., Huang, J., Yimuhan, A., Yuan, N., Chen, C., & Lin, D. (2022). Research advances in mechanical properties and applications of dual network hydrogels. *International Journal of Molecular Sciences*, *23*, 15757-15771.

Niu, H., Wang, F., & Weiss, R. A. (2015). Hydrophibic/hydrophilic triblock copolymers: synthesis and properties of physically crosslinked hydrogels. *Macromolecules*, *48*, 645-654.

Nnadi, B., & Brave, C. (2011). Environmentally friendly superabsorbent polymers for water conservation in agricultural lands. *Journal of Soil Science and Environmental Management*, *2*, 206-211.

Nong, H.T., Tateishi, R., Suriyasak, C., Kobayashi, T., Oyama, Y., Chen, W.J., Matsumoto, R., Hamaoka, N., Iwaya-Inoue, M., & Ishibashi, Y. (2020). Effect of seedling nitrogen condition on subsequent vegetative growth stages and its relationship to the expression of nitrogen transporter genes in rice. *Plants (Besel)*, *9*, 861-872.

Norain, M. N., Shamsiah, A., Abdul, R. H., Nor, A. H., Haslinda, A. M., & Wan, A. W. A. (2014). Correlation analysis on agronomic characters in F2 population derived from MR64 and Pongsu Seribu 2. *Journal of Applied Science and Agriculture*, *9*, 143-147.

Noreen, A., Zia, K. M., Tabasum, S., Khalid, S., & Shareef, R. (2020). A review on grafting of hydroxyethylcellulose for versatile applications. *International Journal of Biological Macromolecules*, *150*, 289-303.

Oguntunde, P. G., Lischeid, G., & Dietrich, O. (2017). Relationship between rice yield and climate variables in southwest Nigeria using multiple linear regression and support vector machine analysis. *International Journal of Biometeorology*, *62*, 459-469.

Oikeh, S.O., Nwilene, F., Diatta, S., Osiname, O., Toure, A., & Okeleye, K.A. (2008). Responses of upland NERICA rice to nitrogen and phosphorus in forest agroecosystem. *Journal of Agronomy*, *100*, 735-741.

Olad, A., Doustdar, F., & Gharekhani, H. (2020). Fabrication and characterization of a starch-based superabsorbent hydrogel composite reinforced with cellulose nanocrystals from potato peel waste. *Colloids and Surfaces A: Physicochemical and Engineering Aspects*, *601*, 124962.

Olad, A., Zebhi, H., Slarai, D., Mirmohseni, A., & Tabar, A.R. (2018). Slow-release NPK fertilizer encapsulated by carboxymethyl cellulose-based nanocomposite with the function of water retention in soil. *Material Science & Engineering C, Materials for Biological Applications*, *90*, 333-340.

Oladipupo, So. O., Hu, X. P., & Appel, A. G. (2020). Essential oil components in superabsorbent polymer gel modify reproduction of *Blatella germanica* (Blatoddea: Ectobiidae). *Journal of Economic Entomology, 113*, 2436-2447.

Oladusu, Y., Rafii, M. Y., Magaji, U., Abdullah, N., Miah, G., Chukwu, S. C., Hussin, G., Ramli, A., & Karim, I. (2018). Genotypic and phenotypic relationship among yield components in rice under tropical conditions. *BioMed Research International, 2018,* 8936767.

Olubanjo, O. O., & Yessoufou, M. A. (2019). Effect of soil compaction on the growth and nutrient uptake of *Zea Mays* L. *Sustainable Agriculture Research*, *8*, 46.

Padhan, B. K., Sathee, L., Kumar, S., Chinnusamy, V., & Kumar, A. (2023). Variation in nitrogen partitioning and reproductive stage nitrogen remobilization determines nitrogen grain production efficiency (NUEg) in diverse rice genotypes under varying nitrogen supply. *Frontiers in Plant Science*, *14*, 1093581.

Pan, T., Hou, S., Liu, Y., & Tan, Q. (2019). Comparison of three models fitting the soil water retention curve in a degraded alpine meadow region. *Scientific Reports*, *9*, 18407.

Panescu, P. H., Browne, M., Chen, K. K., Sack, L., & Maynard, H. D. (2022). Effects of trehalose and polyacrylate-based hydrogels on tomato growth under drought. *AoB Plants*, *14*, 1-10.

Parhi, S. (2017). Cross-linked hydrogels for pharmaceutical applications: a review. *Advanced Pharmaceutical Bulletin*, *7*, 515-530.

Parida, A. K., Sekhar, S., Panda, B. B., Sahu, G., & Shaw, B. P. (2022). Effect of panicle morphology on grain filling and rice yield: genetic control and molecular regulation. *Frontiers in Genetics*, *13*, 1-10.

Park, S., Baker, J. O., Himmel, M. E., Parilla, P. A., & Johnson, D. K. (2010). Cellulose crystallinity index: measurement techniques and their impact on interpreting cellulose performance. *Biotechnology for Biofuels and Bioproducts*, *3*, 10-19.

Parviainen, H., Parviainen, A., Virtanen, T., Kilpeläinen, I., Ahvenainen, P., Serima, R., Grönqvist, S., Maloney, T., & Maunu, S. L. (2014). Dissolution enthalpies of cellulose in ionic liquids. *Carbohydrate Polymers*, *113*, 67-76.

Peck, R. W., Banko, P. C., Donmoyer, K., Scheiner, K., Karmi, R., & Kropidlowski, S. (2017). Efforts to eradicate yellow crazy ants on Johnston Atoll: results from crazy

ant strike team X, XI and XII, June 2015 – December 2016. Technical Report HCSU-081, Hawaii Cooperative Studies Unit, University of Hawaii at Hilo, Hilo, HI.

Peers, S., Montembault, A., & Ladaviere, C. (2020). Chitosan hydrogels for sustained drug delivery. *Journal of Controlled Release*, *326*, 150-163.

Pella, M. C. G., Lima-Tenorio, M. K., Tenorio-Neto, E. T., Guilherme, M. R., Muniz, E. C., & Rubira, A. F. (2018). Chitosan-based hydrogels: from preparation to biomedical applications. *Carbohydrate Polymers*, *196*, 233-245.

Perez Bravo, J. J., & Francois, N. J. (2020). Chitosan/starch matrices prepared by ionotropic gelation: rheological characteristics, swelling behavior and potassium nitrate release kinetics. *Journal of Polymers and the Environment*, *28*, 2681-2690.

Perumal, M., Wasli, M. E., & Ho, S. Y. (2015). Soil morphological and physicochemical properties at reforestation sites after enrichment planting of Shorea Macrophylla in Sampadi Forest Reserve, Sarawak, Malaysia. *Borneo Journal of Resources Science and Technology*, *5*, 28-43.

Peyrusson, F. (2021). Hydrogels improve plant growth in mars analog condition. Frontiers in Astronomy and Space Sciences. Doi: https://doi.org/10.3389/fspas.2021.729278

Phang, S. W., Sin, L. T., Bee, S. T., & Tee, T. T. (2020). Release kinetic model of nitrogen released encapsulated in starch-alginate controlled release urea: diffusion and its decay release. *AIP Conference Proceedings*, *2233*, 1-8.

Piai, J.F., De Moura, M. R., Rubira, A. F., & Muniz, E. C. (2008). Kinetic study of bovine serum albumin (BSA) released from alginate-Ca^{2+}/PNIPAAm hydrogels. *Macromolecular Symposia*, *266*, 108-113.

Poletto, M., Ornaghi, J. H. L., & Zattera, A. J. (2014). Native cellulose: structure, characterization and thermal properties. *Materials*, *7*, 6105-6119.

Pratiwi, G. R., Hanudin, E., Purwanto, B. H., Sulistyaningsih, E., & Hayashi, K. (2021). Rice growth response to CRF fertilizer and biochar in rainfed land under two continuous seasons. *IOP Conference Series: Earth and Environmental Science*, *752*, 1-10.

Putri, D. R., Aprilia, R., & Lubis, R. S. (2020). Analysis of factors affecting production rice in Langkat regency with methods backward in multiple linear regression year 2018. *Journal of Mathematics and Scientific Computing with Applications*, *1*, 23-30.

Qamruzzaman, M., Ahmed, F., & Mondal, M. I. H. (2021). An overview on starch-based sustainable hydrogels: potential applications and aspects. *Journal of Polymers and the Environment*, *30*, 19-50.

Qi, D., Wu, X., & Zhu, J. (2020). Nitrogen and phosphorus losses from paddy fields and the yield of rice with different water and nitrogen management practices. *Scientific Reports*, *10*, 9734-9745.

Qi, H, Chang, C., Zhang, L. (2008). Effects of temperature and molecular weight on dissolution of cellulose in NaOH/urea aqueous solution. *Cellulose*, *15*, 779-787.

Qiao, J., Yang, L., Yan, T., Xue, F., & Zhao, D. (2012). Nitrogen fertilizer reduction in rice production for two consecutive years in the Taihu Lake area. *Agriculture, Ecosystem & Environment*, *146*, 103-112.

Qin, C. C., Abdalkarim, S. Y. H., Zhou, Y., Yu, H. Y., & He, X. (2022). Ultrahigh water-retention cellulose hydrogels as soil amendments for early seed germination under harsh condition. *Journal of Cleaner Production*, *370*, 133602-133612.

Qin, Y., Wang, J., Qiu, C., Xu, X., & Jin, Z. (2019). A dual cross-linked strategy to construct moldable hydrogels with high stretchability, good self-recovery, and self-healing capability. *Journal of Agricultural and Food Chemistry*, *67*, 3966-3980.

Quesada-Perez, M., Maroto-Centeno, J.A., Forcada, J., & Hidalgo-Alvarez, R. (2011). Gel swelling theories: the classical formalism and recent approaches. *Soft Matter*, *7*, 10536-10547.

Raafat, A. I., Eid, M., & El-Arnaouty, M. B. (2012). Radiation synthesis of superabsorbent CMC based hydrogels for agricultural applications. *Nuclear Instruments and Methods in Physics Research Section B Beam Interactions with Materials and Atom*, *283*, 71-76.

Radin Firdaus, R. B., Tan, M. L., Rahmat, S. R., & Gunaratne, M. S. (2020). Paddy, rice and food security in Malaysia: a review of climate change impacts. *Cogent Social Sciences*, *6*, 1-17.

Ramezani, M., Jafari, M., Tavili, A., Javadi, S. A., & Amiri, Q. Z. (2013). The effect of calcium and sodium chloride levels on the dehydration power of hydrophilic polymer. *Journal of Food, Agriculture and Environment*, *11*, 896-898.

Ramli, R. A. (2019). Slow release fertilizer hydrogels: a review. *Polymer Chemistry*, *10*, 6073-6090.

Ramli, R. A., Lian, Y. M., Nor, N. M., & Azman, N. I. Z. (2019). Synthesis, characterization, and morphology study of coco peat-*grafted*-poly(acrylic acid)/NPK slow release fertilizer hydrogel. *Journal of Polymer Research*, *26*, 266-272.

Ramos Campos, E. V., de Oliveira, J. L., Fraceto, L. F., & Singh, B. (2015). Polysaccharides as safer release system for agrochemicals. *Agronomy for Sustainable Development*, *35*, 47-66.

Ranganathan, N., Bensingh, R. J., Kader, M. A., & Nayak, S. K. (2018). Cellulose-based hydrogels for agricultures. In Mondal, M (eds) Cellulose-Based Superabsorbent

Hydrogels. Polymer and Polymeric Composites: A Reference Series. Springer, Cham. Doi: https://doi.org/10.1007/978-3-319-76573-0_34-1

Ransom, C. J., Jolley, V. D., Blair, T. A., Sutton, L. E., & Hopkins, B. G. (2020). Nitrogen release rates from slow- and controlled-release fertilizers influenced by placement and temperature. *Plos One*, *15(6)*, 1-21.

Rashidzadeh, A., & Olad, A. (2014). Slow-released NPK fertilizer encapsulated by NaAlg-g-poly(AA-co-AAm)/MMT superabsorbent nanocomposite. *Carbohydrate Polymers*, *114*, 269-278.

Raucci, M.G., Alvarez-Perez, M.A., Demitri, C., Sannino, A., & Ambrosio, L. (2012). Proliferation and osteoblastic differentiation of hMSCs on cellulose-based hydrogels. *Journal of Applied Biomaterials & Function Materials*, *10*, 302-307.

Rea, R. S., Islam, M. R., Rahman, M. M., & Mix, K. (2019). Study of nitrogen use efficiency and yield of rice influenced by deep placement of nitrogen fertilizers. *SAARC Journal of Agriculture*, *17(1)*, 93-103.

Reis, A. V. G. M., Rubira, A. F., & Muniz, E. C. (2007). Mathematical model for the prediction of the overall profile of in vitro solute release from polymer network. *Journal of Colloid and Interface Science*, *310*, 7.

Rico-García, D., Ruiz-Rubio, L., Pérez-Alvarez, L., Hernández-Olmos, S. L., Guerrero-Ramírez, G. L., & Vilas-Vilela, J. L. (2020). Lignin-based hydrogels: synthesis and applications. *Polymers*, *12*, 81-103.

Riseh, R. S., Vazvani, M. G., Hassanisaadi, M., & Skorik, Y. A. (2023). Micro-/nano-carboxymethyl cellulose as a promising biopolymers with prospects in the agriculture sector: a review. *Polymers (Basel)*, *15*, 440-470.

Rollon, R. J. C., Batac, R. A., Batac, R. A., & Maglines, S. M. (2018). Effects of carbonized rice hull and arbuscular mycorrhizal fungi application on potting media chemical properties, growth and nutrient uptake of falcata (*Paraserianthes falcataria* L.). *International Journal of Agronomy and Agricultural Research*, *13*, 93-101.

Ropek, D., & Kuliskowski, E. (2009). Potential of hydrogel application for plant protection. *Ecological Chemistry and Engineering A*, *16*, 1191-1198.

Rossi, A.M., Villareal, M., Juarez, M.D., & Samman, N.C. (2004). Nitrogen contents in food: A comparison between the kjeldahl and hach methods. *Journal of the Argentine Chemical Society*, *94*, 99-108.

Roth, C. H., Cosijn, M., Carter, C., Chakraborty, A., Das, M., Hamilton, S. H., Jana, A. K., Lim-Kamacho, L., Majumdar, S., Merritt, W. S., Mishra, P., Mishra, R., Nidumolu, U., Rahman, M. W., Ray, D., & Williams, L. J. (2023). Overcoming barriers to social inclusion in agricultural intensification: reflections on a transdisciplinary community development project from India and Bangladesh. *Community Development Journal*, *5*, 1-21.

Roy, A., Bajpai, J., & Bajpai, A. K. (2009). Dynamics of controlled release of chlorpyrifos from swelling and eroding biopolymeric microspheres of calcium alginate and starch. *Carbohydrate Polymers*, *76*, 222-231.

Roy, A., Singh, S. K., Bajpai, J., & Bajpai, A. K. (2014). Controlled pesticides release from biodegradable polymers. *Central European Journal of Chemistry*, *12*, 453-469.

Rozaki, Z., Triyono., Indardi., Salassa, D. I., & Nugroho, R. B. (2020). Farmers' responses to organic rice farming in Indonesia: findings from central Java and south Sulawesi. *Open Agriculture*, *5*, 703-710.

Rust, M. K., Choe, D. H., Wilson-Rankin, E., Campbell, K., Kabashima, J., & Dimson, M. (2017). Controlling yellow jackets with fipronil-based protein baits in urban recreational area. *International Journal of Pest Management*, *63*, 234-241.

Rust, M. K., Soeprono, A., Wright, S., Greenberg, L., Choe, D. H., Boser, C. L., Cory, C., & Hanna, C. (2015). Laboratory and field evaluations of polyacrylamide hydrogel baits against argentine ants (Hymenoptera: Formicidae J.). *Journal of Economic Entomology*, *108*, 1228-1236.

Sabazoodkhiz, R., Rahmaninia, M., & Ramezani, O. (2017). Interaction of chitosan biopolymer with silica nanoparticle as a novel retention/drainage and reinforcement aid in recycled cellulosic fibers. *Cellulose*, *24*, 3433-3444.

Sabbagh, F., Muhamad, I. I., Pa'e, N., & Hashim, Z. (2018). Strategies in improving properties of cellulose based hydrogels for smart applications. *Polymer and Polymeric Composites: A Reference Series*. Doi: https://doi.org/10.1007/978-3-319-76573-0_30-1

Said, M., Atassi, Y., Tally, M., & Khatib, H. (2018). Environmentally friendly chitosan-g-poly(acrylic acid-co-acrylamide)/ground basal superabsorbent composite for agricultural applications. *Journal of Polymers and the Environment*, *26*, 3937-3948.

Saini, A. K., Patel, A. M., Saini, L. H., & Malve, S. H. (2020). Growth, phenology and yield of summer pearl millet (Pennisetum glaucum L.) as affected by varied application of water, nutrients and hydrogel. *International Journal of Ecology and Environmental Sciences*, *2*, 248-252.

Salleh, K. M., Zakaria, S., Sajab, M. S., Gan, S., Chia, C. H., Jaafar, S. N. S., & Amran, U. A. (2018). Chemically crosslinked hydrogel and its driving force towards

superabsorbent behaviour. *International Journal of Biological Macromolecules, 118,* 1422-1430.

Sanchita, B., Borbora, P. D., Manisha, K., Kumar, H. T. & Das, K. (2010). Growth, yield and economics of broccoli under different levels of nitrogen fertigation. *Indian Journal of Horticulture*, *67*, 279-282.

Sannino, A., Demitri, C., & Madaghiele, M. (2009). Biodegradable cellulose-based hydrogel: design and application. *Materials*, *2*, 353-373.

Sarfraz, R., Shakoor, A., Abdullah, M., Arooj, A., Hussain, A., & Xing, S. (2017). Impact of integrated application of biochar and nitrogen fertilizers on maize growth and nitrogen recovery in alkaline calcareous soil. *Soil Science and Plant Nutrition, 63(5),* 488-498.

Saruchi, Kaith, B. S., Jindal, R., & Kapur, G. S. (2013). Enzyme-based green approach for the synthesis of gum tragacanth and acrylic acid cross-linked hydrogel: its utilization in controlled fertilizer release and enhancement of water holding capacity of soil. *Iranian Polymer Journal*, *22*, 561-570.

Satriani, A., Catalano, M., & Scalcione, E. (2018). The role of superabsorbent hydrogel in bean crop cultivation under deficit irrigation conditions. A case-study in Southern Italy. *Agricultural Water Management*, *195*, 114-119.

Schall, K., Tay, J. W., Mulchandani, A., Choe, D. H., & Hoddle, M. (2018). Harnessing hydrogels in the battle against invasive ants: could a hydrogel baiting system solve argentine ant problems in Southern California Citrus? *Citrograph*, *9*, 30-35.

Scheel, R. A., Fusi, A. D., Min, B. C., Thomas, C. M., Ramarao, B. V., & Nomura, C. T. (2019). Increased production of the value-added biopolymers poly(R-3-

hydroxyalkanoate) and poly(γ-glutamic acid) from hydrolysed paper recycling waste fines. *Frontiers in Bioengineering and Biotechnology*, *7*, 1-8.

Seki, Y., Altinisik, A., Demircioglu, B., & Tetik, C. (2014). Carboxymethylcellulose (CMC)-hydroxyethylcellulose (HEC) based hydrogels: synthesis and characterization. *Cellulose*, *21*, 1689-1698.

Sellam, V., & Poovammal, E. (2016). Prediction of crop yield using regression analysis. *Indian Journal of Science and Technology*, *9*, 1-5.

Sellan, G., Brearly, F., & Nilus, R. (2021). Differences in soil properties among contrasting soil types in Northern Borneo. *Journal of Tropical Forest Science*, *33*, 191-202.

Sempeho, S. I., Kim, H. T., Mubofu, E., & Hilonga, A. (2014). Meticulous Overview on the Controlled Release Fertilizers. *Advances in Chemistry*, *2014*, 1-16.

Sennakesavan, G., Mostakhdenim, M., Dkhar, L. K., Seyfoddin, A., & Fatihhi, S. J. (2020). Acrylic acid/acrylamide based hydrogels and its properties – A review. *Polymer Degradation and Stability*, *180*, 109308.

Shah, J. A., Vendl, T., Aulicky, R., Frankova, M., & Stejskal, V. (2022). Gel carriers for plant extracts and synthetic pesticides in rodent and arthropod pest control: An overview. *Gels*, *8*, 522-539.

Sharma, A., Kumar, V., Shahzad, B., Tanveer, M., Sidhu, G. P. S., Handa, N., Kohli, S. K., Yadav, P., Bali, A. S., & Parihar, R. D. (2019). Worldwide pesticide usage and its impacts on ecosystem. *SN Applied Sciences*, *1*, 1446-1461.

Shen, Z., Liao, Q., Hong, Q., & Gong, Y. (2012). An overview of research on agricultural non-point source pollution modelling in China. *Separation and Purification Technology*, *84*, *104-111*.

Shennan, C., Krupntik, T. J., Baird, G., Cohen, H., Forbush, K., Lovell, R., Olimpi, E. M. (2017). Organic and conventional agriculture: a useful framing ?. *Annual Review of Environment and Resources*, *42*, 317-346.

Shetty, R., & Prakash, N. B. (2020). Effect of different biochars on acid soils and growth parameters of rice plants under aluminium toxicity. *Scientific Reports*, *10*, 12249.

Shrestha, J., Kandel, M., Subedi, S., & Shah, K.K. (2020). Role of nutrients in rice (*Oryza Sativa* L.): a review. *Agrica*, *9*, 53-62.

Shrotri, A., Lambert, L. K., Tanksale, A., & Beltramini, J. (2013). Mechanical depolymerisation of acidulated cellulose: understanding the solubility of high molecular weights oligomers. *Green Chemistry*, *15*, 2761-2768.

Sikder, A., Pearce, A. K., Parkinson, A. J., Napier, R., & O'Reilly, R. K. (2021). Recent trends in advanced polymer materials in agriculture related applications. *ACS Applied Polymer Materials*, *3*, 1203-1217.

Singh, B., Sharma, D. K., Kumar, R., & Gupta, A. (2009). Controlled release of a fungicide thiram from starch-alginate-clay based formulation. *Applied Clay Science*, *45*, 76-82.

Singh, H. (2012). Effect of hydrogel on growth, yield and water use efficiency in pearl millet (Pennisetum glaucum) production. *Forage Research*, *38*, 27-28.

Singh, S. P., Singh, R. K., & Kumar, S. (2017). Effect of irrigation schedule, mulching and hydrogel on wheat analysis of soybean (*Glycine max* L.) under drought stress condition. *Pakistan Journal of Biological Science*, *10*, 4190-4196.

Singha, A. K., & Baruah, M. J. (2017). Farmers' adoption behaviour in rice technology: an analysis of adoption behaviour of farmers in rice technology under different farming systems in Assam. *Journal of Human Ecology*, *35*, 167-172.

Sinton, F. V., Sam, L. M., Benedick, S., Jalloh, M. B. (2019). Evaluation of the yield of upland rice varieties under open trial field. *Transaction on Science Technology*, *6*, 253-258.

Song, G., Zhao, H. Q., Liu, Q., & Fan, Z. (2022). A review on biodegradability biliary stents: materials and future trends. *Bioactive Materials*, *17*, 488-495.

Sorieul, M., Dickson, A., Hill, S. J., & Pearson, H. (2016). Plants fibre: molecular structure and biochemical properties, of a complex living material, influencing its deconstruction towards a biobased composite. *Materials*, *9*, 618-653.

Stefan, D. S., Zainescu, G., Manea-Saghin, A. M., Triantaphyllidou, I. E., Tzoumani, I., Tatoulis, T. I., Syriopoulos, G. T., & Meghea, A. (2020). A collagen-based hydrogels composites from hide waste to produce smart fertilizer. *Materials*, *13*,4396-4413.

Suhaimee, S., Rabu, M. R., Ali, A. K., & Ramli, A. (2009). Ex ante assessment on feasibility of Maswangi (MRQ74) commercialization. *Economic and Technology Management Review*, *4*, 49-56.

Sui, B. A., Feng, X. M., Tian, G. L., Hu, X. Y., Shen, Q. R., & Guo, S. (2013). Optimizing nitrogen supply increases rice yield and nitrogen use efficiency by regulating yield formation factors. *Field Crops Researsch*, *150*, 99-107.

Sun, Y., Nan, D., Jin, H., & Qu, Z. (2020). Recent advances of injectable hydrogels for drug delivery and tissue engineering applications. *Polymer Testing, 81*, 106283-106293.

Sun, Z., Yin, X., Ding, J., Yu, D., Hu, M., Sun, X., Tan, Y., Shen, X., Liu, L., Mo, Y., Ouyang, N., Jiang, B., Yuan, G., Duan, M., Yuan, D., & Fang, J. (2017). QTL analysis and dissection of panicle components in rice using advanced backcross populations derived from Oryza sativa cultivars HR1128 and 'Nipponbare'. *PLoS One*, *12*, e0175692.

Supare, K., & Mahanwar, P. (2022). Starch-chitosan hydrogels for the controlled-release of herbicides in agricultural applications: a study on the effect of the concentration of raw materials and crosslinker. *Journal of Polymers and the Environment*, *30*, 2448-2461.

Suresh, R., Prasher, S. O., Patel, R. M., Qi, Z., Elsayed, E., Schwinghamer, T., & Ehsan, A. M. (2018). Super absorbent polymer and irrigation regime effects on growth and water use efficiency of container-grown cherry tomatoes. *Transactions of the ASABE*, *61*, 523-531.

Susanti, D. Y., Sediawan, W. B., Fahrurrozi, M., & Hidayat, M. (2019). A mechanistic model of mass transfer in the extraction of bioactive compounds from intact sorghum pericarp. *Processes*, *7*, 837-856.

Syafrudin, M., Kristanti, R. A., Yuniarto, A., Hadibarata, T., Rhee, J., Al-onazi, W. A., Algarni, T. S., Almarri, A. H., & Al-Mohaimeed, A. M. (2021). *International Journal of Environmental Research and Public Health*, *18*, 468-482.

Tal, A. (2018). Making conventional agriculture environmentally friendly: moving beyond the glorification of organic agriculture and the demonization of conventional agriculture. *Sustainability*, *10*, 1078-1094.

Tan, B. L., Norhaizan, M. E., & Chan, L. C. (2023). Rice bran: from waste to nutritious food ingredients. *Nutrients*, *15(11)*, 2502-2527.

Tanaka, S., Tachibe, S., Wasli, M. E., & Lat, J. (2009). Soil characteristics under cash crop farming in upland areas of Sarawak, Malaysia. *Agriculture Ecosystems & Environment*, *129*, 293-301.

Tang, L., Zhou, J., Bobojonov, I., Zhang, Y., & Glauben, T. (2019). Induce or reduce ? the crowding-in effects of farmers' perception of climate risk on chemical use in China. *Climate Risk Management*, *20*, 27-37.

Tawie, S. (2023, May 23). Sarawak minister says rice production should achieve 60pc self-sufficiency level by 2030. *Malaymail*. https://www.malaymail.com/news/malaysia/2023/05/23/sarawak-minister-says-rice-production-should-achieve-60pc-self-sufficiency-level-by-2030/70591

Tay, J. W., Choe, D. H., Mulchandani, A., & Rust, M. K. (2020). Hydrogels: from controlled release to a new bait delivery for insect pest management. *Journal of Economic Entomology*, *113*, 2061-2068.

Tay, J. W., Hoddle, M. S., Mulchandani, A., & Choe, D. H. (2017). Development of an alginate hydrogel to deliver aqueous bait for pest ant management. *Pest Management Science*, *73*, 2028-2038.

Thivya, P., Akalya, S., & Sinija, V. R. (2022). A comprehensive review on cellulose-based hydrogel and its potential application in the food industry. *Applied Food Research*, *2*, 100161-100171.

Tholiban, D., Tharazi, I., Sulong, A. B., Muhamad, N., Ismail, N. F., Radzi, M. K. F. M., Radzuan, N. A. M., & Hui, D. (2019). Kenaf fiber composites: a review on synthetic and biodegradable polymer matrix. *Jurnal Kejuruteraan*, *31*, 65-76.

Tian, C., Sun, M. X., Zhou, X., Li, J., Xie, G. X., Yang, X. D., & Peng, J. W. (2022). Increased in yield and nitrogen use efficiency of double rice with long-term application of controlled release urea. *Journal of Integrative Agriculture*, *21*, 2106-2118.

Tm, S., Thakur, N., & Sharma, P. (2020). Use of alternative growing media in ornamental plants. *International Journal of Chemical Studies*, *8*, 188-194.

Tredenick, E. C., Farrell, T. W., & Forster, W. A. (2019). Mathematical modelling of hydrophilic ionic fertiliser diffusion in plant cuticles: lipophilic surfactant effects. *Plants*, *8*, 202-222.

Treesuppharat, W., Rojanapanthu, P., Siangsanoh, C., Manuspiya, H., & Ummartyotin, S. (2017). Synthesis and characterization of bacterial cellulose and gelatin-based hydrogel composites for drug delivery systems. *Biotechnology Reports*, *15*, 84-91.

Trenkel, M.E. (2010). Slow-and controlled-release and stabilised fertilizers: an option for enhancing nutrient use efficiency in agriculture. 2nd ed. Paris, France: International Fertilizer Industry Association (IFA).

Tuan Mahamood, N. F. A., Halim, A. H. A., & Zainuddin, N. (2021). Carboxymethyl cellulose hydrogel from biomass waste of oil palm empty fruit bunch using calcium chloride as crosslinking agent. *Polymers*, *13*, 4056-4072.

Tudi, M., Ruan, H. D., Wang, L., Lyu, J., Sadler, S., Connell, D., Chu, C., & Phung, D. T. (2021). Agricultural development, pesticides application and its impact on the environment. *International Journal of Environmental Research and Public Health*, *18*, 1112-1134.

Ul-Islam, M., Ahmad, F., Fatima, A., Shah, N., Yasir, S., Ahmad, M. W., Manan, S., & Ullah, M. W. (2021). Ex situ synthesis and characterization of high strength multipurpose bacterial cellulose-aloe vera hydrogels. *Frontiers in Bioengineering and Biotechnology*, *9*, 601988-601999.

Ullah, F., Othman, M. B. H., Javed, F., Ahmad, Z., & Akil, H. M. (2015). Classification, processing and application of hydrogels: A review. *Materials Science and Engineering C*, *57*, 414-433.

Vakal, V., Pavlenko, I., Vakal, S., Hurets, L., Ochowiak, M. (2020). Mathematical modelling of nutrient released from capsulated fertilizer. *Periodica Polytechnica Chemical Engineering*, *64*, 562-568.

Valente, A. J. M., Cruz, S. M. A., Morán, M. C., Murtinho, D. B., Muniz, E. C., & Miguel, M. G. (2010). Release of DNA from cryogel PVA-DNA membranes. *eXPRESS Polymer Letters*, *4*, 480-487.

Varghese, S. J., Surendran, S., Pillai, A. B., Rajendran, K., & Kitoh, A. (2020). Future changes in rice yield over Kerala using climate change scenario from high resolution global climate model projection. Journal of Earth Science System. Doi: https://doi.org/10.1007/s12040-020-01459-0

Verma, A. K., Sindhu, S. S., Anand, P., Singh, A., Chauhan, V. B. S., & Verma, S. K. (2018). Vermi products and biodegradable superabsorbent polymer improve physiological activities and leaf nutrient contents of gerbera. *Research Journal of Biotechnology*, *13*, 8-18.

Versino, F., Urriza, M., & Garcia, M. A. (2019). Eco-compatible cassava starch films for fertilizer controlled-release. *International Journal of Biological Macromolecules*, *134*, 302-307.

Voon, L.K., Cem, S., Pang, S.C., & Chin, S.F. (2016). Highly porous cellulose beads of controllable sizes derived from egenerated cellulose of printed paper wastes. *Material Letters*, *164*, 264-266.

Wali, A. I., Shaban, A. M., & Bakry, A. B. (2019). Utilization of hydrogel for reducing water irrigation quantities on two wheat cultivars grown under sandy soil conditions field crops. *International Journal of Water Resources and Arid Environment*, *8*, 15-22.

Wang, B., Zhou, G., Guo, S., Li, X., Yuan, J., & Hu, A. (2022). Improving nitrogen use efficiency in rice for sustainable agriculture: strategies and future perspectives. *Life (Basel)*, *12*, 1653-1666.

Wang, C, Bai, J., Tian, P., Xie, R., Duan, Z., Lv, Q., & Tao, Y. (2021). The application status of nanoscale cellulose-based hydrogels in tissue engineering and regenerative biomedicine. *Frontiers in Bioengineering and Biotechnology*, *9*, 732513-732531.

Wang, J., Qiu, Y., Zhang, X., Zhou, Z., Han, X., Zhou, Y., Qin, L., Liu, K., Li, S., Wang, W., Chen, Y., Yang, J., & Liu, L. (2023). Increasing basal nitrogen fertilizer rate improved grain yield, quality and 2-acetyl-1-pyrroline in rice under wheat straw returning. *Frontiers in Plant Science*, *10*, 1-17.

Wang, L., Xue, C., Pan, X., Chen, F., & Liu, Y. (2018). Application of controlled-release urea enhances grain yield and nitrogen use efficiency in irrigated rice in Yangtze River Basin, China. *Frontiers in Plant Science*, *9(999)*, 1-13.

Wang, S., Alva, A. K., Li, Y., & Zhang, M. (2011). A rapid technique for prediction of nutrient release from polymer coated controlled release fertilizers. *Open Journal of Soil Science*, *1*, 40-44.

Wang, X., Yao, Y., Chen, B., Zhang, M., Liu, Z., Wang, Q., & Ma, J. (2021). Paecilomyces variotii extracts and controlled-release urea synergistically increased nitrogen use efficiency and rice yield. *ACS Omega*, *5*, 13303-13311.

Wang, Y., Lu, J., Ren, T., Hussain, S., Guo, C., Wang, S., Cong, R., & Li, X. (2017). Effects of nitrogen and tiller type on grain yield and physiological responses in rice. *AoB Plants*, *9*, 1-14.

Wang, Y., Shaghaleh, H., Hamoud, Y. A., Zhang, S., Li, P., Xu, X., & Liu, H. (2021). Synthesis of a pH-responsive nano-cellulose/sodium alginate/MOFs hydrogel and its application in the regulation of water and N-fertilizer. *International Journal of Biological Macromolecules*, *187*, 262-271.

Watcharamul, S., Lerddamrongchai, S., Siripongpreda, T., Rodtassana, C., Nuisin, R., & Kiatkamjornwong, S. (2022). Effects of carboxymethyl cellulose/nano-calcium carbonate hydrogel amendment of loamy sand soil for maize growth. *ACS Agricultural Science & Technology*, *2*, 1071-1080.

Wei, H., Wang, H., Chu, H., & Li, J. (2019). Preparation and characterization of slow-release and water-retention fertilizer based on starch and halloysite. *International Journal of Biological Macromolecules*, *133*,1210-1218.

Wei, P., Chen, W., Song, Q., Wu, Y., & Yu, Y. (2021). Superabsorbent hydrogels enhanced by quarternized tunicate cellulose nanocrystals with adjustable strength and swelling ratio. *Cellulose*, *28*, 3723-3732.

Wen, P., Han, Y., Wu, Z., He, Y., Ye, B. C., & Wang, J. (2017). Rapid synthesis of a corncob- based semi-penetrating polymer network slow-release nitrogen fertilizer by microwave irradiation to control water and nutrient losses. *Arabian Journal of Chemistry*, *10*, 922-934.

Wiangsamut, B., Lafarge, T.A., Mendoza, T.C., & Pasuquin, E.M. (2013). Agronomic traits and yield components associated with broadcasted and transplanted high yielding rice genotypes. *eSci Journal of Crop Production, 02*, 19-30.

Wlodarczyk, M. (2014). Influence of formulation on mobility of metazachlor in soil. *Environmental Monitoring and Assessment, 186*, 3503-3509.

Wlodarczyk, M., & Siwek, H. (2016). Influence of formulation on mobility of clomazone in soil. *Bulletin of Environmental Contamination and Toxicology, 97*, 582-587.

Wróblewska, K., Chohura, P., Lejcuś, K., Dąbrowska, J., & Bąbelewski, P. (2018). Water absorbing geocomposite: a novel method improving water and fertilizer efficiency in Brunnera macrophylla cultivation. Part II. Properties of the medium and microelement uptake effiency. *Acta Scientiarium Polonorum Hortorum Coltus*, *17*, 57-63.

Wu, W., Nie, L., Liao, Y., Shah, F., Cui, K., Wang, Q., Lian, Y., & Huang, J. (2013). Towards yield improvement of early season rice: other options under double rice-cropping system in central China. *European Journal of Agronomy, 45*, 75-86.

Wuana, R. A., & Okieimen, F. E. (2011). Heavy metals in contaminated soils: a review of sources, chemistry, risks and best available strategies for remediation. *ISRN Ecology, 2011*, 1-20.

Xiang, Y., Zhang, G., Chen, C., Liu, B., Cai, D., & Wu, Z. (2018). Fabrication of a pH responsively controlled release pesticides using an attapulgite-based hydrogel. *ACS Sustainable Chemistry & Engineering*, *6*, 1192-1201.

Xiao, M., Hu, J., & Zhang, L. (2014). Synthesis and swelling behavior of biodegradable cellulose-based hydrogels. *Advanced Materials Research, 1033-1034*, 352-356.

Xiaoyu, N., Yuejin, W., Zhengyan, W., Lin, W., Guannan, Q., & Lixiang, Y. (2013). A novel slow-release urea fertilizer: physical and chemical analysis of its structure and study of its release mechanism. *Biosystems Engineering, 115*, 274-282.

Xin, H. (2022). Double-network tough hydrogels: A brief review on achievements and challenges. *Gels*, *8*, 247-258.

Xiong, D., Chen, J., Yu, T., Gao, W., Ling, X., Li, Y., Peng, S., & Huang, J. (2015). SPAD-based leaf nitrogen estimation is impacted by environmental factors and crop leaf characteristics. *Science Reports*, *5*, 13389-13400.

Xu, C., Cao, L., Bilal, M., Cao, C., Zhao, P., Zhang, H., & Huang, Q. (2021). Multifunctional manganese-based carboxymethyl chitosan hydrogels for pH-triggered pesticide release and enhanced fungicidal activity. *Carbohydrate Polymers*, *262*, 117933-117943.

Xu, H., Yeum, K. J., Yoon, Y. H., & Ju, J. H. (2018). Effect of hydrophilic polymer in three green roof substrates on growth, flower development, and overwintering of *Agastache rugosa* (Korean mint) without irrigation. *Applied Ecology and Environmental Research*, *16*, 5503-5516.

Xu, R., Ma, S., Lin, P., Yu, B., Zhou, F., & Liu, W. (2018). High strength astringent hydrogels using protein as the building block for physically cross-linked multi-network. *ACS Applied Materials & Interfaces*, *10*, 7593-7601.

Yadav, I. C., Devi, N. L., Syed, J. H., Cheng, Z., Li, Z., Zhang, G., & Jones, K. C. (2015). Current status of persistent organic pesticides residues in air, water, and soil, and their possible effect on neighboring countries. A comprehensive review of India. *Science of the Total Environment, 511*, 123-137.

Yan, J., Wu, Q., Qi, D., & Zhu, J. (2022). Rice yield, water productivity, and nitrogen use efficiency responses to nitrogen management strategies under supplementary irrigation for rain-fed rice cultivation. *Agricultural Water Management, 263*, 107486-107496.

Yang, Q., Gao, C., Zhang, X., Tsou, C., Zhao, X., De Guzman, M. R., Pu, Z., Li, X., Lu, Y., & Zeng, C., Yuan, L., Xia, Y., Sheng, Y., & Fu, Y. (2021). A dual physical cross-linking strategy to construct tough hydrogels with strength, excellent fatigue resistance, and stretching-induced strengthening effect. *Macro-molecular Materials and Engineering*, *306*, 1-11.

Yang, S., Fu, S., Li, X., Zhou, Y., & Zhan, H. (2010). Preparation of salt-sensitive and antibacterial hydrogel based on quaternized cellulose. *BioResouces*, *5*, 1114-1125.

Yang, X., & You, X. (2013). Estimating parameter of van genuchten model for soil water retention curve by intelligent algorithms. *Applied Mathematics & International Science*, *7*, 1977-1983.

Yang, Y., Zhang, M., Li, Y.C., Fan, X., & Geng, Y. (2012). Controlled release urea improved nitrogen use efficiency, activities of leaf enzymes, and rice yields. *Soil Science Society of America Journal*, *76*, 2307-2318.

Yang, Y., Zhou, M., Peng, J., Wang, X., Liu, Y., Wang, W., & Wu, D. (2022). Robust, anti-freezing and conductive bonding of chitosan-based double-network hydrogels for stable-performance flexible electronic. *Carbohydrate Polymers*, *276*, 118753-118763.

Yao, F., Huang, J., Cui, K., Nie, L., Xiang, J., Liu, X., Wu, W., Chen, M., & Peng, S. (2012). Agronomic performance of high-yielding rice variety grown under alternate wetting and drying irrigation. *Field Crops Research*, *126*, 16-22.

Ye, C., Ma, H., Huang, X., Xu, C., Chen, S., Chu, G., Zhang, X., & Wang, D. (2022). Effects of increasing panicle-stage N on yield and N use efficiency of indica rice and its relationship with soil fertility. *The Crop Journal*, *10*, 1784-1797.

Yi, J., Gao, J., Zhang, W., Zhao, C., Wang, Y., & Zhen, X. (2019). Differential uptake and utilization of two forms of nitrogen in japonica rice cultivars from north-eastern china. *Frontiers in Plant Science*, *10*, 1-11.

Yi, Z. X., Wang, P., Zhang, H.F., Shen, L.X., Liu, M., & Dai, M.H. (2006). Effects of type and application rate of nitrogen fertilizer on source-sink relationship sin summer maize in North China Plain. *Plant Nutrition and Fertilizer Science*, *12*, 294-300.

Yiau, C. N. (2023, November 6). *Govt targets rice self-sufficiency ratio of 75% by 2025, 80% by 2030.* The Edge Malaysia. https://theedgemalaysia.com/node/688941#:~:text=KUALA%20LUMPUR%20(Nov%206)%3A,at%2062.6%25%20as%20of%202022

Yong, Z. J., Bashir, M. J. K., Ng, C. A., Sethupathi, S., Lim, J. W., & Show, P. L. (2019). Sustainable waste-to-energy development in Malaysia: appraisal of environmental, financial, public issues related with energy recovery from municipal solid waste. *Processes*, *7*, 676-704.

Yuan, M., Sun, Y., Wang, J., Wu, G., Hu, P., Zhang, X., Wang, W., & Jing, Y. (2021). Application of controlled-release compound fertilizer to mechanically dry direct-seeded rice increased rice biomass, nutrient accumulation and yield. *Journal of Plant Nutrition*, *46*, 300-311.

Yuan, N., Xu, L., Wang, H., Fu, Y., Zhang, Z., Liu, L., Wang, C. L., Zhao, J. H., & Rong, J. H. (2016). Dual physically cross-linked double network hydrogels with high mechanical strength, fatigue resistance, notch-insensitivity, and self-healing properties. *ACS Applied Materials & Interfaces*, *8*, 34034-34044.

Zainal, S. H., Mohd, N. H., Suhaili, N., Anuar, F. H., Lazim, A. M., & Othaman, R. (2021). Preparation of cellulose-based hydrogel: A review. *Journals of Materials Research and Technology*, *10*, 935-952.

Zainal, S. H., Nofrianti, R., Lazim, A. M., & Othaman, R. (2019). Cellulose-based hydrogel as halal agricultural medium. *Malaysian Applied Biology*, *48*, 109-113.

Zainol Abidin, S. A. (2023). *Sociological Issues and Challenges of Rice Production in Malaysia*. Food and Fertilizer Technology Center for the Asian and Pacific Region. https://ap.fftc.org.tw/article/3473#:~:text=Statistics%20from%20the%20Department%20of,around%2011.3%25%20within%20six%20years

Zakaria, M. B., & Ghani, N. A. R. N. A. (2022). An analysis of rice supply in Malaysia post Covid-19 – from an agriculture-related fiqh perspective. *International Journal of Academic Research in Accounting Finance and Management Science*, *12(2)*, 150-160.

Zanin, G., Maucieri, D., Ferro, N. D., Bortolini, L., & Borin, M. (2020). Evaluating a controlled-release fertilizer for plant establishment in floating elements for bioretention ponds. *Agronomy*, *10*, 199-213.

Zhang, H., Yang, M., Luan, Q., Tang, H., Huang, F., Xiang, X., Yang, C., & Bao, Y. (2017). Cellulose anionic hydrogels based on cellulose nanofibers as natural stimulants for seed germination and seedling growth. *Journal of Agricultural and Food Chemistry*, *65*, 3785-3791.

Zhang, J., Tong, T., Potcho, P.M., Huang, S., Ma, L., & Tang, X. (2020). Nitrogen effects on yield, quality and physiological characteristics of giant rice. *Agronomy*, *10*, 1816-1831.

Zhang, X., Liu, Y., Lu, P., & Zhang, M. (2020). Preparation and properties of hydrogel based on sawdust cellulose for environmentally friendly slow release fertilizer. *Green Processing and Synthesis*, *9*, 139-152.

Zhang, Y., & Huang, Y. (2020). Rational design of smart hydrogels for biomedical applications. *Frontiers in Chemistry*, *8*, 615665-615675.

Zhang, Z., Rod, M., & Hosseinian, F. A. (2020). A comprehensive review on sustainable industrial vertical farming using film farming technology. *Sustainable Agriculture Research*, *10*, 46-53.

Zhang, Z., Zhu, J., Song, X., Wen, Y., Zhu, C., & Li, J. (2023). Biomass-based single- and double-network hydrogels derived from cellulose microfiber and chitosan for potential application as plant growing substrate. *Carbohydrate Polymers*, *319*, 121170-121180.

Zhao, B., Dong, S., Zhang, J., & Liu, P. (2013). Effects of controlled-release fertilizer on nitrogen use efficiency in summer maize. *PLoS ONE*, *8*, 1-9.

Zhao, C., Gao, Z., Liu, G., Chen, Y., Ni, W., Lu, J., Shi, Y., Qian, Z., Wang, W., & Huo, Z. (2023). Combining controlled-release urea and normal urea to improve the yield, nitrogen use efficiency, and grain quality of single season late *Japonica* rice. *Agronomy*, *13*, 276-289.

Zheng, T., Liang, Y., Ye, S., & He, Z. (2009). Superabsorbent hydrogels as carriers for the controlled-release of urea: experiments and a mathematical model describing the release rate. *Biosystem Engineering*, *102*, 44-50.

Zhu, S. Liu, L., Xu, Y., Yang, Y., & Shi, R. (2020). Application of controlled release urea improved grain yield and nitrogen use efficiency: a meta-analysis. *PLoS ONE*, *15*, 1-15.

LIST OF PUBLICATIONS

Ahmad *et al. Chem. Biol. Technol. Agric.* (2023) 10:36
https://doi.org/10.1186/s40538-023-00407-6

Chemical and Biological Technologies in Agriculture

RESEARCH Open Access

Eco-friendly cellulose-based hydrogels derived from wastepapers as a controlled-release fertilizer

Dayang Fazirah Binyi Abg Ahmad[1], Mohd Effendi Wasli[1], Cindy Soo Yun Tan[2], Zaki Musa[3] and Suk-Fun Chin[1*]

Abstract

In this study, an eco-friendly controlled release fertilizer cellulose-based hydrogel was prepared from cellulose fibers derived from wastepaper, epichlorohydrin (ECH) as a crosslinker and carboxy methyl cellulose (CMC) as a gelling agent. A maximum swelling capacity of 2000% was achieved for cellulose hydrogel with optimum composition. The soil moisture contents in the presence of optimized cellulose hydrogels were determined using the digital moisture meter. Maximum soil moisture of 36.5% was obtained in topsoil, followed by 30.1% in wet clayey soil and 23.4% in sandy soil after 7 days. Urea as a model fertilizer was loaded onto the cellulose hydrogels to control the release of fertilizer. The maximum loading capacity of urea in cellulose hydrogel is 0.51 g/g. The urea-controlled release profiles of the cellulose hydrogel in distilled water and various types of soils were investigated. The formulation of cellulose hydrogels was observed to facilitate the gradual release of urea, with about 74.71% release in topsoil, 73.37% release in wet clayey soil and 71.84% release in sandy soil within 42 days when compared to the free urea which was about 97.32%, 95.09% and 98.47% release in topsoil, wet clayey soils and sandy soils, respectively within 7 days. The result of this study shows that the urea-loaded cellulose hydrogel could be a promising controlled-release fertilizer.

Keywords Controlled-release fertilizers, Carboxymtehyl cellulose, Swelling ratio, Water retention, Sustainable agriculture

*Correspondence:
Suk-Fun Chin
sfchin@unimas.my
Full list of author information is available at the end of the article

Springer Open

© The Author(s) 2023. **Open Access** This article is licensed under a Creative Commons Attribution 4.0 International License, which permits use, sharing, adaptation, distribution and reproduction in any medium or format, as long as you give appropriate credit to the original author(s) and the source, provide a link to the Creative Commons licence, and indicate if changes were made. The images or other third party material in this article are included in the article's Creative Commons licence, unless indicated otherwise in a credit line to the material. If material is not included in the article's Creative Commons licence and your intended use is not permitted by statutory regulation or exceeds the permitted use, you will need to obtain permission directly from the copyright holder. To view a copy of this licence, visit http://creativecommons.org/licenses/by/4.0/. The Creative Commons Public Domain Dedication waiver (http://creativecommons.org/publicdomain/zero/1.0/) applies to the data made available in this article, unless otherwise stated in a credit line to the data.

scientific reports

Check for updates

OPEN

Eco-friendly cellulose hydrogels as controlled release fertilizer for enhanced growth and yield of upland rice

Dayang Fazirah Binti Abg Ahmad[1], Mohd Effendi Wasli[1], Cindy Soo Yun Tan[2], Zaki Musa[3] & Suk-Fun Chin[1]✉

The effect of urea-loaded cellulose hydrogel, a controlled-release fertilizer (CRF) on growth and yield of upland rice were investigated in upland rice. As with the initial research, nitrogen (N) treatments were applied as CRF treatments; T2H (30 kg N ha^{-1}), T3H (60 kg N ha^{-1}), T4H (90 kg N ha^{-1}), T5H (120 kg N ha^{-1}) and recommended dose of fertilizer (RDF) at 120 kg N ha^{-1} RDF (T6U) in split application and T1 (0 N) as control. Results from this study indicated that applying CRF at the optimum N rate, T4H resulted in maximum grain yield, increasing by 71%. The analysis of yield components revealed that higher grain yield in T4H CRF was associated with an increase in panicle number and number of grains per panicle. Maximum grain N uptake of 0.25 g kg^{-1} was also observed in T4H CRF. In addition, T4H CRF recorded the highest harvest index (HI) and N harvest index (NHI) of 45.5% and 67.9%, respectively. Application of T4H CRF also recorded the highest N use efficiency (NUE) and N agronomic efficiency (NAE), 52.6% and 12.8 kg kg^{-1}, respectively. Observations show that CRF with only 75% N applied (T4H) in soil improved grain yield when compared to CRF with 100% N and 100% RDF in farmers' conventional split application. This suggested that CRF with a moderate N application might produce the highest potential yield and improved N efficiencies while enhancing crop production and further increase in N supply did not increase yield and N efficiencies. The results suggest that the application of T4H CRF for upland rice would enhance HI, N efficiencies and improve the yield of upland rice. Also, all growth parameters and yield were positively influenced by the application of CRF as a basal dose compared to split application of conventional urea fertilizers.

Rice (*Oryza sativa* L.) is one of the basic staple foods for more than 3 billion people worldwide. Over two billion people in Asia consume rice and rice-derived products for 60–70% of their energy needs[1,2]. Rice is a staple food for Malaysians of all socioeconomic background. In Malaysia, rice is the main food crop which occupied an area of 685,548 hectares with a production of approximately 2.57 million tons in 2017 but decreased to 2.34 million tons in 2020[3,4]. The self-sufficiency level in Malaysia for rice hovered around 70% from 2008 to 2017[5]. In line with the National Agricultural Policy, the government wishes to increase the rice self-sufficiency level up to 75% by 2025 to ensure food security for people[5]. Meanwhile, in Sarawak, the rice self-sufficiency level was only 38%, while the rest was imported from other countries[6]. The rice self-sufficiency level is significantly low that the Sarawak government has targeted increasing the rice self-sufficiency to 60% by 2030[6,7].

The increase of rice production can be achieved by efficient and good agricultural practices, water[8] and fertilizer inputs[9,10]. However, poor management of plant nutrients and ignorance of the Liebig's Law of Minimum serves as a hurdle in increasing rice production[11]. Most farmers apply conventional fertilizers; it was found that the efficiency of plant uptake of the conventional fertilizers applied is below 50%[12]. Some of the contributory factors that lead to nutrient deficiencies found in crops are due to losses through heavy leaching, surface runoff, reaction with organic compounds in the soils, vaporization and volatilization[13–15]. Better fertilizer management is required as it is known that long-term cropping will alter the availability of soil nutrients[16,17]. A promising strategy to overcome these challenges is the encapsulation of fertilizers in superabsorbent hydrogels

[1]Faculty of Resource Science and Technology, Universiti Malaysia Sarawak, 94300 Kota Samarahan, Sarawak, Malaysia. [2]Faculty of Applied Science, Universiti Teknologi MARA, 94300 Kota Samarahan, Sarawak, Malaysia. [3]Malaysian Agricultural Research and Development Institute (MARDI), Jalan Santubong, Petra Jaya, 93050 Kuching, Sarawak, Malaysia. ✉email: sfchin@unimas.my

APPENDICES

Appendix 1: Kjeldahl Procedure and the Nessler Method

Objectives:

To determine the available nitrogen in the water and soil sample by Kjeldahl procedure and the Nessler method.

Introduction:

The test for Kjedahl nitrogen, also referred to as crude protein, is used to determine ammonia and organic nitrogen present in a sample. Only small fractions of nitrite and nitrate nitrogen are included in the test. A preliminary digestion is used to oxidize carbon compounds to carbon dioxide, and to convert organic forms of any nitrogen present (amino acidsn proteins, peptides) to ammonia. The traditional digestion uses sulfuric acid and various combinations of metallic catalysts and salts. Digestion of at least 2 hours is followed by addition of sodium hydroxide to the digest and then distillation of the ammonia into a boric acid or buffer solution. Ammonia in the distillate is measured with the back titration or nesslerization. This procedure requires several hours for reagent preparation, digestion, distillation, and final measurement.

The Hach Digesdahl Digestion Apparatus and the Peroxide Digestion Method allow completion of the Kjeldahl test within 15 minutes, depending on the nature of the sample. First, the sample is charred in the concentrated sulfuric acid. 50 % hydrogen peroxide is fed into the reaction mixture, where it oxidizes organic carbonaceous matter and converts organic nitrogen into ammonium bisulphate.

Digestion apparatus

The Digesdahl Digestion Apparatus includes a fractioning column. Hydrogen peroxide, added slowly, trickles into the reaction mixture in the flask. The temperature of the reaction is maintained near the boiling point of sulphuric acid (300 °C). vapours from the reaction rise to the column where SO_2 and water vapours are drawn off by an aspirator. Hydrogen peroxide vapours condense in the column and return to the reaction mixture.

It should be noted that no metal catalysts or salts are used in the digestion. The digest is suitable for nesslerization for final measurement without an intermediate distillation step. The digest is also suitable for mineral analysis of Ca, Mg, Mn, K, P, and Zn. See Nitrogen, Ammonia for more information about the Nessler method.

Significance of Soil Analysis:

1. It increases the knowledge of what nutrients are especially available in our soil.
2. It reduces the environmental impacts due to soil amendments.
3. It increases the efficiency of resource inputs such as fertilisers and water.
4. It helps to predict the nutritional values needed for crop production.
5. It helps to evaluate the fertility status of soils of a country or a state or a district.

Procedure for Taking Good Soil Samples:

1. Determine the soil unit (or plot).
2. Make a traverse over the soil unit (or plot).
3. Clean the site (with spade) from where soil sample is to be collected.
4. Insert the spade into soil.
5. Standing on the opposite side, again insert the spade into soil.
6. A lump of soil is removed.

7. A pit of ‘V’ shape is formed. Its depth should be 0-6" or 0-9" or 0-12" (i.e., Depth of tillage).
8. Take out the soil-slice (like a bread slice) of ½ inch thick from both the exposed surface of the pit from top to bottom. This slice is also termed furrow-slice. To collect the soil-slice spade may be used. Collect the soil samples in a polyethylene bucket.
9. Collect furrow-slices from 8-10 or sometimes 20-30 sites. Select the sites at random in a zigzag (or criss-cross) manner. Distribute the sites throughout the entire soil unit (plot). In lieu of spade auger may be used. Do not take the prohibited samples and local problem soils.
10. Furnish the following information in two sheets of thick paper with the sample. One sheet is folded and kept inside the bag. Another sheet is folded and attached to the bag.

Apparatus:

Kjeldahl Digestion Assembly, Ammonia Distillation Assembly.

Principle:

The Kjeldahl method permits the available nitrogen to be precisely determined in the plant and in the soil. The method of determination involves three successive phases which are,

1. Digestion of the organic material to convert nitrogen into HNO_3.
2. Distillation of the released Ammonia into an absorbing surface or medium.
3. Volumetric analysis of the Ammonia formed during the digestion process.

Digestion:

Digestion of the organic material is carried out by digesting the sample with Con. H_2SO_4 in the presence of $CuSO_4.H_2O$ as a catalyst and K_2SO_4 which raise the digestion temperature. The organic material decomposes into several components, i.e.,

$C \rightarrow CO_2$, $O \rightarrow H_2O$ and $N \rightarrow NH_3$

In the organic matter, some nitrates are present, most of which are lost during the digestion. The loss may be disregarded for most soils. Since the amount of NO_3^- - N is far lesser than the Organic Nitrogen.

$2\ C_6H_3\ (OH)\ NH_2COO + 26\ H_2SO_4 \rightarrow (NH_4)_2SO_4 + 25\ SO_2 + 14\ CO_2 + 28H_2O$

Distillation:

The Ammonia content of the digest is determined by distillation with excess NaOH and absorption of the evolved NH_3 is in standard HCl.

$(NH_4)_2SO_4 + 2\ NaOH \rightarrow Na_2SO_4 + 2\ NH_3 + 2\ H_2O$

$NH_3 + HCl \rightarrow NH_4Cl$

Volumetric Analysis:

The excess of standard HCl is titrated against standard NaOH using Methyl Red as an indicator. The decrease in the multi equivalence of acid as determined by acid-base titration, which gives a measure of the N content of the sample. The end point is determined by a change of colour from pink to yellow.

$2\ HCl + 2\ NaOH \rightarrow 2\ NaCl + H_2O$

Significance:

The chemical analysis of the soil for nitrogen is less precise when the requirement for this element needs to be forecast over a longer period of time, as they vary not only with species, but with the phase of growth and season as well. Therefore the chemical test for NO_3^- and $NH4^+$signifies the momentary status when the sample is taken and measures must be taken instantaneously. The analysis of the extractableNitrogen content of the soil using a given extractable method.

In reaction to crop response study provides a basis of Nitrogen fertility levels, which will rationalize the use efficiency of Nitrogen fertilizer content of the soil are also needed for the

evaluation of C-N ratios of soils which give an indication of the process of transformation of organic Nitrogen to available Nitrogen like ammoniated nitrate Nitrogen.

Procedure:

a. Digestion of Water and Soil:

1. Water and soil sample were taken and placed in a 500 mL Kjeldahl flask.
2. 30 mL of concentrated sulphuric acid (H_2SO_4), 10 mL of hydrogen peroxide (H_2O_2), and 2 boiling chips were added into the Kjeldahl flask containing soil sample.
3. The mixture in the Kjeldahl flask was mixed well and allowed to stand for at least 30 minutes with frequent shaking or until complete solution results.
4. The solution was digested at 450-500 °C using Kjeldahl digestion apparatus in a fume hood. The solution was digested until greenish colour of the solution (upon heating) turns clear.
5. After, the digested sample was cooled to room temperature and transferred into a 100 mL conical flask. The digested solution was diluted with distilled water until 100 mL. The solution was shaken and mixed well.
6. The digested solution sometimes contain impurities and appeared yellowish. The solution was filtered using filtered paper several times until the solution turned clear.

b. The Nessler Method

The digested solution (from no. 6 in step a) was used in the Nessler method.

Instrument – specific information

Table 1 shows all of the instruments that have the program for this test. The table also shows sample cell and orientation requirements for specific instruments.

To use the table, select an instrument, then read across to find the applicable information for this test.

Table 1: Instrument – specific information

Instrument	Sample cell orientation	Sample cell
DR 6000 DR 3800 DR2800 DR 2700 DR 1900	The fine line is to the right	2495402 
DR 5000 DR 3900	The fill line is toward the user	
DR 900	The orientation mark is towards the user	2401906 

Before starting

Hach no longer offers the Digesdahl Digestion Apparatus. Hach does offer an EPA approved method for TKN following the TKN method using TNT880.
Install the instrument cap on the DR 900 cell holder before ZERO or READ is pushed
For the best results, measure the reagent blank value for each new lot of reagent. Replace the sample with deionized water in the test procedure to determine the reagent blank value. Subtract the reagent blank value from the sample results automatically with the reagent blank adjust option.
If the Pour-Thru Cell is used (for applicable instruments), clean the cell periodically. Pour a few sodium thiosulphate pentahydrate crystals into the cell funnel or rinse the cell with a solution of sodium thiosulphate. Flush the crystals through the funnel and cell with enough deionized water to dissolve. Rinse the cell with deionized water.
The Nessler reagent contains mercuric iodide. Both the reacted sample and blank will contain mercury. Do not pour these solutions down the drain. Collect the reacted samples and the blank for proper disposal.
Hold the reagent droppers and dropper bottles vertically, not at an angle, when the reagent is added.
Use the standard adjust option with each new lot of reagent for the best results. Refer to the standard solution method in accuracy check.
Review the Safety Data Sheets (MSDS/SDS) for the chemicals that are used. Use the recommended personal protective equipment.
Dispose of reacted solutions according to local, state and federal regulations. Refer to the Safety Data Sheets for disposal information for used reagents. Refer to the environmental, health and safety staff for your facility and/or local regulatory agencies for further disposal information.

Items to collect

Description	Quantity
Boiling chips, silicon carbide	2-2
Cylinder, graduated mixing, 25 mL	2
Finger cots	2
Digesdahl Digestion Apparatus (Obsolete, no replacement available)	1
Safety shield	1
Hydrogen Peroxide, 50 %	20 mL
Mineral Stabilizer	6 drops
Nessler Reagent	2 mL
Polyvinyl Alcohol Dispersing Agent	6 drops
Potassium Hydroxide (KOH) Standard Solution, 1.0 N	Varies
Potassium Hydroxide (KOH) Standard Solution, 8.0 N	Varies
Sulfuric Acid, ACS, concentrated	6 mL
TKN Indicator Solution	2 drops
Pipette, TenSette, 0.1 – 1.0 mL, plus tips	1
Sample cells	2

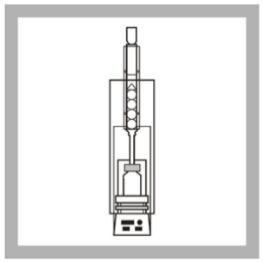
Sample collection and storage

1. samples were collected in clean glass or plastic bottles.
2. If the sample contains chlorine, one drop of 1.0 N sodium thiosulfate was added for each 0.3 mg/L chlorine in 1 L of sample.
3. To preserve samples for later analysis, the sample pH was adjusted to less than 2 with concentrated H_2SO_4 (approximately 2 mL per L). no acid addition is necessary if the sample is tested immediately.
4. The preserved samples were kept at or below 6 °C (43 °F) for a maximum of 28 days.
5. The sample temperature was allowed to increase to room temperature before analysis.
6. Before analysis, the pH was adjusted to ~7 with 5 N sodium hydroxide solution.
7. The test result was corrected for the dilution caused by the volume additions.

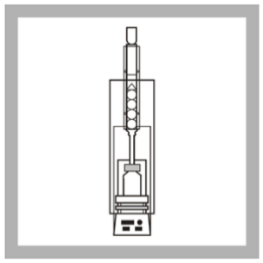
Test procedure



1. Program 399 N, TKN was started.



2. The sample was prepared. The Digesdahl Digestion Apparatus Instruction Manual was used to digest the sample amount.



3. The blank was prepared. An amount of deionized water was digested for use as the blank.



4. A pipette was used to move an analysis volume of the digested sample to a graduated mixing cylinder.



5. A pipette was used to transfer an equal amount of digested deionized water ta a second graduated cylinder.



6. 1 drop of TKN indicator was added to each cylinder.



7. If the aliquot is less than 1 mL, go to step 8. If the aliquot is greater than 1 mL, drops of 8.0 KOH must be added to each cylinder until the first flesh of blue colour shows.the stopper was added in the cylinder and inverted after each addition.



8. 1.0 N KOH was added to each cylinder, one drop at a time. The solution was mixed after each addition. The step was continued until the first permanent blue colour shows.



9. Both cylinders were filled to the 20 mL mark with deionized water.



10. Three drops of mineral stabiliser were added to each cylinder.



11. The stoppers were put in the mixing cylinders and inverted to mix.



12. Three drops of polyvinyl alcohol dispersing agent were added to each cylinder.



13. The stoppers were put in the mixing cylinders and inverted to mix.



14. Both cylinders were filled to the 25 mL mark with deionized water.



15. The stoppers were put in the mixing cylinders and inverted to mix.



16. A pipette was used to add 1.0 mL of the Nessler reagent to each cylinder.



17. The stoppers were put in the mixing cylinders and inverted to mix. The solution should not be hazy.



18. The instrument timer was started. A 2 minute reaction was started.



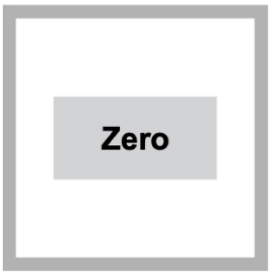
19. When the timer expires, the content of each cylinder was poured into separate sample cells.



20. The blank sample cell was cleaned.



21. The blank was inserted into the cell holder.



22. **ZERO** was pushed. 0 mg/L TKN was shown in the display.



23. The prepared sample was cleaned.



24. The prepared sample was placed into the cell holder.



25. **READ** was pushed. Results were shown in mg/L TKN.



26. The sample TKN was calculated in ppm:

$TKN = (75 \times A) / (B \times C)$

A: mg/L read from display

B: g (or mL of water) sample taken from the digestion

C: mL analysis volume of the digested sample

Digested sample volume

Table 2: Aqueous samples (solutions or suspensions in water – less than 1 % solid

Expected nitrogen concentration (mg/L)	Analysis volume (mL)
0.5 – 26	10
2 – 112	5
11 – 560	2
45 – 2250	1
425 – 22500	0.5

Table 3: Dry samples

Expected nitrogen concentration (mg/L)	Analysis volume (mL)
42 – 2200	10
106 – 5600	5
350 – 18,000	2
1000 – 56,000	1
4200 – 220,000	0.5

Accuracy check

Digestion method

To validate the digestion method, the Primary Standards for Kjeldahl Nitrogen that are given in the Accuracy Check section of the *Digesdahl® Digestion Apparatus Instruction Manual*[2] were used. The accuracy check procedure was used to find the digestion efficiency and the amount of bound nitrogen that is released during digestion.

The digested Kjeldahl standard in the Nessler test procedure was used to measure the TKN of the primary standard. The TKN value should be within ± 3% of the value of the prepared Kjeldahl standard.

Standard solution method

Items to collect:

- 1.0-mg/L NH_3–N standard solution
- TKN indicator
- Dropper
- 25-mL graduated mixing cylinders (2)
- Deionized water
- Mineral Stabilizer
- Polyvinyl Alcohol Dispersing agent

1. **One drop of TKN Indicator was added to each 25-mL graduated mixing cylinder.**

2. **One cylinder was filled to the 20-mL mark with deionized water. The other cylinder was filled to the 20-mL mark with a 1.0-mg/L NH_3–N standard solution.**
3. **3 drops of Mineral Stabilizer was added to each cylinder. The solution was inverted several times to mix.**
4. **3 drops of Polyvinyl Alcohol Dispersing agent was added to each cylinder. The solution was inverted several times to mix.**
5. **The steps were continued with the TKN procedure to measure the concentration of the standard solution. Accurate calibrations will show 26–27 mg/L TKN.**

Note: The factory calibration can be adjusted slightly with the standard adjust option so that the instrument shows the expected value of the standard solution. The adjusted calibration is then used for all test results. This adjustment can increase the test accuracy when there are small variations in the reagents or instruments.

Method performance

The method performance data that follows was derived from laboratory tests that were measured on a spectrophotometer during ideal test conditions. Users can get different results under different test conditions.

Program	Standard	Precision (95 % confidence interval)	Sensitivity (Concentration change per 0.010 Abs Change)
399	76 mg/L NH_3 – N	70 – 82 mg/L NH_3 – N	1 mg/L NH_3 – N

Summary of method

The term Total Kjeldahl Nitrogen refers to the combination of ammonia and organic nitrogen. However, only the organic nitrogen compounds that are present as organically bound nitrogen in the trinegative state are determined in this test. Nitrogen in this form is converted into ammonium salts by the action of sulfuric acid and hydrogen peroxide. The ammonia is then analyzed by a modified Nessler method test. The measurement wavelength is 460 nm for spectrophotometers or 420 nm for colorimeters.

Pollution prevention and waste management

The Nessler reagent contains mercuric iodide. The reacted samples and blanks will contain mercury and must be disposed of as a hazardous waste. Dispose of reacted solutions according to local, state and federal regulations.

Appendix 2: Maximum swelling percentage of cellulose hydrogels at varied concentrations (% w/v) of cellulose fibers.

Cellulose hydrogels	Maximum swelling percentage (%)	Mean	Variance, s^2	Standard Deviation, σ	95 % Confidence Level (Statistical significance of 5 %)
C1	1533.255	1534.633	25.99	5.0978	1534.633 ± 5.769 (± 0.38 %)
	1530.371				
	1540.282				
C2	1885.801	1885.611	21.84	4.6728	1885.611 ± 5.288 (± 0.28 %)
	1890.191				
	1880.854				
C3	2054.072	2055.093	0.87	0.9309	2055.093 ± 1.053 (± 0.05 %)
	2060.151				
	2065.091				

Appendix 2 continued

C4	1701.171	1704.136	27.86	5.2781	1704.127 ± 5.973 (± 0.35 %)
	1710.223				
	1700.972				
C5	1286.123	1285.710	20.47	4.5242	1285.707 ± 5.12 (± 0.4 %)
	1290.014				
	1280.991				

Appendix 3: Maximum swelling percentage of cellulose hydrogels at various concentrations of CMC

Cellulose hydrogels	Maximum swelling percentage (%)	Mean	Variance, s^2	Standard Deviation, σ	95 % Confidence Level (Statistical significance of 5 %)
CMC1.75	2054.019	2055.093	0.87	0.9309	2055.093 ± 1.053 (± 0.05 %)
	2060.158				
	2065.099				
CMC2.0	1072.656	1073.172	2.65	1.6276	1073.173 ± 1.842 (± 0.17 %)
	1071.915				
	1075.018				
CMC2.5	1107.543	1107.600	6.66	2.5815	1107.600 ± 2.921 (± 0.26 %)
	1110.239				
	1105.077				

Appendix 3 continued

CMC3.0	1200.558	1202.953	5.06	2.2501	1202.953 ± 2.546 (± 0.21 %)
	1205.016				
	1203.356				
CMC3.5	1485.452	1484.331	22.48	4.7411	1485.331 ± 5.365 (± 0.36 %)
	1480.534				
	1490.016				
CMC4.0	1685.557	1685.261	24.62	4.9614	1685.261 ± 5.614 (± 0.33 %)
	1690.074				
	1680.167				
CMC4.5	2023.881	2024.030	15.383	3.9221	2024.027 ± 4.438 (± 0.22 %)
	2020.185				
	2028.027				

Appendix 3 continued

CMC5.0	2038.555	2039.041	0.83	0.9099	2039.041 ± 1.03 (± 0.05 %)
	2040.097				
	2038.486				

Appendix 4: Soil moisture content

Cellulose hydrogels		Soil moisture (%)	Mean	Variance, s^2	Standard Deviation, σ	95 % Confidence Level (Statistical significance of 5 %)
With cellulose hydrogel C3	**Topsoil**	36.511	36.497	0.25	0.5001	36.497 ± 0.566 (± 1.55 %)
		35.992				
		36.996				
	Wet clayey soil	30.094	30.133	0.003	0.0577	30.133 ± 0.065 (± 0.22 %)
		30.213				
		30.115				
	Sandy soil	23.421	23.433	0.003	0.0578	23.433 ± 0.065 (± 0.28 %)
		23.533				
		23.412				

Appendix 4 continued

Cellulose hydrogels		Soil moisture (%)	Mean	Variance, s^2	Standard Deviation, σ	95 % Confidence Level (Statistical significance of 5 %)
Without cellulose hydrogel C3	**Topsoil**	28.991	28.826	0.08	0.2743	28.827 ± 0.31 (± 1.08 %)
		28.515				
		28.982				
	Wet clayey soil	24.428	24.642	0.18	0.4219	24.643 ± 0.477 (± 1.94 %)
		24.385				
		25.137				
	Sandy soil	18.913	18.927	0.003	0.0569	18.927 ± 0.064 (± 0.34 %)
		18.9952				
		18.881				

Appendix 5: Loading capacity of cellulose hydrogel C3

Duration (h)	**Loading capacity ($g\ g^{-1}$)**	**Mean**	**Variance, s^2**	**Standard Deviation, σ**	**95 % Confidence Level (Statistical significance of 5 %)**
24	0.382	0.381	3.3333	0.0006	0.381 ± 0.0007 (± 0.17 %)
	0.381				
	0.381				
48	0.511	0.511	0.0002	0.0140	0.509 ± 0.016 (± 3.12 %)
	0.523				
	0.495				
72	0.517	0.514	0.0001	0.0103	0.514 ± 0.0166 (± 2.26 %)
	0.503				
	0.523				

Appendix 5 continued

96	0.517	0.514	0.0003	0.0192	0.514 ± 0.022 (± 4.23 %)
	0.531				
	0.493				
120	0.517	0.515	6.3333	0.0025	0.515 ± 0.003 (± 0.55 %)
	0.512				
	0.515				

Appendix 6: Release behavior of cellulose hydrogel C3 and free urea in water

Duration (days)		Release rate (%)	Mean	Variance, s^2	Standard Deviation, σ	95 % Confidence Level (Statistical significance of 5 %)
Release of free urea in water	**1**	98.702	98.737	1.09	1.0429	98.737 ± 1.18 (± 1.20 %)
		99.797				
		97.712				
	3	98.981	98.558	0.34	0.5822	98.558 ± 0.659 (± 0.67 %)
		98.799				
		97.894				
	5	98.898	98.907	0.02	0.1462	98.907 ± 0.165 (± 0.17 %)
		98.765				
		99.057				

Appendix 6 continued

Release of free urea in water	**7**	98.376	98.566	0.07	0.2699	98.566 ± 0.305 (± 0.31 %)
		98.875				
		98.447				
	11	98.228	98.623	0.53	0.7308	98.624 ± 0.827 (± 0.84 %)
		98.176				
		99.467				
	14	98.845	98.598	0.14	0.3691	98.596 ± 0.418 (± 0.42 %)
		98.172				
		98.771				
	22	97.999	98.527	0.31	0.5570	98.527 ± 0.630 (± 0.64 %)
		98.472				
		99.109				

Appendix 6 continued

Release of free urea in water	**30**	98.099	98.721	0.29	0.5549	98.721 ± 0.617 (± 0.62 %)
		98.941				
		99.166				
	48	98.869	98.867	0.002	0.0485	98.867 ± 0.055 (± 0.06 %)
		98.914				
		98.817				
	60	98.844	98.507	0.23	0.4845	98.507 ± 0.548 (± 0.56 %)
		98.726				
		97.952				
	72	98.772	98.718	0.03	0.1615	98.718 ± 0.183 (± 0.19 %)
		98.845				
		98.536				

Appendix 6 continued

Duration (days)		Release rate (%)	Mean	Variance, s^2	Standard Deviation, σ	95 % Confidence Level (Statistical significance of 5 %)
Release of urea from cellulose hydrogel C3 in water	**1**	50.711	50.767	0.002	0.0494	50.767 ± 0.056 (± 0.11 %)
		50.788				
		50.803				
	3	57.471	57.394	0.007	0.0813	57.394 ± 0.092 (± 0.16 %)
		57.309				
		57.402				
	5	66.099	66.134	0.003	0.0577	66.134 ± 0.065 (± 0.10 %)
		66.103				
		66.201				

Appendix 6 continued

Release of urea from cellulose hydrogel C3 in water	**7**	71.259	71.264	0.002	0.0462	71.264 ± 0.052 (± 0.07 %)
		71.221				
		71.313				
	11	75.291	75.235	0.011	0.1072	75.235 ± 0.121 (± 0.16 %)
		75.302				
		75.111				
	14	76.445	76.422	0.010	0.1009	76.422 ± 0.144 (± 0.15 %)
		76.312				
		76.510				
	22	79.317	79.319	0.011	0.1075	79.319 ± 0.122 (± 0.15 %)
		79.212				
		79.427				

Appendix 6 continued

Release of urea from cellulose hydrogel C3 in water	**30**	80.468	80.463	0.002	0.0402	80.463 ± 0.045 (± 0.06 %)
		80.421				
		80.501				
	48	80.491	80.467	0.001	0.0339	80.467 ± 0.038 (± 0.05 %)
		80.481				
		80.428				
	60	80.389	80.468	0.005	0.0689	80.468 ± 0.078 (± 0.10 %)
		80.516				
		80.499				
	72	80.464	0.471	0.003	0.0538	80.471 ± 0.061 (± 0.08 %)
		80.421				
		80.528				

Appendix 7: Release behavior of cellulose hydrogel C3 and free urea in soils

Duration (days)		Release rate (%)	Mean	Variance, s^2	Standard Deviation, σ	95 % Confidence Level (Statistical significance of 5 %)
Release of free urea in topsoil	**1**	95.022	95.082	0.003	0.0517	95.082 ± 0.059 (± 0.06 %)
		95.114				
		95.109				
	3	95.049	95.096	0.002	0.0405	95.096 ± 0.046 (± 0.05 %)
		95.121				
		95.117				
	5	95.127	95.102	0.002	0.0427	95.102 ± 0.048 (± 0.05 %)
		95.129				
		95.053				
	7	96.002	95.414	0.259	0.5090	95.414 ± 0.576 (± 0.60 %)
		95.129				
		95.112				

Appendix 7 continued

Release of free urea in topsoil	**11**	96.013	96.164	0.017	0.1308	96.164 ± 0.148 (± 0.15 %)
		96.237				
		96.242				
	14	96.021	96.174	0.017	0.1325	96.174 ± 0.15 (± 0.16 %)
		96.242				
		96.258				
	22	97.011	96.523	0.179	0.4236	96.523 ± 0.479 (± 0.50 %)
		96.247				
		96.312				
	30	96.338	96.589	0.123	0.3604	96.589 ± 0.408 (± 0.42 %)
		97.002				
		96.427				

Appendix 7 continued

Release of free urea in topsoil	**48**	97.102	96.833	0.151	0.3894	96.834 ± 0.441 (± 0.46 %)
		96.387				
		97.012				
	60	96.792	96.705	0.122	0.3496	96.706 ± 0.396 (± 0.41 %)
		96.321				
		97.004				
	72	97.249	96.831	0.142	0.3770	96.831 ± 0.427 (± 0.44 %)
		96.684				
		97.259				

Appendix 7 continued

Duration (days)		Release rate (%)	Mean	Variance, s^2	Standard Deviation, σ	95 % Confidence Level (Statistical significance of 5 %)
Release of free urea in wet clayey soil	**1**	95.031	95.052	0.003	0.0518	95.052 ± 0.062 (± 0.07 %)
		95.115				
		95.011				
	3	95.102	95.088	0.002	0.0476	95.088 ± 0.054 (± 0.06 %)
		95.127				
		95.035				
	5	95.119	95.125	8.633	0.0093	95.125 ± 0.011 (± 0.01 %)
		95.136				
		95.121				
	7	95.124	95.425	0.260	0.5101	95.425 ± 0.577 (± 0.60 %)
		95.137				
		96.104				

Appendix 7 continued

Release of free urea in wet clayey soil	**11**	96.124	96.135	8.933	0.0095	96.135 ± 0.011 (± 0.01 %)
		96.138				
		96.142				
	14	96.275	96.188	0.015	0.1231	96.188 ± 0.139 (± 0.14 %)
		96.243				
		96.047				
	22	97.309	96.536	0.197	0.4438	96.536 ± 0.502 (± 0.52 %)
		96.251				
		96.047				
	30	96.511	96.674	0.099	0.3161	96.674 ± 0.358 (± 0.37 %)
		96.472				
		97.038				

Appendix 7 continued

Release of free urea in wet clayey soil	**48**	97.024	96.832	0.159	0.3998	96.832 ± 0.452 (± 0.47 %)
		96.372				
		97.099				
	60	97.016	96.708	0.116	0.3409	96.708 ± 0.386 (± 0.40 %)
		96.768				
		96.341				
	72	97.074	96.972	0.044	0.2089	96.972 ± 0.236 (± 0.24 %)
		96.732				
		97.111				

Appendix 7 continued

Duration (days)		Release rate (%)	Mean	Variance, s^2	Standard Deviation, σ	95 % Confidence Level (Statistical significance of 5 %)
Release of free urea in sandy soil	**1**	95.031	95.052	0.003	0.0518	95.052 ± 0.062 (± 0.07 %)
		95.115				
		95.011				
	3	95.102	95.088	0.002	0.0476	95.088 ± 0.054 (± 0.06 %)
		95.127				
		95.035				
	5	95.119	95.125	8.633	0.0093	95.125 ± 0.011 (± 0.01 %)
		95.136				
		95.121				
	7	95.124	95.425	0.260	0.5101	95.425 ± 0.577 (± 0.60 %)
		95.137				
		96.104				

Appendix 7 continued

Release of free urea in sandy soil	**11**	96.52	96.137	0.0003	0.01680	96.137 ± 0.019 (± 0.02 %)
		96.119				
		96.141				
	14	96.241	96.209	0.009	0.0957	96.209 ± 0.108 (± 0.11 %)
		96.101				
		96.284				
	22	96.247	96.538	0.407	0.6378	96.538 ± 0.722 (± 0.75 %)
		96.097				
		97.269				
	30	96.271	96.632	0.255	0.5051	96.632 ± 0.572 (± 0.59 %)
		96.415				
		97.209				

Appendix 7 continued

Release of free urea in sandy soil	**48**	97.101	96.872	0.176	0.4194	96.872 ± 0.475 (± 0.49 %)
		96.388				
		97.127				
	60	97.115	96.063	0.108	0.3281	96.063 ± 0.371 (± 0.38 %)
		96.712				
		96.361				
	72	97.084	96.766	0.246	0.4956	96.766 ± 0.561 (± 0.58 %)
		96.195				
		97.019				

Appendix 7 continued

Duration (days)		Release rate (%)	Mean	Variance, s^2	Standard Deviation, σ	95 % Confidence Level (Statistical significance of 5 %)
Release of urea from cellulose hydrogel C3 in topsoil	**1**	47.712	47.703	5.433	0.0074	47.704 ± 0.008 (± 0.02 %)
		47.698				
		47.701				
	3	52.923	52.872	0.004	0.0650	52.872 ± 0.074 (± 0.14 %)
		52.799				
		52.895				
	5	55.901	56.903	6.033	0.0078	55.903 ± 0.009 (± 0.02 %)
		55.897				
		55.912				
	7	56.341	56.342	1.733	0.0042	56.342 ± 0.005 (± 0.01 %)
		56.339				
		56.347				

Appendix 7 continued

Release of urea from cellulose hydrogel C3 in topsoil	**11**	63.223	63.218	3.733	0.0061	63.218 ± 0.007 (± 0.01 %)
		63.219				
		63.211				
	14	66.091	66.093	8.400	0.0092	66.093 ± 0.010 (± 0.02 %)
		66.103				
		66.085				
	22	71.842	71.844	4.433	0.0067	71.844 ± 0.008 (± 0.01 %)
		71.838				
		71.851				
	30	74.711	74.711	0.0001	0.0115	74.711 ± 0.013 (± 0.02 %)
		74.699				
		74.722				

Appendix 7 continued

Release of urea from cellulose hydrogel C3 in topsoil	**48**	75.998	76.182	0.114	0.3376	76.182 ± 0.502 (± 0.66 %)
		75.977				
		76.572				
	60	75.981	76.184	0.118	0.3441	76.184 ± 0.389 (± 0.51 %)
		75.989				
		75.581				
	72	75.993	76.184	0.107	0.3276	76.184 ± 0.371 (± 0.49 %)
		75.996				
		77.562				

Appendix 7 continued

Duration (days)		Release rate (%)	Mean	Variance, s^2	Standard Deviation, σ	95 % Confidence Level (Statistical significance of 5 %)
Release of urea from cellulose hydrogel C3 in wet clayey soil	**1**	42.141	42.143	2.233	0.0047	42.143 ± 0.005 (± 0.01 %)
		42.139				
		42.148				
	3	47.893	47.892	3.099	0.0056	47.892 ± 0.006 (± 0.01 %)
		47.897				
		47.886				
	5	51.724	51.724	1.633	0.0040	51.724 ± 0.005 (± 0.01 %)
		51.721				
		51.729				
	7	56.322	56.322	1.233	0.0035	56.322 ± 0.004 (± 0.01 %)
		56.326				
		56.319				

Appendix 7 continued

Release of urea from cellulose hydrogel C3 in wet clayey soil	**11**	60.544	60.541	1.233	0.0035	60.541 ± 0.004 (± 0.01 %)
		60.541				
		60.537				
	14	63.222	63.224	4.433	0.0067	63.224 ± 0.008(± 0.01 %)
		63.218				
		63.231				
	22	68.972	68.975	3.033	0.0055	68.975 ± 0.006 (± 0.01 %)
		68.981				
		68.971				
	30	73.372	73.374	1.4333	0.0038	73.374 ± 0.004 (± 0.01 %)
		73.371				
		73.378				

Appendix 7 continued

Release of urea from cellulose hydrogel C3 in wet clayey soil	**48**	73.375	73.375	4.233	0.0065	73.375 ± 0.007 (± 0.01 %)
		73.381				
		73.368				
	60	73.379	73.372	4.233	0.0065	73.372 ± 0.007 (± 0.01 %)
		73.366				
		73.372				
	72	73.385	73.377	4.433	0.0067	73.377 ± 0.008 (± 0.01 %)
		73.374				
		73.373				

Appendix 7 continued

Duration (days)		Release rate (%)	Mean	Variance, s^2	Standard Deviation, σ	95 % Confidence Level (Statistical significance of 5 %)
Release of urea from cellulose hydrogel C3 in sandy soil	**1**	45.985	45.982	9.333	0.003	45.982 ± 0.003 (± 0.01 %)
		45.981				
		45.979				
	3	46.931	46.932	1.633	0.0040	46.932 ± 0.005 (± 0.01 %)
		46.936				
		46.928				
	5	49.809	49.812	9.333	0.0031	49.812 ± 0.003 (± 0.01 %)
		49.811				
		49.815				
	7	55.165	55.174	6.5333	0.0091	55.174 ± 0.009 (± 0.02 %)
		55.175				
		55.181				

Appendix 7 continued

Release of urea from cellulose hydrogel C3 in sandy soil	**11**	59.779	59.772	4.933	0.0070	59.772 ± 0.008 (± 0.01 %)
		59.765				
		59.773				
	14	61.302	61.304	4.633	0.0068	61.304 ± 0.008 (± 0.01 %)
		61.312				
		61.299				
	22	67.822	67.823	5.033	0.0071	67.823 ± 0.008 (± 0.01 %)
		67.831				
		67.817				
	30	71.841	71.842	4.933	0.0070	71.842 ± 0.008 (± 0.01 %)
		71.835				
		71.849				

Appendix 7 continued

Release of urea from cellulose hydrogel C3 in sandy soil	**48**	71.844	71.844	4.899	0.0069	71.844 ± 0.008 (± 0.01 %)
		71.851				
		71.837				
	60	71.847	71.851	3.033	0.0055	71.851 ± 0.006 (± 0.01 %)
		71.848				
		71.857				
	72	71.845	71.854	8.133	0.0090	71.854 ± 0.010 (± 0.01 %)
		71.855				
		71.863				

Appendix 8: The effect of N level on the plant height (cm)

Days after sowing (DAS)		Plant height (cm)	Mean	Variance, s^2	Standard Deviation, σ	95 % Confidence Level (Statistical significance of 5 %)
T1	**15**	30.061	30.068	8.933	0.0095	30.068 ± 0.011 (± 0.04 %)
		30.064				
		30.065				
		30.072				
		30.079				
	35	39.229	39.234	2.533	0.0050	39.234 ± 0.006 (± 0.01 %)
		39.235				
		39.239				
		39.232				
		39.237				
	55	45.097	45.104	4.899	0.0069	45.104 ± 0.008 (± 0.02 %)
		45.099				
		45.104				
		45.108				
		45.111				

Appendix 8 continued

T1	**75**	58.361	58.367	3.233	0.0057	58.367 ± 0.006 (± 0.01 %)
		58.363				
		58.367				
		58.369				
		58.372				
	85	80.304	80.301	6.333	0.0025	80.301 ± 0.003 (± 0.00 %)
		80.301				
		80.299				
		80. 302				
		80.302				
	99	86.241	86.234	8.933	0.0095	86.234 ± 0.011 (± 0.01 %)
		86.237				
		86.223				
		86.235				
		86.235				

Appendix 8 continued

T1	**115**	86.009	86.021	0.0002	0.0149	86.021 ± 0.017 (± 0.02 %)
		86.017				
		86.038				
		86.022				
		86.022				
	130	86.117	86.148	0.002	0.0464	86.148 ± 0.053 (± 0.06 %)
		86.201				
		86.125				
		86.199				
		86.197				

Appendix 8 continued

Days after sowing (DAS)		Plant height (cm)	Mean	Variance, s^2	Standard Deviation, σ	95 % Confidence Level (Statistical significance of 5 %)
T2H	**15**	28.019	28.063	0.006	0.0742	28.063 ± 0.084 (± 0.30 %)
		28.022				
		28.149				
		28.054				
		28.061				
	35	41.014	41.044	0.001	0.0295	41.044 ± 0.033 (± 0.08 %)
		41.073				
		41.045				
		41.044				
		41.044				
	55	48.991	49.025	0.001	0.0428	49.025 ± 0.048 (± 0.10 %)
		49.073				
		49.011				
		49.022				
		49.025				

Appendix 8 continued

T2H	**75**	67.324	67.333	7.633	0.0087	67.333 ± 0.009 (± 0.01 %)
		67.336				
		67.341				
		67.331				
		67.335				
	85	90.587	90.649	0.003	0.0565	90.649 ± 0.064 (± 0.07 %)
		90.661				
		90.698				
		90.641				
		90.646				
	99	94.056	94.048	0.001	0.0298	94.048 ± 0.034 (± 0.04 %)
		94.073				
		94.015				
		94.047				
		94.049				

Appendix 8 continued

T2H	**115**	94.002	94.051	0.003	0.0567	94.051 ± 0.064 (± 0.07 %)
		94.113				
		94.037				
		94.044				
		94.051				
	130	94.105	94.138	0.002	0.0509	94.138 ± 0.058 (± 0.06 %)
		94.113				
		94.197				
		94.127				
		94.133				

Appendix 8 continued

Days after sowing (DAS)		Plant height (cm)	Mean	Variance, s^2	Standard Deviation, σ	95 % Confidence Level (Statistical significance of 5 %)
T3H	**15**	33.661	33.664	7.233	0.008	33.664 ± 0.010 (± 0.03 %)
		33.658				
		33.674				
		33.662				
		33.663				
	35	53.333	53.336	4.133	0.0064	53.336 ± 0.007 (± 0.01 %)
		53.331				
		53.343				
		53.335				
		53.335				
	55	65.114	65.224	0.011	0.1041	65.224 ± 0.118 (± 0.18 %)
		65.237				
		65.321				
		65.222				
		65.222				

Appendix 8 continued

T3H	**75**	90.669	90.649	0.003	0.0535	90.649 ± 0.061 (± 0.07 %)
		90.588				
		90.689				
		90.649				
		90.649				
	85	100.327	100.337	9.233	0.0096	100.337 ± 0.011 (± 0.01 %)
		100.339				
		100.346				
		100.338				
		100.338				
	99	109.113	109.144	0.008	0.0915	109.144 ± 0.104 (± 0.09 %)
		109.072				
		109.247				
		109.142				
		109.142				

Appendix 8 continued

T3H	**115**	109.521	109.353	0.023	0.1523	109.354 ± 0.172 (± 0.16 %)
		109.317				
		109.223				
		109.227				
		109.228				
	130	109.541	96.381	0.019	0.1412	96.381 ± 0.16 (± 0.15 %)
		109.328				
		109.274				
		109.325				
		109.325				

Appendix 8 continued

Days after sowing (DAS)		Plant height (cm)	Mean	Variance, s^2	Standard Deviation, σ	95 % Confidence Level (Statistical significance of 5 %)
T4H	**15**	30.121	30.122	1.733	0.0042	30.122 ± 0.005 (± 0.02 %)
		30.127				
		30.119				
		30.120				
		30.120				
	35	53.333	53.336	4.133	0.0064	53.336 ± 0.007 (± 0.01 %)
		53.331				
		53.343				
		53.335				
		53.336				
	55	70.557	70.565	5.199	0.0072	70.565 ± 0.008 (± 0.01 %)
		70.567				
		70.571				
		70.565				
		70.564				

Appendix 8 continued

T4H	**75**	121.329	121.335	3.633	0.0060	121.335 ± 0.007 (± 0.01 %)
		121.334				
		121.341				
		121.334				
		121.327				
	85	125.201	125.206	2.533	0.0050	125.206 ± 0.006 (± 0.00 %)
		125.211				
		125.205				
		125.203				
		125.203				
	99	129.533	129.584	0.002	0.0455	129.584 ± 0.052 (± 0.04 %)
		129.597				
		129.621				
		129.535				
		129.537				

Appendix 8 continued

T4H	**115**	129.542	129.587	0.002	0.0401	129.587 ± 0.045 (± 0.03 %)
		129.602				
		129.618				
		129.585				
		129.585				
	130	129.562	129.601	0.001	0.0342	129.601 ± 0.039 (± 0.03 %)
		129.613				
		129.627				
		129.602				
		129.601				

Appendix 8 continued

Days after sowing (DAS)		Plant height (cm)	Mean	Variance, s^2	Standard Deviation, σ	95 % Confidence Level (Statistical significance of 5 %)
T5H	**15**	32.309	32.306	4.899	0.0069	32.306 ± 0.008 (± 0.02 %)
		32.311				
		32.298				
		32.306				
		32.306				
	35	69.337	69.346	0.001	0.0234	69.346 ± 0.027 (± 0.04 %)
		69.329				
		69.373				
		69.344				
		69.344				
	55	89.333	89.337	1.633	0.0040	89.337 ± 0.005 (± 0.01 %)
		89.341				
		89.336				
		89.335				
		89.335				

Appendix 8 continued

T5H	**75**	105.019	105.124	0.0109	0.1045	105.124 ± 0.118 (± 0.11 %)
		105.124				
		105.228				
		105.124				
		105.124				
	85	114.121	114.122	1.733	0.0042	114.122 ± 0.005 (± 0.00 %)
		114.119				
		114.112				
		114.120				
		114.120				
	99	129.621	129.606	0.002	0.0431	129.606 ± 0.045 (± 0.04 %)
		120.557				
		120.639				
		120.605				
		120.605				

Appendix 8 continued

T5H	**115**	129.632	129.613	0.002	0.0459	129.613 ± 0.052 (± 0.04 %)
		129.561				
		129.647				
		129.614				
		129.617				
	130	120.631	129.612	0.002	0.0428	129.612 ± 0.048 (± 0.04 %)
		129.563				
		129.642				
		129.610				
		129.615				

Appendix 8 continued

Days after sowing (DAS)		Plant height (cm)	Mean	Variance, s^2	Standard Deviation, σ	95 % Confidence Level (Statistical significance of 5 %)
T6U	**15**	36.331	36.325	4.001	0.0241	36.325 ± 0.027 (± 0.08 %)
		36.298				
		36.345				
		36.323				
		36.325				
	35	75.412	75.414	0.001	0.0360	75.414 ± 0.041 (± 0.05 %)
		75.379				
		75.451				
		75.410				
		75.414				
	55	91.012	91.039	0.001	0.0275	91.039 ± 0.312 (± 0.03 %)
		91.037				
		91.067				
		91.038				
		91.041				

Appendix 8 continued

T6U	**75**	109.988	110.023	0.001	0.0315	110.023 ± 0.036 (± 0.03 %)
		110.032				
		110.049				
		110.021				
		110.025				
	85	115.213	115.475	0.089	0.2991	115.475 ± 0.338 (± 0.29 %)
		115.801				
		115.412				
		115.474				
		115.476				
	99	122.433	122.434	5.699	0.0075	122.434± 0.009 (± 0.01 %)
		122.427				
		122.442				
		122.432				
		122.432				

Appendix 8 continued

T6U	**115**	122.417	122.439	0.001	0.0225	122.439 ± 0.026 (± 0.02 %)
		122.438				
		122.462				
		122.432				
		122.435				
	130	122.411	122.437	0.001	0.0243	122.437 ± 0.028 (± 0.02 %)
		122.442				
		122.459				
		122.435				
		122.436				

Appendix 9: The effect of N level on the chlorophyll content (SPAD) of the rice plants

N treatments	Chlorophyll content (SPAD)	Mean	Variance, s^2	Standard Deviation, σ	95 % Confidence Level (Statistical significance of 5 %)
T1	28.592	28.575	0.001	0.0275	28.575 ± 0.031 (± 0.11 %)
	28.543				
	28.589				
	28.575				
	28.575				
T2H	34.352	34.585	0.113	0.3364	34.585 ± 0.381 (± 1.10 %)
	34.433				
	34.971				
	34.584				
	34.585				
T3H	35.147	35.167	0.001	0.0224	35.167 ± 0.025 (± 0.07 %)
	35.162				
	35.191				
	35.167				
	35.167				

Appendix 9 continued

T5H	37.991	38.107	0.0108	0.1039	38.107 ± 0.118 (± 0.31 %)
	38.192				
	38.137				
	38.105				
	38.105				
T6U	31.721	31.714	0.001	0.0239	31.714 ± 0.027 (± 0.09 %)
	31.687				
	31.733				
	31.712				
	31.712				

Appendix 10: The effect of N treatments on the number of panicles per plant, number of grains per panicle, grain, and straw yield

N treatments	Number of panicles per plant (or pot)	Mean	Variance, s^2	Standard Deviation, σ	95 % Confidence Level (Statistical significance of 5 %)
T1	6	5.7	0.3	0.58	5.7 ± 0.3 (± 5.8 %)
	6				
	6				
	5				
	5				
T2H	7	6.7	0.3	0.58	6.7 ± 0.3 (± 5.0 %)
	7				
	7				
	6				
	6				
T3H	8	8.7	0.3	0.58	8.7 ± 0.3 (± 5.0 %)
	9				
	9				
	8				
	8				

Appendix 10 continued

T4H	11	12.0	1.0	1.0	12.0 ± 0.6 (± 4.81 %)
	12				
	13				
	12				
	12				
T5H	10	10.7	0.3	0.58	10.7 ± 0.3 (± 3.13 %)
	11				
	11				
	10				
	11				
T6U	8	7.6	0.33	0.58	7.6 ± 0.3 (± 4.35 %)
	8				
	7				
	7				
	7				

Appendix 10 continued

N treatments	Number of grains per panicle	Mean	Variance, s^2	Standard Deviation, σ	95 % Confidence Level (Statistical significance of 5 %)
T1	110	110.0	4.0	2.0	110 ± 1.2 (± 1.7 %)
	112				
	108				
	110				
	110				
T2H	117	116.3	16.3	4.0	116.3 ± 2.3 (± 2.0 %)
	112				
	120				
	116				
	116				
T3H	117	117.7	1.3	1.2	117.7 ± 0.7 (± 0.6 %)
	117				
	119				
	115				
	117				

Appendix 10 continued

T4H	134	134.3	0.3	0.6	134.3 ± 0.3 (± 0.3 %)
	134				
	135				
	135				
	134				
T5H	123	128.3	25.3	5.0	128.3 ± 2.9 (± 2.26 %)
	129				
	133				
	128				
	128				
T6U	119	123.0	16.0	4.0	123.0 ± 2.3 (± 1.9 %)
	123				
	127				
	123				
	123				

Appendix 10 continued

N treatments	Grain yield (g per pot)	Mean	Variance, s^2	Standard Deviation, σ	95 % Confidence Level (Statistical significance of 5 %)
T1	19.659	19.667	5.633	0.0075	19.667 ± 0.009 (± 0.04 %)
	19.674				
	19.667				
	19.666				
	19.666				
T2H	22.509	22.524	0.001	0.0234	22.524 ± 0.027 (± 0.12 %)
	22.512				
	22.551				
	22.523				
	22.523				
T3H	25.788	25.789	6.433	0.0080	25.789 ± 0.009 (± 0.04 %)
	25.781				
	25.797				
	25.785				
	25.785				

Appendix 10 continued

T4H	33.649	33.653	2.233	0.047	33.653 ± 0.005 (± 0.02 %)
	33.651				
	33.658				
	33.653				
	22.653				
T5H	31.045	31.046	3.099	0.0056	31.046 ± 0.006 (± 0.002 %)
	31.051				
	31.041				
	31.045				
	31.045				
T6U	28.845	28.846	1.733	0.0416	28.846 ± 0.005 (± 0.02 %)
	28.851				
	28.843				
	28.845				
	28.345				

Appendix 10 continued

N treatments	Straw yield (g per pot)	Mean	Variance, s^2	Standard Deviation, σ	95 % Confidence Level (Statistical significance of 5 %)
T1	29.987	30.028	0.004	0.0659	30.028 ± 0.075 (± 0.25 %)
	29.993				
	30.103				
	30.027				
	30.027				
T2H	34.749	34.754	5.733	0.0076	34.754 ± 0.009 (± 0.02 %)
	34.751				
	34.763				
	34.752				
	34.752				
T3H	35.089	35.096	9.733	0.0099	35.096 ± 0.011 (± 0.03 %)
	35.107				
	35.091				
	35.095				
	35.095				

Appendix 10 continued

T4H	39.136	39.128	5.633	0.0075	39.128 ± 0.008 (± 0.02 %)
	39.128				
	39.121				
	39.127				
	39.127				
T5H	40.147	40.136	0.0001	0.0100	40.136 ± 0.011 (± 0.03 %)
	40.128				
	40.132				
	40.135				
	40.135				
T6U	36.754	36.752	3.233	0.0057	36.752 ± 0.006 (± 0.02 %)
	36.757				
	36.746				
	36.753				
	36.753				

Appendix 11: Harvest index (HI) of rice with different N treatments

N treatments	Harvest index (HI)	Mean	Variance, s^2	Standard Deviation, σ	95 % Confidence Level (Statistical significance of 5 %)
T1	36.624	36.623	4.333	0.0021	36.623 ± 0.002 (± 0.01 %)
	36.621				
	36.625				
	36.623				
	36.623				
T2H	39.018	39.011	6.533	0.0081	39.011 ± 0.009 (± 0.02 %)
	39.002				
	39.012				
	39.010				
	39.010				
T3H	40.891	40.892	2.533	0.0050	40.892 ± 0.006 (± 0.01 %)
	40.887				
	40.897				
	40.891				
	40.891				

Appendix 11 continued

T4H	45.489	45.513	0.001	0.0240	45.513 ± 0.003(± 0.06 %)
	45.512				
	45.537				
	45.513				
	45.513				
T5H	42.864	42.864	6.333	0.0025	42.864 ± 0.004 (± 0.01 %)
	42.861				
	42.866				
	42.864				
	42.864				
T6U	42.027	42.045	0.002	0.0439	42.045 ± 0.049 (± 0.12 %)
	42.095				
	42.013				
	42.045				
	42.045				

Appendix 12: The effect of N levels on the N uptake of the rice plants

N treatments	N uptake ($g\ Kg^{-1}$)	Mean	Variance, s^2	Standard Deviation, σ	95 % Confidence Level (Statistical significance of 5 %)
T1	0.034	0.033	2.333	0.0015	0.033 ± 0.001 (± 2.70 %)
	0.031				
	0.033				
	0.033				
	0.033				
T2H	0.084	0.088	1.333	0.0036	0.088 ± 0.002 (± 2.37 %)
	0.089				
	0.091				
	0.088				
	0.088				
T3H	0.091	0.092	1.733	0.0042	0.092 ± 0.002 (± 2.60 %)
	0.089				
	0.097				
	0.091				
	0.091				

Appendix 12 continued

T4H	0.253	0.254	1.333	0.0036	0.0254 ± 0.002 (± 0.82 %)
	0.251				
	0.258				
	0.253				
	0.254				
T5H	0.223	0.224	3.733	0.0061	0.224 ± 0.004 (± 1.57 %)
	0.219				
	0.231				
	0.224				
	0.224				
T6U	0.194	0.191	6.333	0.0079	0.191 ± 0.005 (± 2.40 %)
	0.182				
	0.197				
	0.191				
	0.191				

Appendix 13: The effect of N levels on Nitrogen Harvest Index (NHI) of the rice plants

N treatments	N Harvest Index (%)	Mean	Variance, s^2	Standard Deviation, σ	95 % Confidence Level (Statistical significance of 5 %)
T1	50.428	50.429	0.0001	0.0120	50.429 ± 0.014 (± 0.03 %)
	50.417				
	50.441				
	50.428				
	50.428				
T2H	53.047	53.031	0.0002	0.0146	53.031 ± 0.017 (± 0.03 %)
	53.019				
	53.026				
	53.031				
	53.031				
T3H	58.894	58.901	4.2999	0.0066	58.901 ± 0.007 (± 0.01 %)
	58.902				
	58.907				
	58.901				
	58.901				

Appendix 13 continued

T4H	67.928	67.928	0.0002	0.0130	67.928 ± 0.015 (± 0.02 %)
	67.916				
	67.942				
	67.928				
	67.928				
T5H	61.327	61.331	0.0002	0.0154	61.331 ± 0.017 (± 0.03 %)
	61.318				
	61.348				
	61.331				
	61.331				
T6U	60.504	60.506	9.4333	0.0097	60.506 ± 0.011 (± 0.02 %)
	60.517				
	60.498				
	60.505				
	60.505				

Appendix 14: The effect of N level on nitrogen use efficiency (NUE) of the rice plants

N treatments	N use efficiency (%)	Mean	Variance, s^2	Standard Deviation, σ	95 % Confidence Level (Statistical significance of 5 %)
T2H	40.112	40.084	0.0014	0.0370	40.084 ± 0.042 (± 0.10 %)
	40.098				
	40.042				
	40.83				
	40.083				
T3H	46.214	46.244	0.0225	0.1498	46.244 ± 0.170 (± 0.37 %)
	46.407				
	46.112				
	46.242				
	46.242				
T4H	52.621	52.622	8.1333	0.0090	52.622 ± 0.011 (± 0.02 %)
	52.613				
	52.631				
	52.621				
	52.621				

Appendix 14 continued

T5H	35.473	35.473	3.0333	0.0055	35.473 ± 0.006 (± 0.02 %)
	35.467				
	35.478				
	35.473				
	35.473				
T6U	31.172	31.174	0.001	0.0226	31.174 ± 0.026 (± 0.08 %)
	31.153				
	31.198				
	31.172				
	31.172				

Appendix 15: The effect of N levels on agronomic nitrogen efficiency (NAE) of the rice plants

N treatments	N agronomic efficiency (Kg Kg^{-1})	Mean	Variance, s^2	Standard Deviation, σ	95 % Confidence Level (Statistical significance of 5 %)
T2H	3.331	3.334	9.333	0.0031	3.334 ± 0.003 (± 0.10 %)
	3.337				
	3.335				
	3.335				
	3.335				
T3H	6.153	6.152	2.099	0.0046	6.152 ± 0.005 (± 0.08 %)
	6.147				
	6.156				
	6.152				
	6.152				
T4H	12.784	12.784	6.333	0.0025	12.784 ± 0.003 (± 0.02 %)
	12.786				
	12.781				
	12.84				
	12.784				

Appendix 15 continued

T5H	7.501	7.507	3.233	0.0057	7.507 ± 0.006 (± 0.09 %)
	7.506				
	7.512				
	7.506				
	7.605				
T6U	5.733	5.732	9.333	0.0031	5.732 ± 0.003 (± 0.06 %)
	5.735				
	5.729				
	5.732				
	5.732				

Appendix 16: Dry matter accumulation in rice as influenced by N rates application over the crop growth stages

N level	Growing stage	Total dry matter (g per pot)	Mean	Variance, s^2	Standard Deviation, σ	95 % Confidence Level (Statistical significance of 5 %)
T1	**15**	1.987	2.041	0.002	0.0484	2.041 ± 0.055 (± 2.68 %)
		2.081				
		2.054				
	30	25.579	25.634	0.003	0.0523	25.634 ± 0.059 (± 0.23 %)
		25.683				
		25.641				
	45	40.908	40.933	0.001	0.0307	40.933 ± 0.035 (± 0.08 %)
		40.923				
		40.967				
	60	79.697	79.706	7.433	0.0086	79.706 ± 0.009 (± 0.01 %)
		79.714				
		79.708				

Appendix 16 continued

T1	**75**	122.235	122.235	0.001	0.0275	122.235 ± 0.031 (± 0.03 %)
		122.262				
		122.207				
	90	116.112	116.169	0.011	0.1031	116.169 ± 0.117 (± 0.10 %)
		116.107				
		116.288				
	105	108.084	108.091	0.001	0.0227	108.091 ± 0.026 (± 0.02 %)
		108.116				
		108.072				
	120	90.127	90.166	0.004	0.0627	90.166 ± 0.071 (± 0.08 %)
		90.238				
		90.132				

Appendix 16 continued

N level	Growing stage	Total dry matter (g per pot)	Mean	Variance, s^2	Standard Deviation, σ	95 % Confidence Level (Statistical significance of 5 %)
T2H	**15**	3.102	3.107	1.733	0.0042	3.107 ± 0.005 (± 0.15 %)
		3.110				
		3.108				
	30	25.731	25.735	3.033	0.0055	25.735 ± 0.006 (± 0.02 %)
		25.732				
		25.741				
	45	41.714	42.042	0.334	0.5779	42.042 ± 0.654 (± 1.56 %)
		41.702				
		42.709				
	60	100.299	100.304	4.633	0.0068	100.304 ± 0.008 (± 0.01 %)
		100.312				
		100.302				

Appendix 16 continued

T2H	**75**	131.128	131.126	0.001	0.0226	131.126 ± 0.026 (± 0.02 %)
		131.102				
		131.147				
	90	126.107	126.135	0.001	0.0252	126.135 ± 0.029 (± 0.02 %)
		126.142				
		126.156				
	105	120.088	120.065	0.001	0.0272	120.065 ± 0.031 (± 0.03 %)
		120.035				
		120.072				
	120	107.121	107.171	0.002	0.0442	107.171 ± 0.050 (± 0.05 %)
		107.187				
		107.205				

Appendix 16 continued

N level	Growing stage	Total dry matter (g per pot)	Mean	Variance, s^2	Standard Deviation, σ	95 % Confidence Level (Statistical significance of 5 %)
T3H	**15**	3.248	3.211	0.001	0.0348	3.211 ± 0.040 (± 1.23 %)
		3.179				
		3.205				
	30	25.711	25.711	4.899	0.0069	25.711 ± 0.008 (± 0.03 %)
		25.704				
		25.718				
	45	41.472	41.501	0.001	41.501	41.501 ± 0.028 (± 0.07 %)
		41.518				
		41.512				
	60	107.102	107.082	0.001	0.0237	107.082 ± 0.027 (± 0.03 %)
		107.089				
		107.056				

Appendix 16 continued

T3H	**75**	137.097	137.106	6.033	0.0078	137.106 ± 0.009 (± 0.01 %)
		137.112				
		137.108				
	90	129.051	129.083	0.001	0.0278	129.083 ± 0.031 (± 0.02 %)
		129.097				
		129.101				
	105	123.112	123.142	0.004	0.0619	123.142 ± 0.070 (± 0.06 %)
		123.102				
		123.214				
	120	114.089	114.109	0.001	0.0237	114.109 ± 0.027 (± 0.02 %)
		114.102				
		114.135				

Appendix 16 continued

N level	Growing stage	Total dry matter (g per pot)	Mean	Variance, s^2	Standard Deviation, σ	95 % Confidence Level (Statistical significance of 5 %)
T4H	**15**	9.112	9.095	0.001	0.0247	0.095 ± 0.028 (± 0.31 %)
		9.067				
		9.107				
	30	35.556	35.592	0.001	0.0312	31.592 ± 0.035 (± 0.01 %)
		35.608				
		35.612				
	45	74.357	74.393	0.001	0.0329	74.393 ± 0.037 (± 0.05 %)
		74.402				
		74.421				
	60	125.397	125.213	0.025	0.1595	125.213 ± 0.18 (± 0.14 %)
		125.128				
		125.114				

Appendix 16 continued

T4H	**75**	171.116	171.126	8.399	0.0092	171.126 ± 0.010 (± 0.01 %)
		171.128				
		171.134				
	90	169.069	169.058	0.001	0.0325	169.058 ± 0.037 (± 0.02 %)
		169.083				
		169.021				
	105	151.098	151.103	2.533	0.0050	151.103 ± 0.006 (± 0.00 %)
		151.102				
		151.108				
	120	149.141	149.121	0.001	0.0278	149.121 ± 0.031 (± 0.02 %)
		149.132				
		149.089				

Appendix 16 continued

N level	Growing stage	Total dry matter (g per pot)	Mean	Variance, s^2	Standard Deviation, σ	95 % Confidence Level (Statistical significance of 5 %)
T5H	**15**	8.992	9.069	0.0045	0.0669	9.069 ± 0.076 (± 0.83 %)
		9.102				
		9.113				
	30	34.251	34.251	1.233	0.0035	34.251 ± 0.004 (± 0.01 %)
		34.248				
		24.255				
	45	62.311	62.317	0.001	62.317	62.317 ± 0.04 (± 0.06 %)
		62.289				
		62.352				
	60	117.128	117.158	0.004	0.0669	117.158 ± 0.08 (± 0.06 %)
		117.112				
		117.235				

Appendix 16 continued

T5H	**75**	162.113	162.107	0.001	0.0279	162.107 ± 0.032 (± 0.02 %)
		162.077				
		162.132				
	90	159.099	159.088	0.001	0.0306	159.088 ± 0.035 (± 0.02 %)
		159.053				
		159.111				
	105	149.011	149.046	0.001	0.0316	149.046 ± 0.36 (± 0.02 %)
		149.056				
		149.072				
	120	137.051	137.081	0.001	0.0267	137.081 ± 0.030 (± 0.02 %)
		137.101				
		137.092				

Appendix 16 continued

N level	Growing stage	Total dry matter (g per pot)	Mean	Variance, s^2	Standard Deviation, σ	95 % Confidence Level (Statistical significance of 5 %)
T6U	**15**	8.102	8.035	0.014	0.1198	8.035 ± 0.14 (± 1.69 %)
		8.107				
		7.897				
	30	34.221	34.223	3.233	0.0057	34.223 ± 0.006 (± 0.02 %)
		24.218				
		34.229				
	45	57.291	57.299	4.633	0.0068	57.299 ± 0.008 (± 0.01 %)
		57.304				
		57.301				
	60	116.113	116.121	5.633	0.0075	116.121 ± 0.009 (± 0.01 %)
		116.121				
		116.128				

Appendix 16 continued

T6U	**75**	148.751	149.024	0.0565	0.2377	149.024 ± 0.27 (± 0.18 %)
		149.133				
		149.187				
	90	145.151	145.120	0.001	0.0266	145.120 ± 0.030 (± 0.02 %)
		145.103				
		145.107				
	105	139.991	140.030	0.004	0.0622	140.030 ± 0.07 (± 0.05 %)
		139.998				
		140.102				
	120	134.054	134.045	0.001	0.0225	134.045 ± 0.026 (± 0.02 %)
		134.061				
		134.019				

Appendix17: Pattern of dry matter partitioning to different parts of rice as influenced by time course and nitrogen level

N level	Growing stage	Total dry matter (g per pot)	Mean	Variance, s^2	Standard Deviation, σ	95 % Confidence Level (Statistical significance of 5 %)
T1 Leaf	**15**	1.024	1.041	0.002	0.0403	1.041 ± 0.046 (± 4.38 %)
		1.012				
		1.087				
	30	6.612	6.613	2.100	0.0046	6.613 ± 0.006 (± 0.08 %)
		6.618				
		6.609				
	45	9.588	9.595	4.433	0.0067	9.595 ± 0.008 (± 0.08 %)
		9.597				
		9.601				
	60	8.697	8.705	7.433	0.0086	8.705 ± 0.010 (± 0.11 %)
		8.703				
		8.714				

Appendix 17 continued

T1 **Leaf**	**75**	8.799	8.801	0.001	0.0268	8.801 ± 0.03 (± 0.34 %)
		8.794				
		8.831				
	90	8.418	8.417	3.633	0.0060	8.417 ± 0.007 (± 0.08 %)
		8.423				
		8.411				
	105	6.189	6.198	6.933	0.0083	6.198 ± 0.009 (± 0.15 %)
		6.201				
		6.205				
	120	5.503	5.508	2.533	0.0050	2.533 ± 0.006 (± 0.10 %)
		5.509				
		5.519				

Appendix 17 continued

N level	Growing stage	Total dry matter (g per pot)	Mean	Variance, s^2	Standard Deviation, σ	95 % Confidence Level (Statistical significance of 5 %)
T1 Sheath	**15**	1.128	1.145	0.001	0.0239	1.145 ± 0.027 (± 2.36 %)
		1.134				
		1.172				
	30	6.512	6.507	3.233	0.0057	6.507 ± 0.006 (± 0.10 %)
		6.509				
		6.501				
	45	9.788	9.794	5.433	0.0074	9.794 ± 0.008 (± 0.09 %)
		9.791				
		9.802				
	60	22.597	22.604	3.733	0.0061	22.604 ± 0.007 (± 0.03 %)
		22.605				
		22.609				

Appendix 17 continued

T1 Sheath	**75**	21.215	21.214	1.733	0.0042	21.214 ± 0.005 (± 0.02 %)
		21.209				
		21.217				
	90	18.896	18.905	9.033	0.0095	18.905 ± 0.011 (± 0.06 %)
		18.905				
		18.915				
	105	18.701	18.706	2.533	0.0050	18.706 ± 0.006 (± 0.03 %)
		18.705				
		18.711				
	120	14.299	14.302	1.733	0.0042	14.302 ± 0.005 (± 0.03 %)
		14.301				
		14.307				

Appendix 17 continued

N level	Growing stage	Total dry matter (g per pot)	Mean	Variance, s^2	Standard Deviation, σ	95 % Confidence Level (Statistical significance of 5 %)
T1 Stem	**15**	1.104	1.117	5.033	0.0071	1.117 ± 0.008 (± 0.72 %)
		1.113				
		1.118				
	30	7.293	7.302	6.299	0.0079	7.302 ± 0.009 (± 0.12 %)
		7.305				
		7.308				
	45	25.197	25.201	3.433	0.0059	25.201 ± 0.007 (± 0.03 %)
		15.199				
		26.208				
	60	26.809	26.814	4.633	0.0068	26.814 ± 0.008 (± 0.03 %)
		26.812				
		26.822				

Appendix 17 continued

T1 **Stem**	**75**	35.191	35.199	6.399	0.0080	35.199 ± 0.009 (± 0.03 %)
		35.199				
		35.207				
	90	30.021	30.025	1.233	0.0035	30.025 ± 0.004 (± 0.01 %)
		30.025				
		30.028				
	105	22.334	22.334	4.233	0.0065	22.334 ± 0.007 (± 0.03 %)
		22.341				
		22.328				
	120	16.697	16.704	4.933	0.0070	16.704 ± 0.008 (± 0.05 %)
		16.705				
		16.711				

Appendix 17 continued

N level	Growing stage	Total dry matter (g per pot)	Mean	Variance, s^2	Standard Deviation, σ	95 % Confidence Level (Statistical significance of 5 %)
T1 Panicle	**15**	1.891	1.967	0.004	0.0659	1.967 ± 0.038 (± 1.94 %)
		1.997				
		2.012				
	30	10.129	10.125	8.233	0.0091	10.125 ± 0.005 (± 0.05 %)
		10.115				
		10.132				
	45	24.909	24.914	4.633	0.0068	24.914 ± 0.008 (± 0.03 %)
		24.912				
		24.922				
	60	36.799	36.803	2.033	0.0045	36.803 ± 0.005 (± 0.01 %)
		36.803				
		36.808				

Appendix 17 continued

T1 **Panicle**	**75**	55.124	55.128	1.633	0.0040	55.128 ± 0.005 (± 0.01 %)
		55.129				
		55.132				
	90	43.501	43.506	3.733	0.0061	43.506 ± 0.007 (± 0.02 %)
		43.505				
		43.513				
	105	33.703	33.706	1.299	0.0036	33.706 ± 0.004 (± 0.01 %)
		333.705				
		33.710				
	120	23.211	23.207	2.033	0.0045	23.207 ± 0.005 (± 0.02 %)
		23.202				
		23.207				

Appendix 17 continued

N level	Growing stage	Total dry matter (g per pot)	Mean	Variance, s^2	Standard Deviation, σ	95 % Confidence Level (Statistical significance of 5 %)
T2H Leaf	**15**	1.112	1.104	8.233	0.0091	1.104 ± 0.010 (± 0.93 %)
		1.105				
		1.094				
	30	4.722	4.727	2.533	0.0050	4.727 ± 0.006 (± 0.12 %)
		4.728				
		4.732				
	45	8.209	8.204	3.033	0.0055	8.204 ± 0.006 (± 0.08 %)
		8.204				
		8.198				
	60	7.892	7.903	9.433	0.0097	7.903 ± 0.011 (± 0.14 %)
		7.905				
		7.911				

Appendix 17 continued

T2H Leaf	**75**	8.902	8.908	0.0060	3.633	8.908 ± 0.007 (± 0.08 %)
		8.907				
		8.914				
	90	9.111	9.117	5.199	0.0072	9.117 ± 0.008 (± 0.09 %)
		9.115				
		9.125				
	105	6.206	6.213	3.733	0.0061	6.213 ± 0.007 (± 0.11 %)
		6.214				
		6.218				
	120	6.897	6.902	2.533	0.0050	6.902 ± 0.006 (± 0.08 %)
		6.901				
		6.907				

Appendix 17 continued

N level	Growing stage	Total dry matter (g per pot)	Mean	Variance, s^2	Standard Deviation, σ	95 % Confidence Level (Statistical significance of 5 %)
T2H Sheath	**15**	1.367	1.341	0.001	0.0225	1.341 ± 0.026 (± 1.90%)
		1.322				
		1.325				
	30	8.698	8.707	7.233	0.0085	8.707± 0.009 (± 0.11 %)
		8.707				
		8.715				
	45	9.319	9.339	0.001	0.0227	9.339 ± 0.026 (± 0.28 %)
		9.336				
		9.364				
	60	20.204	20.178	0.003	0.0509	20.178 ± 0.058 (± 0.29 %)
		20.210				
		20.199				

Appendix 17 continued

T2H Sheath	**75**	27.312	27.339	0.001	0.0275	27.339 ± 0.031 (± 0.11 %)
		27.338				
		27.367				
	90	21.778	21.804	0.001	0.0246	21.804 ± 0.028 (± 0.13 %)
		21.806				
		21.827				
	105	19.299	19.321	0.001	0.0243	19.321 ± 0.028 (± 0.14 %)
		19.316				
		19.347				
	120	14.905	14.929	0.001	0.0236	14.929 ± 0.003 (± 0.18 %)
		14.932				
		14.952				

Appendix 17 continued

N level	Growing stage	Total dry matter (g per pot)	Mean	Variance, s^2	Standard Deviation, σ	95 % Confidence Level (Statistical significance of 5 %)
T2H Stem	**15**	1.781	1.827	0.050	0.0025	1.827 ± 0.029 (± 1.59 %)
		1.822				
		1.881				
	30	9.218	9.222	0.005	2.033	9.222 ± 0.005 (± 0.06 %)
		9.222				
		9.227				
	45	13.801	13.807	3.033	0.0055	13.807 ± 0.006 (± 0.05 %)
		13.807				
		13.812				
	60	30.016	30.021	3.233	0.0057	30.021 ± 0.007 (± 0.02 %)
		30.019				
		30.027				

Appendix 17 continued

T2H Stem	**75**	40.038	40.070	0.001	0.0303	40.070 ± 0.034 (± 0.09 %)
		40.075				
		40.098				
	90	35.198	35.221	0.001	0.0241	35.221 ± 0.027 (± 0.08 %)
		35.218				
		35.246				
	105	31.122	31.125	1.233	0.0035	31.125 ± 0.004 (± 0.01 %)
		31.125				
		31.129				
	120	20.114	20.120	5.033	0.0071	20.120 ± 0.008 (± 0.04 %)
		20.119				
		20.123				

Appendix 17 continued

N level	Growing stage	Total dry matter (g per pot)	Mean	Variance, s^2	Standard Deviation, σ	95 % Confidence Level (Statistical significance of 5 %)
T2H Panicle	**15**	1.712	1.718	4.233	0.0065	1.718 ± 0.007 (± 0.43 %)
		1.718				
		1.725				
	30	9.798	9.803	3.233	0.0057	9.803 ± 0.006 (± 0.07 %)
		9.801				
		9.809				
	45	18.333	18.326	5.699	0.0075	18.326 ± 0.009 (± 0.05 %)
		18.327				
		18.318				
	60	45.504	45.509	1.733	0.0042	45.509 ± 0.005 (± 0.01 %)
		45.510				
		45.512				

Appendix 17 continued

T2H Panicle	**75**	60.705	60.711	3.633	0.0060	60.711 ± 0.007 (± 0.01 %)
		60.712				
		60.717				
	90	55.509	55.513	2.033	0.0045	55.513 ± 0.005 (± 0.01 %)
		55.513				
		55.518				
	105	41.097	41.101	1.299	0.0036	41.101 ± 0.004 (± 0.01 %)
		41.102				
		41.104				
	120	30.001	30.009	4.633	0.0068	30.009 ± 0.008 (± 0.03 %)
		30.011				
		30.014				

Appendix 17 continued

N level	Growing stage	Total dry matter (g per pot)	Mean	Variance, s^2	Standard Deviation, σ	95 % Confidence Level (Statistical significance of 5 %)
T3H Leaf	**15**	1.327	1.341	0.0002	0.0136	1.341 ± 0.008 (± 0.58 %)
		1.343				
		1.359				
	30	2.981	2.986	2.5333	0.0050	2.986 ± 0.006 (± 0.19 %)
		2.985				
		2.991				
	45	5.013	5.016	9.3333	0.0031	5.016 ± 0.003 (± 0.07 %)
		5.017				
		5.019				
	60	8.793	8.799	3.0333	0.0055	8.799 ± 0.006 (± 0.07 %)
		8.799				
		8.804				

Appendix 17 continued

T3H Leaf	**75**	9.211	9.215	1.5999	0.0039	9.215 ± 0.006 (± 0.06 %)
		9.215				
		9.219				
	90	9.281	9.286	3.7333	0.0061	9.286 ± 0.007 (± 0.07 %)
		9.285				
		9.293				
	105	7.110	7.114	1.2333	0.0035	7.114 ± 0.004 (± 0.06 %)
		7.114				
		7.117				
	120	7.485	7.495	9.2333	0.0096	7.495 ± 0.011 (± 0.15 %)
		7.497				
		7.504				

Appendix 17 continued

N level	Growing stage	Total dry matter (g per pot)	Mean	Variance, s^2	Standard Deviation, σ	95 % Confidence Level (Statistical significance of 5 %)
T3H Sheath	**15**	1.495	1.505	7.6333	0.0087	1.505 ± 0.009 (± 0.66 %)
		1.507				
		1.512				
	30	6.709	6.712	1.2333	0.0035	6.712 ± 0.004 (± 0.006 %)
		6.712				
		6.716				
	45	9.401	9.407	3.0333	0.0055	9.407 ± 0.006 (± 0.07 %)
		9.407				
		9.412				
	60	14.398	14.407	7.2333	0.0085	14.407 ± 0.009 (± 0.07 %)
		14.407				
		14.415				

Appendix 17 continued

T3H Sheath	**75**	17.312	17.319	4.9333	0.0070	17.319 ± 0.008 (± 0.05 %)
		17.318				
		17.326				
	90	16.293	16.299	3.6000	0.0060	16.299 ± 0.007 (± 0.04 %)
		16.299				
		16.305				
	105	13.512	13.516	2.0333	0.0045	13.516 ± 0.005 (± 0.04 %)
		13.516				
		13.521				
	120	19.211	19.218	3.7333	0.00611	19.218 ± 0.007 (± 0.04 %)
		19.219				
		19.233				

Appendix 17 continued

N level	Growing stage	Total dry matter (g per pot)	Mean	Variance, s^2	Standard Deviation, σ	95 % Confidence Level (Statistical significance of 5 %)
T3H Stem	**15**	1.903	1.908	2.5333	0.0050	1.908 ± 0.006 (± 0.30 %)
		1.907				
		1.913				
	30	7.397	7.405	1.6666	0.0040	7.405 ± 0.005 (± 0.06 %)
		7.401				
		7.405				
	45	12.202	12.206	1.2333	0.0035	12.206 ± 0.004 (± 0.03 %)
		12.206				
		12.209				
	60	30.011	30.014	1.2333	0.0035	30.014 ± 0.004 (± 0.01 %)
		30.014				
		30.018				

Appendix 17 continued

T3H Stem	**75**	43.199	43.204	2.2333	0.0047	43.204 ± 0.005 (± 0.01 %)
		43.206				
		43.208				
	90	40.881	40.885	1.6333	0.0040	40.885 ± 0.005 (± 0.01 %)
		40.884				
		40.889				
	105	32.104	32.108	1.6333	0.0040	32.108 ± 0.005 (± 0.01 %)
		32.109				
		32.112				
	120	27.809	27.813	1.5999	0.0039	27.813 ± 0.005 (± 0.02 %)
		27.813				
		27.817				

Appendix 17 continued

N level	Growing level	Total dry matter (g per pot)	Mean	Variance, s^2	Standard Deviation, σ	95 % Confidence Level (Statistical significance of 5 %)
T3H Panicle	**15**	1.781	1.784	1.2333	0.0035	1.784 ± 0.004 (± 0.22 %)
		1.784				
		1.788				
	30	8.299	8.302	9.3333	0.0031	8.302 ± 0.003 (± 0.04 %)
		8.301				
		8.305				
	45	19.897	19.969	0.0039	0.0621	19.969 ± 0.007 (± 0.35 %)
		20.002				
		20.007				
	60	46.208	46.213	3.0333	0.0055	46.213 ± 0.006 (± 0.01 %)
		46.213				
		46.219				

Appendix 17 continued

T3H Panicle	**75**	63.321	63.326	2.5333	0.0050	63.326 ± 0.006 (± 0.01 %)
		63.327				
		63.331				
	90	49.899	49.902	9.3333	0.0031	49.902 ± 0.003 (± 0.01 %)
		49.901				
		49.905				
	105	40.013	40.017	1.6333	0.0040	40.017 ± 0.005 (± 0.01 %)
		40.016				
		40.021				
	120	33.512	33.519	5.8333	0.0076	33.519 ± 0.008 (± 0.03 %)
		33.517				
		33.527				

Appendix 17 continued

N level	Growing stage	Total dry matter (g per pot)	Mean	Variance, s^2	Standard Deviation, σ	95 % Confidence Level (Statistical significance of 5 %)
T4H Leaf	**15**	2.781	2.786	2.7333	0.0061	2.786 ± 0.007 (± 0.25 %)
		2.785				
		2.793				
	30	4.913	4.916	9.3333	0.0031	4.916 ± 0.003 (± 0.07 %)
		4.915				
		4.919				
	45	6.211	6.218	4.9333	0.0070	6.218 ± 0.008 (± 0.13 %)
		6.217				
		6.225				
	60	10.102	10.110	5.8333	0.0076	10.110 ± 0.009 (± 0.09 %)
		10.112				
		10.117				

Appendix 17 continued

T4H	**75**	13.713	13.716	9.3333	0.0031	13.716 ± 0.003 (± 0.03 %)
Leaf		13.715				
		13.719				
	90	10.909	10.912	8.9999	0.0029	10.912 ± 0.003 (± 0.03 %)
		10.912				
		10.915				
	105	9.312	9.317	2.4999	0.0049	9.317 ± 0.006 (± 0.06 %)
		9.317				
		9.322				
	120	8.712	8.715	6.3333	0.0025	8.715 ± 0.003 (± 0.03 %)
		8.715				
		8.717				

Appendix 17 continued

N level	Growing stage	Total dry matter (g per pot)	Mean	Variance, s^2	Standard Deviation, σ	95 % Confidence Level (Statistical significance of 5 %)
T4H Sheath	**15**	2.812	2.815	6.3333	0.0025	2.815 ± 0.003 (± 0.10 %)
		2.815				
		2.817				
	30	8.099	8.103	1.6333	0.0040	8.103 ± 0.005 (± 0.06 %)
		8.102				
		8.107				
	45	14.698	14.703	2.4999	0.0049	14.703 ± 0.006 (± 0.04 %)
		14.703				
		14.708				
	60	29.277	29.297	0.0004	0.0190	29.297 ± 0.022 (± 0.07 %)
		29.298				
		29.315				

Appendix 17 continued

T4H Sheath	**75**	35.409	35.414	2.5333	0.0050	35.414 ± 0.006 (± 0.02 %)
		35.413				
		35.419				
	90	30.004	30.041	0.0038	0.0618	30.041 ± 0.069 (± 0.23 %)
		30.006				
		30.112				
	105	25.495	25.501	4.4333	0.0067	25.501 ± 0.008 (± 0.03 %)
		25.499				
		25.508				
	120	19.717	19.722	3.0333	0.0055	19.722 ± 0.006 (± 0.03 %)
		19.722				
		19.728				

Appendix 17 continued

N level	Growing stage	Total dry matter (g per pot)	Mean	Variance, s^2	Standard Deviation, σ	95 % Confidence Level (Statistical significance of 5 %)
T4H Stem	**15**	2.853	2.865	0.0002	0.0132	2.865 ± 0.015 (± 0.52 %)
		2.862				
		2.879				
	30	8.731	8.756	0.0005	0.0217	8.756 ± 0.025 (± 0.28 %)
		8.722				
		8.764				
	45	18.412	18.442	0.0008	0.0279	18.442 ± 0.032 (± 0.17 %)
		18.448				
		18.467				
	60	35.114	35.124	8.6333	0.0093	35.124 ± 0.011 (± 0.03 %)
		35.127				
		35.132				

Appendix 17 continued

T4H Stem	**75**	52.805	52.813	9.4333	0.0097	52.813 ± 0.011 (± 0.02 %)
		52.811				
		52.824				
	90	53.337	53.345	5.6333	0.0075	53.345 ± 0.008 (± 0.02 %)
		53.345				
		53.352				
	105	35.889	35.903	0.0002	0.0127	35.903 ± 0.014 (± 0.04 %)
		35.905				
		35.914				
	120	30.104	30.115	9.4333	0.0097	30.115 ± 0.011 (± 0.04 %)
		30.117				
		30.123				

Appendix 17 continued

N level	Growing stage	Total dry matter (g per pot)	Mean	Variance, s^2	Standard Deviation, σ	95 % Confidence Level (Statistical significance of 5 %)
T4H Panicle	**15**	2.781	2.786	3.7333	0.0061	2.786 ± 0.007 (± 0.25 %)
		2.785				
		2.793				
	30	9.117	9.123	3.0999	0.0056	9.123 ± 0.006 (± 0.07 %)
		9.124				
		9.128				
	45	24.297	24.304	4.2333	0.0065	24.304 ± 0.007 (± 0.03 %)
		24.304				
		24.310				
	60	50.012	50.018	4.2333	0.0065	50.018 ± 0.007 (± 0.01 %)
		50.018				
		50.025				

Appendix 17 continued

T4H Panicle	**75**	70.088	70.092	2.0333	0.0045	70.092 ± 0.005 (± 0.01 %)
		70.093				
		70.097				
	90	62.312	62.326	0.0002	0.0127	62.326 ± 0.014 (± 0.02 %)
		62.328				
		62.337				
	105	58.697	58.709	0.0001	0.0108	58.709 ± 0.012 (± 0.02 %)
		58.712				
		58.718				
	120	57.209	57.219	0.0001	0.0111	57.219 ± 0.013 (± 0.02 %)
		57.218				
		57.231				

Appendix 17 continued

N level	Growing stage	Total dry matter (g per pot)	Mean	Variance, s^2	Standard Deviation, σ	95 % Confidence Level (Statistical significance of 5 %)
T5H Leaf	**15**	1.891	1.899	9.6999	0.0098	1.899 ± 0.011 (± 0.59 %)
		1.896				
		1.910				
	30	3.347	3.361	0.0002	0.0129	3.361 ± 0.015 (± 0.43 %)
		3.365				
		3.372				
	45	5.412	5.423	0.0001	0.0115	5.423 ± 0.013 (± 0.24 %)
		5.423				
		5.435				
	60	9.101	9.114	0.0002	0.0135	9.114 ± 0.015 (± 0.17 %)
		9.114				
		9.128				

Appendix 17 continued

T5H Leaf	**75**	13.895	13.908	0.0002	0.0130	13.908 ± 0.015 (± 0.11 %)
		13.908				
		13.921				
	90	9.712	9.725	0.0002	0.0135	9.725 ± 0.015 (± 0.16 %)
		9.725				
		9.739				
	105	9.297	9.308	0.0001	0.0105	9.308 ± 0.012 (± 0.13 %)
		9.309				
		9.318				
	120	8.214	8.224	0.0001	0.0105	8.224 ± 0.011 (± 0.14 %)
		8.223				
		8.2352				

Appendix 17 continued

N level	Growing level	Total dry matter (g per pot)	Mean	Variance, s^2	Standard Deviation, σ	95 % Confidence Level (Statistical significance of 5 %)
T5H Sheath	**15**	1.989	2.026	0.0012	0.0344	2.026 ± 0.02 (± 0.98 %)
		2.032				
		2.057				
	30	6.308	6.318	0.0001	0.0100	6.318 ± 0.011 (± 0.18 %)
		6.317				
		6.328				
	45	14.794	14.806	0.0002	0.0125	14.806 ± 0.014 (± 0.10 %)
		14.805				
		14.819				
	60	27.218	27.232	0.0002	0.0135	27.232 ± 0.015 (± 0.06 %)
		27.232				
		27.245				

Appendix 17 continued

T5H Sheath	**75**	32.404	32.421	0.0003	0.0175	32.421 ± 0.019 (± 0.06 %)
		32.421				
		32.439				
	90	29.328	29.344	0.0003	0.0165	29.344 ± 0.019 (± 0.06 %)
		29.344				
		29.361				
	105	25.019	25.036	0.0003	0.0189	25.036 ± 0.021 (± 0.08 %)
		25.033				
		25.056				
	120	19.899	19.915	0.0003	0.0184	19.915 ± 0.021 (± 0.10 %)
		19.910				
		19.935				

Appendix 17 continued

N level	Growing level	Total dry matter (g per pot)	Mean	Variance, s^2	Standard Deviation, σ	95 % Confidence Level (Statistical significance of 5 %)
T5H Stem	**15**	2.287	2.293	3.6666	0.0060	2.293 ± 0.007 (± 0.30 %)
		2.293				
		2.299				
	30	2.978	2.989	0.0001	0.0106	2.989 ± 0.012 (± 0.40 %)
		2.991				
		2.999				
	45	17.112	17.124	0.0002	0.0125	17.124 ± 0.014 (± 0.08 %)
		17.124				
		17.137				
	60	31.712	31.728	0.0003	0.0165	31.728 ± 0.019 (± 0.06 %)
		31.728				
		31.745				

Appendix 17 continued

T5H Stem	**75**	48.424	38.446	0.0006	0.0006	38.446 ± 0.028 (± 0.06 %)
		48.441				
		48.472				
	90	40.891	40.906	0.0003	0.0160	40.906 ± 0.018 (± 0.04 %)
		40.905				
		40.923				
	105	35.111	35.129	0.0003	0.0180	35.129 ± 0.020 (± 0.06 %)
		35.129				
		35.147				
	120	30.024	30.043	0.0004	0.0196	30.043 ± 0.022 (± 0.07 %)
		30.041				
		30.063				

Appendix 17 continued

N level	Growing stage	Total dry matter (g per pot)	Mean	Variance, s^2	Standard Deviation, σ	95 % Confidence Level (Statistical significance of 5 %)
T5H Panicle	**15**	2.435	2.449	0.0003	0.0164	2.449 ± 0.019 (± 0.76 %)
		2.445				
		2.467				
	30	9.978	9.981	1.2333	0.0035	9.981 ± 0.004 (± 0.04 %)
		9.981				
		9.985				
	45	25.112	25.127	0.0002	0.0145	25.127 ± 0.016 (± 0.07 %)
		25.127				
		24.141				
	60	47.331	47.347	0.0002	0.0155	47.347 ± 0.018 (± 0.04 %)
		47.348				
		47.362				

Appendix 17 continued

T5H Panicle	**75**	66.434	66.455	0.0005	0.0221	66.455 ± 0.025 (± 0.04 %)
		66.452				
		66.478				
	90	58.712	58.727	0.0002	0.0145	58.727 ± 0.0164 (± 0.03 %)
		58.728				
		58.741				
	105	56.222	56.238	0.0002	0.0150	56.238 ± 0.017 (± 0.03 %)
		56.239				
		56.252				
	120	52.299	52.310	0.0001	0.0121	52.310 ± 0.014 (± 0.03 %)
		52.309				
		52.323				

Appendix 17 continued

N level	Growing stage	Total dry matter (g per pot)	Mean	Variance, s^2	Standard Deviation, σ	95 % Confidence Level (Statistical significance of 5 %)
T6U Leaf	**15**	1.723	1.738	0.0003	0.0168	1.738 ± 0.009 (± 0.56 %)
		1.734				
		1.756				
	30	3.331	3.338	3.7333	0.0061	3.338 ± 0.007 (± 0.21 %)
		3.339				
		3.343				
	45	3.368	3.377	7.4333	0.0086	3.377 ± 0.009 (± 0.29 %)
		3.379				
		3.385				
	60	8.801	8.812	0.0001	0.0110	8.812 ± 0.012 (± 0.14 %)
		8.812				
		8.823				

Appendix 17 continued

T6U **Leaf**	**75**	10.899	10.907	0.0002	0.0122	10.907 ± 0.012 (± 0.13 %)
		10.901				
		10.921				
	90	8.201	8.208	3.7333	0.0061	8.208 ± 0.007 (± 0.08 %)
		8.209				
		8.213				
	105	8.112	8.116	2.0333	0.0045	8.116 ± 0.005 (± 0.06 %)
		8.116				
		8.121				
	120	7.302	7.308	3.6333	0.0060	7.308 ± 0.007 (± 0.09 %)
		7.309				
		7.314				

Appendix 17 continued

N level	Growing stage	Total dry matter (g per pot)	Mean	Variance, s^2	Standard Deviation, σ	95 % Confidence Level (Statistical significance of 5 %)
T6U Sheath	**15**	1.667	1.673	3.6333	0.0060	1.673 ± 0.007 (± 0.41 %)
		1.674				
		1.679				
	30	6.213	6.219	4.9333	0.0070	6.219 ± 0.008 (± 0.13 %)
		6.219				
		6.227				
	45	13.201	13.208	7.8999	0.0089	13.208 ± 0.010 (± 0.08 %)
		13.205				
		13.218				
	60	26.978	26.984	4.2999	0.0066	26.984 ± 0.007 (± 0.03 %)
		26.983				
		26.991				

Appendix 17 continued

T6U Sheath	**75**	29.211	29.217	3.6333	0.0060	29.217 ± 0.007 (± 0.02 %)
		29.218				
		29.223				
	90	28.298	28.305	4.2333	0.0065	28.305 ± 0.007 (± 0.03 %)
		28.305				
		28.311				
	105	24.211	24.217	2.6333	0.0051	24.217 ± 0.006 (± 0.02 %)
		24.218				
		24.221				
	120	17.212	17.218	3.0999	0.0056	17.218 ± 0.006 (± 0.04 %)
		17.219				
		17.223				

Appendix 17 continued

N level	Growing stage	Total dry matter (g per pot)	Mean	Variance, s^2	Standard Deviation, σ	95 % Confidence Level (Statistical significance of 5 %)
T6U Stem	**15**	2.347	2.358	0.0002	0.0128	2.358 ± 0.014 (± 0.61 %)
		2.355				
		2.372				
	30	8.278	8.284	5.0333	0.0071	8.284 ± 0.008 (± 0.10 %)
		8.283				
		8.292				
	45	12.581	12.587	4.2333	0.0065	12.587 ± 0.007 (± 0.06 %)
		12.587				
		12.594				
	60	30.014	30.019	3.0333	0.0055	30.019 ± 0.006 (± 0.02 %)
		30.019				
		30.025				

Appendix 17 continued

T6U Stem	**75**	45.299	45.307	5.6333	0.0075	45.307 ± 0.008 (± 0.02 %)
		45.307				
		45.314				
	90	40.101	40.108	4.9333	0.0070	40.108 ± 0.008 (± 0.02 %)
		40.107				
		40.115				
	105	35.097	35.104	4.2333	0.0065	35.104 ± 0.007 (± 0.02 %)
		35.104				
		35.110				
	120	27.602	27.609	4.2333	0.0065	27.609 ± 0.007 (± 0.03 %)
		27.609				
		27.615				

Appendix 17 continued

N level	Growing stage	Total dry matter (g per pot)	Mean	Variance, s^2	Standard Deviation, σ	95 % Confidence Level (Statistical significance of 5 %)
T6U Panicle	**15**	2.437	2.447	0.0001	0.0106	2.447 ± 0.012 (± 0.49 %)
		2.445				
		2.458				
	30	10.001	10.005	2.0333	0.0045	10.005 ± 0.005 (± 0.05 %)
		10.005				
		10.010				
	45	20.007	20.010	1.7333	0.0042	20.010 ± 0.005 (± 0.02 %)
		20.009				
		20.015				
	60	47.107	47.112	3.7333	0.0061	47.112 ± 0.007 (± 0.01 %)
		47.111				
		47.119				

Appendix 17 continued

T6U Panicle	**75**	62.299	62.305	2.6333	0.0051	62.305 ± 0.006 (± 0.01 %)
		62.306				
		62.309				
	90	55.101	55.108	4.2333	0.0065	55.108 ± 0.007 (± 0.01 %)
		55.108				
		55.114				
	105	53.214	53.219	3.0333	0.0055	53.219 ± 0.006 (± 0.01 %)
		53.219				
		53.225				
	120	49.699	49.705	4.2333	0.0065	49.705 ± 0.009 (± 0.02 %)
		49.705				
		49.712				

Appendix 18: Correlation Regression Analysis

Graph	Equation	R^2	P value	95 % Confidence Level (Statistical significance of 5 %)	Slope standard error
(a) Number of grains / panicle vs. grain yield (g per pot)	y = 0.4753x – 31.35	0.9607	0.0001	0.4244 – 0.5263	0.0240
(b) Panicle number / pot vs. grain yield (g per pot)	y = 0.1968x + 7.714	0.8544	0.0001	1.538 – 2.399	0.2031
(c) Grain yield (g per pot) / harvest index (HI)	y = 0.6090x + 24.83	0.7881	0.0001	0.4415 – 0.7763	0.0789
(d) N uptake (g Kg^{-1}) / panicle number	y = 2.072x + 5.592	0.7885	0.0001	1.498 – 2.646	0.2708

(e) N uptake (g Kg^{-1}) / number of grains per panicle	y = 9.172x + 105.2	0.8643	0.0001	7.245 – 11.0	0.9086

Appendix 19: Weight loss of cellulose hydrogels CRF during the degradation time throughout the rice cultivation period

W_i	W_f	Percentage difference (%)	Mean, %	Variance, s^2	Standard Deviation, σ	95 % Confidence Level (Statistical significance of 5 %)
104.357	2.548	97.56	97.56	1.000	0.001	97.56 ± 0.001 (± 0.00 %)
104.359	2.551	97.56				
104.361	2.551	97.56				